THE UNIVERSITY *of* EDINBURGH

Spatial Variability of Nitrous Oxide Flux Measurements at the Plot, Field and Farm Scale

Nicholas Jon Cowan [1, 2]

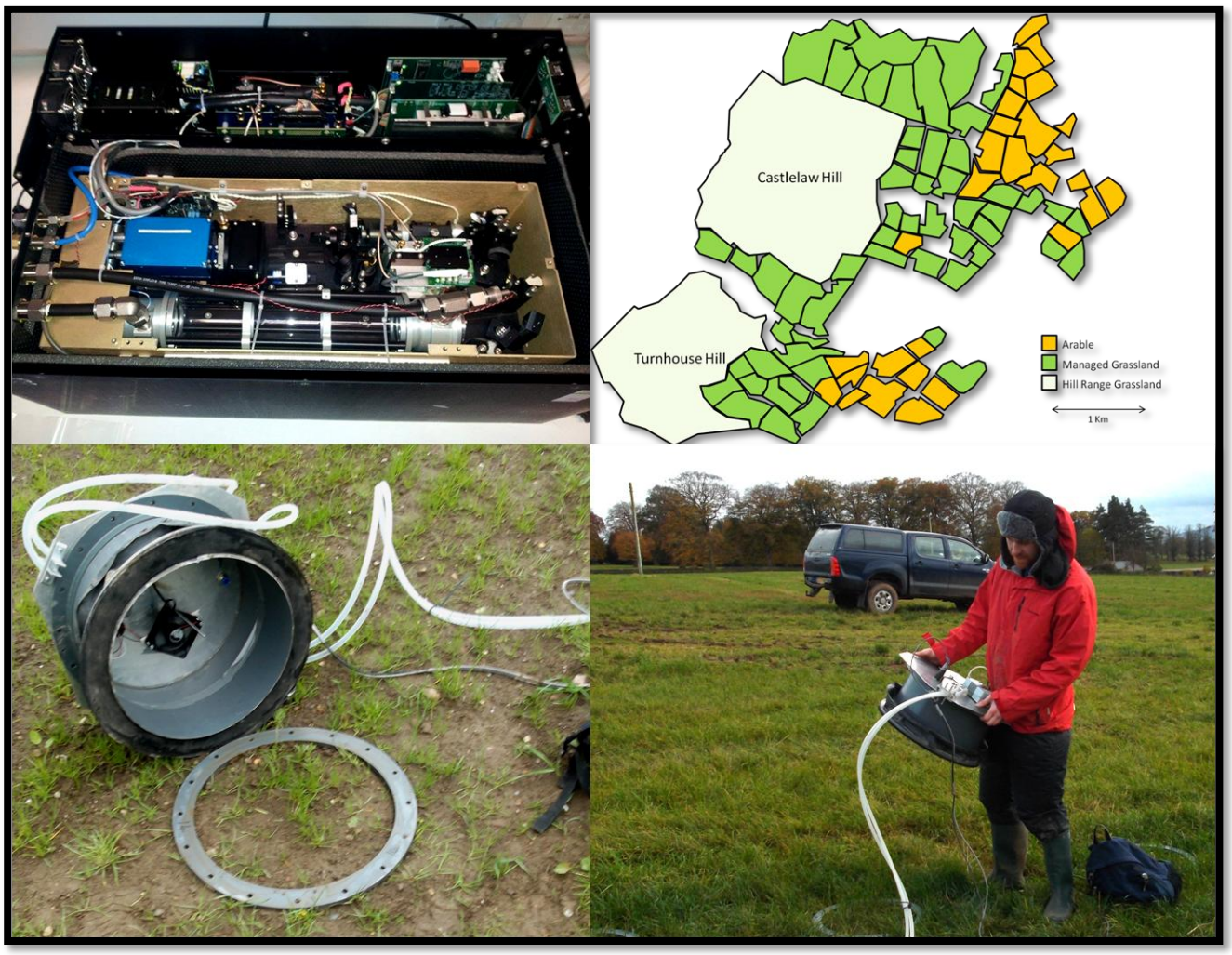

Doctor of Philosophy

University of Edinburgh

September 2014

[1] School of Geosciences, University of Edinburgh, the King's Buildings, Edinburgh

[2] Centre for Ecology and Hydrology, Penicuik, Edinburgh

Declaration

I declare that this thesis and the papers within it have been composed by myself and that no part of this thesis has been submitted for any other degree or qualification. The work described is my own unless stated otherwise.

Nicholas Cowan

September 2014

Summary

Nitrous oxide (N_2O) is a potent greenhouse gas (GHG) which is released naturally into the atmosphere as a by-product of the microbial processes of nitrification and denitrification. Agricultural activities are believed to account for up to 80% of anthropogenic N_2O emissions at a global scale; however, these estimates are prone to large uncertainties due to the large temporal and spatial variability associated with flux measurements. This thesis contains five studies which aimed to improve the ability to measure and predict N_2O emissions from agricultural activities.

A closed loop dynamic chamber was developed using a quantum cascade laser (QCL). This method provided high precision chamber measurements of N_2O flux from soils with a detection limit below 4 μg N_2O-N m^{-2} h^{-1}. Using the dynamic chamber method allowed for a detailed investigation of uncertainties in individual measurements including contributions from regression fitting, temperature and pressure. The lack of negative fluxes measured that were outwith the detection limits of the methodology (0.3% of all measurements) highlighted that the uptake of N_2O reported in some previous literature is likely to have been the result of detection limits of measurement methods applied.

Spatial variability of N_2O flux was investigated at the plot, field and farm scale. Fluxes were measured from a grassland field plot before and after a tillage event. These measurements highlighted the large spatially variability present in N_2O fluxes from agricultural soils. Fluxes varied by up to three orders of magnitude over distances less than 5 metres after the tillage event. A field scale experiment carried out on grazed grassland investigated relationships between soil properties and N_2O flux. This study found that N_2O emissions correlated strongly with available nitrogen content in the soil and that animal waste was likely responsible for the spatial variability of N_2O flux observed at the field scale. A farm scale inventory of N_2O emissions was carried out investigating several large point sources of N_2O and emissions from the wider field coverage. The inventory estimates that nitrogen fertiliser application is the single largest N_2O source from the livestock farm accounting for 49% of annual emissions.

Acknowledgements

I would like to thank my supervisors Ute Skiba, Daniela Famulari and David Reay for all of the support and guidance they have provided throughout my PhD. I also wish to thank them for the trust they put in me by offering me the studentship and giving me the opportunity to work with them for the past three years. Throughout this time I have learned many new skills from them for which I am extremely grateful. A special thank you to Pete Levy who was willing to spend many hours of his time teaching me many of the analysis and coding skills which have improved my research skills a great deal during my studentship.

I would like to thank Margaret Anderson, Julia Drewer, Albert Johnston and all other members of staff at the Centre of Ecology and Hydrology in Edinburgh who have helped me in a wide variety of ways during my time there. These people have consistently helped me in a friendly manner in all my endeavours and made me feel like an integrated member of a wider team which I am glad to have been a part of.

I would like to thank University of Edinburgh, Scotland's Rural College (SRUC) and the Agricultural Development and Advisory Service (ADAS) for providing the field sites from which N_2O fluxes could be measured. I thank Ainsley Bagnall (SRUC) for providing the chamber and flux data from the Crichton field site. I thank Wim Bosma, farm manager for the Easter Bush field site, who provided me with the opportunity to carry out the experiments at Easter Bush Farm. I thank Alex Moir for providing the field sites and farm data for the farm scale work.

I also thank DEFRA and the UK Devolved Administrations for financial support through the UK GHG Platform project AC0116 (The InveN_2Ory project).

A special mention goes to my parents and my wife Linda. They have supported me fully throughout my studentship and have consistently provided me with the motivation I needed to continue through challenging times.

Contents

Chapter 1

Outline of thesis

This thesis is a compilation of studies I have carried out during my PhD studentship which aimed to improve the ability to accurately measure and predict anthropogenic emissions of the trace greenhouse gas, nitrous oxide (N_2O). These studies were focussed mainly on N_2O released due to agricultural practices commonly carried out across the UK. The thesis will begin with an introduction explaining the global impact that atmospheric N_2O has on the environment and then summarise the major natural and anthropogenic sources of N_2O emissions. The variety of methods available to measure and predict emissions from agricultural soils will be discussed as well as the advantages and disadvantages associated with each approach. A methodology section will then outline the field sites and measurement methods that were used during my studies which will include details on instrumentation and calculations used throughout the thesis.

Chapters 4 to 8 contain five studies which I carried out during my PhD studentship under the supervision of colleagues at the Centre for Ecology and Hydrology (CEH). The first study outlines a new dynamic chamber method for measuring fluxes of N_2O from soils which provides various advantages over current static chamber methodology. The second study used the dynamic chamber method to measure spatial variability of N_2O fluxes at a plot scale after a grazed grassland tillage event. The third study was an investigation of the spatial variability of N_2O fluxes at a field scale across grazed grassland during summer from which a field scale inventory of N_2O flux was created. The fourth study involved combining farm management data and over 500 chamber measurements of N_2O flux from a livestock farm over the period of a year and developing a simple model to predict N_2O emissions at a farm scale. The final study is an investigation into the causes of negative flux measurements of N_2O which attempts to explain why N_2O uptake is sometimes observed in agricultural soils.

The final section of the thesis will discuss the results of the studies described in Chapters 4 to 8 and provide additional conclusions summarizing the findings. The validity of the assumptions and models used and the scale of uncertainties calculated during these studies will also be discussed. These conclusions will assess the difficulties encountered during the experiments and suggest how experiences gained from the work can contribute to further developments in the future study of N_2O emissions from soil.

Further work which was originally planned to be part of the thesis included eddy covariance measurements and modelling of the collected data sets using the DAYCENT model. Initially it had been planned to record eddy covariance measurements of N_2O over several months from a grassland field after a tillage event. An unexpected and long lasting change in the predominant wind direction from South-westerly to North-easterly prevented these measurements of the tilled field due to the fixed positioning of the eddy covariance tower and the inability to change the tillage date or location. Chambers were used as an alternative method to measure N_2O from the tillage experiment as presented in Chapter 5. Modelling work was attempted using the DAYCENT model in partnership with the University of Aberdeen. This work was cancelled near the end of the studentship due to the lack of available time and financial resources.

Figure 1.1 Myself at the permanent CEH Easter Bush field site 2012.

Chapter 2

Scientific background

2.1 Greenhouse gases

The greenhouse effect is the process in which thermal radiation emitted from a planetary surface is absorbed by atmospheric gases, and is re-radiated in all directions (Berger & Tricot, 1992). This effect results in a net increase in the temperature of the atmosphere dependent on the concentrations of the relevant gases in the atmosphere. Gases which contribute to the greenhouse effect are called greenhouse gases (GHGs). The gases which contribute most to the greenhouse effect are water vapour, carbon dioxide (CO_2), methane (CH_4), tropospheric Ozone (O_3) and nitrous oxide (N_2O) (IPCC, 2013). The greenhouse effect is estimated to increase the surface temperature of the Earth from approximately -18 °C to 14 °C making it essential to human life on Earth (IPCC, 2007).

Anthropogenic activities have significantly increased the concentrations of GHGs present in the atmosphere since pre-industrial times (Machida *et al.*, 1995; Karl & Trenberth, 2003; IPCC, 2013). The burning of fossil fuels, industrial processes, widespread agriculture, deforestation of large areas of woodland and rainforest and other changes in land use have all contributed to rising concentrations of CO_2, CH_4 and N_2O in the atmosphere (IPCC, 2013). CO_2 has a relatively weak radiative efficiency (1.4×10^{-5} W m^{-2} ppb^{-1}); however, it is by far the most significant greenhouse gas due to its high concentration in the atmosphere (~ 390 ppm) compared to other greenhouse gases with stronger radiative efficiency such as CH_4 (~ 1774 ppb, 3.7×10^{-4} W m^{-2} ppb^{-1}) and N_2O (~ 325 ppb, 3.03×10^{-3} W m^{-2} ppb^{-1}) (IPCC, 2007; IPCC, 2013). The accumulation of GHGs in the atmosphere has become a major environmental, economic and political issue as it has become apparent that an increased greenhouse effect will increase global temperatures, alter the balance of the climate system and have drastic effects on Earth's ecosystems. Even relatively small increases in global temperatures may have many significant negative impacts for humans including lower crop yields, increased rates of desertification, droughts, rising sea levels and increased frequency of extreme weather events (Schneider, 1989; Parry *et al.*, 2004).

Due to the large contribution that CO_2 has on the greenhouse effect the majority of climate change research undertaken by the scientific community has focussed on processes concerning CO_2 and the evaluation

of its global and international emission inventories. Estimates of global anthropogenic CO_2 emissions are based primarily on the consumption of fossil fuels which can be calculated empirically as fossil fuel consumption is relatively simple to measure and record based on economic data. Less research has been carried out investigating other greenhouse gases and their inventories which despite their importance, remain poorly understood. Using the current estimates available, the IPCC estimated that non-CO_2 gases (such as CH_4, halocarbons and N_2O) contribute almost as much to global radiative forcing as CO_2 does (Figure 2.1). Understanding the processes which release and remove these gases from the atmosphere is vital in fully understanding climate change and predicting future environmental alteration that anthropogenic influence will have.

In order to mitigate and manage GHG emissions, the environmental processes in which they are involved must first be understood. In the cases of CH_4 and N_2O emissions, there remain many factors that the scientific community cannot predict accurately given the large variability between experimental results and lack of data gathered. N_2O emissions have proven particularly difficult to predict due to the many environmental factors that can change emissions significantly over short periods of time and the difficulties involved in measuring a gas with such low concentrations in the atmosphere (Rypdal & Winiwarter, 2001). Currently the IPCC believes that N_2O contributes approximately 6% of the total radioactive forcing caused by human activities; however, given that it has such a large global warming potential (GWP), approximately 300 times greater than an equivalent mass of CO_2 over a period of 100 years (IPCC, 2013), it is important to investigate the sources of this gas and how mitigation efforts can be improved.

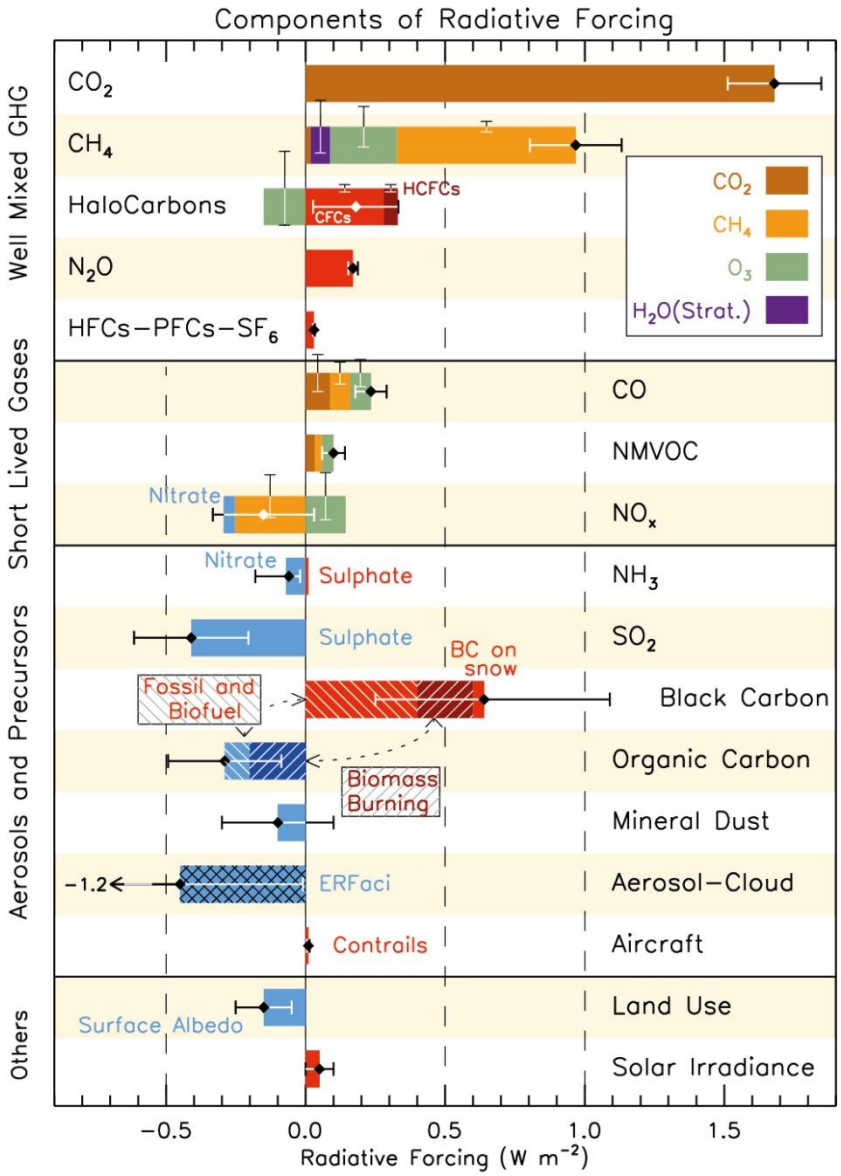

Figure 2.1 IPCC estimate of global average radiative forcing for the year 2011 (Image taken from IPCC, 2013)

2.2 Atmospheric chemistry of N_2O

As well as being a powerful GHG, N_2O also plays a significant role in the catalytic destruction of stratospheric ozone (Ravishankara *et al.*, 2009). Stratospheric N_2O reacts with ozone (O_3) and reduces the ability of the atmosphere to filter out harmful UV radiation. The strong chemical bonds formed between the atoms in N_2O molecules mean that it remains almost completely chemically inert in the troposphere with an atmospheric lifetime of approximately 120 years (IPCC, 2007). This results in a relatively even tropospheric mixing ratio up to altitudes of roughly 17 km where N_2O is lost by transport to the stratosphere.

In the stratosphere N_2O decays through a variety of processes which involves powerful UV radiation from the sun. Approximately 80% of N_2O is decomposed into nitrogen N_2 and a singlet oxygen atom (O_1) by photolysis (Equation 2.1*).* The other 20% of N_2O reacts with O_1 atoms to form 2 NO molecules (Equation 2.2*)* (Schlesinger, 1997). The NO produced from N_2O destroys stratospheric ozone (O_3) in a series of reactions:

$$N_2O + h\nu \rightarrow N_2 + O_1 \qquad \text{(Eq. 2.1)}$$

$$N_2O + O_1 \rightarrow 2NO$$

$$NO + O_3 \rightarrow NO_2 + O_2$$

$$O_3 \rightarrow O + O_2$$

$$\underline{NO_2 + O \rightarrow NO + O_2}$$

$$2O_3 \rightarrow 3O_2 \qquad \text{(Eq. 2.2)}$$

NO_2 is removed from the stratosphere by reacting with hydroxyl radicals (OH*) to form nitric acid (HNO_3) (Equation 2.3). HNO_3 is soluble in water and returns to earth as acid rain completing the natural nitrogen cycle.

$$NO_2 + OH^* \rightarrow HNO_3 \qquad \text{(Eq. 2.3)}$$

Due to the long atmospheric life and high potential to destroy O_3, N_2O has a relatively high ozone depletion potential (ODP). Since the ban on the use of chlorofluorocarbons (CFC's) in the 1980's N_2O has become the largest single contributor to stratospheric ozone destruction (Ravishankara *et al.,* 2009). When CFC concentrations were higher in the atmosphere in the 1970s it was believed that N_2O could react with CFCs in a destructive process in the presence of UV light. Since the widespread removal of CFCs from commercial and industrial use this effect has become less significant in terms of ODP as atmospheric CFC concentrations have dropped substantially (McFarland & Kaye, 1992).

Samples taken from ice cores have shown that the concentration of N_2O in the atmosphere had remained fairly constant for thousands of years (Leuenberger & Siegenthaler, 1992; Machida *et al.*, 1995) until around 300 years ago when it started to increase from pre-industrial concentrations of approximately 270 ppb to current concentrations above 320 ppb (IPPC, 2007; IPCC, 2013). It is believed that the increase in atmospheric N_2O concentrations is a direct result of human activity (Hirsch *et al.*, 2006; Park *et al.*, 2012) and atmospheric concentrations of N_2O are estimated to be increasing at a rate of 0.7 to 0.8 ppb per year as a result of these

activities (Prinn *et al.*, 2000; Park *et al.*, 2012). Although it is difficult to quantify the contribution that individual natural and anthropogenic sources have on global emissions of N_2O it is clear that human activity is the main contributing factor to the 20% rise in atmospheric concentration of N_2O since pre-industrial times.

The combination of a high GWP and high ODP of N_2O make it a significant cause for concern, especially at the current rate of increasing atmospheric concentrations. Furthermore, if action is not taken to mitigate emissions, the consequences will be longer lasting than other GHGs due to the estimated 120 year lifetime of N_2O. Once released, there is very little that can be done to reduce atmospheric N_2O concentrations except to wait for natural processes to occur in the stratosphere.

2.3 Natural sources of N_2O

N_2O can be formed naturally by processes which involve high energy such as forest fires and lightning strikes. These sources are estimated to account for up to 5% of natural N_2O emissions (IPCC, 2013). The remaining 95% of natural emissions of N_2O originate from processes which are carried out in soils and aquatic environments where microbial life is present. The microbial processes of nitrification and denitrification are considered to be the most significant contributors to global N_2O production (e.g. Davidson, 2009; Kool, 2011). These processes play a significant role in the natural nitrogen cycle in which ammonia (NH_4^+) and nitrate (NO_3^-) are converted into nitrogen gas (N_2) which is released into the atmosphere. N_2O is released as a product or by-product of these processes depending on the microbial life and environmental conditions present.

One basic description of how microbial activity emits N_2O from soils is the 'hole in the pipe' model (Figure 2.2) (Davidson, 2000). This model represents a flow of nitrogen compounds passing through leaking pipes with flow rates analogous to rates of nitrification and denitrification. NO and N_2O gas 'leak' from holes in the pipes as the microbial processes are carried out. The sizes of these holes (and therefore the rate at which gases leak) are relative to variable soil properties which affect the rates of the microbial processes (such as acidity, water content, redox potential, etc.). Although this model cannot account for all of the factors which influence N_2O production, it is a useful concept in explaining some common trends in N_2O flux measurements.

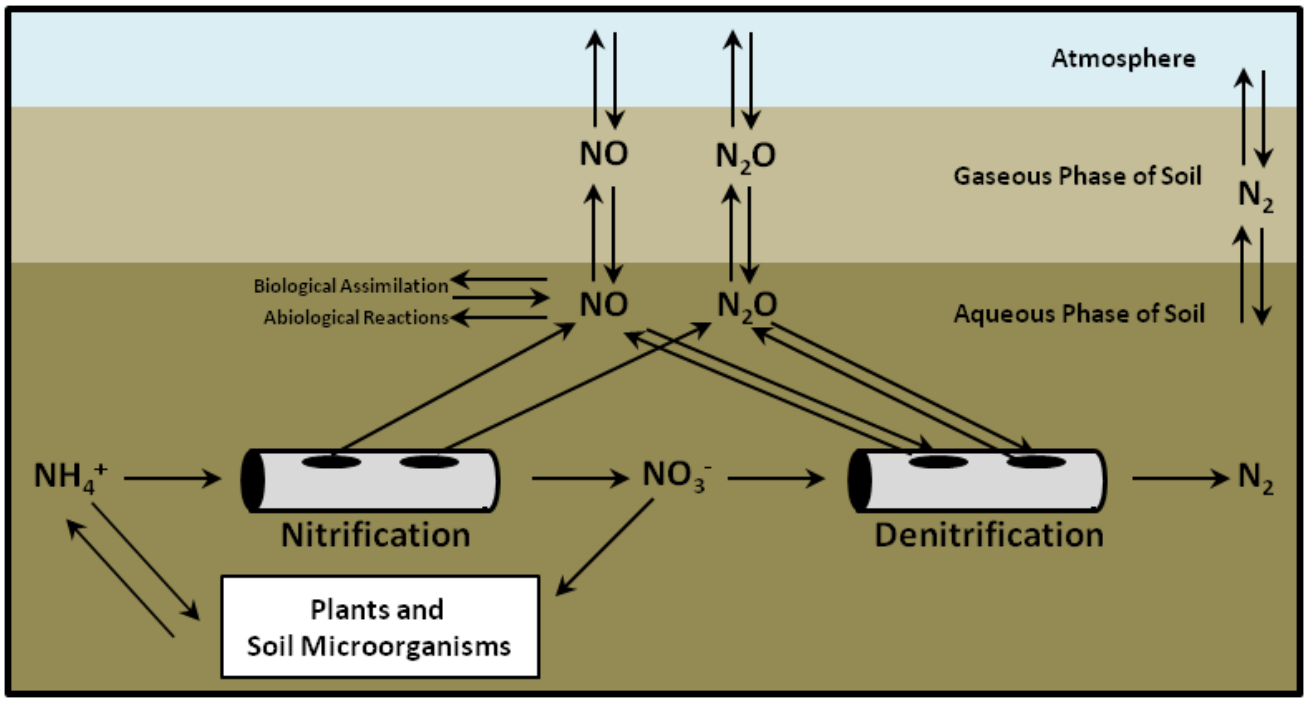

Figure 2.2 The hole in the pipe model is a simplified description of the production and subsequent emissions of N_2O from soils as a by-product of the microbial processes of nitrification and denitrification (Image redrawn from Davidson, 2000).

In reality the formation of N_2O is much more complicated. The processes of nitrification and denitrification rarely occur in isolation. Multiple N_2O producing microbial processes often occur at the same time in soils, each competing for rate-limiting compounds containing nitrogen, carbon or oxygen (See Figure 2.3) (Stevens *et al.*, 1997; Bateman & Baggs, 2005). The rate of each of these processes can also respond differently to soil properties such as pH, temperature and moisture. The heterogeneous nature of soils means that multiple micro-sites in which conditions favour alternate processes can exist in soils over relatively short distances.

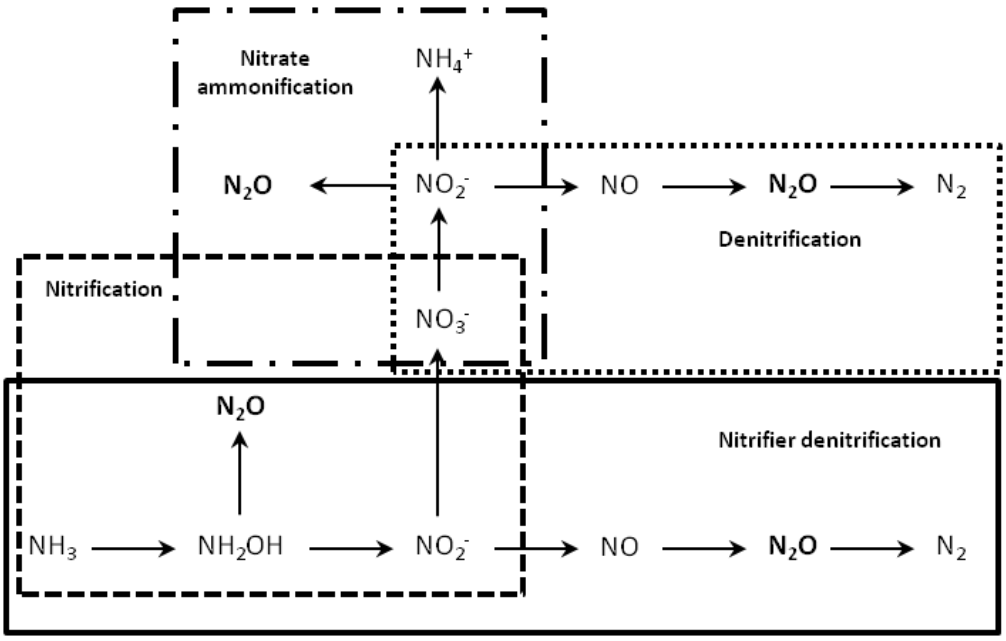

Figure 2.3 A summary of numerous identified pathways in which N_2O emissions are released by microbial processes in soils (Image redrawn from Baggs, 2008).

2.4 Nitrification

Nitrification is the process in which NH_4^+ is converted into NO_3^- by oxidising bacteria which gain energy from the conversion (See Equation 2.4 & Figure 2.3). The rate of NH_4^+ oxidation is often driven by the availability of NH_4^+ present in the soil. Soil pH is also a significant factor in nitrification rate as the acidity of soils affects the protonation of NH_3 and regulates the availability of NH_4^+. Nitrification is an aerobic process which requires the presence of oxygen, so nitrification occurs most readily in oxygen-rich environments such at the very surface layers of soils and sediments. Many factors may influence O_2 availability in soils such as the soil moisture content, composition and porosity of soils. In very wet soils there is often a lack of oxygen which can prevent nitrification processes from taking place (Bateman & Baggs, 2005).

$$2NH_4^+ + 3O_2 \rightarrow 2NO_2^- + 4H^+ + 2H_2O + \text{Energy} \qquad \text{(Eq. 2.4)}$$

2.5 Denitrification

Denitrification is the process in which NO_3^- is converted to N_2 by denitrifying bacteria (See Equation 2.5 & Figure 2.3). This is the final step in the nitrogen cycle in which nitrogen from the biosphere is returned to the atmosphere as N_2. Under anaerobic (oxygen-poor) conditions facultative anaerobic bacteria use NO_3^- as an

electron acceptor in the respiration of organic material (Davidson, 1991). Some archaea and fungi are also capable of denitrifying (Shoun *et al.*, 1992; Cabello *et al.*, 2004). Denitrification occurs in a stepwise fashion in the soil often leaving intermediate products that can accumulate in soils depending on environmental conditions (See Equation 2.5 & Figure 2.3). In certain conditions some bacteria will only produce N_2 while others will produce a mixture of both N_2 and N_2O.

The rate of microbial denitrification in soils is often controlled primarily by nitrogen, carbon and oxygen availability, although pH, temperature and other variables also influence the production of N_2O (Hofstra & Bouwman, 2005; Saggar *et al.*, 2013). Denitrification is an anaerobic process; therefore high soil moisture content can improve conditions for denitrifying microbes by limiting oxygen availability (Bateman & Baggs, 2005).

$$5(CH_2O) + 4NO_3^- + 4H^+ \rightarrow 5CO_2^- + 7H_2O + 2N_2 + \text{Energy} \qquad \text{(Eq. 2.5)}$$

2.6 Anthropogenic sources of N_2O

The largest estimated sources of anthropogenic emissions of N_2O at the global scale are agricultural soils, aquatic environments, biomass and fuel combustion, industrial processes and sewage (See Figure 2.4). It has been estimated that anthropogenic sources account for approximately 39% of global annual emissions of N_2O (IPCC, 2013); however, these estimates are subject to large uncertainties (estimate ranges from 15 to 62% of global annual emissions). Quantifying anthropogenic emissions from sources such as soils and aquatic environments is difficult as human activities can influence existing natural processes in a variety of unpredictable ways. Since the invention of the Haber-Bosch process at the beginning of the 20th century (which allowed mass production of synthetic ammonia fertilisers) the amount of available nitrogen in the global nitrogen cycle has increased dramatically. This increase in nitrogen availability has led to an increase in N_2O emissions from many soils and aquatic environments into which nitrogen compounds have leached (Reay *et al.*, 2012; Fowler *et al.*, 2013).

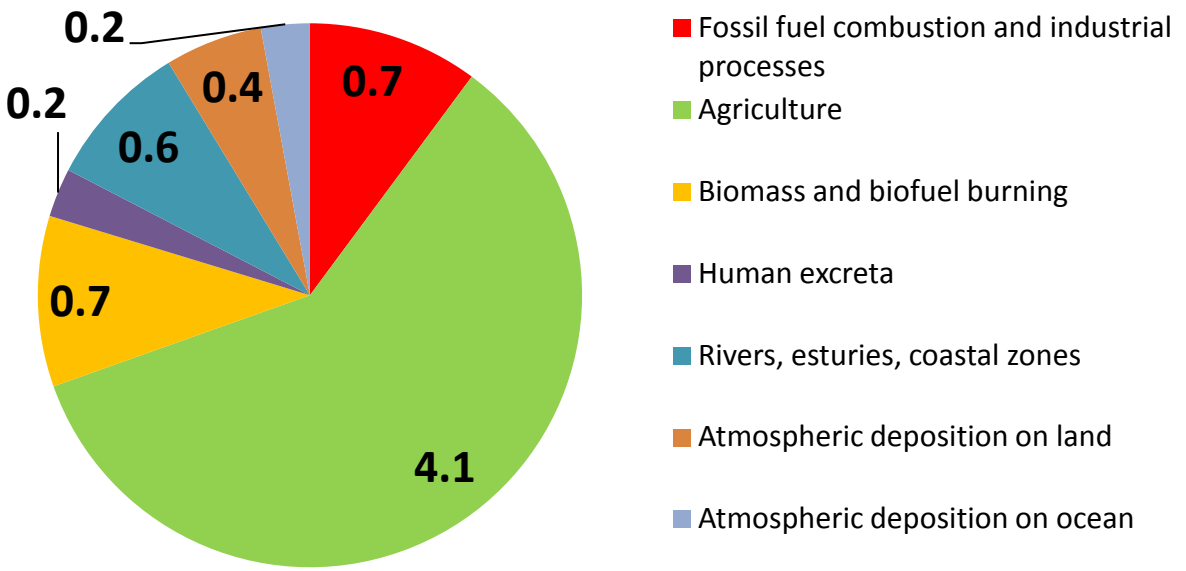

Figure 2.4 IPCC estimate of global N_2O emissions from anthropogenic sources TgN yr^{-1} (IPCC, 2013).

2.7 Agricultural sources of N_2O

The 2013 IPCC report states that agriculture is the single largest source of anthropogenic N_2O emissions (See Figure 2.4). The additional nitrogen applied to soils in the form of nitrogen fertilisers or livestock waste accounts for the majority of agricultural emissions of N_2O. Although classed as separate sources in the IPCC report, if all of the N_2O emissions associated with agricultural activities were combined they would account for as much as 60−80% of all anthropogenic N_2O emissions (IPCC, 2013; Beauchamp, 1997). A large majority of emissions from industrial sources are due to the production of synthetic fertilisers (nitric and adipic acid production) and emissions from coastal zones and rivers are influenced significantly by nitrogen fertilisers leaching into ground waters (Kroeze *et al.*, 2010; Beaulieu *et al.*, 2011). Land clearance, biomass burning, fossil fuel burning and atmospheric deposition are also largely influenced by agricultural activities. These combined factors make agricultural practices by far the most significant source of anthropogenic N_2O emissions.

Since the 1900s the use of synthetic fertilisers has increased dramatically (Davidson, 2009). A greater number of livestock used to feed a growing world population has also led to an increase in the use of farm manures and slurry on crops. Productivity in arable areas has increased significantly due to the addition of nitrogen containing fertilisers which has become a powerful driving force behind the increase in human population over the past 100 years. This increase in agricultural activity has come at a cost to the environment. Increasing the nitrogen applied to soils has altered the natural nitrogen cycle in a variety of ways which are

harmful to human health and the wider environment. Many aquatic environments that are used as sources of drinking water in areas with high intensity agriculture contain high concentrations of nitrogen compounds which exceed the recommended guidelines given by the World Health Organisation (WHO). Atmospheric nitrogen compounds such as NH_3 and NO_x have also been linked to respiratory disease and unintentional nitrogen deposition can damage nitrogen sensitive environments (Sala *et al.*, 2000).

Experiments carried out investigating microbial emissions of N_2O from fertilised fields have estimated that fields treated with synthetic fertilisers emit the equivalent of 0.2 to 3 percent of the total nitrogen applied as N_2O (Mosier, 1996; IPCC, 2007). Due to the heterogeneity of soil conditions and the numerous environmental and meteorological factors which influence rates of nitrification and denitrification it is difficult to accurately predict the magnitude of N_2O emissions from fertiliser treatments of agricultural soils at large scales (Parkin, 1987; Zhu *et al*., 2013; Chadwick *et al*., 2014).

Emission factors are often used to estimate N_2O released as a result of nitrogen fertilisation events. Emission factors are estimated values of the percentage of total nitrogen in an applied fertiliser which is then converted into N_2O-N and released into the environment as a result of the fertilisation event. These estimates are based on past experiments in which N_2O emissions were monitored from multiple fertilisation events. These values are often highly uncertain and may only represent a certain regional area or set of meteorological circumstances (Lesschen *et al*., 2011; Skiba *et al*., 2012). The IPCC uses a simplistic N_2O emission factor of 1% of total applied nitrogen to calculate global estimate of N_2O emissions as a direct result of nitrogen fertilisation events. This value is based on numerous studies in which N_2O emissions from fertiliser events were investigated around the world (IPCC, 2007; IPCC, 2013).

Farm management practices such as tillage events can have short term and long term effects on microbial activity (Pinto *et al.*, 2004; Mutegi *et al.*, 2010). Tillage timing and method can be an important factor in controlling N_2O emissions as tillage can control the moisture content and oxygen availability of the top layer of soils. Tillage can aerate or compact the soil depending on which method is used which affects the oxygen concentration and therefore the rates of nitrification and denitrification (Bateman & Baggs, 2005). Soil conditions after tillage events may increase or decrease the emission factor of a nitrogen fertilisation event depending on the environmental conditions (Yamulki & Jarvis, 2002; Petersen *et al.*, 2008; Mutegi *et al.*, 2010).

Another growing source of anthropogenic N_2O emissions from agriculture is the rising amount of animal waste generated by livestock (Chadwick *et al*., 1999). Livestock numbers have been increasing with the rise in world population. The demand for animal products is increasing significantly in developing countries in which animal protein is still considered a relatively small part of most people's diets compared to the more developed countries. This in turn leads to larger areas of agricultural land receiving synthetic fertilisers in order to feed grazing animals, and also larger volumes of animal waste produced, both of which increase N_2O emitting microbial activity (Chadwick *et al*., 1999; Saggar, 2004; Montes *et al*., 2013).

Ruminant animals excrete between 75% and 95% of the nitrogen they ingest in the form of urine or dung (Eckard, 2010). Animal waste such as manure can be stored from barns and used as a source of organic fertiliser on agricultural fields or it can be left to decay where the animals graze. Animal droppings increase the nutrients available in soils (in the form of available nitrogen and organic carbon) for microbial processes to take place which in turn increases N_2O emissions from areas which receive animal waste. Dung heaps and slurry silos are large sources of N_2O (Chadwick *et al*., 1999; Amon *et al*., 2001; Skiba *et al*., 2006). The application timing, application method and location of manure and slurry fertilisers all contribute to the resultant N_2O emissions (Velthof *et al*., 2003; Vallejo, 2006; Chadwick *et al*., 2011).

2.8 N_2O measurement methodology

The majority of N_2O measurements and data sets that contribute to the IPCC N_2O emission inventories are obtained using the closed, non-steady-state (or "static") chamber method (e.g. Hutchinson & Mosier, 1981; Jones *et al*., 2011; de Klein & Harvey, 2013). Static chambers are simply airtight chambers that can be placed on a small area of soil (~1m^2). The chambers are cheap to make and easy to use in a variety of environments. Typically, the static chamber method requires a frame (or chamber base) which is inserted into the soil which provides a gas tight seal between the chamber and the soil. The chamber (or a lid) is then placed on top of the frame in a manner which creates an airtight seal between the interior of the chamber and the atmosphere. Draft excluding material is often fitted to create an airtight seal between the base and the top of the chambers. Once enclosed, gas concentrations within the chamber can be sampled manually via a syringe, or by an automatic sampling system. Typically two to five gas samples are sampled from the chamber at set time intervals over a sixty minute enclosure period. These samples can then be analysed by a gas chromatography (GC) instrument fitted with an electron capture detector (ECD). The flux from the enclosed area of soil is determined using Equation 2.6. Rate of change of the concentration of N_2O calculated from static chambers are often poorly

constrained due to uncertainty in regression methods applied (Pedersen *et al.*, 2010). The resolution of GC instruments also tends to be rather low (less than 1 ppb) when measuring N_2O, which can contribute to higher uncertainty in measurements.

$$F = \frac{dC}{dt_0} . \frac{\rho V}{A} \quad \text{(Eq. 2.6)}$$

Where F is gas flux from the soil (nmol m^{-2} s^{-1}), dC/dt_0 is the initial rate of change in concentration with time in nmol $mol^{-1}s^{-1}$, ρ is the density of air in mol m^{-3}, V is the volume of the chamber in m^3 and A is the ground area enclosed by the chamber in m^2.

Another form of chamber method used to measure N_2O from soils is the non-steady-state flow-through (or closed loop dynamic) chamber method. This is similar to the static chamber method; however, instead of permanently removing gas samples from the chamber, the dynamic chamber method circulates air from the chamber to an analyser and back again for a continuous analysis of mixing ratios within the chamber. The dynamic chamber method allows the use of infrared laser technology to measure N_2O concentrations instead of GC instruments (Hensen *et al.*, 2006; Laville *et al.*, 2011; Grossel *et al.*, 2014). The dynamic chamber method is able to measure N_2O fluxes with a higher precision than the static chamber method but it is limited by the logistical constraints of operation in the field, and the high cost of the instrumentation (Hensen *et al*., 2006; Hensen *et al*., 2013).

Chamber methods have several weaknesses that can result in large uncertainties when it comes to monitoring fluxes and estimating emission factors. Chamber methods which require manual measurements to be carried out are often limited in terms of the times that measurements can take place and the number of measurements that can be made over a given time period. This results in few data points which require a large amount of gap filling between measurement dates. Automated chambers are also limited in terms of how many measurements can be made, although measurements are easier to make during night using an automated setup (Smith and Dobbie, 2001). The biggest weakness of the chamber method is the inability to interpolate measurements over large scales due to the spatial variability of N_2O fluxes which can vary by several orders of magnitude over relatively short distances (several metres) (Parkin, 1987; Zhu *et al*., 2013; Chadwick *et al*., 2014). Chamber measurements are unable to represent this variability due to the small surface area of the soil covered during measurements.

An alternative method used to measure N_2O from agricultural soils is eddy covariance. Eddy covariance is micrometeorological method capable of constantly measuring integrated fluxes of N_2O from a large area (greater than 100 m^2) over a long period of time. The strength of the eddy covariance method is that it is capable of interpolating N_2O flux measurements over a large area and it is not prone to the same uncertainties caused by spatial variability that chamber measurements suffer from. The method relies on instrumentation capable of measuring gas transport by 3–D wind speed in real time and small concentration changes in the gas being monitored. The eddy covariance method measures and calculates vertical turbulent fluxes within atmospheric boundary layers. It is a statistical method which analyses high-frequency wind and scalar atmospheric data series, and yields values of fluxes of these properties. In simple terms, during conditions when a turbulent flow of wind is present the vertical flux is equal to the mean product of air density, vertical wind speed and the mixing ratio of the gas of interest (Equation 2.7). Measurements are continuous, non-destructive, non-intrusive and ideal for agricultural land such as grazed grasslands and tall arable crops. This method has been successfully applied to many fields to study N_2O fluxes. (e.g. Eugster *et al.*, 2007; Kroon *et al*., 2010; Jones *et al.*, 2011)

$$F = \overline{\rho_{aws}} \qquad \text{(Eq. 2.7)}$$

Where F is the vertical flux, ρ_a is mean product of air density, w is the mean product of vertical wind speed and s is the mean product of mixing ratio of the gas of interest.

The eddy covariance method still has a number of limitations. Practical problems encountered when measuring N_2O fluxes include dealing with the effects of heat and water vapour, damping of gas concentrations by sampling tubes and correct alignment of the sonic anemometer (Denmead, 2008). Eddy covariance measurements do not account for spatial variability and do not observe hot spots of emissions in the area that is measured. The equipment used for eddy covariance requires a flat canopy and in some cases can require a large constant power supply (mains power or generator). There are corrections that can be applied to account for terrain that is not flat, although this complicates the data processing significantly. Measurements of particular areas also rely on wind direction leaving experiments open to distortion from weather conditions. All of these factors can make eddy covariance more complicated; however, it is still considered the most practical and accurate way to measure N_2O fluxes from a large homogeneous area.

There has been some research into how chamber and micrometeorological techniques compare (Christensen *et al.*, 1996; Laville *et al.*, 1999; Jones *et al.*, 2011). There is usually some disagreement between results from the different techniques due to the nature of the measurements. Chamber methods will pick up on some high emission peaks and some very low ones. The flux estimates obtained chamber methods will depend very much on the locations of the measurements. The eddy covariance technique may give a more accurate integrated flux value for the area being investigated over a given time; however, it will provide little spatial information on where emissions have been high or low. Data gathered using the eddy covariance method will also depend heavily on wind speed and direction as these factors will determine the footprint area of the measured flux.

2.9 N_2O models and inventories

N_2O released due to agricultural activities on a large scale is very difficult to predict due to the large number of poorly constrained variables which influence the microbial processes responsible for N_2O fluxes. N_2O emissions and rates of flux from the processes of nitrification and denitrification still remain poorly understood due to the numerous factors which influence emissions from soils. The high spatial and temporal variability of N_2O emissions from soils and the limited number of data points made available through flux measurement methods, often with high uncertainty, also prevent accurate emission estimates in many cases. The large variety of soil types, environmental conditions and farm management methods make scaling up to national or global scales very difficult without having to make many large assumptions.

The IPCC introduced the concept of 'tiered reporting' for greenhouse gases and other pollutants in 2006. Tiers represent a level of complexity in a particular set of activity data or emission estimates made using models or emission factors. In the case of N_2O, the most basic emission estimates which use data on a global or national scale are classed as Tier 1. An example of a Tier 1 emission estimate is the use of a 1% emission factor of N_2O-N released from nitrogen fertiliser which is applied to estimate N_2O emissions from agricultural fertiliser applications on a global scale. Tier 2 is more complex than Tier 1 and requires an element of local or regional data. Tier 2 emission estimates may be based entirely on measurements made in a specific country or regional scale. An example of a Tier 2 emission estimate would be a relationship described between N_2O flux measurements, soil type and rainfall. Using this data, localised emission estimates can be made on a finer resolution than a Tier 1 approach would allow. Tier 2 emission estimates are required for more accurate national GHG accounting which is becoming increasingly important as governments try to reach emission reduction

targets. Tier 3 reporting is the most complex and requires the most specific data sets. Tier 3 emission estimates require multiple measurements of various properties which would contribute to estimating N_2O flux. An example of a Tier 3 estimate would be the use of a process based model which requires many soil measurements and meteorological data to predict flux on a daily basis from a particular soil type or field. Currently Tier 3 reporting for N_2O is rarely applied due to the complexity required and the limitations in N_2O measurement methodology.

Several methods are currently used to estimate N_2O emissions on a global scale despite significant limitations which arise from missing data. A top down approach can be used as an estimate of global anthropogenic emissions of N_2O (Crutzen *et al.*, 2008). This method requires measurements of changes in the global concentrations of N_2O in the atmosphere and the rate of sinks of N_2O on a global scale. Based on these measurements an emission factor for anthropogenic sources of N_2O can be estimated using pre-industrial estimates of annual emissions of approximately 10.2 Tg N_2O-N as a background level. This background estimate is obtained from ice core measurements of N_2O which date long before the industrial revolution in the 18^{th} century. Taking better defined measurements into account such as N_2O emissions due to fossil fuel combustion and industrial activities an emission factor for reactive nitrogen applied in to agricultural soils can be estimated. This method estimates that three to five percent of additional nitrogen added to soils is eventually converted into N_2O (Crutzen, 2008). The strength of this method is that it does not rely on flux measurements which suffer from spatial and temporal variability; however, this is also a weakness as it provides no spatial information on specific sources of N_2O or how to mitigate these emissions.

A bottom up approach is far more complicated as many sources have to be considered separately. To estimate N_2O flux using a bottom up approach each known source of N_2O must be assigned an associated emission factor based on past measurements. Multiple experiments from different soil types and climates around the world can provide an estimate of these emission factors which account for a wide range of environments and conditions. Emission factors are also calculated for significant N_2O flux events such as nitrogen applications (IPCC, 2007; Lesschen *et al*., 2011; Skiba *et al*., 2012). N_2O flux estimates can be calculated at the plot, field, national or global scales using the relevant emission factors so long as information on agricultural management is available in these areas. The strengths of using a Tier 2 rather than Tier 1 bottom up approach is that it allows a more detailed regional analysis of the sources of N_2O from different areas, thus allowing policy makers to focus mitigation strategies on sources that contribute most significantly to N_2O emissions. The weakness of the

method is that the emission factors can have large uncertainties associated with them that may propagate significantly depending on scale.

Several computer simulation models have been created to assist in N_2O emission estimates which also use a bottom up approach. The two most commonly used biogeochemical simulators require soil property inputs to predict emissions of carbon and nitrogen compounds produced through microbial processes in agricultural soils. The two most commonly used models for estimating N_2O emissions are DNDC (Denitrification-Decomposition) and daily DAYCENT (Del Grosso *et al*., 2006; Giltrap *et al*., 2010). These models require inputs of soil properties such as nitrogen and carbon stocks, pH, soil type, management practices and crop type. These properties are combined with meteorological measurements such as temperature and rainfall to predict microbial activity and the rates at which soils release GHGs into the atmosphere. The models use a mixture of emission factors and known biogeochemical pathways to estimate how soils will react to certain conditions over a given period of time. These models have been generated through years of soil measurements and experiments including measurements of gas fluxes using various methodologies. Advantages of using biogeochemical models is that they provide long term flux estimates which factor in a large variety of variables in the soil. Currently the major weakness of these models is that estimates of N_2O fluxes are often far from actual flux measurements made at field sites. Although agreement is observed in some cases there is still a lot of uncertainty in these models which prevent them being used confidently at large scales.

2.10 Uncertainties in N_2O flux measurements

Currently measurements, estimates and models of N_2O fluxes all have very large uncertainties associated with them. Large uncertainties in N_2O fluxes often prevent effective research into mitigation strategies as conclusive results are difficult to reach between research groups. Creating national or global inventories is also difficult due to the many large uncertainties involved. The IPCC currently estimates that approximately 17.9 TgN yr^{-1} of N_2O is released into the atmosphere every year; however, due to experimentation and modelling uncertainties it is estimated that the true annual value of N_2O released on a year to year basis could lie anywhere between 8.1 to 30.7 TgN yr^{-1} (an uncertainty greater than 50%) (IPCC, 2013).

There are a variety of reasons for large uncertainties in N_2O estimates. One of the most significant is the lack of data recorded at a global level. Many terrestrial and aquatic sources are yet to be characterised for N_2O emissions and many assumptions are made in estimating emissions from these areas when global estimates

are made. A lack of research carried out at a global scale also means that even the most basic of soil maps for many wide ranging environments are unavailable for modelling purposes. A lack of sufficient meteorological data recorded from many of these areas is also a limiting factor for modellers. Without basic data sets from which to base assumptions or compare measurements there is little that can be done to improve emission estimates from these areas without the need for further research.

The limitations of simplistic measurement methods used to make flux measurements from soils are also a cause for uncertainties in N_2O emission estimates. The static chamber method has many large uncertainties associated with it including low instrument resolution and poorly defined regression estimates (Kroon *et al.*, 2008; Pedersen *et al.*, 2010; Parkin *et al.*, 2012). Chamber methodology coupled with a lack of a clear understanding of what causes the large spatial variability in N_2O emissions from soils prevent effective interpolation of fluxes over a large scale. Without an effective measurement strategy any estimate of N_2O will be subject to these errors which can be an order of magnitude larger than the reported flux. The precision of eddy covariance flux measurements of N_2O have also been limited in the past due to instrumental resolution. Eddy covariance is a complicated statistical method with large room for error. Temperamental instruments requiring a daily input of liquid nitrogen coolant combined with fragile lasers with high sensitivity to temperature and electrical noise are prone to reporting fluxes with high uncertainties.

Uncertainties in instrumental detection limits and the inability to realistically determine precise values for these limits can cause controversy between researchers. Many experiments report negative fluxes of N_2O in soil measurements (Ryden, 1981; Papen *et al*., 2001; Butterbach-Bahl *et al*., 2002; Flechard *et al*., 2005). There is some controversy into whether this observation is a measurement of real uptake of N_2O in soils or if it is an artefact of measurement methodology (Chapuis-Lardy *et al*., 2007). Negative fluxes often fall within the uncertainty range of the instruments used to measure N_2O; however, this is not always the case and it is believed that denitrification in soils can reduce atmospheric N_2O to N_2 (Okereke, 1993; Davidson et al., 2000). It is possible that the observations are a mixture of both and care should be taken when negative fluxes are measured.

2.11 INVEN$_2$ORY project

The research carried out in this thesis contributed to the *InveN$_2$Ory* project which is part of the Agricultural UK Greenhouse Gas Platform (See www.GHGPlatform.org.uk). The Agricultural Greenhouse Gas Research Platform is a research programme funded by DEFRA (Department for Environment, Food and Rural Affairs)

and the devolved administration governments. The *InveN_2Ory* project seeks to improve the accuracy and resolution of N_2O emission estimates from agricultural sources across the UK, which will provide the evidence for a UK specific method of calculating nitrous oxide emissions on a national scale. This thesis contains scientific developments which contribute to Work Package 5 (WP5) of the *InveN_2Ory* project. WP5 focuses on the verification of measured and modelled emissions of N_2O which occur at a range of temporal and spatial scales.

This study aimed to:

a) improve N_2O flux measurement methodology to provide an N_2O chamber flux methodology with lower uncertainty than previous methods allowed
b) investigate and identify the causes of spatial variability in N_2O flux measurements caused by agricultural activities at the plot, field and farm scales
c) create a farm scale inventory of N_2O for a typical Scottish livestock farm using on site measurements.

Chapter 3

Materials and methods

3.1 Field sites

This thesis contains several studies investigating measurements of N_2O flux from agricultural soils in the UK which were carried out between summer 2011 to summer 2013. The majority of these measurements were carried out at Easter Bush Farm Estate near Penicuik (Scotland) (55° 51' 55.7036"N, 3° 12' 44.3549"W). Easter Bush Farm Estate is a combination of several university run farms which are owned by both the Scotland's Rural College (SRUC) and the University of Edinburgh (UoE) and are run for commercial and research purposes. The estate covers over 1000 ha of land which consists of a mixture of intensively managed arable and pasture grassland fields and hill ranges in which animals can roam and graze freely (Figure 3.1). Arable fields at the farm are primarily used to grow barley and silage grass for animal feed, although occasionally oil seed rape and other crops are grown either for commercial or research purposes. The estate provided for approximately 1600 ewes and 300 cattle during the measurement period according to farm records. The livestock at the estate are primarily bred as a source of meat and no dairy production occurs at any of the farms.

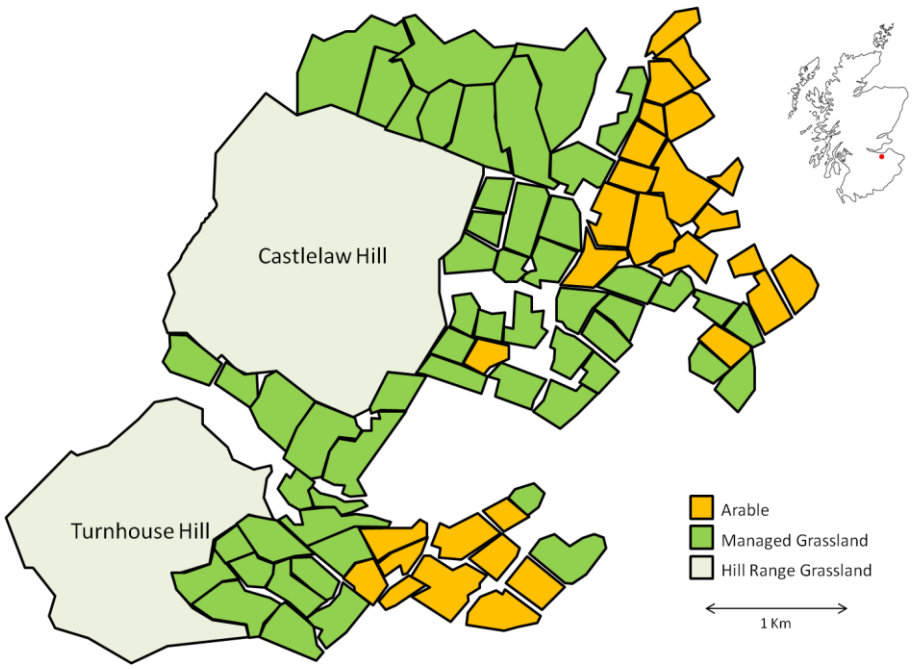

Figure 3.1 Field outlines and overview of Easter Bush Farm Estate near Penicuik (Scotland). The combination of several small farm areas consists of primarily grazing and arable fields which contribute to feeding the large number of livestock within the estate.

Easter Bush Farm Estate is situated at approximately 200 m above sea level near the South East foot of the Pentland Hills Regional Park. A permanent weather monitoring station (run by the Centre for Ecology and Hydrology) records local meteorological data for the farm area. Trends in annual temperature recorded at the monitoring station were fairly consistent over the 2 year measurement period at the site (Figure 3.2). Mean daily temperatures at the estate varied from slightly negative values in winter to above 15 ˚C in summer. Daily temperatures recorded were considered typical for the year in which measurements took place. Seasonal temperature changes at the farm estate have been fairly consistent throughout the past 10 years (Figure 3.3b). The annual precipitation recorded for the estate over the past 10 years is 921 mm (SD ± 201 mm) (Figure 3.3a). During 2012, annual precipitation was significantly larger than that of 2011 and 2013. The estate received a lot more rainfall during spring and summer months during 2012 than it had done in previous years (See Figure 3.2). All meteorological data was recorded by staff from the Centre for Ecology and Hydrology (Edinburgh) at the Easter Bush meteorological monitoring station.

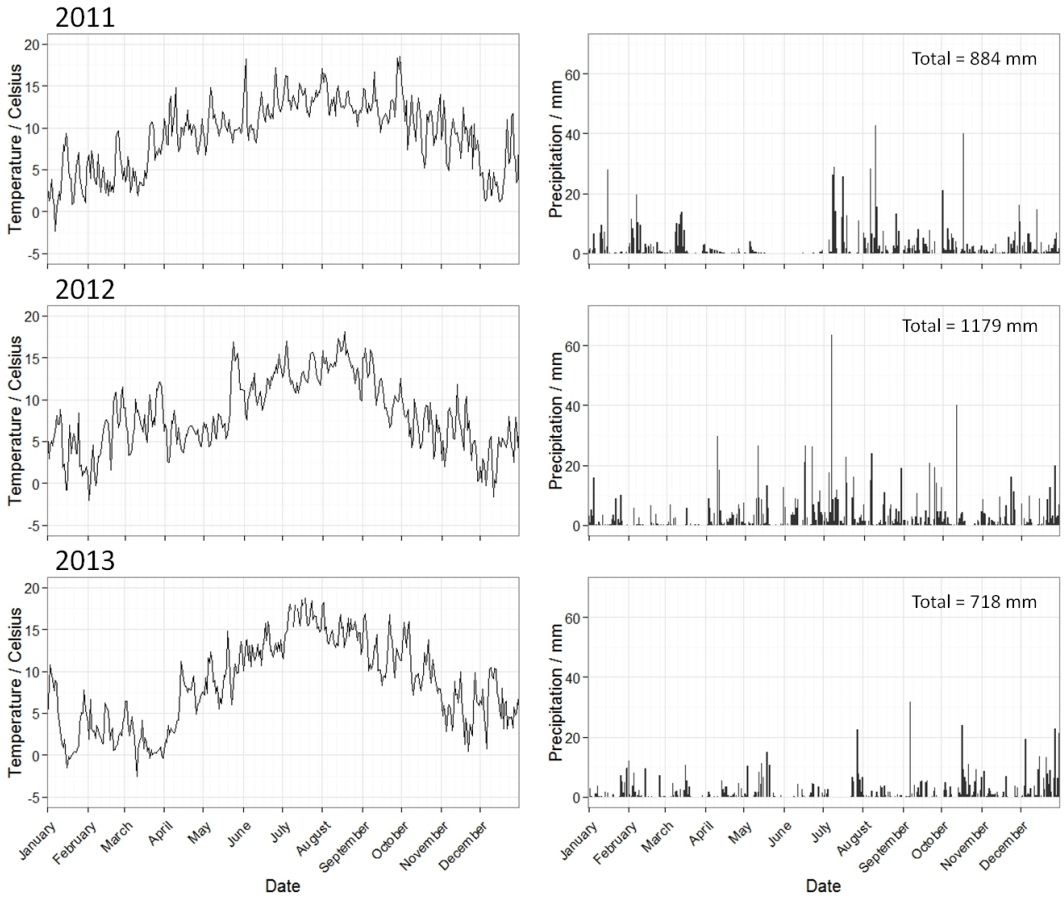

Figure 3.2 Average daily temperatures and daily precipitation values as recorded by the Easter Bush permanent meteorological monitoring station for the years 2011 to 2013.

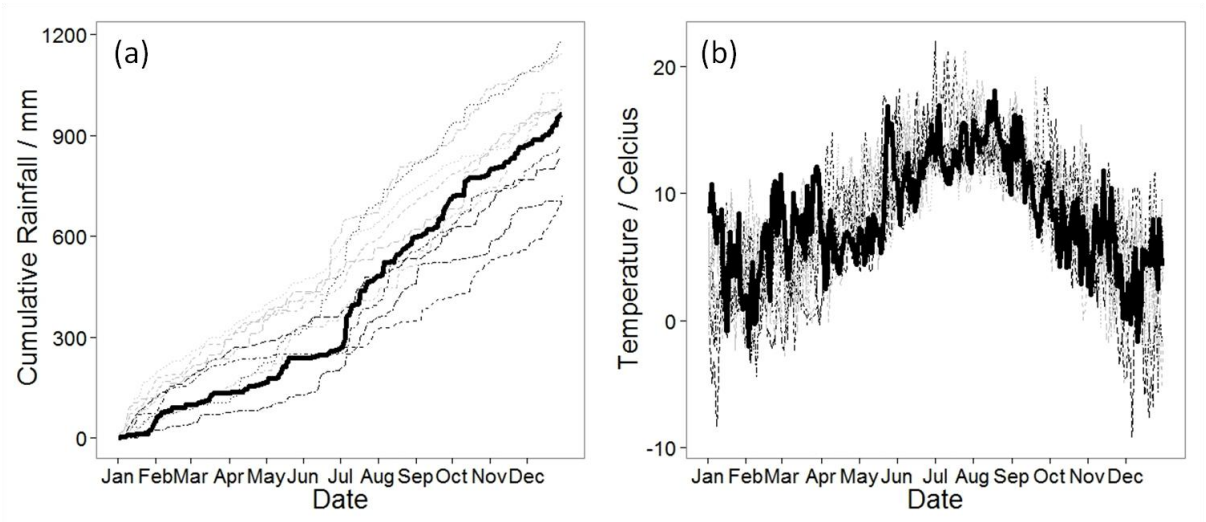

Figure 3.3 (a) Cumulative annual rainfall and (b) daily average temperature were plotted for the past 10 years of meteorological measurements recorded at the Easter Bush Estate. The period where most measurements were made between the summer of 2012 and autumn of 2013 is represented with a solid black line in both figures.

Flux measurements were also made at two other UK locations. This work was carried out to verify flux measurement methodologies in a national project (InveN_2Ory; http://www.ghgplatform.org.uk/) (See Chapter 4). Firstly, measurements were made at an SRUC field site in Dumfries (SW Scotland) in October 2012. The field site was a silage grass field with sandy loam soil texture which had recently been used to graze cattle. The measurement area consisted of 15 individual 8 m^2 plots which had received various fertiliser treatments. The fertiliser treatments used at this site were synthetic urine, cattle urine, cattle urine mixed with dicyandiamide (DCD) and cattle dung. A similar set of measurements were also carried out in March 2013 in Rosemaund (near Hereford, West England). This field site was set up in an arable winter wheat field with silty clay loam soil texture and was managed by the agricultural development advisory service (ADAS). During this experiment plots were fertilised with cattle slurry (applied via surface broadcast), cattle slurry (applied via trailing hose), layer manure (top dressed) and broiler litter (For further information see Chapters 4 and 8).

3.2 Quantum Cascade Laser

A quantum cascade laser (QCL) rapid gas analyser (CW-QC-TILDAS-76-CS, Aerodyne Research Inc., Billerica, MA, USA) was used to measure N_2O during my research (Figure 3.4). The QCL is capable of measuring atmospheric gas concentrations using tuneable infrared differential absorption spectroscopy (Zahniser *et al.*, 2009) at a rate of 20 Hz (typically used for eddy covariance measurements). The gases

measured by the instrument are determined by the specific laser diode fitted. The diodes are exchangeable between the instruments (blue box, Figure 3.4) and different diodes operate at different temperatures. The diode used in the work described in this thesis could measure CO_2 (2242.90 cm^{-1}), N_2O (2242.45 cm^{-1}) and H_2O (2242.73 cm^{-1}) at an operating temperature of between -23 to -26 ˚C. The temperature of the laser was regulated by a thermoelectric peltier cooler which automatically adjusted temperature to keep the laser stable. In order to help the peltier temperature remain stable, a solid-state cooling system was used to keep the internal insulated area of the instrument at a constant temperature of 10 ˚C by circulating a cooled solution of water and ethanol (20%) through a sealed closed loop system of tubing tubing within the instrument (Figure 3.4).

The QCL instrument uses, with a 0.5-litre multi-pass absorption cell, with an optical path length of 76 metres (Figure 3.4). The cell was kept at a constant low pressure (approximately 6 kPa / 45 Torr) using a dry-scroll vacuum pump which pumped a constant flow of air through the sample cell. An infra-red laser is emitted from the laser diode when a small voltage is applied. This laser is reflected through several mirrors into the absorption cell then out of the cell and into an infrared detector. The inlet of the QCL was fitted with a manual ball valve and a needle valve to control the air flow rate and cell pressure, as well as a safety valve attached to the pump to prevent back-flow. A 0.45 µm particle filter was attached to the inlet of the absorption cell to avoid particulates damaging the fragile mirrors inside the sample cell.

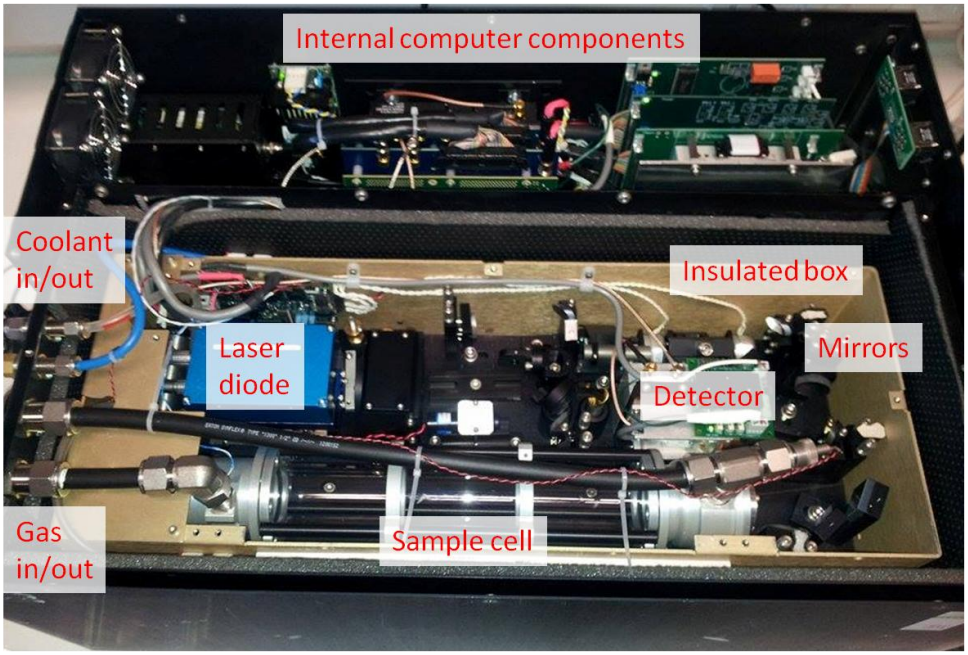

Figure 3.4 An internal photograph of the compact continuous wave quantum cascade laser used in this thesis (CW-QC-TILDAS-76-CS, Aerodyne Research Inc).

3.3 Dynamic chamber method

The dynamic chamber flux measurement method was developed as a primary aim of this thesis (See Chapter 4). The initial design of the method was based on the fast box method outlined in Hensen *et al*., 2006 in which a twin diode laser (TDL) measured CH_4 and N_2O mixing ratios at a frequency of 2 Hz from a chamber (See Figure 3.5a). Air flow was circulated by a vacuum pump between the TDL and chamber with a flow rate of 4 l min^{-1} in a closed loop. This method was adapted for use with a modern QCL instrument which worked similarly in principle to the TDL analyser, but was more robust, did not require liquid nitrogen coolant and could provide a higher measurement precision (30 pmol mol^{-1} compared with the 5 nmol mol^{-1}).

A chamber was designed using a static chamber base. These bases were made by cutting 22 cm sections of a 38 cm diameter PVC drainpipe. Flanges were attached at both ends of the chamber base. An aluminium lid was attached to the top of the chamber base permanently using epoxy resin and silica sealant. A 1 cm layer of closed cell neoprene sponge was fitted around the bottom flange. The chamber was fitted with an internal fan (3000 rpm, Delta Electronics Inc., Taipei, Taiwan) and air temperature probe (CS109, Campbell Scientific, Logan, UT, USA). A pressure sensor (CS100, Campbell Scientific, UT, USA) fitted to the lid of the chamber measured the internal air pressure. All fittings on the lid of the chamber were sealed with silicone sealant to avoid gas leakage (See Figure 3.5b).

Steel cutting rings were made which had similar PVC flanges attached as the chamber. These could be inserted into to soil (on average 5 cm) to form an airtight seal (See Figure 3.5c). During measurements the chamber was placed on these rings. The neoprene sponge formed an airtight seal between the cutting ring and the chamber. Rings were inserted into the soil several minutes before measurements were taken. The rings could be inserted relatively easily into wet soils. On hard surfaces the rings could be stamped into the ground taking care not to break the plastic flange.

Two 30 m lengths of 9.5 mm ID Tygon® tubing were attached to both the inlet of the QCL and the outlet of a dry-scroll vacuum pump (SH-110, Varian Vacuum Technologies, Lexington MA, USA). This provided a 30 m radius from the QCL in which the chamber could be placed. A flow rate of approximately 6 to 7 L min^{-1} was used between the QCL and the chamber. During the development phase and fixed location measurements the instruments were powered by a mains power supply. During field measurements the instrumentation was secured inside a four wheel drive vehicle to allow for mobile measurements around the farm estate which was powered by a diesel generator kept on a tow trailer (See Figure 3.5d).

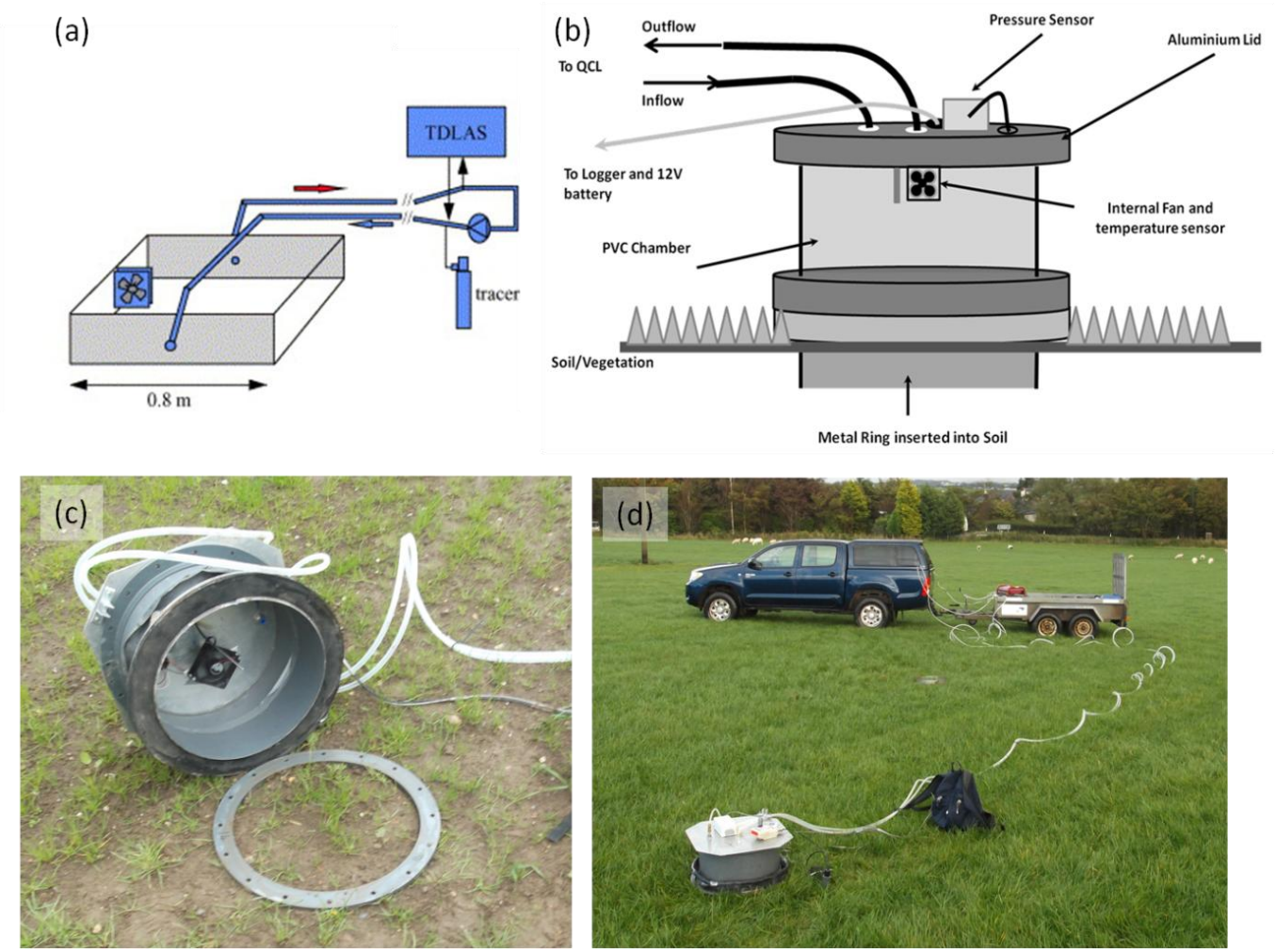

Figure 3.5 (a) The setup of the fast box method as described in Hensen *et al*., 2006. (b) Schematic of the dynamic chamber design used in this thesis (as described in Chapter 4). (c) Steel cutting rings were inserted into the soil prior to dynamic chamber measurements. The dynamic chamber was placed on top of these rings during enclosure periods. (d) The instrumentation required to run the dynamic chamber method could be mounted on an off-road vehicle and powered by a diesel generator for mobile measurements.

3.4 Static chamber method

The static chamber method was used during a verification of the dynamic chamber method and was not used to quantify fluxes from any of the agricultural sources reported in this thesis (See Chapter 4). Static chamber measurements were carried at the Dumfries field site by SRUC research staff. These results are presented in Chapter 4.

The methodology used at the Dumfries field site is outlined in Chadwick *et al*., 2014. Chamber bases were inserted into the soil which extended approximately 15 to 20 cm from the soil surface. The chambers were circular with the same diameter as the dynamic chamber design. The chambers were non-vented and they did not contain fans. Aluminium lids lined with draught excluding material were placed on top of the chamber bases creating an airtight seal and were held in place using four strong clips. The chamber lids contained a three way sealed tap from which a gas sample from within the chamber could be drawn.

Only one sample was taken from the chamber forty minutes after enclosure. Gas samples were removed using a 20 ml syringe and injected into 20 ml pre-evacuated vials. All of the samples were analysed on a 7890A GC System fitted with an ECD and FID detector (Agilent Technologies, CA, USA). Ten measurements of atmospheric concentrations of N_2O were made on days which the chambers were sampled. This provided a mean background concentration for the day. Using a linear fit between the background concentration and the measured concentration from within the chamber dc/dt was calculated for each chamber measurement. Using the chamber volume, cross-sectional area coverage, and atmospheric air pressure and temperature, flux was calculated using Equation 2.6.

Static chamber measurements were usually carried out by SRUC staff in the morning between 10:00 to 12:00. During the verification experiment the dynamic chamber was used to measure fluxes from each of the chamber bases directly. This was possible as the flange of the dynamic chamber was the same diameter as that of the chamber bases used by SRUC. The dynamic chamber fit on top of the chamber base from which a flux measurement could be made in a similar manner as would be done from the steel cutting rings (See Figure 3.6). The total volume of the dynamic chamber and chamber base were taken into account for flux calculations.

Figure 3.6 The dynamic chamber was placed on top of static chamber bases at the Dumfries field site to verify static chamber flux measurements. The rubber flap was rolled down prior to measurements to avoid wind penetration of the neoprene sponge seal.

3.5 Soil measurements

After flux measurements made during the project a variety of soil properties were often measured. Soil temperature was recorded on-site using a temperature probe (ETI Ltd, Worthing, UK) which was inserted approximately 5 to 10 cm into the soil. Volumetric water content of the soil was also measured on-site using a portable hand held moisture meter (HH2, Delta-T, Cambridge, UK). Typically three volumetric water content measurements were made from each measurement location and a mean value was calculated. Two types of soil samples were also often collected during fieldwork, usually immediately after a flux measurement was complete. A 5 cm deep 'wet' soil sample was collected using a 2 cm wide corer which was inserted into a sealable plastic bag. The samples were kept in a cool box and put into frozen storage (-18 ˚C) after measurements were complete (within six hours of sampling). Bulk density soil samples were taken using a sharp metal cutting cylinder (7.4 cm diameter, 5 cm deep) which was carefully hammered into undisturbed soil. This provided an undisturbed soil sample with a known volume from which the soil density (bulk density) could be measured. These soils were also stored in sealable plastic bags, but were not required to be frozen, as chemical analysis was not carried out on the samples. Samples were kept refrigerated (below 5 ˚C) over a short period (less than a week) before oven drying.

Wet soil samples were defrosted in a refrigerated room (5 ˚C) over night prior to analysis. The pH of the soil samples were measured using the method outlined in Rowell, 1994. 10 g of air dried soil was placed in a small plastic cup. 20 ml of deionised H_2O was added to the soil and the mixture was shaken and left for 60 minutes. A pH meter (MP220, Mettler Toledo, Columbus, Ohio, USA) was used to measure pH in the soil solution.

NH_4^+ and NO_3^- were extracted from the wet soil samples using KCl extraction as outlined in Rowell, 1994 (p 226). Soil (15 g) was added to a flask and mixed with 50 ml of 1 mol L^{-1} KCl solution. The solution was shaken automatically using an orbital shaker for 60 minutes. The mixture was filtered using 2.5 µm filter paper (Fisherbrand, Hampton, New Hampshire, USA) and the solution was stored and frozen in 20 ml sterilised plastic vials. Concentrations of NH_4^+ and NO_3^- were measured using a Bran and Luebbe AutoAnalyser (SPX Flow Technology, Norderstedt, Germany). Available nitrogen content in the soils was calculated using Equation 3.1.

$$N = \frac{C \times V}{m} \quad \text{(Eq. 3.1)}$$

Where N is the mass of nitrogen in the form of NH_4^+ or NO_3^- in mg (per g of dry soil), C is the concentration of NH_4^+ or NO_3^- measured in the analysis of KCl extract in mg L^{-1}, V is the volume of solution in which the soil sample was mixed with KCl in L, and m is the mass of dry soil mixed with the KCl solution in g.

Separate soil samples used to measure bulk density were also taken immediately after the flux measurement using a sharp metal cutting cylinder (7.4 cm diameter, 5 cm deep) which was carefully hammered into undisturbed soil. These samples were used to calculate soil moisture content (via oven drying at 100 ˚C) which also provided the dry soil mass. Bulk density was calculated by dividing the volume of the cutting ring by the mass of dry soil. A sub sample of the dried soils was taken to be ground (via ball milling) for elemental analysis of total carbon and nitrogen content of the soil (vario EL cube, Elemaentar, Hanau, Germany). WFPS was calculated from the bulk density soil samples as described in Rowell, 1994 (See Equation 3.2).

$$WFPS = \frac{V_{cont} \times 100}{1 - \left(\frac{r_b}{r_d}\right)} \quad \text{(Eq. 3.2)}$$

Where WFPS is the percentage of porous volume in the soil filled by water, V_{cont} is the volumetric water content of the soil, r_b is the bulk density of the soil in g cm^{-3} and r_d is the particle density of the soil (assumed as 2.65 g cm^{-3}) (Rowell, 1994).

3.6 Statistical analysis

3.6.1 HMR regression package

The N_2O mixing ratio measurements recorded by the dynamic chamber method required the application of a linear or non-linear regression fitting to calculate flux from the soil surface. To optimise data handling and processing time, these calculations were carried out using the HMR package, a freely available package for the statistical software R (Pedersen *et al.*, 2010). Originally designed to be used with static chamber measurements, the HMR package calculates both linear and non-linear fitting parameters for a set of mixing ratio measurements. The non-linear regression uses the HM (Hutchinson & Mosier, 1981) method to calculate flux at t= 0. The package presents the data for each chamber enclosure with the relevant regression fitting parameters (Figure 3.7). The package can recomend a particular fit, but the option remains for the user to make a judgment based on visual inspection (Figure 3.7). This method was used throughout the thesis to calculate flux from dynamic chamber measurerments. The majority of the three minute measurements (>90%) fit linear regression best, although the difference between linear and non-linear regression estimates during a three minute enclosure time is usually minimal (See Figure 3.7).

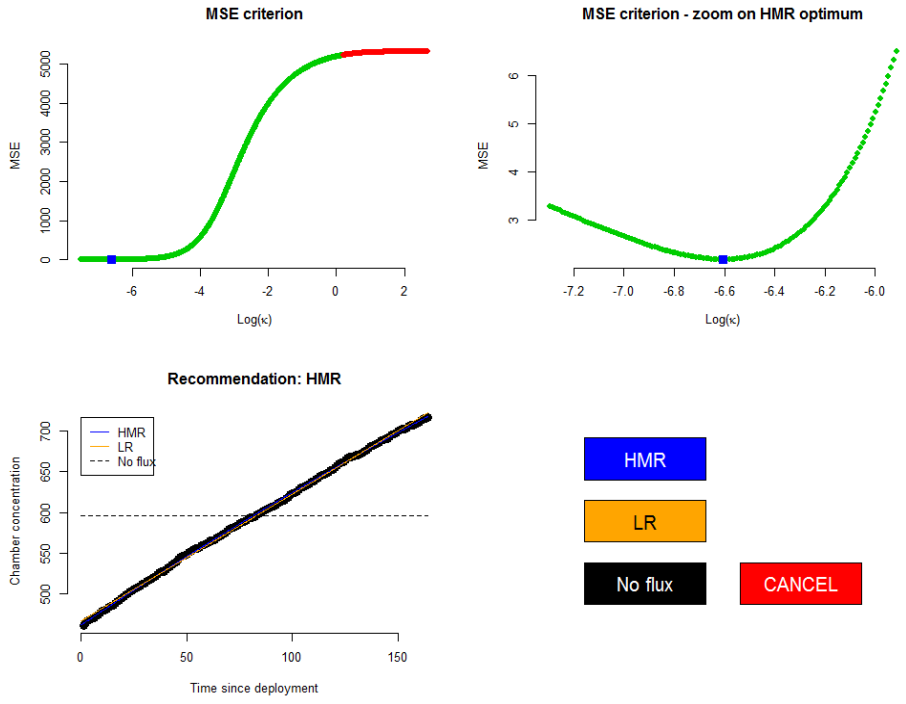

Figure 3.7 The HMR package allows users to investigate the fitting parameters of linear and non-linear regression for each chamber measurement. The package requests that users make a decision of best fit for each measurement based on the observations.

3.6.2 Data distribution

The normality of data is examined throughout the thesis and displayed in some cases using distribution plots. N_2O fluxes measured from agricultural soils throughout the thesis consistently follow a log or $\log_{10}$ distribution which is referred to as geometric in the text (See Chapters 7 & 8). Comparisons of arithmetic and geometric data analysis are made throughout the thesis as both are commonly used in N_2O literature. The geometric mean of a data set is simply the mean of the log values of the measurements which is then converted back to a real value. The geometric mean is similar in magnitude to a median value which is sometimes used to describe N_2O measurements in literature due to the large spatial variability of flux measurements. A geometric distribution of measurement data is also observed in some soil measurements such as available NH_4^+ and NO_3^-. The geometric mean values of these measurements can be used in multiple linear regression models in place of more commonly used arithmetic values which may provide better correlation between variables.

3.6.3 Multiple linear regression

Multiple linear regression is carried out in several of the chapters of this thesis. Multiple linear regression attempts to model the relationship between multiple explanatory variables and a response variable by fitting a linear equation to observed data. This method is primarily used in the thesis to investigate correlation between soil properties and N_2O flux. As soil measurements were often made from the same location that flux was measured, a direct comparison between the results was possible in most cases. Multiple linear regression was run using the basic 'stat' package available on statistical software R. The 'lm' fitting function available in the package can be used to carry out regression, single stratum analysis of variance and analysis of covariance. The basic summary output for the regression is shown in the text (See Tables 6.2, 7.5 & 8.2)

3.6.4 Local polynomial regression fitting

The majority of measurements presented in this thesis have a degree of spatial variability associated with them and interpolation is carried out using various methods. One method used to visualise measurements on a 2D plot is local polynomial regression fitting. The LOESS (Local regESSion) method combines multiple regression models to interpolate measurement data between points. The method combines a mixture of linear and non-linear (polynomial) regression to fit simple localized models to measurement data. As N_2O spatial variability is often unpredictable the method is better at providing a qualitative than quantitative interpolation; however it

does allow some spatial patterns to be observed (See Figures 5.7 & 9.2). The 'loess' function was run using the basic 'stat' package available on statistical software R.

3.7 Quality control of measurements

Quality control of flux measurements was managed in a variety of ways. The high frequency mixing ratio measurements recorded using the dynamic chamber method revealed spikes in measurement data by simple visual inspection in most cases. Large spikes in measurements were usually the result of pressure changes caused by kinking of tubing during measurements but could also be caused by contamination or a soil disturbance near a measurement location. These spikes could increase gas concentration measurements up to thousands of ppb; however, they were often short lived and most problems in gas measurements could be witnessed immediately while the sampling was underway. A repetition of the measurement could be made in these cases and therefore data was rarely lost due to these issues.

Flux regression calculations were made on a case to case basis in which the rate of change of concentration within each chamber was examined in detail (See Section 3.6.1). Using the HMR method the fitting parameters of each flux can be examined in detail which can be used to identify if a measurement has failed in some way. Leaks in the closed loop system were the only common cause of discarded measurements. These could be identified by increased noise and sharp decreases in concentration measurements during an enclosure period (See Chapter 4). CO_2 measurements were the best indicator of any leakage or contamination during enclosure periods due to the high atmospheric concentrations. Using the HMR method it was usually obvious if a measurement had failed as interference was easy to identify visually due to the high frequency of measurement points and high precision of the gas analyser.

Quality control of soil measurements was more difficult due to the heterogeneous nature of the soils and the wide range of conditions present in agricultural soils. It can be uncertain whether a particularly high or low outlier measurement of available nitrogen or carbon content is a true value in some cases. Generally measurements fell within a consistent range and those that did not were reanalysed when possible. Any data that was discarded during the thesis tended to be due to problems with lab analysis (NH_4^+ contamination in filter papers) or instrumental calibration (pH meter). This occurrence was rare and could usually be identified by testing known standards. When possible, samples were reanalysed to fill missing data.

Chapter 4

An improved method for measuring soil N_2O fluxes using a quantum cascade laser with a dynamic chamber

Summary

A dynamic chamber method was developed to measure fluxes of N_2O from soils with greater accuracy than previously possible, through the use of a quantum cascade laser (QCL). The dynamic method was compared with the conventional static chamber method, where samples are analysed subsequently on a gas chromatograph. Results suggest that the dynamic method is capable of measuring soil N_2O fluxes with an uncertainty of typically less than 1–2 μg N_2O-N m^{-2} $hour^{-1}$ (0.24–0.48 g N_2O-N ha^{-1} day^{-1}), much less than the conventional static chamber method, because of the greater precision and temporal resolution of the QCL. The continuous record of N_2O and CO_2 concentration at 1 Hz during chamber closure provides an insight into the effects that enclosure time and the use of different regression methods may introduce when employed with static chamber systems similar in design. Results suggest that long enclosure times can contribute significantly to uncertainty in chamber flux measurements. Nonlinear models are less influenced by effects of long enclosure time, but even these do not always adequately describe the observed concentrations when enclosure time exceeds 10 minutes, especially with large fluxes.

Work presented in this chapter is based on the manuscript published as: Cowan, N. J., Famulari, D., Levy, P. E., Anderson, M., Bell, M. J., Rees, R. M., Reay, D. S., and Skiba, U. M.: An improved method for measuring soil N_2O fluxes using a quantum cascade laser with a dynamic chamber, European Journal of Soil Science, 65, 643-652, 2014

4.1 Introduction

Nitrous oxide (N_2O) is a potent greenhouse gas (GHG) and the single largest contributor to global stratospheric ozone depletion (Ravishankara *et al.*, 2009). The majority of N_2O is released into the atmosphere by the natural microbial processes of nitrification and denitrification (e.g. Davidson *et al.*, 2000), but human activities (such as the wide scale use of nitrogen fertilizers) have resulted in a significant increase in global N_2O emissions since pre-industrial times (IPCC, 2007). Global N_2O fluxes have large uncertainties associated with them (55–75%) (IPCC, 2007) because of the large temporal and spatial variability of N_2O fluxes, and the uncertainty inherent in the methodology predominantly used to measure them (Folorunso & Rolston, 1985; Velthof *et al.*, 1996).

Almost all measurements use the closed, non-steady-state (or 'static') chamber method (Hutchinson & Mosier, 1981), because of its simplicity and small cost (de Klein & Harvey, 2013). In this method, gas samples are extracted from a chamber sealed on the soil surface during a 30–60 minute incubation period, and later analysed using a gas chromatograph (GC) instrument. The flux is inferred from the rate of change in gas concentration within the chamber. Because of the constraints imposed by the logistics of extracting samples and subsequent laboratory analysis, the sample size is typically limited to 2–4 samples per chamber closure. Consequently the fluxes calculated by any regression model are poorly constrained (Pedersen *et al.*, 2010). Furthermore, data can be noisy, and it is not always clear which regression model is the most appropriate for fitting to the data (Levy *et al.*, 2011). The resolution of GC instruments tends to be poor (>10 nmol mol^{-1} for N_2O), meaning that small fluxes may not be clearly detectable.

Previous attempts to improve the precision of N_2O flux measurements, using infrared spectroscopy to measure concentration changes of N_2O within chambers, were limited by the poor resolution of the instruments available (Yamulki & Jarvis, 1999; Laville *et al.*, 2011), the logistical constraints of operation, and cost (Hensen *et al.*, 2006; Hensen *et al.*, 2013). However, advances in infrared laser technology have recently produced fast-response (> 10 Hz) N_2O analysers with improved sensitivity (< 5 nmol mol^{-1}), capable of operating in the field (Laville *et al.*, 1999; Jones *et al.*, 2011). In this study, we used a commercially-available infrared continuous wave quantum cascade laser (QCL) with a resolution of 30 pmol mol^{-1}. Pulsed QCL instruments (resolution of 1.5 nmol mol^{-1}) have been used successfully to measure N_2O fluxes using the eddy covariance method (Eugster *et al.*, 2007; Kroon *et al.*, 2007; Kort *et al.*, 2011). The objective of this work was to incorporate this instrument into a dynamic non-steady-state chamber design, which allows for improved accuracy and precision when measuring N_2O fluxes. This method would also then be able to verify measurements made with less precise methodologies such as static chambers. In this paper we describe the system design, the analysis of the high-

resolution data obtained, and comparison with conventional static chamber measurements. Costs and benefits of the dynamic chamber/QCL system are compared with the conventional static chamber system.

4.2 Materials and methods

A non-steady-state flow-through (or dynamic) chamber system was constructed (Livingston & Hutchinson, 1995; Hensen *et al.*, 2006) hereafter referred to as the dynamic chamber method, in which a closed volume of air was circulated between a chamber and the QCL gas analyser *via* a pump (Figure 4.1). A compact continuous wave quantum cascade laser (CW-QC-TILDAS-76-CS, Aerodyne Research Inc., Billerica, MA, USA) was used to measure gas concentrations within the chamber. This instrument uses tuneable infrared differential absorption spectroscopy (Zahniser *et al.*, 2009), with a 0.5-litre multi-pass absorption cell, with an optical path length of 76 metres. The laser source requires a very stable temperature to operate, and a solid-state cooling system (Thermocube, SS cooling systems, New York, USA) kept the system at a constant temperature of 10 ˚C by pumping a cooled solution of water and ethanol (20%). The cell was kept at a constant low pressure (approximately 6 kPa / 45 Torr) using a dry-scroll vacuum pump (SH-110, Varian Vacuum Technologies, Lexington MA, USA). The inlet of the QCL was fitted with a manual ball valve and a needle valve to control the air flow rate and cell pressure, as well as a safety valve attached to the pump to prevent back-flow. A 0.45 micron particle filter was attached to the inlet of the absorption cell.

The chamber consisted of a cylindrical polyvinyl chloride (PVC) plastic pipe of 38 cm inner diameter (ID) and 22 cm height. The chamber had PVC flanges fitted at the top and bottom. A 3 mm thick square aluminium metal lid was fitted to the top of the tube and sealed with epoxy resin and silicon sealant. A 1 cm layer of closed cell neoprene sponge was fitted around the bottom flange. The chamber was placed onto a collar which could be inserted several cm into the soil (on average 5 cm). The collar consisted of a PVC flange attached to a stainless steel ring (2-mm thickness, 6-cm height). The closed cell neoprene sponge attached to the underside of the chamber formed an airtight seal with the collar.

The chamber was fitted with an internal fan (3000 rpm, Delta Electronics, Taipei, Taiwan) and air temperature probe (CS109, Campbell Scientific, Logan, UT, USA). A pressure sensor (CS100, Campbell Scientific, UT, USA) fitted to the lid of the chamber measured the internal air pressure. All fittings on the lid of the chamber were sealed with silicone sealant to avoid gas leakage. The temperature and pressure sensors were connected to a data logger (CR1000, Campbell Scientific, UT, USA) which stored data every second. The

chamber was fitted with a rubber flap (1 mm thickness, 6 cm width) which could be rolled down to shield the seal formed between the neoprene sponge and the base of the collar or chamber from wind.

Two 30 m lengths of 9.5 mm ID Tygon® tubing were attached to both the inlet of the QCL and the outlet of the pump. This provided a 30-m radius from the QCL in which the chamber could be placed. Tygon® tubing was used as it allowed flexibility in the movement of the chamber and does not interact with N_2O. A flow rate of approximately 6 to 7 L minute^{-1} was used between the QCL and the chamber. There was a lag time of approximately 20 seconds between gas leaving the chamber and entering the analyser. Prior to each measurement, the chamber was purged with ambient air for one minute, and the data for the first minute following closure was discarded. The chamber volume was estimated after each measurement by recording depth from the chamber top to the soil surface at ten points. The typical volume of the enclosed system was 0.03 m^3 with a cross sectional area of 0.12 m^2.

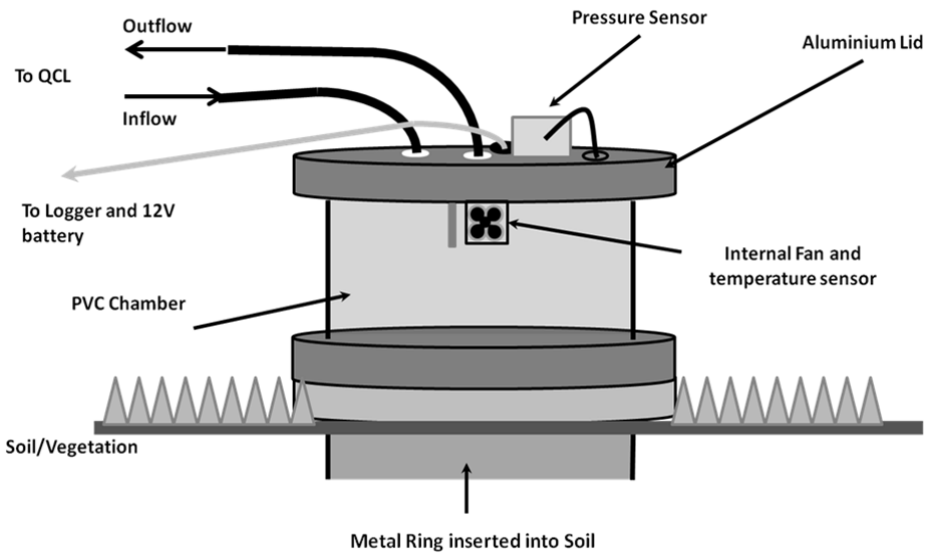

Figure 4.1 Schematic diagram of the dynamic chamber used for more detail.

To investigate the effect that circulating air through the chamber had on internal pressure, we made measurements in the lab with the chamber sealed on an impermeable metal base. Care was taken to ensure that the chamber was completely sealed by using strong clamps and bolts to seal between the neoprene layer and the metal base. In these measurements, the chamber was fitted with a very sensitive differential pressure sensor (PX654, Omega Engineering Inc., Stamford, CT, US) with a precision of 0.1 Pa (Figure 4.2). A flow rate of 6 L min^{-1} reduced pressure in the chamber by approximately 3 Pa (because of the drop in static pressure with

fluid speed). This drop in pressure was considered to be negligible when compared to the natural variation in air pressure caused by wind and temperature variation (>100 Pa).

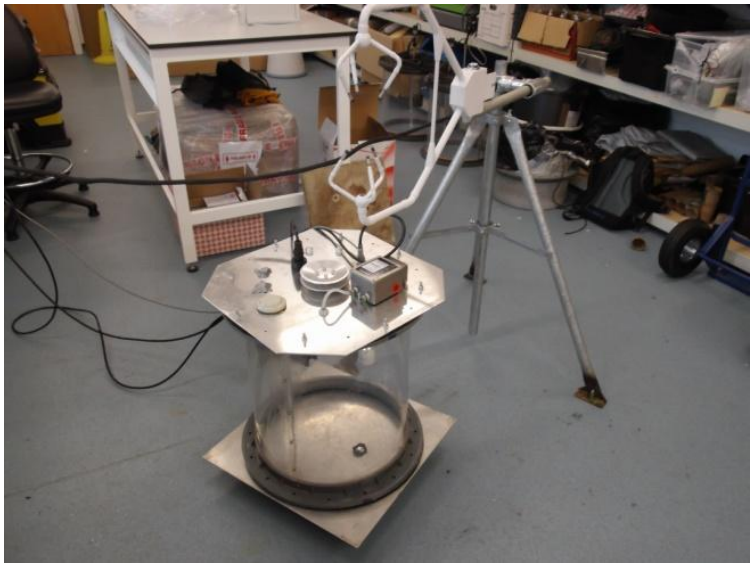

Figure 4.2 A photograph taken during testing of a chamber similar in design to the dynamic chamber described is this paper. A sensitive differential pressure sensor is attached to the lid of the chamber to identify any effects that changes in wind speed, the use of vents or the flow rate within a closed loop system has within the chamber.

Field measurements were made at two locations. Firstly, we measured on grass turf at our institute (near Penicuik, Scotland, 55° 51' 42.827"N, 3° 12' 21.6393"W), where we enhanced N_2O fluxes by applying 50 g of ammonium nitrate dissolved in 5 litres of water and spread over 10 m^2 (17.5 kg N ha^{-1}). Four collar rings were inserted into the treated area and one collar ring was inserted into an untreated area as a control. Measurements were made from each of the five chambers on four separate days, each lasting approximately one hour. Secondly, we made measurements in a grazed field using both chamber methods from the same collars at Crichton near Dumfries, SW Scotland (55° 2' 31.3238"N, 3° 35' 16.4393"W) where different fertilizer types (synthetic urine, cattle urine, cattle urine mixed with dicyandiamide (DCD) and cattle dung) had been applied at rates of 425, 435, 435 and 720 kg N ha^{-1} respectively (Figure 4.3).

Figure 4.3 Measurements were made at the Dumfries field site set up and maintained by SRUC. Dynamic chamber measurements were made from consecutive plots of different fertiliser treatments from static chamber and cutting ring bases. The QCL was housed in a tow van and powered by a diesel generator at the site.

Fluxes of N_2O were calculated using linear and non-linear asymptotic regression methods (Equations (4.1)–(4.4)) using the HMR package for the statistical software R (Pedersen *et al.*, 2010). The regression method that provided the best fit for the time series of concentration was chosen for each individual measurement, using goodness-of-fit statistics and visual inspection.

(i) Linear regression. Fluxes are calculated using the standard line of best fit through the data:

$$C_t = a + b \times t, \qquad \text{(Eq. 4.1)}$$

where C_t is the gas concentration at time t, and dC/dt is:

$$\frac{dC}{dt_0} = b \qquad \text{(Eq. 4.2)}$$

(ii) HM model. This is a commonly used non-linear model derived by Hutchinson & Mosier (1981) with a negative exponential form of curvature. The change in C with t is given by:

$$C_t = C_{max} - (C_{max} - C_0)\exp(-kt), \quad \text{(Eq. 4.3)}$$

where C_0 is the initial concentration, C_{max} is the value at equilibrium and k is a constant, and calculates dC/dt_0 as:

$$\frac{dC}{dt_0} = k(C_{max} - C_0) \quad . \quad \text{(Eq. 4)}$$

Once the rate of change in concentration of a particular gas is known it can then be used to calculate soil flux for each measurement (See Equation 4.5). The flux can then be converted to the appropriate units by simple unit conversion factors.

$$F = \frac{dC}{dt_0} \cdot \frac{\rho V}{A} \quad \text{(Eq. 4.5)}$$

Where F is gas flux from the soil (nmol m^{-2} s^{-1}), dC/dt_0 is the initial rate of change in concentration with time in nmol mol^{-1} s^{-1}, ρ is the density of air in mol m^{-3}, V is the volume of the chamber in m^3 and A is the ground area enclosed by the chamber in m^2.

Static chamber measurements were made at the Crichton site using identical chambers, following an existing protocol (see www.GHGPlatform.org.uk). Chambers were sealed for 40 minutes, then a single sample taken *via* a three-way tap in the lid. All gas samples were collected with a 20 ml syringe and stored in evacuated 20 ml glass vials. Rather than sampling gas concentration at the time of closure, this was estimated from 10 samples of ambient air collected during the measurement day. All of the samples were analysed on a 7890A GC System fitted with an ECD and FID detector (Agilent Technologies, Santa Clara, CA, USA) at SRUC. The concentration change inside the static chambers was calculated by subtracting the concentration of N_2O measured within the chamber (at t = 40 minutes) from the daily average ambient N_2O concentration. Using Equation 4.5, the flux of N_2O from each chamber was calculated assuming that the concentration change within the chamber was linear. The static and dynamic chamber methods were compared by measuring on the same collars on the same day or within 24 hours. Static chamber measurements were carried out in the early morning, and then dynamic chamber measurements were made throughout the day.

4.3 *Results and discussion*

4.3.1 Effects of wind

In initial tests, strong gusts of wind (>10 m s^{-1}) did have a clear influence on the observed concentrations within the chamber, presumably by inducing air flow between the neoprene gasket and the collar (Figure). To counter this, a ring of rubber made from a bicycle inner-tube was used to form a skirt which could be rolled to cover the seal between the chamber and the collar (Figure 4.5). Subsequent to fitting this skirt, no further effects of wind on the concentrations within the chamber were observed, and the concentration pattern was as shown in Figure 4.6. Effects of wind were only observable with the high frequency concentration measurements from the QCL, and would not be detected in conventional static chambers, where concentration measurements are made at much lower time frequency (>600 s).

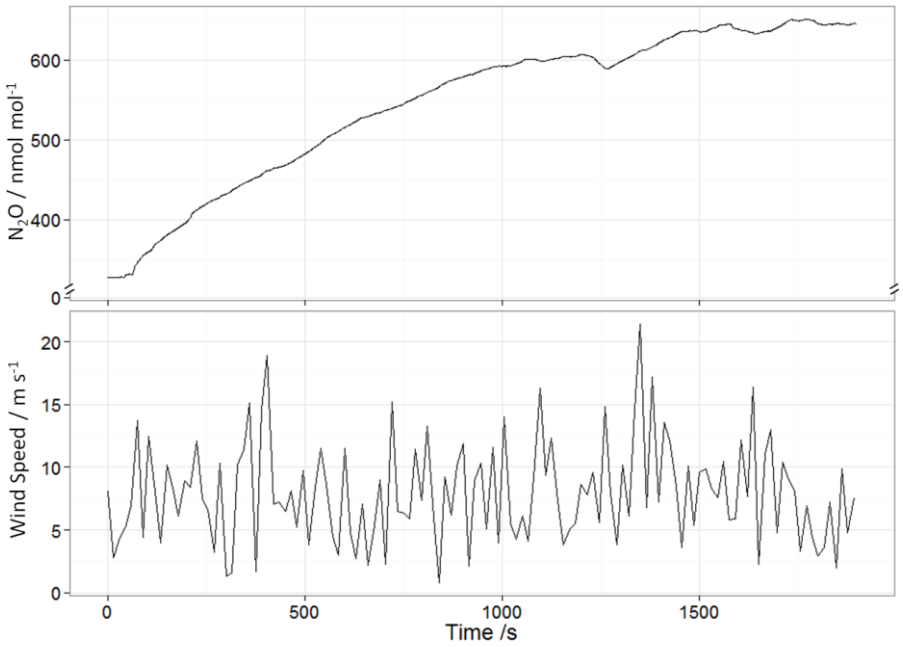

Figure 4.4 Example of N_2O concentration measurements affected by wind over a 30 min period without the use of the wind-blocking skirt. Concentration changes within the chamber should look close to linear (as in Figure 4.6), but an influence of gusts is apparent. The effect is more obvious when higher gas concentrations are present within the chamber due to a proportional dilution effect when ambient air contaminates the enclosed air. Measurement made on mown grass with added ammonium nitrate, at CEH Edinburgh, UK, March 2012.

Figure 4.5 A skirt made from a rubber bicycle tyre was fitted to the chamber to prevent wind disrupting measurements. Prior to this, the neoprenes sponge fitted to the bottom of the chamber was expected to prevent a draught between the flanges between the chamber and base (left). The skirt was folded down across the connection between the chamber and chamber base to prevent leaks caused by high winds (right).

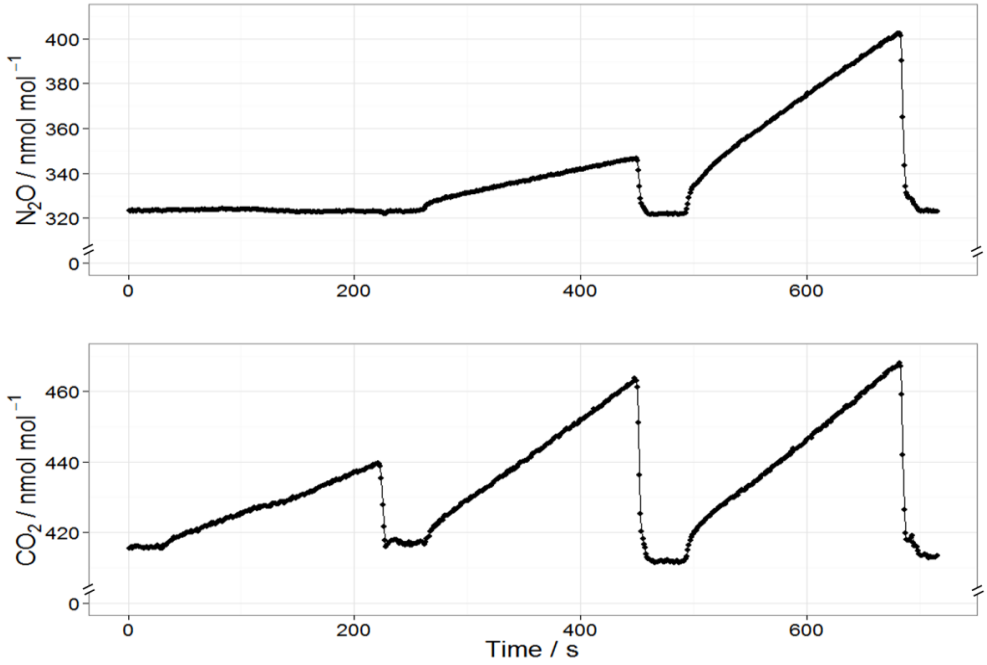

Figure 4.6 Example of N_2O and CO_2 concentration measurements recorded at 1 Hz by a QCL during three chamber measurements using the dynamic chamber from three different nearby locations within close range. Fluxes are calculated from the change in concentration over time. Each measurement lasts approximately 180 seconds of which the first 60 seconds are discarded from the regression analysis. Measurements were made on multiple grassland plots with synthetic urine fertiliser applied. (Crichton, Dumfries, SW Scotland, November 2012)

4.3.2 The influence of enclosure time on calculated flux

Figure 4.7 shows the concentration increase within chambers over the course of twenty one hour-long measurements made on metal collars inserted into fertilized grassland soil. The plots are ranked in order of magnitude of flux calculated using linear regression, increasing top-left to bottom-right (labelled 1 to 20 in sequential measurement order).

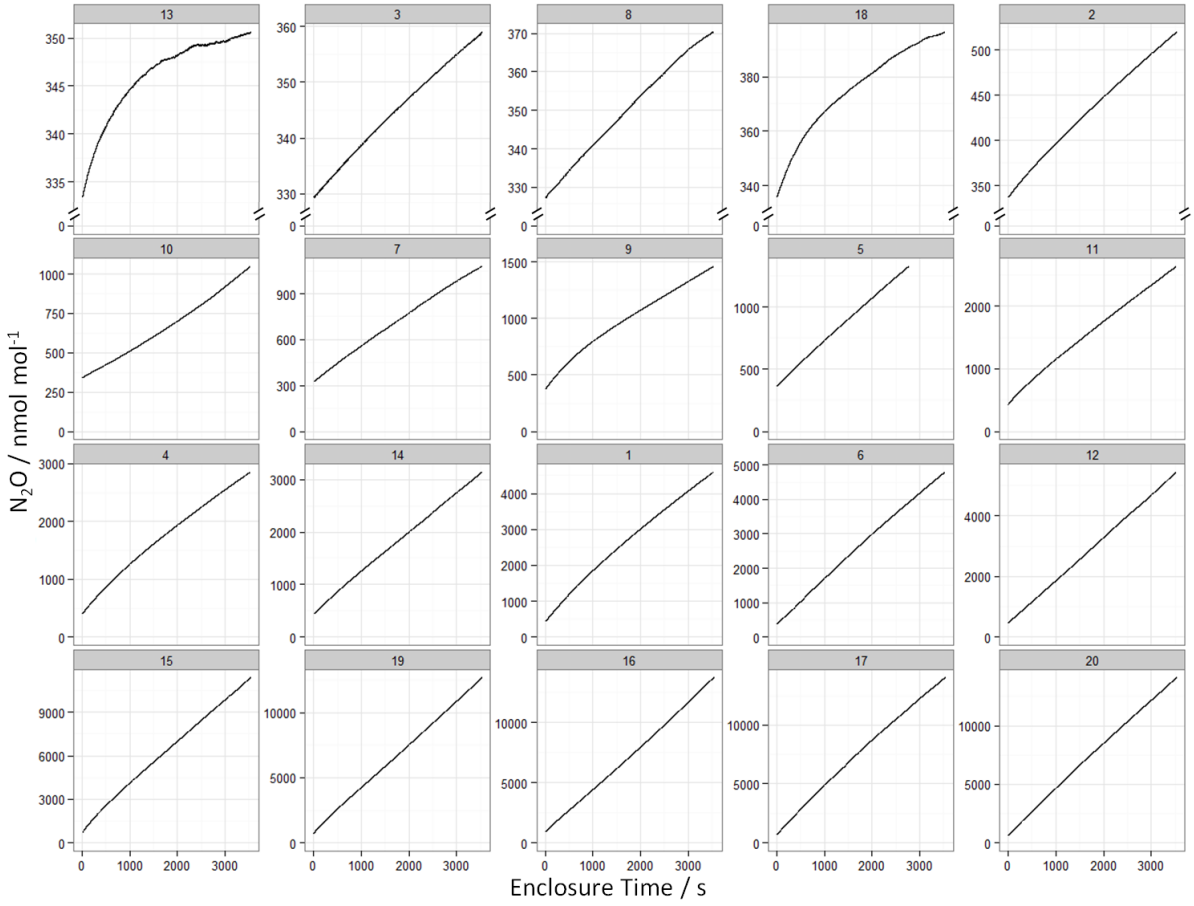

Figure 4.7 *C*oncentration increase over time within the chamber over the course of 20 hour-long measurements. The plots are ranked in order of magnitude of flux, increasing top-left (#13) to bottom-right (#20), labelled by an arbitrary measurement number. Measurement made on mown grass with added ammonium nitrate on 16 of the 20 plots (see Table 4.1): CEH Edinburgh, March 2012.

The plots in Figure 4.7 show that there is little instrumental noise in the measurements, and there is a clear change in concentration with time, irrespective of flux magnitude. Almost all of the concentration changes appear to be close to linear with time, with only a few exceptions. The fluxes calculated from the chambers over

a 60 min measurement period using linear and non-linear regression are shown in Table 4.1. The R^2 values for both linear and non-linear fits exceed 0.99 for most of the measurements; however, there are significant differences in the flux calculated using the different regression methods. Flux calculated using linear regression is smaller than those calculated using non-linear regression for all 20 measurements. The 95% confidence intervals estimated from the fitted regressions are also shown in Table 4.1.

Table 4.1 A comparison of N_2O fluxes (μg N_2O-N m^{-2} h^{-1}) calculated using linear and non-linear regression from hour long measurements using the dynamic chamber method. The table is arranged in order of increasing flux.

		Linear			Non-linear		
Plot number	Added N Treatment	Flux	95% confidence interval	R^2	Flux	95% confidence interval	R^2
13	N	4	125	0.84	17	1.3	0.98
3	N	9	14	0.99	10	0.2	0.99
8	N	13	14	0.99	15	0.6	0.99
18	N	16	70	0.95	35	2.0	0.99
2	Y	53	14	0.99	62	0.3	0.99
10	Y	204	20	0.99	230	3.0	0.99
7	Y	220	10	0.99	248	0.3	0.99
9	Y	298	32	0.99	425	1.3	0.99
5	Y	363	1	0.99	405	0.0	0.99
11	Y	628	12	0.99	719	0.4	0.99
4	Y	705	21	0.99	906	0.5	0.99
14	Y	781	6	0.99	882	0.7	0.99
1	Y	1203	20	0.99	1509	0.5	0.99
6	Y	1277	9	0.99	1444	0.3	0.99
12	Y	1440	2	0.99	1626	1.1	0.99
15	Y	3049	10	0.99	3445	0.6	0.99
19	Y	3420	3	0.99	3862	1.1	0.99
16	Y	3708	7	0.99	4184	1.6	0.99
17	Y	3850	12	0.99	4428	0.2	0.99
20	Y	3923	7	0.99	4433	0.4	0.99

Figure 4.8 shows the fluxes calculated from these data over a range of possible enclosure times, and with both linear and non-linear fitted models. Despite the appearance of linearity in Figure 4.7, the calculated fluxes for the different time periods deviate from the flux calculated after three minutes, and this deviation generally increases with the magnitude of the flux (note that the fluxes are all shown on the same absolute scale.) At the extreme, this can be approximately 1.5 nmol m^{-2} s^{-1} or 40% of the flux. Although a non-linear

model should be much less sensitive to enclosure time, even this progressively deviates from the flux calculated after three minutes. In two cases, the non-linear model deviates more than the linear one (measurements 12 & 16), but in these instances, the curves are slightly convex, and non-linear fitting to these data would usually be rejected.

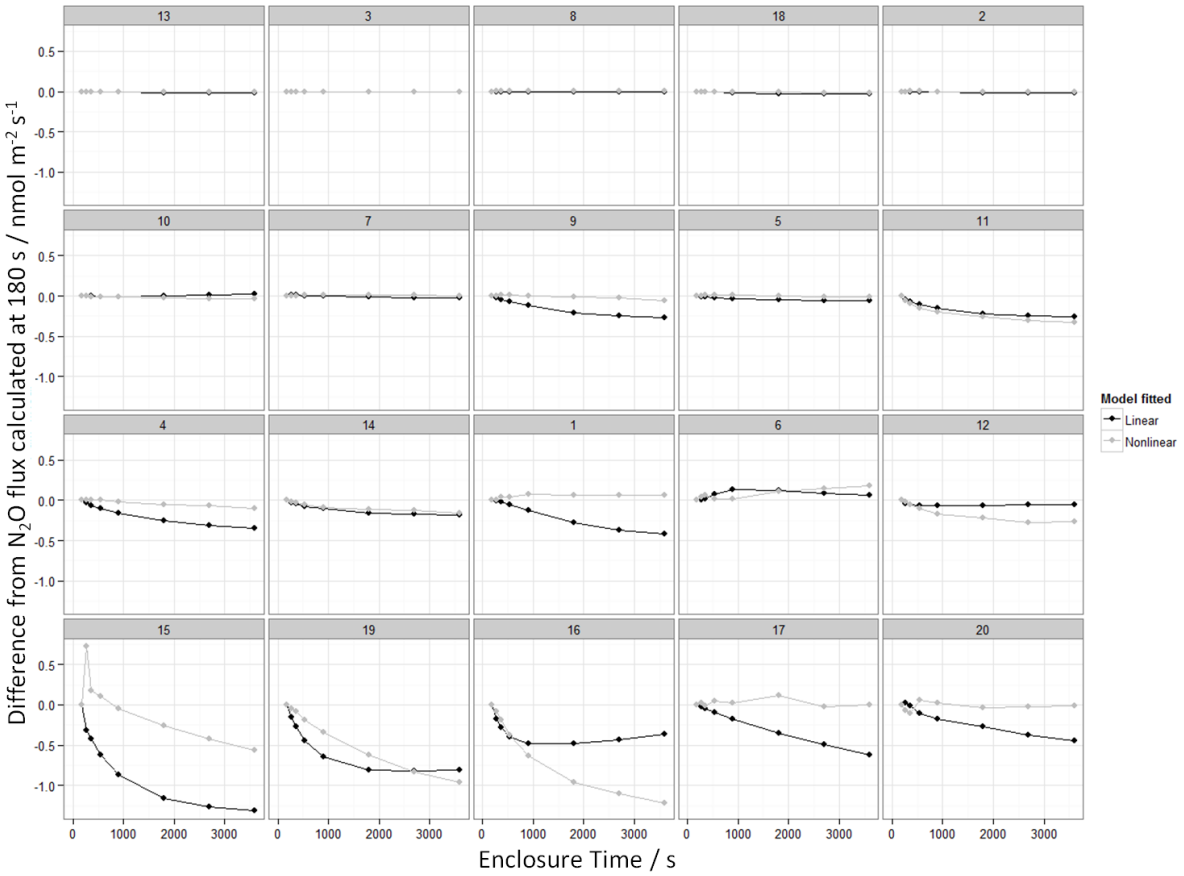

Figure 4.8 Fluxes calculated from the hour-long measurements (from Figure 4.7) over a range of possible enclosure times, and with both linear and nonlinear fitted models. Note that the fluxes are all shown on the same absolute scale.

We would conclude from these results that fluxes should be calculated using chamber enclosure times of considerably less than one hour. Whilst an effect of enclosure time might be expected if using a linear model whenever there is any degree of curvature in the rate of change in concentration, this is not expected when using a non-linear model. In principle, a non-linear model should account for the effects of feedbacks which change the rate of change in concentration over time (most obviously, the build-up of N_2O within the chamber slows the rate of diffusion from the soil, and increases the loss of N_2O to ambient air through any leaks present). Our

empirical results show that the variation in the rate of change in concentration over time is not always well represented by any model. For example, while the curvature in measurements 9, 13 & 18 is accounted for well, there are changes in curvature in measurements 11 & 15 which are not captured by the model. Presumably this arises because of some artefact of the chamber, measuring environment or instrument which changes over time.

On the basis of these results, it could be argued that the most reliable approach is to use a short enclosure time, typically less than five minutes, where model assumptions are best met. This seems to provide a sufficiently long-enough data-run to establish a good fit, and be short enough to reduce any measurement artefacts which may change over time. One might attempt to find an optimal enclosure time by assessing the marginal increase in information with change in goodness-of-fit as enclosure time increases. More simply, the model residuals can be plotted against enclosure time, and the longest enclosure time chosen where no trend is present in the residuals.

The choice of regression model used to calculate fluxes from chamber measurements is recognised as one of the largest sources of uncertainty (Kroon *et al.*, 2008; Pedersen *et al.*, 2010; Parkin *et al.*, 2012). We would also conclude that a non-linear model fit needs to be included whenever enclosure times are long, as they are more robust than the linear model to any artefact of enclosure time. It should be noted that statistical null-hypothesis testing of linear versus non-linear model fits is not pertinent, and failure to detect a statistical difference can be misconstrued as equivalence. For example, in measurement number 11, fluxes calculated by linear and non-linear models differ by 20%, but no statistically significant difference can be detected. With only three to five points as conventionally available from GC-based methods, there would be no chance of detecting any such statistical difference.

4.3.3 Comparison of dynamic and static chamber methods

Comparison of static and dynamic chambers at identical locations showed under-estimation in the flux measured with the static chamber measurements than from the dynamic chamber (R^2 value of 0.71); however this relationship is dominated by a small number of measurements with much influence (Figure 4.9). A bias towards smaller flux measurements using the static chamber method may arise because of the implicit assumption of linearity over the 40 min enclosure time (there was only one sample taken, and an estimate of initial concentration). The lack of agreement between individual measurements using both methods in this experiment is probably caused by the large uncertainty in the static chamber method. Although there was inevitably some

delay between measurements at the same locations by the two methods (typically one to five hours, but as much as 24 hours in a few cases), the time delay did not explain any of the difference in the measured fluxes. Nor was any pattern related to diurnal temperature change apparent.

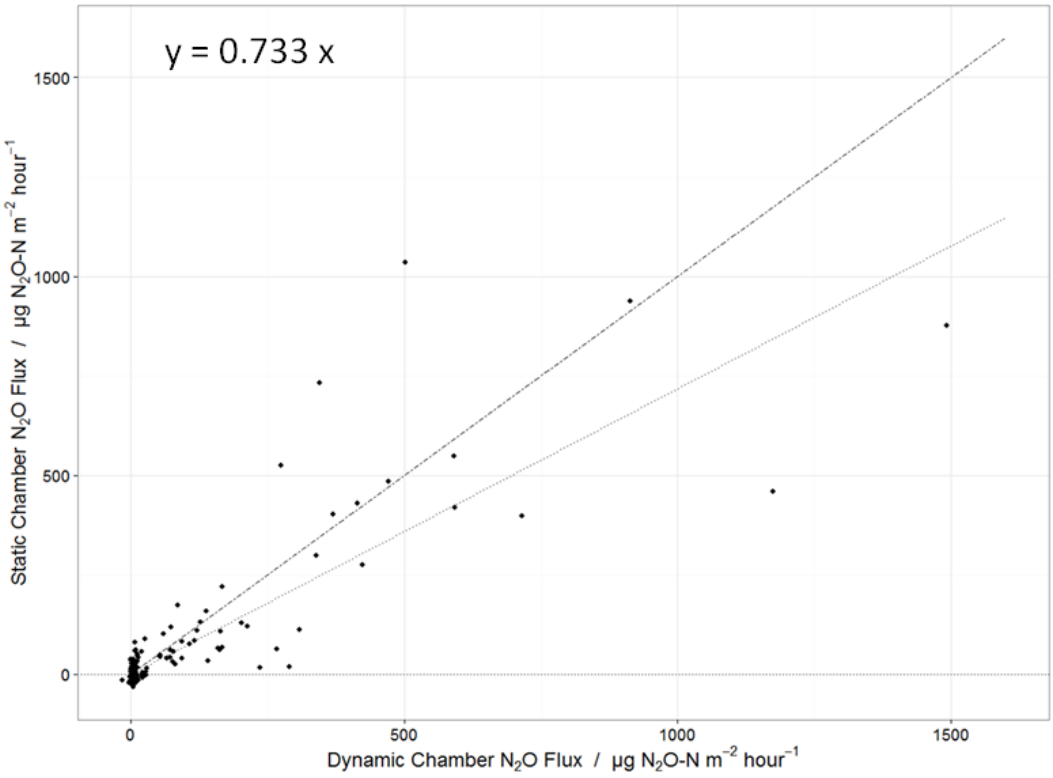

Figure 4.9 A direct comparison of N_2O flux measurements made using the dynamic and static chamber methods at a SRUC field site in Dumfries (October to November 2012). The dashed line represents the 1:1 relationship. The dotted line is the line of least-squares best fit through all data points.

Background fluxes measured in the non-fertilized control plots of the field experiment using the static chamber method ranged between -32 to 44 µg N_2O-N m^{-2} h^{-1}. In comparison, fluxes measured from the same locations using the dynamic QCL method were consistently below 10 µg N_2O-N m^{-2} h^{-1}, with calculated uncertainty of approximately 1 µg N_2O-N m^{-2} h^{-1}. The mean flux values calculated from all control plot measurements from the dynamic and static chamber methods are 2.5 and 5.4 µg N_2O-N m^{-2} h^{-1}, respectively, using linear regression. Both methods report similar mean flux values for the control plots; however the range of flux measurements from the control plots differs considerably between the methods (Figure 4.10). The small range of fluxes measured with the dynamic chamber suggests that the method is able to provide measurements of small N_2O flux with greater consistency and precision than the static chamber is able to.

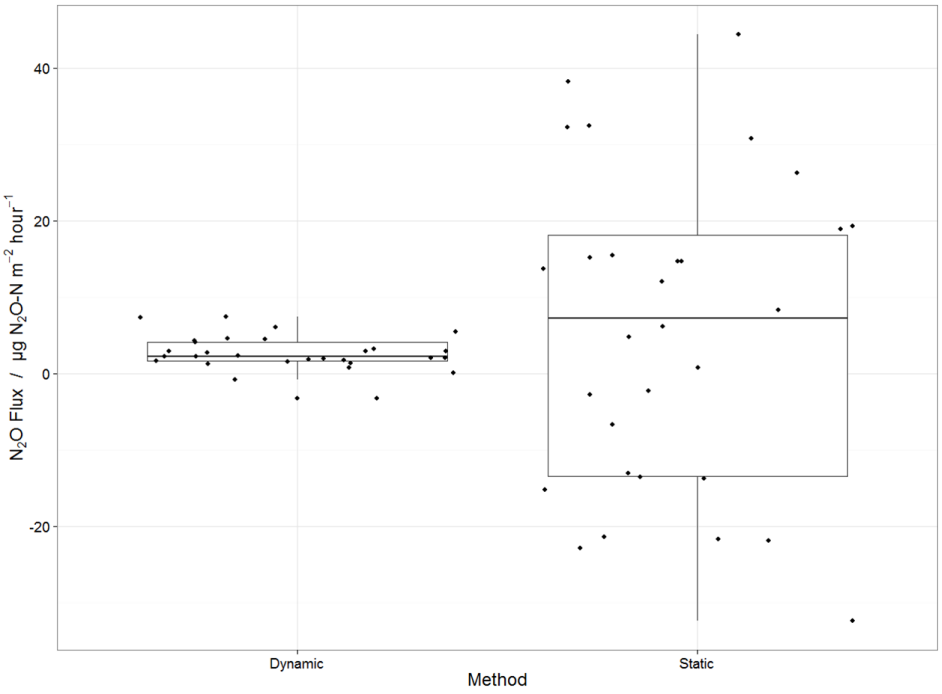

Figure 4.10 A comparison of N_2O fluxes measured from untreated control plots using both dynamic and static chamber methods. The box plot represents the 25th and 75th percentile ranges. The ability of the dynamic chamber method to measure background flux precisely is highlighted by the small range of uncertainty.

4.3.4 Uncertainty analysis

For each measurement, we estimated the uncertainty associated with each of the terms in Equation (4.5), and propagated these to estimate the total uncertainty in the flux. Uncertainty in dC/dt was obtained from the 95% confidence interval in the regression slope parameter. Uncertainty in the chamber volume was estimated by taking several measurements of height in each chamber, and taking the 95% confidence interval in the calculated chamber volume. Including estimates of the volume of vegetation, this gave values of approximately 10% of the total volume. Uncertainty in the air density term (ρ) arises from uncertainties in the temperature and pressure measurements. The 95% confidence interval for the mean temperature and pressure was calculated from the 1 Hz data, and added to the instrumental precision of the temperature probe (0.4 °C) and pressure sensor (50 Pa). For the static chambers measurements, it was not possible to calculate regression uncertainty as concentration during chamber closure was only measured once. However, a previous study has estimated that the realistic confidence intervals based on uncertainty arising from instrumental errors and poor fitting to the model are typically of an order of 20% that of the measured flux, although this can vary substantially (Levy *et al.*, 2011).

The results of the one-hour long and the comparison measurements suggest that the uncertainty in flux due to d*C*/d*t* can be large (minimum of approximately 20 µg N_2O-N m^{-2} h^{-1}) using the static chamber method, but is reduced to typically <10 µg N_2O-N m^{-2} h^{-1} in the dynamic QCL chamber method. Uncertainties from the temperature and pressure measurements are small and should apply to both methods (ranging from 0 to 2.83 µg N_2O-N m^{-2} h^{-1}). In the dynamic chamber method, only the volume term remains as a significant source of error; this is because errors in volume scale linearly with flux. Only occasionally does the uncertainty in d*C*/d*t* contribute significantly, where there is not a good relationship with concentration measurements (Figure 4.11).

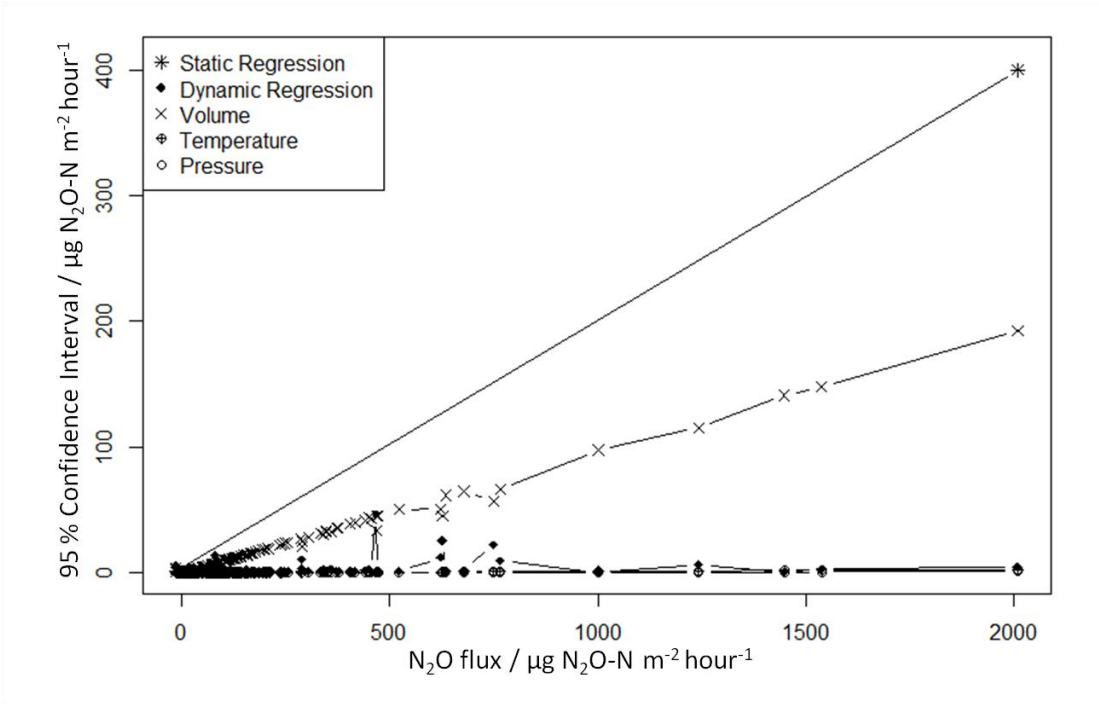

Figure 4.11 A representation of all of the calculated uncertainties made using the dynamic chamber method at the Crichton field site. The estimated uncertainty in dC/dt in static chambers (20%) is added as a comparison with literature estimates (Levy *et al.*, 2011). Uncertainty in volume of the chamber was calculated using chamber height measurements provided by SRUC. The results demonstrate the improved ability to measure dC/dt precisely using the dynamic chamber method.

The dynamic chamber used with the QCL provides more data than the static chamber method from which uncertainties from individual chamber measurements can be confidently estimated. This allows a detailed investigation of how to improve flux measurements as well as providing a clearer picture of the true spatial variability of N_2O fluxes from soils. The largest source of error in static chambers comes from estimating d*C*/d*t*

(Levy *et al.*, 2011). This uncertainty is not as large using the dynamic chamber method. The largest source of error which could be eliminated from the dynamic chamber method is that of volume. The volume uncertainty can be difficult to address on non-uniform soils. Paying more attention to measuring the volume of vegetation and measuring the soil microtopography would be ways to improve the chamber volume estimation, as simple steps to increase the accuracy of chamber methods.

4.3.5 Advantages and disadvantages

The dynamic chamber method is adaptable and able to work with a variety of instruments and chamber designs. A significant advantage of this particular arrangement is that the high-precision laser instrument can be used for both micrometeorological measurements and chambers alternately. The principal advantage of linking this laser to a dynamic chamber over conventional static chambers is the high resolution of N_2O concentration measurements. Uncertainty calculated in the smallest flux measurements was typically less than 4 μg N_2O-N m^{-2} $hour^{-1}$, defined as the 95% confidence interval in the estimate of the flux, and this may be interpreted as a limit of detection for the measurement system (*sensu* Parkin *et al*., 2012), although definitions in the literature vary. The development of these methods is important to improving the accuracy of GHG measurements which can then provide reliable information on the efficacy of mitigation of N_2O from a variety of agricultural sources.

Currently the biggest drawbacks of using the QCL system are the initial setup cost and the power requirements of the system. The mobility of the instrumentation is limited as a mains power supply or generator is required, thus limiting the spatial coverage of the system. To avoid long lag times we limited the tubing to 30 m, which limited the distance accessible for measurements. However, the QCL instrument is relatively robust to vibrations and temperature changes and is capable of being mounted in an off-road vehicle without significantly altering the detection limit of the system. A mobile system such as this would allow a wide area to be sampled. There are difficulties in using the dynamic chamber methods to make a large number of simultaneous measurements often demanded by field experiments comparing different treatments. However, because each measurement is short and no further laboratory analysis is required, we estimate that a larger number of flux measurements can be made per hour of effort (Table 4.2). Combined with the greater precision of the measurements, this yields an estimate of the mean or total flux from the sample area with less uncertainty than when using conventional static chambers.

The main disadvantages of the method are the large capital cost and the technical complexity of the instrument. With current trends in laser-based gas analysers, prices will decrease and ease-of-use will improve, and this gap in affordability and practicality between the methods will reduce.

Table 4.2 Cost-benefit analysis of QCL dynamic chamber and GC static chamber methods.

	QCL Dynamic Chamber	GC Static Chamber
Capital cost	£ 90 k	£ 14 k
Flux measurement time (minutes)	5	60
Number of simultaneous measurements	1	up to 10
Laboratory analysis time (minutes)	0	60
Number of measurements per hour of effort	12	5
Detection limit (μg N_2O-N m^{-2} $hour^{-1}$)	4	40

4.4 Conclusions

Using precise, fast-response gas analysers such as a QCL in combination with chambers provides more reliable data than the conventional static chamber/GC approach. Fluxes and their associated physical and statistical uncertainties can be properly quantified, even when fluxes are very small (below 10 μg N_2O-N m^{-2} $hour^{-1}$). It is important that errors and uncertainties in these systems are understood, and the dynamic chamber methodology gives us insights that were previously unavailable. The enhanced precision, ability to measure several gases including isotopologues will advance our understanding of soil processes and associated emissions of N_2O and CH_4. Dynamic and static chamber methods can deliver roughly the same number of flux measurements in the field (up to ten) within one hour, assuming four samples are withdrawn from static chambers within this one hour, but the dynamic chamber method has no subsequent laboratory sample analysis stage, which can take several days. Currently high costs, power consumption, weight and lack of portability limit the use of fast dynamic chamber approaches to measure N_2O or CH_4 fluxes. In time, these restrictions will be lessened, as developments in lower power laser technology become available.

Chapter 5

The influence of tillage on N_2O fluxes from an intensively managed grazed grassland in Scotland

Summary

A high resolution dynamic chamber method was used to measure fluxes of N_2O from intensively managed grazed grassland in Scotland before and after a tillage event in May 2012. N_2O fluxes from the tilled field were compared with those measured from a similarly managed adjacent grazed grassland field over a four month period which remained un-tilled. The tillage event increased N_2O emissions for 58 to 79 days; over this period the net contribution of the tillage event was estimated to be 114 to 457 g N_2O-N ha^{-1}. Spatial variability of N_2O flux increased significantly after the tillage event with fluxes varying by up to three orders of magnitude (range: -2−890 µg N_2O-N m^{-2} h^{-1}) over very short distances (2–5 m). Measurements of soil moisture suggest that N_2O fluxes are significantly higher after tillage events in soils where water filled pore space (WFPS) exceeded 50%.

Work presented in this chapter is based on the manuscript submitted as: N. J. Cowan, D. Famulari, P. E. Levy, M. Anderson, D. S. Reay, U. M. Skiba: The influence of tillage on N_2O fluxes from an intensively managed grazed grassland in Scotland, in Journal of Plant and Soil, August 2014)

5.1 Introduction

Modern agriculture and intensive land management practices are estimated to contribute over 40% of total global anthropogenic emissions of the greenhouse gas (GHG) nitrous oxide (N_2O) (IPCC, 2013). N_2O is a naturally occurring GHG released into the atmosphere by the microbial processes of nitrification and denitrification which occur in soils and aquatic systems (e.g. Davidson *et al.*, 2000; Seitzinger *et al.*, 2000). Human activities which alter environmental conditions can have an impact on natural microbial processes which in turn can increase N_2O emissions. Agricultural activities such as the use of nitrogen fertilisers, livestock production and land use changes are all important sources of anthropogenic N_2O from agricultural soils (Fowler *et al.*, 2013).

There is still large uncertainty associated with the quantification of N_2O emissions released from agricultural soils on a national and global scale due to the large spatial and temporal variability of N_2O fluxes measured (Mathieu *et al.*, 2006; Jahangir *et al.*, 2011). Many past experiments have measured the release of N_2O from soils after the application of nitrogen fertilisers - which are believed to be the most significant contributor to the rise of N_2O emissions since pre-industrial times (e.g. Dobbie *et al.*, 1999; Bouwman *et al.*, 2002). Other causes of N_2O emissions from agricultural soils, such as tillage and soil disturbance, are less well documented.

Unlike arable fields, many of which are tilled annually, grasslands are only tilled occasionally, either for conversion to arable use or to improve grass sward productivity. A freshly sown grass seed will provide a faster growing healthier grass crop for grazing animals. The regularity of sward renewal depends primarily on the condition of the grass available for grazing and desired stocking density and is entirely dependent on the opinion and experience of farm managers in different climates.

The use of nitrogen fertilisers (Yamulki & Jarvis, 2002; Abdalla *et al.*, 2010), the presence of crop residues (Baggs *et al.*, 2003), soil compaction (Yamulki & Jarvis, 2002; Ball *et al.*, 2008), the regularity and method of tillage (Sheehy *et al.*, 2013), rainfall and temperature (Dobbie *et al.*, 1999; Ussiri *et al.*, 2009; Merbold *et al.*, 2014) have been shown to affect tillage induced N_2O emissions. Changes in N_2O emissions after tillage events are believed to be due to altering the bulk density, WFPS and oxygen availability in soils which can lead to an increase or decrease in denitrification rates depending on environmental conditions (Palma *et al.*, 1997; Elmi *et al.*, 2003).

The large number of contributing factors can lead to a wide variety of results between experiments carried out at different field sites under different meteorological environments. As a result, tillage events in agricultural fields have been reported to have very different effects on N_2O depending on the numerous conditions present and experimental design, some have shown large increases in N_2O emissions (i,e. Yamulki & Jarvis, 2002; Pinto *et al.*, 2004; Omonode *et al.*, 2011) whereas others have shown a small or negative effect of tillage (i.e. Rochette, 2008; Tan *et al.*, 2009; Boeckx *et al.*, 2011: Merbold *et al.*, 2014). Improving our understanding of N_2O fluxes released from tillage events is important, considering that agriculture accounts for approximately 70% of the total land coverage in the UK (DEFRA, 2012) and it is possible that even small perturbations in fluxes caused by tillage events can contribute significantly to the total national inventory of anthropogenic N_2O emissions.

The aim of this work was to add to the understanding of the magnitude and drivers of N_2O fluxes from grasslands tilled for sward renewal and to investigate how the spatial variability of N_2O fluxes changes with time after the tillage event.

5.2 Materials and method

Nitrous oxide fluxes were measured from an area of intensively managed, grazed grassland (Easter Bush, Scotland, 55° 51' 55.2976"N, 3° 12' 22.1655"W) before and after a tillage event on the 1st of May 2012, and were compared with fluxes measured from an adjacent grassland which remained un-tilled (Jones *et al*, 2011). The climate is temperate maritime, with an average annual rainfall of 921 mm and average annual air temperature of 9 ^{o}C (in the period 2002–2010). The two 5.4 ha fields have been managed for intensive livestock production for at least 20 years, and since 2002 were predominately grazed by sheep. The average stocking densities were 0.7 LSU ha^{-1} (livestock units) and average N fertiliser application rates of approx 200 kg N ha^{-1} y^{-1}. Mainly NH_4NO_3 or NPK compound fertilisers were applied in three split applications usually between March and July (Skiba *et al.*, 2012).

The soils are clay loams with a sand/silt/clay texture of 28/20/52 and 24/19/57 for the top 30 cm in the un-tilled and tilled fields, respectively with a pH of 5.1 (in H_2O). They are classed as imperfectly drained Macmerry soil of the Rowanhill association (eutric cambisol, FAO classification). A drainage system had been installed about 50 years ago, but is no longer functioning well, resulting in frequent occurrence of surface water during rainy periods. The fields had not been tilled for at least 20 years, and the farmer had reported reduced

fertility and productivity. This together with the poor drainage led to the decision to till both fields. In the first stage, only one field (also called the South Field in Jones *et al*., 2011) was tilled. In preparation glycophosphate was applied to kill the grass three days prior ploughing on the 1st of May 2012 to a depth of 30 cm (Figure 5.1). Two days after ploughing the field was harrowed, then rolled and sown with *Lolium perenne* three days after ploughing. The un-tilled field (also called the North field in Jones *et al*., 2011) was managed as usual and grazed by sheep (approximately 30 sheep ha^{-1}).

Figure 5.1 The tilled field was originally a grassland pasture used to graze sheep. The field was ploughed to a depth of 30 cm on the 1st of May 2012.

Nitrous oxide flux measurements from both fields were made using the dynamic chamber method over a four-month period (April to July 2012) before and after the tillage event on the 1st May 2012 (Table 5.1). Before tillage, flux measurements were made in the middle of April (12 and 14 days before tillage from the field to be tilled and 7 days before tillage from the field to remain grassland) as a background estimate of flux rates and of the natural spatial variability of N_2O fluxes. Measurements could not be made on the day of tillage as the instrumentation and chambers would have obstructed the farm machinery during the ploughing, harrowing and seeding of the field. From then on measurements were made 1, 2, 3, 4, 6, 8, 20, 58 and 79 days after the tillage event. Only a smaller number of measurements were made regularly on the un-tilled adjacent grassland (Table 5.1). The number and frequency of flux measurements was restricted and uneven across the two fields due to the multiple stages of the tillage event in which farm vehicles required unrestricted access, the fragility of the sown

grass seed in wet conditions, limited availability of the quantum cascade laser (QCL) or heavy precipitation and our primary focus being to observe temporal and spatial changes of the N_2O flux from the tilled field.

Table 5.1 Tillage management and flux measurements which were made during the experiment using the dynamic chamber method on both the tilled and un-tilled fields.

Date	Days after tillage	Management	No. of measurements made in tilled field	No. of measurements made in un-tilled field
16th April	-14		34	0
18th April	-12		34	0
23rd April	-7		0	14
1st May	0	Tillage	0	0
2nd May	1		25	5
3rd May	2	Harrowed	40	5
4th May	3	Rolled & Sown	25	5
5th May	4		30	5
7th May	6		30	5
9th May	8		30	5
21st May	20		15	0
28th June	58		10	0
19th July	79		15	15

Nitrous oxide flux measurements were made using a closed loop dynamic chamber system which circulated air between a flux chamber and a quantum cascade laser (QCL) gas analyser via a vacuum pump (SH-110, Varian Inc, CA, USA) as described in Chapter 4. A compact continuous wave QCL (CW-QC-TILDAS-76-CS, Aerodyne Research Inc., Billerica, MA, USA) was used to measure gas mixing ratios within the chamber at a rate of 1 Hz with a detection limit of 30 nmol mol^{-1} for N_2O. The chamber (of 38 cm inner diameter (ID) and 22 cm height) was placed onto an aluminium collar inserted several cm into the soil (on average 5 cm) prior to a measurement. Two 30 m lengths of 3/8 inch ID Tygon® tubing connected the chamber to the inlet of the QCL and the outlet of the pump to form a closed loop of airflow within the system. This provided a 30 m radius from the QCL in which the chamber could be placed (Figure 5.2). The length of the tubing was limited by the strain on the vacuum pump and the lag time between the chamber and analyser. A flow rate of approximately 6 to 7 L min^{-1} was used between the QCL and the chamber with a lag time of approximately 22 seconds between the chamber and analyser. Measurements were made for three minutes, collecting 180 data points, which were logged by the QCL computer (See Chapter 4).

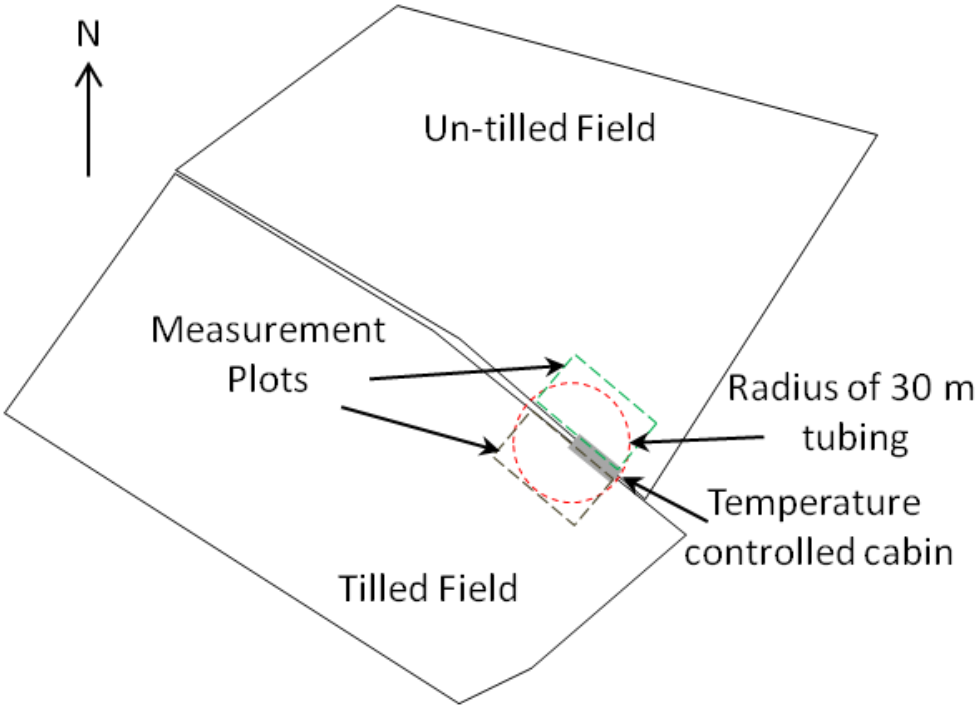

Figure 5.2 The QCL gas analyser was housed in a temperature controlled cabin situated between the tilled and un-tilled field. The gas tubing allowed a 30 m radius around the position of the QCL from which flux measurements could be made. This allowed for a small plot from each field to be sampled from.

Fluxes of N_2O were calculated using both linear and non-linear asymptotic regression methods using the HMR package for the statistical software R (Pedersen *et al.*, 2010; Levy *et al.*, 2011). Using a mixture of goodness-of-fit statistics and visual inspection, the regression method that provided the best fit for the time series of mixing ratios of N_2O was chosen for each individual measurement. The rate of change in mixing ratio was used to calculate the flux for each measurement (Equation 5.1). The minimum detection range of the method was approximately 4 µg N_2O-N m^{-2} h^{-1}.

$$F = \frac{dC}{dt_0} \cdot \frac{\rho V}{A} \qquad \text{(Eq. 5.1)}$$

Where F is gas flux from the soil (µmol m^{-2} s^{-1}), dC/dt_0 is the initial rate of change in mixing ratio with time in µmol $mol^{-1}s^{-1,}$ ρ is the density of air in mol m^{-3}, V is the volume of the chamber in m^3 and A is the ground area enclosed by the chamber in m^2.

During the study changes in bulk density and total carbon (C) and nitrogen (N) content from both fields were measured. Soil moisture content was measured from the tilled field only. Between the 22nd of February and

9th of March 2012 a total of 63 soil cores were collected from the fields (35 and 28 from the tilled and untilled fields respectively) as part of a separate soil analysis experiment carried out in the fields. These cores were made using 60 cm deep sharpened stainless steel tubes (6 cm diameter) which were hammered into the ground. Once removed from the corer the soil cores were cut into 12 cm sections for analysis. The results obtained from the top 12 cm of the soil cores are reported in this study. 35 soil cores, approximately 12 cm deep with a diameter of 5 cm, were taken from the fields 5 weeks after the tillage event (18 and 17 from the tilled and untilled fields respectively). These cores were collected using 20 cm long sharpened plastic tubes (5.5 cm diameter) which were hammered into the ground. All soil samples were kept in sealed bags and stored in a refrigerated area (<5 ˚C) before analysis. The soils were oven dried (100 ˚C) and ground via ball milling for total carbon and nitrogen analysis via elemental analysis (vario EL cube, Elemaentar, Hanau, Germany).

Volumetric soil moisture measurements were made 6 and 8 days after the tillage event using moisture probe (Theta kit, MEA, Adelaide, South Australia). Water filled pore space (WFPS) was calculated from the measured volumetric water content, bulk density and standard particle density of the soil (Equation 5.2).

$$\mathrm{WFPS} = \frac{V_{cont} \times 100}{1 - \left(\frac{r_b}{r_d}\right)} \qquad \text{(Eq. 5.2)}$$

Where WFPS is the percentage of porous volume in the soil filled by water, V_{cont} is the volumetric water content of the soil, r_b is the bulk density of the soil in g cm^{-3} (after tillage) and r_d is the particle density of the soil (assumed as 2.65 g cm^{-3}) (Rowell, 1994).

WFPS for the tilled field plot was mapped the using local polynomial regression fitting (See Section 3.6.4). Soil moisture measurements made 7 and 9 days after tillage were made on a grid of 10 x 5 m on both days. WFPS interpolation was estimated using a 2nd degree polynomial function on a 0,5 m grid with a span (α) of 0.75.Rainfall (tipping bucket) and air temperature (3 m from the soil surface) are continuously recorded (30 min averages) at CEH's field station, which is situated between the two fields (See Figure 5.3).

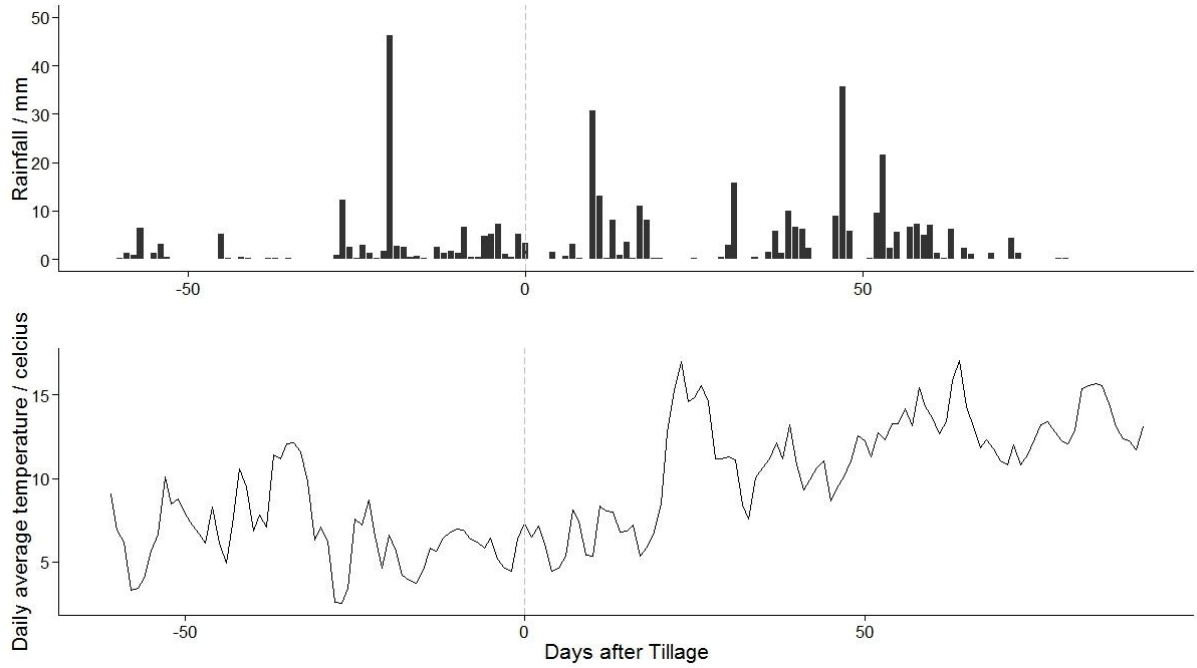

Figure 5.3 Accumulated daily rainfall and average daily air temperature at height 3 m recorded at the Easter Bush field site from March to August 2012

5.3 Results

5.3.1 Comparison of N_2O fluxes measured from the tilled and un-tilled fields

N_2O fluxes were measured before the tillage event from the to-be-tilled field (34 measurements on two occasions 15 and 13 days before tillage) and from the untilled field (14 days before the tillage event) were very small. Fluxes from the to-be-tilled field ranged between -1 to 8 µg N_2O-N m^{-2} h^{-1} with a mean value of 1 µg N_2O-N m^{-2} h^{-1} (Figure 5.4a), and fluxes from the untilled field ranged between -2 to 13 µg N_2O-N m^{-2} h^{-1} (Figure 5.4b) with a mean value of 3 µg N_2O-N m^{-2} h^{-1} (See Table 5.2).

N_2O emissions increased significantly after the tillage event, with mean flux values measured as 79 and 109 µg N_2O-N m^{-2} h^{-1} on the first and second days after tillage respectively (See Figure 5.4a & Table 5.2). Fluxes as high as 890 µg N_2O-N m^{-2} h^{-1} were measured from the tilled field during this period. The daily mean flux remained significantly higher (19–55 µg N_2O-N m^{-2} h^{-1}) at least for the next five measurement dates (3 to 20 days) after the tillage event. Fifty eight days after tillage the flux magnitude returned to values which were not significantly different to background emissions (< 3 µg N_2O-N m^{-2} h^{-1}, p= 0.26) (Figure 5.4a). Seventy nine days after the tillage event fluxes measured from the tilled and un-tilled field were 0.34 and

-0.01 µg N_2O-N m^{-2} h^{-1} respectively and were not significantly different (p-value = 0.71). Fewer flux measurements were made on the un-tilled field (Figure 5.4b). Fluxes from this field varied little (between -2 to 14 µg N_2O-N m^{-2} h^{-1}) over the four month period between April and July when compared to the tilled field. The fluxes observed from the un-tilled field were very small, varying in magnitude similar to the detection limit of the method (mean flux values between -1 to 4 µg N_2O-N m^{-2} h^{-1}) (Figure 5.4b). The mean fluxes measured during from the tilled and un-tilled field during the first 20 days were 55 and 3 µg N_2O-N m^{-2} h^{-1} (p-value = <0.01). Assuming similar N_2O fluxes from both fields under same conditions (Skiba *et al*., 2012) this suggests that the tillage event increased N_2O emissions by seventeen fold for the first twenty days after tillage.

Table 5.2 A comparison of mean fluxes measured from the tilled and un-tilled fields. Standard deviation and p-values indicating a statistical significance between fluxes measured from the fields are included.

		Tilled		Un-tilled		
Date	Days after Tillage	Mean flux	S.D.	Mean flux	S.D.	p-value
April[a]	Before Tillage	1.1	1.7	3.1	2.6	0.02
02/05/2012	1	73	82	4.1	4.6	< 0.01
03/05/2012	2	110	171	1.9	1.5	< 0.01
04/05/2012	3	44	105	1.8	2.1	0.06
05/05/2012	4	37	74	3.1	1.5	0.02
07/05/2012	6	20	28	3.2	3.2	< 0.01
09/05/2012	8	27	32	5.3	5.3	< 0.01
21/05/2012	20	55	29	1.3[b]	4.4[b]	< 0.01
28/06/2012	58	3.2	4.6	1.3[b]	4.4[b]	0.26
19/07/2012	79	0.3	1.5	-0.01	3.2	0.71

[a] Multiple dates (See Table 5.1 for details), [b] missing data filled using combination of measurements made 8 and 79 days after tillage event

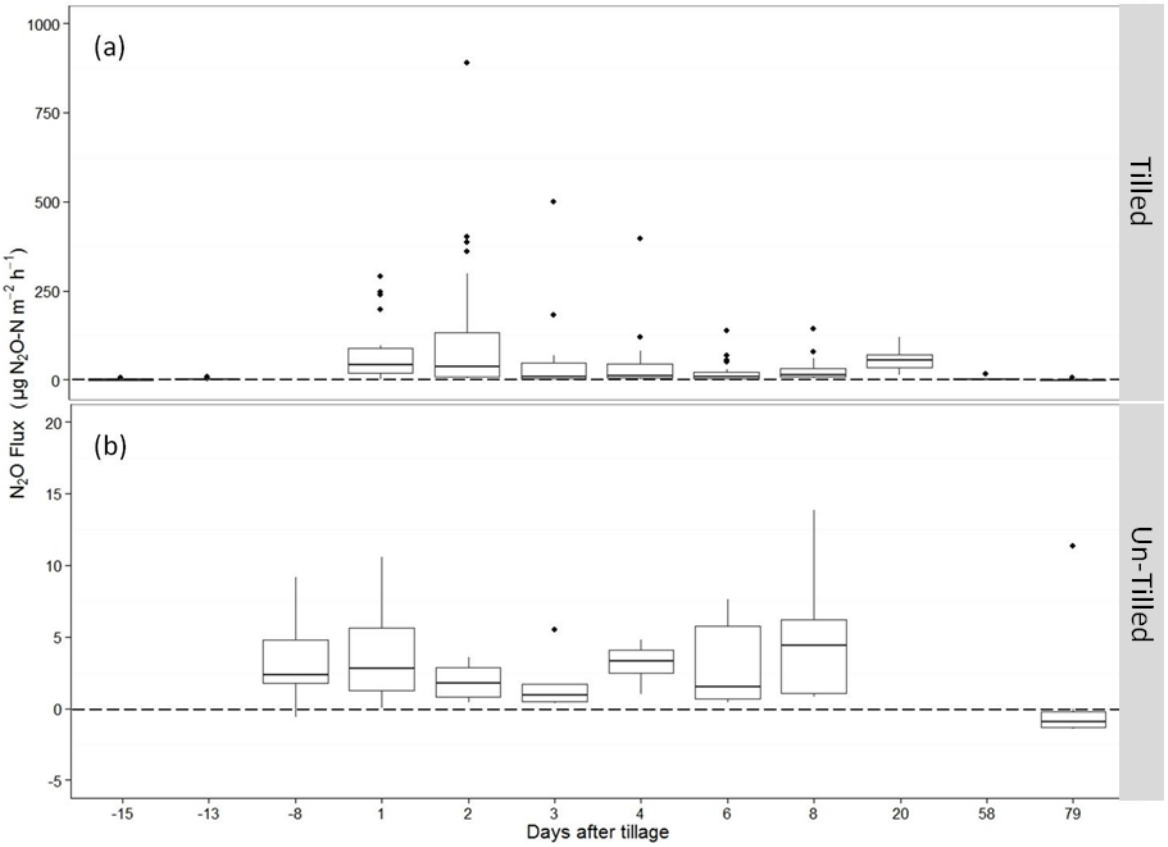

Figure 5.4 N_2O fluxes measured from the tilled field (a) and un-tilled field (b) at Easter Bush. Tillage occurred on the 1st May 2012. The box plots represent the mean, first and third quartiles of fluxes measured on each day that measurements took place. Measurements outside the third quartile are included as points on the plot. (Note the scale difference in flux between the graphs).

5.3.2 The effect of tillage on soil properties

Soil measurements made five weeks after the tillage event were compared with measurements from the fields taken 1 month before tillage (Table 5.3). The comparisons show that the bulk density of soil in the top 12 cm of the tilled did not change significantly due the tillage event (p-value = 0.8) (Table 5.3). Carbon and nitrogen content of the soil in the tilled field was also not significantly different 5 weeks after tillage event and remained at approximately 30 and 2.6 g kg^{-1} respectively (See Table 5.3).

Significant differences in soil properties were observed in soil samples taken from the un-tilled field before and after the tillage event (See Table 5.3). It is likely that these large differences are due to the sampling locations rather than any change at the field scale. The measurements made before the tillage event spanned the

entire area of the field whilst the soil samples made after the tillage event were only taken from the small plots from which chamber measurements had taken place. The comparison of soil properties between both fields before the tillage event shows that mean values of bulk density, and carbon and nitrogen content were similar over the field as a whole (See Table 5.3). No spatial patterns were observed in the soil properties measured within the small measurement plots in which flux measurements took place, and no spatial relationship was observed between N_2O flux and carbon or nitrogen content in these areas.

Table 5.3 Soil measurements made from the tilled and un-tilled fields a month before and five weeks after tillage (Standard deviation included). Significance in statistical differences between the tilled and untilled fields and difference between samples taken prior to and after the tillage event from each field are included (p-values).

	n	Bulk density (g cm^{-3})	S.D.	Total carbon content (g kg^{-1})	S.D.	Total nitrogen content (g kg^{-1})	S.D.
Tilled							
Before	35	0.79	0.13	30.2	7.2	2.6	0.6
After	18	0.79	0.08	30.4	6.3	2.6	0.6
p-value[a]		0.8		0.9		1.0	
Un-tilled							
Before	28	0.74	0.06	33.0	6.5	2.7	0.6
After	17	0.86	0.13	19.0	5.9	2.1	0.5
p-value[a]		< 0.01		< 0.01		0.012	
Tilled and un-tilled							
p-value (before)[b]		0.011		0.110		0.459	
p-value (after)[b]		0.123		< 0.01		0.025	

[a] Statistical significance between soils before and after tillage, [b] Statistical significance between tilled and untilled field.

5.3.3 Spatial variability of N_2O fluxes after the tillage event

Fluxes of N_2O measured from the tilled field were very variable, even over short distances during each of the measurement days (Figure 5.5). A large flux 'hotspot' area can be seen in fluxes in the days immediately after tillage near the centre of the plot (X= 20 m, Y =15 m). Fluxes measured in the area left of the centre of the plot appear to be higher than those throughout the rest of the plot. Most of the largest fluxes were measured in this area of the plot. 58 days after tillage the majority of the fluxes had returned to pre-tillage magnitude (below 10 µg N_2O-N m^{-2} h^{-1}).

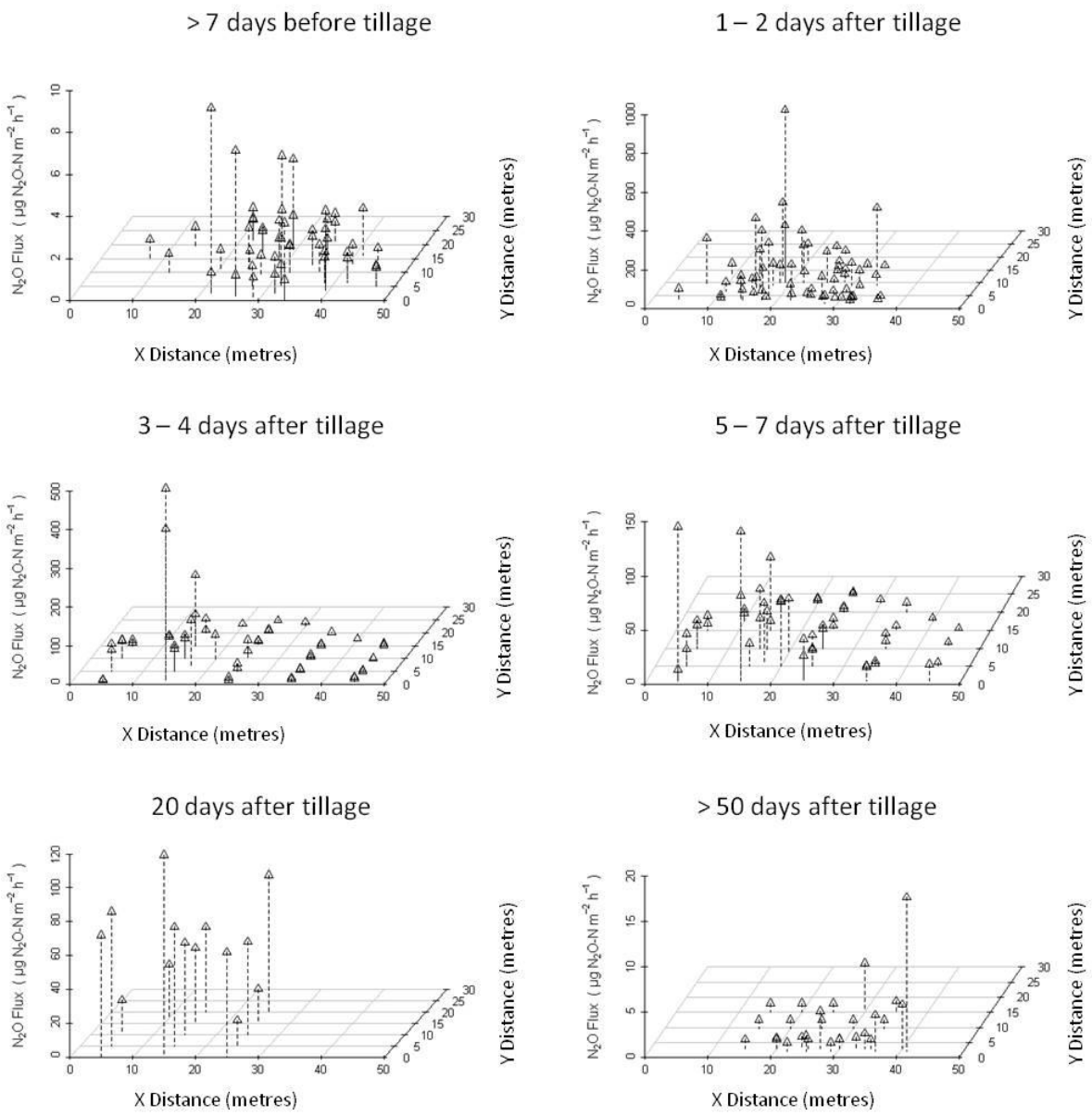

Figure 5.5 A representation of the spatial variability of N_2O fluxes measured from the ploughed field as 3D scatter plots split into 6 periods over which measurements took place. (Note the scale difference in flux between the graphs)

The main reason for the spatial variability observed in flux measurements in this study is believed to be variations in the WFPS content of the soil. During the four month measurement period there was a large area of constantly wet, poorly drained soil near the centre left of the measurement plot that was clearly visible by eye (Figure 5.6).

Figure 5.6 A large poorly drained area of soil was present in the measurement plot of the tilled field. This area of soil remained damper than the surrounding soil during the duration of the experiment. Surface water was often visible after rainfall events as in the photograph.

This patch of soil became boggy during periods of wet weather (Figure 5.3) and never fully dried during drier days. Soil moisture measurements made 7 and 9 days after tillage provided a general map of the moisture distribution in the plot (Figure 5.7). Individual WFPS measurements measured on these occasions varied from 27 to over 90%. The soil moisture measurements reveal that that the centre left area of the plot was significantly wetter than its surroundings. The area of high WFPS corresponds well with the highest fluxes measured during the experiment. Most of the fluxes that exceed 100 μg N_2O-N m^{-2} h^{-1} came from the damp central area of the plot as highlighted in Figure 5.7 by the white dots.

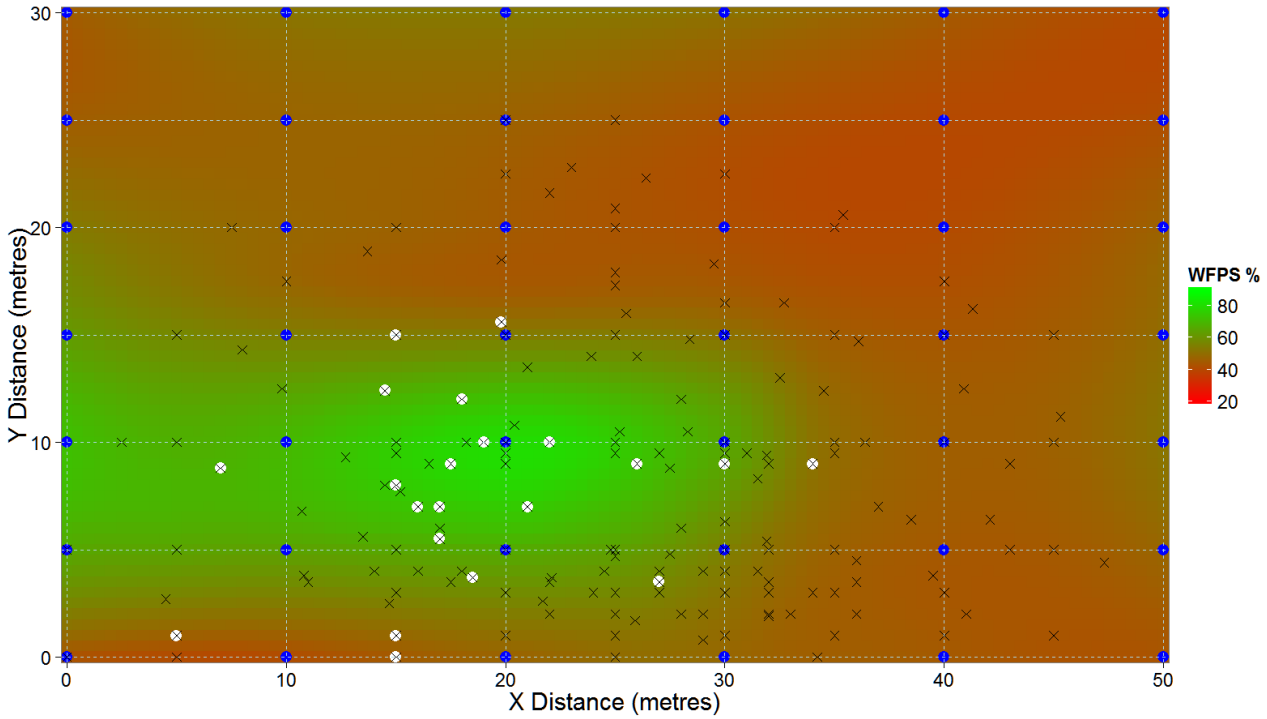

Figure 5.7 A representation of the average spatial variability of soil moisture plotted using local polynomial regression fitting with data measured from the tilled field 7 and 9 days after tillage.

5.4 Discussion

Before tillage, neither of the two fields had received any nitrogen fertiliser since early July 2011. Therefore N_2O fluxes were at background levels (1.1 ± 1.7 µg N_2O-N m^{-2} h^{-1} and 3.1 ± 2.6 µg N_2O-N m^{-2} h^{-1} for the tilled and non-tilled fields, respectively) and similar in magnitude to background fluxes measured from the same fields between 2007 and 2010 (Skiba *et al.*, 2012). Many of the background fluxes from both fields (89%) were below the 4 µg N_2O-N m^{-2} h^{-1} detection limit of the methodology and no clear patterns in spatial variability were observed in these measurements. From the background fluxes measured in this study it would be difficult to prove if meteorological effects such as temperature or rainfall (and resultant changes in WFPS) have a considerable impact on N_2O flux from the fields. Microbial emissions of N_2O have both been shown to respond to changes in moisture and temperature in previous experiments (Dobbie and Smith, 2001; Ussiri *et al.*, 2009).

Figure 5.4b implies that flux measurements from the un-tilled field remained at background levels throughout the measurement period. This was not strictly true, as the non-tilled field was fertilised with 70 kg NH_4NO_3 ha^{-1} on the 28th May 2012. Previous work at the field site (Skiba *et al.*, 2012) and the general

literature (i.e. Bouwman, 1996) has shown that fertiliser induced elevated N_2O emissions only last for 1–3 weeks. The next measurement date after fertilisation was on 19th July, which was well beyond this three week window, and any elevated N_2O fluxes would have returned to the background levels we recorded then.

The comparison of background fluxes (both before tillage and from the untilled field) with fluxes measured from the tilled field show that the tillage event was directly responsible for the increased N_2O fluxes. Elevated N_2O fluxes lasted over 58 to 79 days. Fluxes measured from the tilled field vary significantly throughout the plot, ranging from -1 to 890 µg N_2O-N m^{-2} h^{-1} over the four month measurement period. This range of fluxes compares with those that may be expected after the application of nitrogen fertilisers (Cowan *et al*., 2014). The magnitude and spatial variability of the fluxes recoded in this study are comparable with a tillage experiment carried out on a long term perennial pasture, used for grazing cattle in Spain (Pinto *et al.*, 2004). In this experiment daily fluxes measured over the first five days from non-fertilised soils ranged from 900 to 5200 µg N_2O-N m^{-2} day^{-1} depending on tillage method. This compared well with the range of daily mean values of measured in this study (880 to 2600 µg N_2O-N m^{-2} day^{-1}).

Soil moisture content appeared to have an impact on the magnitude of N_2O flux from the tilled field. After the tillage event, the largest recorded fluxes were measured in the area of the plot where WFPS exceeded 50% (range 50 to 90%). It is unclear if this was also true before the tillage event as the measured fluxes were close to the detection range of the dynamic chamber system. Similar relationships between WFPS and N_2O flux from tilled soils have been observed in previous grassland tillage experiments (Pinto *et al.*, 2004; Yamulki & Jarvis, 2002, Merbold *et al*., 2014) and also from arable soils (Petersen *et al.*, 2008; Mutegi *et al.*, 2010). In these experiments significantly higher fluxes were recorded from tilled soils with higher WFPS ranging from 40 to 90%.

Reasons for the relationship observed between N_2O flux and WFPS are not straightforward. Gas diffusion rates, availability of nutrients, and the effects that these have on soil microbial nitrification and denitrification rates are complex. The high moisture contents together with decomposition and mineralisation of the old grass residues and soil organic matter may have provided the low oxygen conditions and carbon and nitrogen needed for denitrification to proceed, either to N_2O, or N_2 under very anaerobic conditions (Linn and Doran, 1984; Davidson *et al*., 2000). The possibility of full denitrification from N_2 means that areas of very high soil moisture contents may not always have the largest N_2O fluxes, as shown in Figure 5.7 which may explain in part, the observation of fluxes smaller and larger than 100 µg N_2O-N m^{-2} h^{-1} within the very wet area of the plot.

The large spatial variability and long stretches of time between measurements of fluxes in this study make it difficult to estimate a cumulative flux for the tillage event. Three methods were used to calculate N_2O released from the tilled field over the 80 day period that measurements took place. The simplest of these methods was to use a linear interpolation of the arithmetic daily mean fluxes (as reported in Table 5.2) and subtract an estimate of background N_2O fluxes which would have been released had the tillage event not occurred. Using this method it was estimated that 478 g N_2O-N ha^{-1} was released from the tilled field over a period of 80 days after the tillage event. Background emissions were estimated to be 22 g N_2O-N ha^{-1} resulting in a net emission of 457 g N_2O-N ha^{-1} due to the tillage event over the 80 day period.

A similar approach was used with daily geometric means (mean of $\log_{10}$ N_2O flux values) instead of arithmetic. This option seemed more appropriate due to the geometric distribution of the N_2O flux measurements and the small number of very high flux measurements which significantly increased the daily arithmetic mean. Geometric linear interpolation method resulted in a lower net emission of 342 g N_2O-N ha^{-1}.

A more complex method to estimate the net emission from the event was to treat the fluxes as an exponential decay after the tillage event. This assumes that N_2O flux was highest at the time of tillage and constantly fell at an exponential rate after the event, which agrees with the majority of observed measurements. An exponential decay fit was estimated by fitting a linear regression through $\log_{10}$ values of flux over time. This method takes into account all flux measurements made within the plot after the tillage event (Figure 5.8a). The exponential decay was then used to integrate daily flux estimates over the four month period. The exponential decay estimates that N_2O flux from the tilled field reaches a pre-tillage magnitude of 1 µg N_2O-N m^{-2} h^{-1} after 74 days (Figure 5.8b). Daily mean fluxes estimated by the decay are in the order of 20 to 30 µg N_2O-N m^{-2} h^{-1} the first 48 hours after tillage. These values are significantly less than the mean values reported in Table 5.2. Net emission of N_2O released from the tilled field using the exponential decay method is estimated at 114 g N_2O-N ha^{-1}.

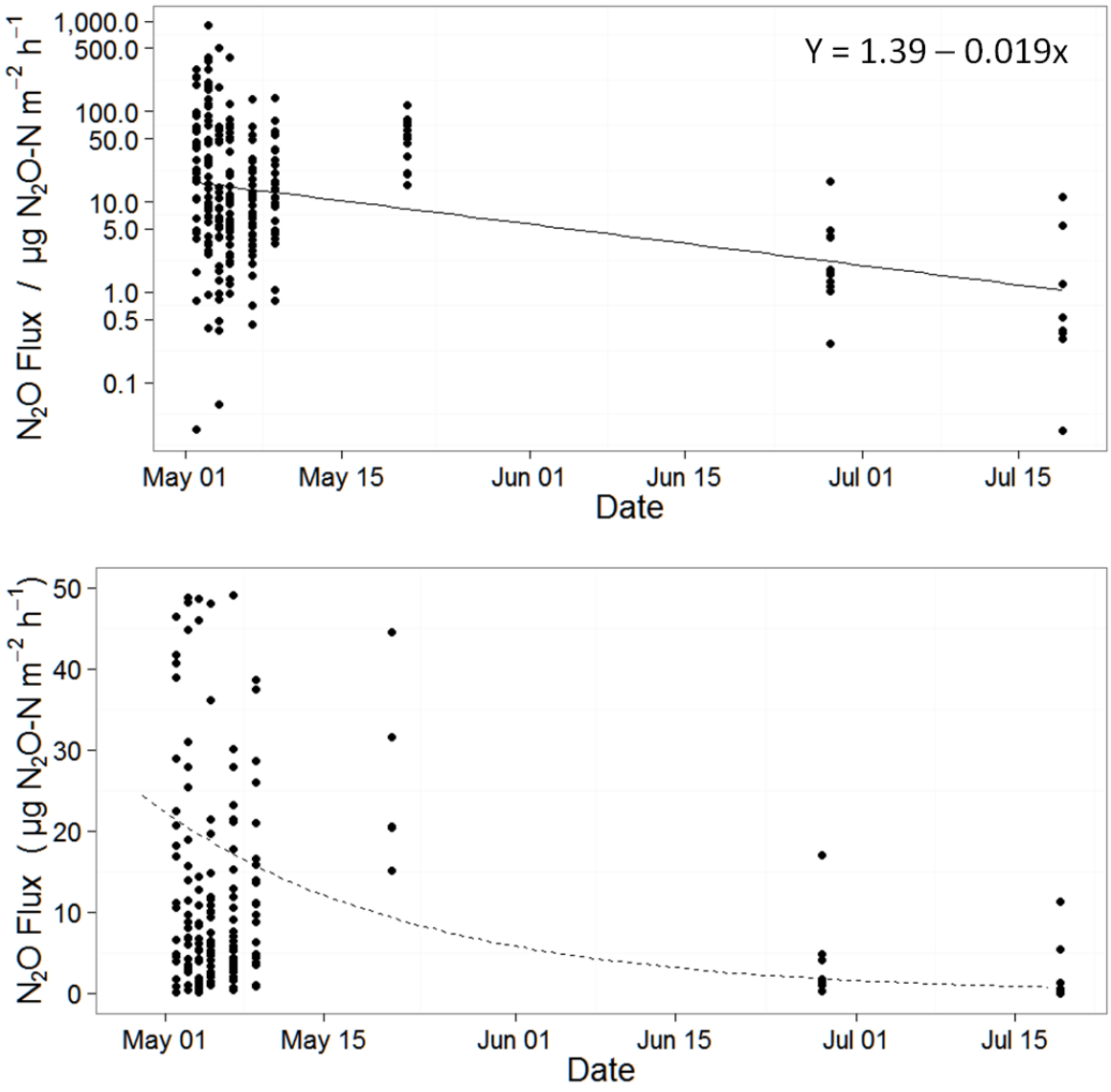

Figure 5.8 (a) Linear regression was used to fit a correlation between all $\log_{10}(N_2O)$ flux measurements and time after the tillage event. (b) This relationship was used to estimate daily fluxes over the 4 month measurement period which fit an exponential decay. The plot excludes flux measurements over 50 µg N_2O-N m^{-2} h^{-1} to show the fit in greater detail.

Emission factors from a typical fertiliser event can be used to draw comparisons between the estimated emissions of N_2O from the tillage event with that from nitrogen fertilisers used on the field. A typical nitrogen fertilisation event on the tilled field would normally use 70 kg N ha^{-1}. Using the IPCC N_2O direct emission factor (EF1) of 1% of applied nitrogen (IPCC, 2007) it can be estimated that a typical fertilisation event on the field would emit close to 700 g N_2O-N ha^{-1}. Past work has also been carried out on this field in which a method

to calculate a local emission factor for nitrogen fertiliser events was developed based on rainfall and fertiliser input (Skiba *et al*., 2012). This relationship predicts the emission factor of a nitrogen fertiliser event using the summed cumulative rainfall one week previous and three weeks after the event. A total of 105 mm of rain fell in this period resulting in an emission factor estimate of 2.9% for this particular date. Using this emission factor it can be estimated that an average fertilisation event on the field would emit close to 2000 g N_2O-N ha^{-1}, which is considerably higher than the 700 g N_2O-N ha^{-1} estimated using the IPCC method (Figure 5.9).

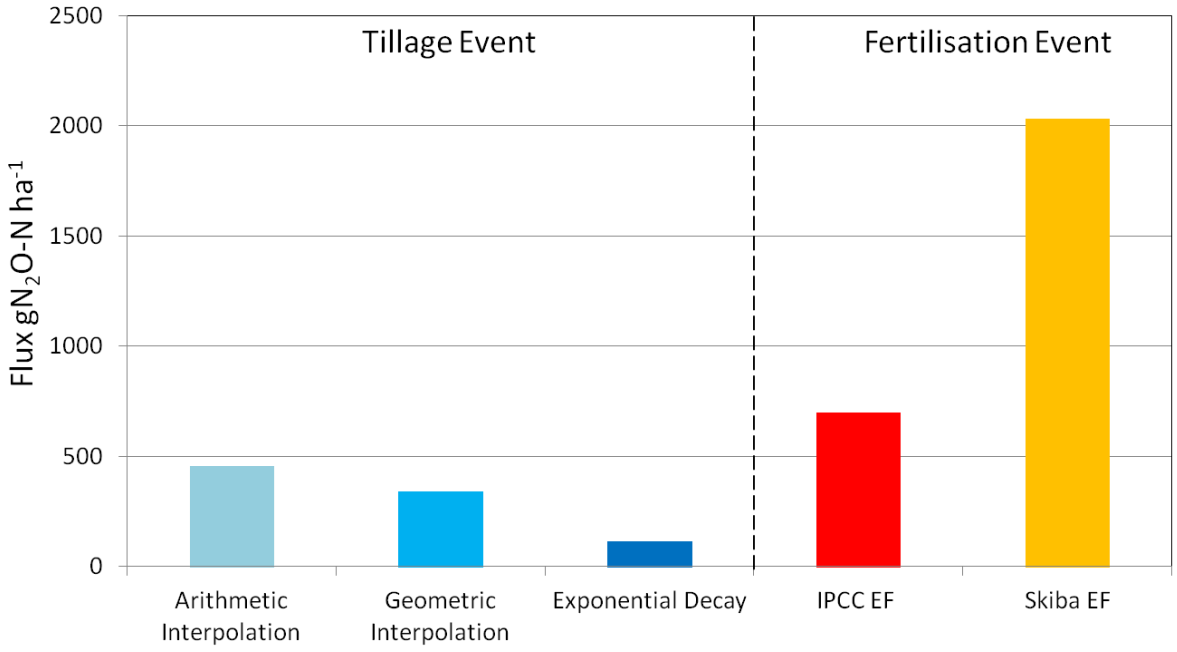

Figure 5.9 A comparison of the four month cumulative flux estimates for the Easter Bush tillage event (left) with the estimated N_2O flux from a typical 70 kg ha^{-1}fertiliser event at the field site (right).

The arithmetic mean, geometric mean and exponential decay methods estimate that cumulative emissions of 457, 342 and 114 g N_2O-N ha^{-1} are released over an 80 day period due to the tillage event respectively (Figure 5.9). This highlights the large uncertainty in calculating cumulative fluxes of N_2O using chamber methods and the significance of using different statistical methods to analyse and interpolate between measurements. This uncertainty is also observed when using chamber methods to measure N_2O fluxes from fertilisation events due to the same spatial variability and temporal gap filling involved. Using emission factors of 1 and 2.9% (described above) a range of 700 to 2000 g N_2O-N ha^{-1} is estimated for a typical fertilisation event in the field. Using these results it could be suggested that the tillage event can contribute from as much as 65% to as little as 5% of emissions associated with a typical fertilisation event at the field scale. This high

uncertainty in cumulative flux estimates highlights the need for better understanding of emissions of N_2O from tillage events and further research into how to interpolate N_2O measurement data.

5.5 Conclusion

The results from this experiment suggest that tillage events result in a short term increase in N_2O fluxes released from grassland fields. Due to the small spatial scale of the experiment, the N_2O emissions from tillage estimated in this paper (100 to 450 g N_2O-N ha^{-1}) is representative of a specific type of soil over a limited range of environmental conditions. This makes it a challenge to draw an accurate representation of the impact of tillage practices on a wider landscape containing different soil types, vegetation and densities, all of which are influenced by highly variable environmental conditions. The release of N_2O measured during this experiment (comparable to 5 to 65% of N_2O emissions expected from a nitrogen fertiliser event) suggests that any large scale national or global N_2O greenhouse gas budget would be incomplete without some estimated contribution from tillage. The study also highlights the need for better understanding of experimental design and statistical analysis of measurements in this particular subject in order to improve comparison between field sites and identify the true drivers of N_2O emissions in different climates. Tillage has often been dismissed as a small contributor to total N_2O emissions from agriculture; this work proves that in some conditions this may not be the case.

Chapter 6

Spatial variability and hotspots of soil N_2O fluxes from intensively grazed grassland

Summary

One hundred N_2O flux measurements were made from an area of intensively managed grazed grassland in central Scotland using a high resolution dynamic chamber method. The field contained a variety of features from which N_2O fluxes were measured including a manure heap, patches of decaying grass silage, and areas of increased sheep activity. Individual fluxes varied significantly across the field varying from 2 to 79,000 μg N_2O-N m^{-2} h^{-1}. Soil samples were collected at 55 locations to investigate relationships between soil properties and N_2O flux. Fluxes of N_2O correlated strongly with soil NO_3^- concentrations. Distribution of NO_3^- and the high spatial variability of N_2O flux across the field are shown to be linked to the distribution of waste from grazing animals and the resultant reactive nitrogen compounds in the soil which are made available for microbiological processes. Features within the field such as shaded areas and manure heaps contained significantly higher available nitrogen than the rest of the field. Although these features only represented 1.1% of the area of the field, they contributed to over 55% of the total estimated daily N_2O flux.

(Work presented in this chapter is based on the manuscript published as: N. J. Cowan, P. Norman, D. Famulari, P. E. Levy, D. S. Reay, U. M. Skiba: Spatial variability and hotspots of soil N_2O fluxes from intensively grazed grassland, to Journal of Biogeosciences, September 2014)

6.1 Introduction

Nitrous oxide (N_2O) is the single largest contributor to global stratospheric ozone depletion (Ravishankara *et al*., 2009) and a potent greenhouse gas (GHG). N_2O is formed naturally in soils and aquatic environments, primarily as a by-product of the microbial processes of nitrification and denitrification (e.g. Davidson *et al*., 2000; Wrage *et al*., 2001). Agricultural activities such as the use of nitrogen fertilisers and livestock farming have dramatically altered the natural nitrogen cycle in agricultural environments resulting in significantly increased global emissions of N_2O since pre-industrial times (IPCC, 2013). Agriculture is believed to be the largest source of global anthropogenic N_2O emissions with estimates as high as 80% of all anthropogenic emissions due directly or indirectly to agricultural activities (Isermann, 1994; IPCC, 2013).

Large scale N_2O flux estimates for terrestrial sources are often subject to large and poorly defined uncertainties which can limit the effectiveness of mitigation efforts in the agricultural sector (e.g. Bouwman *et al*., 1995; Oenema *et al*., 2005). Even estimates of N_2O fluxes from agricultural sources at much finer scales (i.e. the plot and farm scale) can be highly uncertain. This is predominately caused by the large temporal and spatial variability of N_2O fluxes due to the high heterogeneity of soil properties and microbiological processes (Parkin, 1987; Zhu *et al*., 2013; Chadwick *et al*., 2014). Soil properties which are believed to increase N_2O emissions by influencing the nitrification and denitrification processes include available nitrogen (in the form of ammonium (NH_4^+) and nitrate (NO_3^-)), available organic carbon, oxygen supply and pH (Davidson, 2000; Bateman and Baggs, 2005). Although it is known that these properties can alter N_2O production in soils, it is still difficult to accurately simulate the net effect on N_2O fluxes from areas (that are often considered to be homogeneous land cover) such as agricultural fields used for arable crops and grazing of livestock due to the heterogeneous nature of microbial populations and nitrogen availability in soils (Oenema *et al*., 1997; Conen *et al*., 2000; Jarecki *et al*., 2008).

The two main flux measurement methods applied to the field scale for N_2O in agricultural areas are the flux chamber method and the eddy covariance method (e.g. Jones *et al*., 2011; Skiba *et al*., 2012). Chamber fluxes are measured over a number of enclosed areas (typically smaller than 1 m^2) on a field, and a mean or median flux estimate is extrapolated to the farm, field or regional scale: the combination of up-scaling with the large spatial variability of N_2O sources often results in very significant uncertainty when estimating N_2O fluxes (Velthof *et al*., 1996). The advantage of using the eddy covariance method is that it can measure and integrate flux data directly over areas greater than 100 m^2 continuously without disturbing the soil or air environment.

For large homogeneous areas, which are well represented by an integrated value of flux, the eddy covariance approach is ideal, but it does not address the issue of spatial variability on reported fluxes within the measurement area. Eddy covariance also requires fast, sensitive equipment that often demands high power supply and so it can be an expensive option (Hensen *et al*., 2013).

In this experiment a high precision dynamic chamber method (See Chapter 4) was used to make 100 flux measurements of N_2O from an intensively managed grassland field which contained several features associated with elevated N_2O fluxes. Soil NH_4^+, NO_3^-, total carbon, total nitrogen, water filled pore space (WFPS), bulk density and pH were recorded from 55 out of 100 flux measurement locations. The aims of the experiment were: i) to measure the spatial variability of N_2O fluxes at a field scale, ii) to try to identify the main drivers of this variability, and iii) to provide better understanding of how N_2O flux estimates from agricultural soils can be improved.

6.2 Materials and methods

6.2.1 Field site

Flux measurements were carried out at an intensively managed grassland field owned by the University of Edinburgh (55° 52' 1.2144"N, 3° 12' 39.564"W) (Figure 6.1). This 6.78 ha field contained approximately 140 sheep (a mixture of ewes and lambs) during the three day measurement period between the 8th to the 10th of July 2013. This field had been used to graze predominately sheep for at least the last decade with regular nitrogen fertiliser application. The field contained several interesting features that provided the opportunity to measure N_2O fluxes from soils with a wide range of properties. The majority of the field (98.6% of the study area) could be classed as typical grazed grassland in which sheep were free to roam during the measurement period. The sheep had been present on the field for several months giving us the opportunity to measure from suspected hotspots of N_2O flux where sheep droppings had collected on the grass.

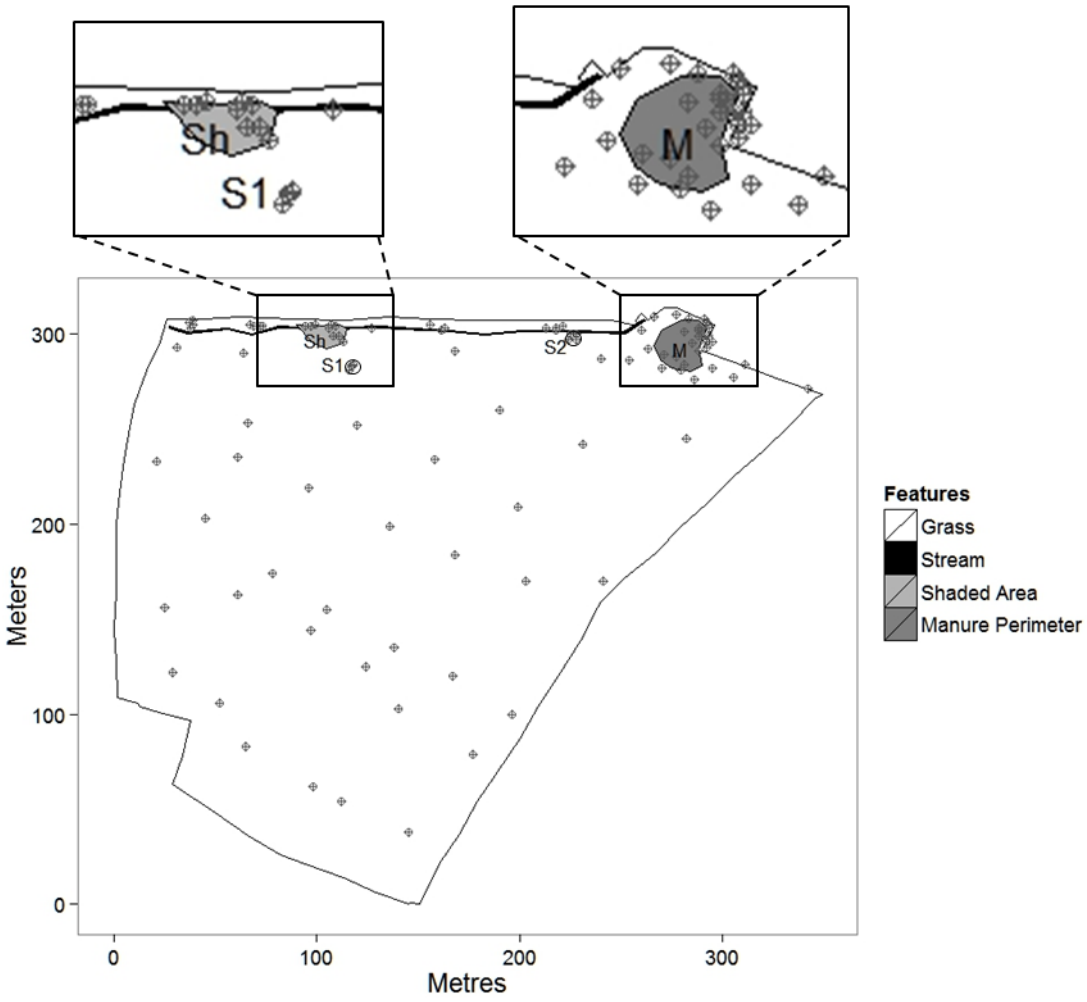

Figure 6.1 The locations of 100 flux measurements (markers) made over a 6.78 ha grazed grassland field using the closed loop dynamic chamber method (bottom). Details of the high density measurement areas in the north of the field are expanded (top). Features present in the field are outlined, including the tree shaded area (Sh), the two small patches of silage remains (S1 & S2) and the manure heap (M). The stream runs across the North of the field through the shaded area.

A drinking trough was situated in a shaded area under several large mature trees with wide leaf coverage at the north end of the field. The sheep had spent a lot of time in this shaded area due to the warm weather two to three weeks before measurements were made (Figure 6.2). This behaviour was observed during recent measurements carried out in adjacent fields unrelated to this study. Several flux measurements were made in the shaded area to investigate the effect that the recent increase in sheep density in this area had on N_2O flux.

Figure 6.2 The sheep preferred to spend time in the shaded area under two large trees at the north side of the field. The sheep would move from the shade to graze, then return to rest and drink from the stream during the measurement period.

Patches of decayed grass silage were visible in two small areas of the field. These patches remained after silage bales had been placed in the fields to feed sheep over the winter months (Figure 6.3). The patches had scarred the grassland leaving small areas of bare soil with decayed grass matter still present. Fluxes from both of these patches were measured during the experiment. A small running stream crosses the north side of the field which helped with drainage. Several flux measurements were made from the stream using the dynamic chamber to investigate if it was a significant source of N_2O.

Figure 6.3 Silage bales placed in the field in winter (left) had decayed away to small scarred patches visible in the grassland field (right).

One particular area of interest was a large manure heap which was situated in the Northeast corner of the field (Figure 6.4). This heap was a semi-permanent feature which had been used to fertilise a nearby barley field on several occasions. The heap reached a height of up to three metres and covered approximately 100 m^2 of the field, with a wider perimeter of contaminated soil. The area of influence of the manure heap contamination was uncertain due to consistent build up and removal of the heap over several years. A scarred area around the heap was visible with no grass present for several metres (See Figure 6.4). The scarred grassland was used as an indicator of the area of contamination of the manure heap. Measurements were made on the heap, from soils near the base of the heap and on the contaminated soils surrounding the heap at varying distances to investigate the spatial variability of this particular feature of the field.

Figure 6.4 A scarred area was visible in the grass where the manure heap had previously been before application to nearby fields (left). The remaining heap covered an area of soil approximately 100 m^2 which varied in height and manure type.

6.2.2 *Dynamic chamber method*

N_2O flux measurements were made using a non-steady-state flow-through (or closed dynamic) chamber system which circulated air between a flux chamber and a quantum cascade laser (QCL) gas analyser via an air pump (SH-110, Varian Inc, CA, USA) (for a full description of the system see Chapter 4). A compact continuous wave QCL (CW-QC-TILDAS-76-CS, Aerodyne Research Inc., Billerica, MA, USA) was used to measure gas mixing ratios within the dynamic chamber system (with a detection limit of approximately 30 nmol $mol^{-1}s^{-1}$ for N_2O). The instrument was secured inside a four wheel drive vehicle to allow mobile measurements. A diesel generator was kept on a tow trailer which provided electricity to the system. The chamber was placed onto circular aluminium collars which were inserted several cm into the soil (on average 5 cm) and almost flush to

the soil, prior to each measurement. Neoprene sponge formed an airtight seal between the chamber and the collar. When used to measure from the stream in the field the chamber was held steady in place by hand with the bottom slightly under the surface of the water. Two 30 m lengths of 3/8 inch ID Tygon® tubing were attached to both the inlet of the analyser and the outlet of the pump. This provided a 30 m radius from the vehicle in which the chamber could be placed. A flow rate of approximately 6 to 7 L min^{-1} was used between the analyser and the chamber.

Fluxes of N_2O were calculated using linear and non-linear asymptotic regression methods using the HMR package for the statistical software R (Pedersen *et al*., 2010; Levy *et al*., 2011). Using a mixture of goodness-of-fit statistics and visual inspection the regression method that provided the best fit for the time series of concentration was chosen for each individual measurement. The rate of change in concentration of a particular gas can then be used to calculate the soil flux for each measurement according to Equation 6.1.

$$F = \frac{dC}{dt_0} . \frac{\rho V}{A} \qquad \text{(Eq. 6.1)}$$

Where F is gas flux from the soil (nmol m^{-2} s^{-1}), dC/dt_0 is the initial rate of change in concentration with time in nmol $mol^{-1}s^{-1,}$ ρ is the density of air in mol m^{-3}, V is the volume of the chamber in m^3 and A is the ground area enclosed by the chamber in m^2.

6.2.3 Soil sampling and analysis

Fifty five of the one hundred locations from which dynamic chamber measurements were made were selected for soil analysis. From these locations 5 cm deep soil samples were taken from inside the chamber collar using a 2 cm wide corer immediately after the flux measurement was completed. These soils were used to calculate soil pH and available nitrogen in the form of ammonium (NH_4^+) and nitrate (NO_3^-) via KCl extraction (see below). Soil cores were taken immediately after the flux measurement using a sharp metal cutting cylinder (7.4 cm diameter, 5 cm deep) which was carefully hammered into undisturbed soil. Samples were used to calculate total carbon and nitrogen content of the soil, soil moisture content (via oven drying at 100 ˚C) and WFPS as well as bulk density. WFPS was calculated from the bulk density soil samples using Equation 6.2 (Rowell, 1994).

$$WFPS = \frac{V_{cont} \times 100}{1 - \left(\frac{r_b}{r_d}\right)} \qquad \text{(Eq. 6.2)}$$

Where WFPS is the percentage of porous volume in the soil filled by water, V_{cont} is the volumetric water content of the soil, r_b is the bulk density of the soil in g cm^{-3} and r_d is the particle density of the soil (assumed as 2.65 g cm^{-3}) (Rowell, 1994).

KCl extractions were carried out on 15 g un-dried soil samples (kept frozen until extraction) using 1 mol L^{-1} KCl solution. Concentrations of NH_4^+ and NO_3^- were measured using a Bran and Luebbe AutoAnalyser (SPX Flow Technology, Norderstedt, Germany). The mass of available nitrogen in the soil was calculated using Equation 6.3.

$$N = \frac{C \times V}{m} \quad \text{(Eq. 6.3)}$$

Where N is the mass of nitrogen in the form of NH_4^+ or NO_3^- in g (per kg of soil), C is the concentration of NH_4^+ or NO_3^- measured in the analysis of KCl extract in mg L^{-1}, V is the volume of solution in which the soil sample was mixed with KCl in L, and m is the mass of dry soil mixed with the KCl solution in g.

6.2.4 Sampling locations

Flux measurement locations for the majority of the filed coverage were chosen at intervals with some degree of randomness while driving back and forward across the field. A selection of feature areas in which multiple measurements were made in close proximity were also included (See Figure 6.1). 50 measurements were made on what was considered 'normal' grassland across the field. This provided an estimate of the spatial variability of N_2O flux across the field without interference from the hotspot features. Chamber placement on the grassland area included some locations where sheep droppings were present. These locations were noted during measurements when visible.

Two features which were measured in more detail were patches of the field which contained the remains of decayed grass silage and a large area shaded by trees in which the sheep had spent much of their time due to the warm weather (See Figures 6.2 & 6.3). A total of seven flux measurements were made over two patches of decayed grass silage. Only small residues of the grass silage were visible, mixed in with the soil in these areas as the sheep had consumed the majority of it months before the measurement period. The patches were easily visible due to the lack of grass on the bare soil where the silage bales had been left. Five flux measurements were made in the shaded area in which the sheep had access to a water trough. The precise area

which had been influenced by increased sheep activity was difficult to measure for certain, although an increased number of animal droppings, clumps of wool and damp urine patches were visible in this area of the field.

Flux measurements were made using the chamber from a stream: nine sampling points were chosen where the stream was wide enough to fit the chamber onto the surface of the water. The stream was approximately 5 m away from the North edge of the study area. These measurements of flux were not as reliable as the measurements made on the soil, due to the unavoidable disturbance on water pressure and flow caused by the chamber. These flux estimates can still be used as a rough approximation of the N_2O which is emitted from the stream as it passes through this field.

Ten N_2O flux measurements were made directly on top of the manure heap located on the field (See Figure 6.4) at differing heights (0.5 to 3 m). Care was made not to physically disturb the chamber during measurements to prevent additional gases escaping from the porous manure surface. Seven sampling points were taken near the foot of the heap where the manure met the soil. 6 flux measurements were made at distances of 5 to 10 metres and a further five more were made at 10–20 m from the heap.

6.3 Results

6.3.1 Variation in N_2O fluxes at the field scale

The three day measurement period (8th to 10th July 2013) was very dry with no rainfall and relatively low soil moisture contents (ranging from 9 to 50% WFPS). Daily temperatures were similar, with mean daytime soils temperatures recorded as 15.7, 16.6 and 15.9 ˚C on the 8th, 9th and 10th of July respectively.

Fluxes from the grassland followed a geometric (log-normal) distribution ranging between 2 to 227 µg N_2O-N m^{-2} h^{-1}, with arithmetic and geometric mean values of 25 and 13 µg N_2O-N m^{-2} h^{-1} respectively (Figure 6.5). No negative fluxes of N_2O were measured during this experiment at any of the locations. Droppings were present at locations where the two largest fluxes were measured from the grassland (227 and 132 µg N_2O-N m^{-2} h^{-1}), although fluxes measured at other locations which contained droppings were not always larger than those observed on clear (dropping-free) grassland (Figure 6.5).

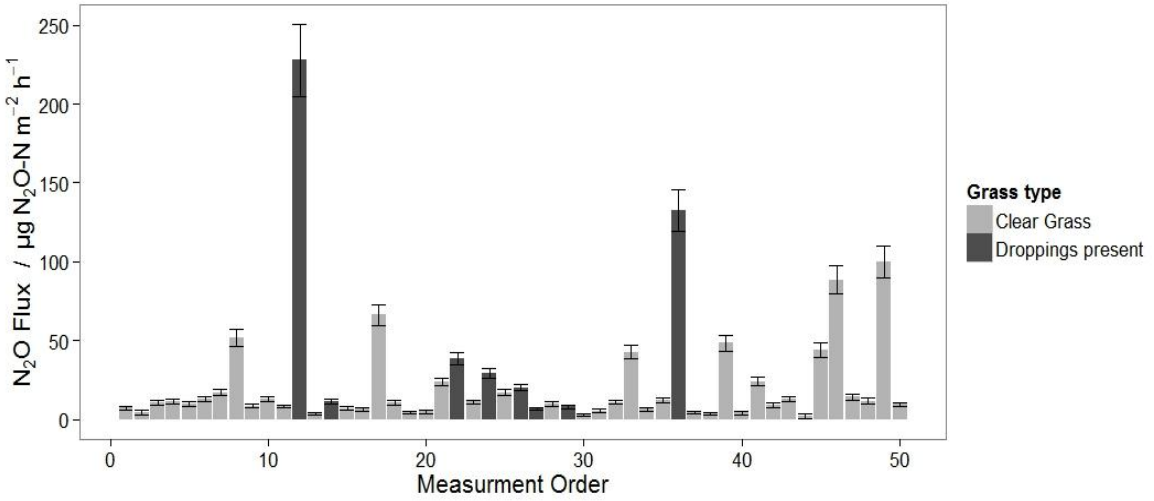

Figure 6.5 Fifty flux measurements of N_2O were made on grazed grassland: the sampled locations which contained visible sheep droppings are represented by the darker bars. Error bars represent the uncertainty in each flux measurement which was calculated using a propagation of regression, volume, temperature and pressure uncertainties (See Chapter 4).

6.3.2 Silage and Shaded Patch Fluxes

N_2O fluxes measured from these plots were higher than those measured from the grassland area. Fluxes varied from 1160 to 13,400 µg N_2O-N m^{-2} h^{-1} (Figure 6.6a). The arithmetic and geometric mean values of these fluxes were 3750 and 2660 µg N_2O-N m^{-2} h^{-1} respectively.

These fluxes varied between 200 and 9600 µg N_2O-N m^{-2} h^{-1} (Figure 6.6b). The arithmetic and geometric mean values of these fluxes were 2983 and 1217 µg N_2O-N m^{-2} h^{-1} respectively. The two measurements made in the centre of the shaded area appeared to contain more animal droppings and emit higher fluxes, whereas the outer perimeter appeared more similar to the surrounding grassland area and fluxes were lower. It was likely that the additional presence of sheep had influenced N_2O production in this area, although the effect of the shade (on soil moisture content) and a difference in organic material composition (due to leaf litter) provided by the tree may have also contributed.

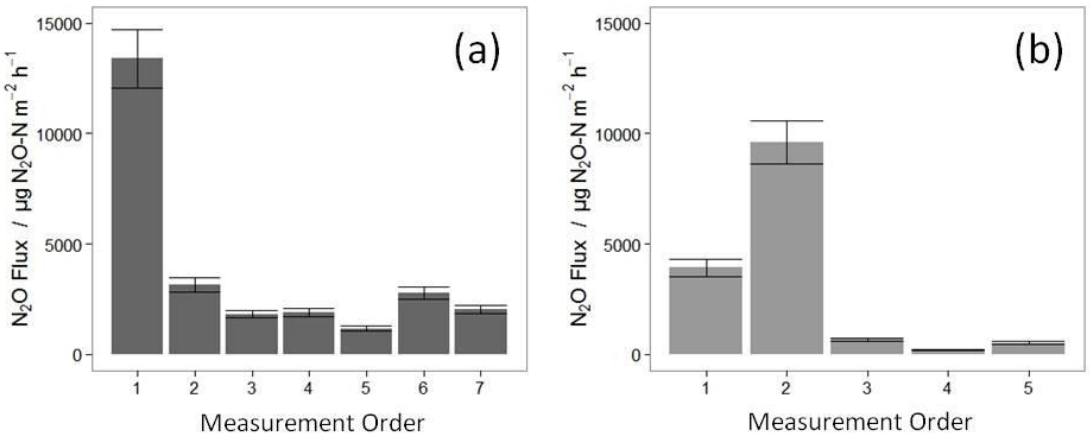

Figure 6.6 (a) Flux measurements made on patches of decayed grass silage. Measurements 1–3 were taken from the first patch (referred as S1 in Figure 6.1) and the remaining four were measured from the second (referred as S2 in Figure 6.1). (b) Flux measurements made from a shaded area with increased sheep density. The first two of these measurements were made near the centre of the shaded area. Fluxes from both features were made during the same three day measurement period between the 8th to the 10th of July 2013. Error bars represent the uncertainty in flux measurement calculated using a propagation of errors from regression, volume, temperature and pressure (as described in Chapter 4).

6.3.3 Drainage stream fluxes

Fluxes from the stream varied from 1 to 22 µg N_2O-N m^{-2} h^{-1} (Figure 6.7) with arithmetic and geometric mean values of 9.5 and 7.1 µg N_2O-N m^{-2} h^{-1} respectively. These fluxes were similar in magnitude to some of those measured from the grassland area, although hotspots were not observed in the stream, even in areas with higher turbulence in which de-gassing of N_2O would be expected to be higher (Reay et al., 2003). Uncertainty in flux measurements from the stream was generally larger than for equivalent fluxes measured from the grassland soils due to higher uncertainty in the regression analysis. The concentration change within the chamber did not follow the linear or non-linear models as well as fluxes measured from soils. The surface area of the stream crossing the field was approximated at 183 m^2 using a combination of GPS coordinates and water body width measurements. It is not possible to determine whether N_2O fluxes from the stream were a result of nitrogen input from the grazed field in the experiment, or from sources further up the stream. It is also not possible to determine the magnitude of N_2O fluxes which may have occurred further downstream as a result of inputs from the field. The measurements were made only as an indicator of the fluxes from the stream within the field area.

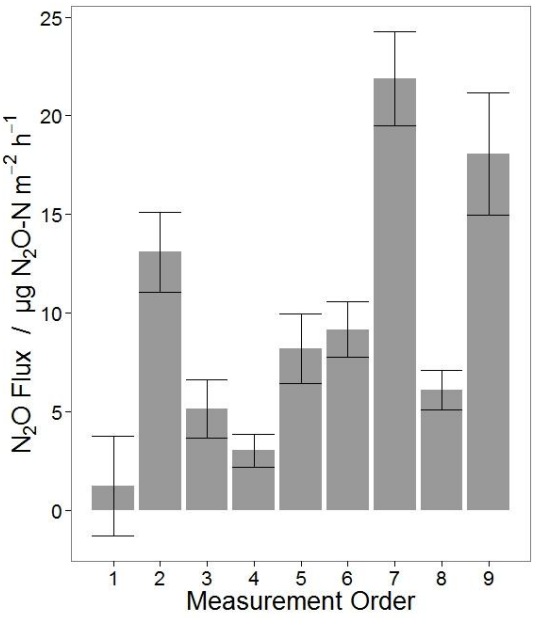

Figure 6.7 N_2O fluxes measured from different locations in a drainage stream in the grazed grassland field. Hotspots of N_2O flux were not observed in the stream measurements. Uncertainty was calculated for each measurement, as was done for the fluxes measured from soils in the field.

6.3.4 Manure heap fluxes

Fluxes varied in magnitude significantly across the manure heap with measured values ranging between approximately 660 to 79,000 µg N_2O-N m^{-2} h^{-1} (Figure 6.8). Two of the measurements recorded very high N_2O fluxes exceeding 35,000 µg N_2O-N m^{-2} h^{-1}. No relationship between depth of the heap and N_2O flux was observed from these measurements. Seven sampling points were taken near the foot of the heap: fluxes recorded from these locations showed a similar mixture of very large and comparatively small fluxes of N_2O, varying by up to three orders of magnitude, between 85 and 31,250 µg N_2O-N m^{-2} h^{-1}. Again, no clear spatial pattern was observed in the fluxes around the heap. A further 6 flux measurements were made at distances of 5 to 10 metres and five more were made at 10–20 m from the heap. The arithmetic and geometric mean fluxes recorded from the 5 to 10 metre range were 6800 and 2000 µg N_2O-N m^{-2} h^{-1} respectively. The arithmetic and geometric mean fluxes recorded from the 10 to 20 metre were 466 and 91 µg N_2O-N m^{-2} h^{-1} respectively. These results suggest that the influence of the manure heap on N_2O fluxes decreases rapidly after a distance of approximately 10 metres (See Figure 6.8).

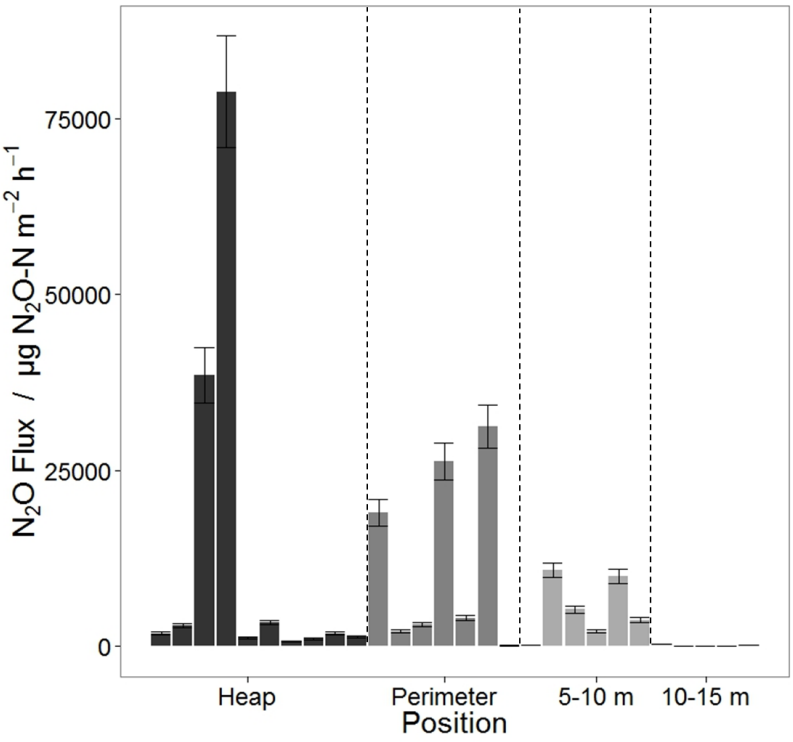

Figure 6.8 N_2O flux measurements from a semi-permanent manure heap located on the grassland field. Vertical dashed lines split the measurements into groups separated by distance from the heap with the left side of the figure being the nearest and right side the furthest from heap The darkest bars in the figure represent measurements made on top of the actual manure heap. Next are the measurements made from the base of the heap, then those made 5 to 10 m and 10 to 15 m from the heap.

6.3.5 Variation in soil properties at the field scale

Soil measurements were made from 55 of the 100 flux measurement locations (Table 6.1). The majority of these samples (n = 38) were taken from the grassland area to assess the natural heterogeneity of the soil throughout the field. The remaining soil samples were taken from the visible hotspot features of the field to investigate the causes of elevated N_2O emissions (n = 17).

The most variable of the soil properties across the grassland area were the concentrations of the available reactive nitrogen in the form of NH_4^+ and NO_3^- (See Table 6.1). Locations with elevated NH_4^+ also generally recorded higher NO_3^- concentrations, although this relationship was not consistent at all locations (R^2 = 0.56). Soil samples taken from patches of decayed grass silage and the shaded area indicated that these small areas had significantly greater concentrations of NH_4^+ and NO_3^- ($p < 0.01$) compared to the grassland area.

Reactive nitrogen concentrations in soils from the perimeter of the manure heap also showed wide variations, with some extremely large (2.2 g N kg^{-1}) and small (0.1 g N kg^{-1}) values being measured (Table 6.1).

Total carbon and nitrogen content of the soil from the grassland area showed less variation than the reactive nitrogen content, with a small number of elevated outlier values. The ratio of carbon to nitrogen content of the soils (12:1) was consistent across the measurement locations (R^2 = 0.94). Total soil carbon and nitrogen concentrations from the shaded area and silage remains were similar in magnitude to the grassland area measurements. The manure heap perimeter was the exception to this, presenting some very high concentrations of carbon and nitrogen. Total carbon and nitrogen content of the soils around the manure heap varied from small concentrations similar to the grassland soil (8 g N kg^{-1} and 107 g C kg^{-1}) to concentrations as large as 34 g N kg^{-1} and 355 g C kg^{-1} (Table 6.1).

Soil pH varied little between most of the measurement locations in the grassland area with the majority of the grazed field confidently estimated at pH levels of 5.6 +/- 0.34 (n = 38), in agreement with measurements made in similar managed grazed fields in this area. Soil pH from the silage remains and tree shaded area was generally more alkaline (pH 6.9 +/- 1.5) than from the grassland area. The soils from the manure heap perimeter were highly alkaline (pH 8.3 +/- 0.85) (Table 6.1).

WFPS values were relatively consistent across the field with the majority of measurements ranging between 20 to 25%. The bulk density of the soil in the field was also fairly consistent ranging between 0.65 to 0.80 g cm^{-3}. Due to the heterogeneous nature of soils there were several outliers for each of the soil properties measured across the field (Table 6.1).

Table 6.1 Summary of relevant soil properties of all 55 soil measurements made during flux measurements. Soil samples were taken from inside the chamber area immediately after flux measurements were completed. The mean values and range (in brackets) of measurements from each variable within the field are included in the table.

Feature	**Soil Samples** (n)	**Area** (m^2)	**NH_4^+** (g N / kg)	**NO_3^-** (g N / kg)	**Total Carbon** (g C / kg)	**Total Nitrogen** (g N / kg)	**pH**	**WFPS** (%)	**Bulk Density** (g / cm^3)
Grass	38	66861	0.06 (0.01 – 0.75)	0.02 (0.00 – 0.20)	60 (44 – 104)	4.7 (3.4 –9.5)	5.6 (4.7 – 6.6)	25 (9 – 37)	0.8 (0.6 – 1.0)
Silage remains	5	36	0.25 (0.04 – 0.93)	0.161 (0.05 – 0.24)	77 (44 – 119)	5.9 (3.8 – 8.5)	6.4 (5.2 – 8.3)	43 (38 – 50)	0.9 (0.7 – 1.1)
Shaded area	3	210	0.29 (0.04 – 0.49)	0.09 (0.01 – 0.24)	52 (10 – 106)	4.3 (0.8 – 9.2)	7.4 (6.1 – 3.2)	34 (24 – 44)	1.0 (0.8 – 1.1)
Stream	0	183	NA	NA	NA	NA	NA	NA	NA
Manure heap	0	102	NA	NA	NA	NA	NA	NA	NA
Manure heap perimeter	7	a	0.99 (0.09 – 2.18)	0.10 (0.000 – 0.59)	217 (108 – 355)	18.8 (8.0 – 34.1)	8.3 (7.0 – 9.4)	23 (14 – 32)	0.4 (0.2 – 0.9)
Manure perimeter (5- 10 m)	1	b	0.04	0.40	52	5.4	6.0	34	1.0
Manure perimeter (10 – 15 m)	1	406	0.01	0.00	112	9.6	7.2	11	0.8

[a] As Manure heap [b] Total manure perimeter area of influence estimated as 406 m

6.3.6 Correlation between soil properties and N_2O flux

Multiple linear regression was used to investigate the relationships between the soil properties presented in Table 6.1 (also soil porosity) and N_2O flux (See Section 3.6.3). Due to the wide ranging and uneven distribution of measurements for both N_2O flux and soil properties, the common logarithm (hereafter referred to as $\log_{10}$) of several of these measurements (N_2O flux, NH_4^+, NO_3^- , total carbon and total nitrogen content) was used for the multiple linear regression. Correlations of soil properties were carried out using multiple linear regression in the statistical software R. The soil properties from all of the features in the field were processed together as one group (n= 55).

Linear regression was first of all carried out using all of the measured soil properties for each of the fits. After the initial fit, the properties which were not statistically significant ($p > 0.1$) were removed and the fit

was run again using only the significant values (See Table 6.2). Concentrations of NH_4^+ in soils were found to correlate well with pH and total carbon and nitrogen (R^2 = 0.64) (Figure 6.9a). High total carbon and nitrogen contents were indicative of an increased presence of total organic carbon (TOC) in the soils.

Concentrations of NO_3^- correlated strongest with TOC and NH_4^+ present in the soil (R^2 = 0.77) (Figure 6.9b). NO_3^- concentrations were presumed to be indicative of microbial nitrification activity in the soil as it is the primary product of this process. Fluxes of N_2O ($log_{10}(N_2O)$) correlated strongly with NO_3^-, pH and WFPS (R^2 = 0.86) (Figure 6.9c). The soil property with the most significant correlation with N_2O flux was NO_3^- (See Table 6.2).

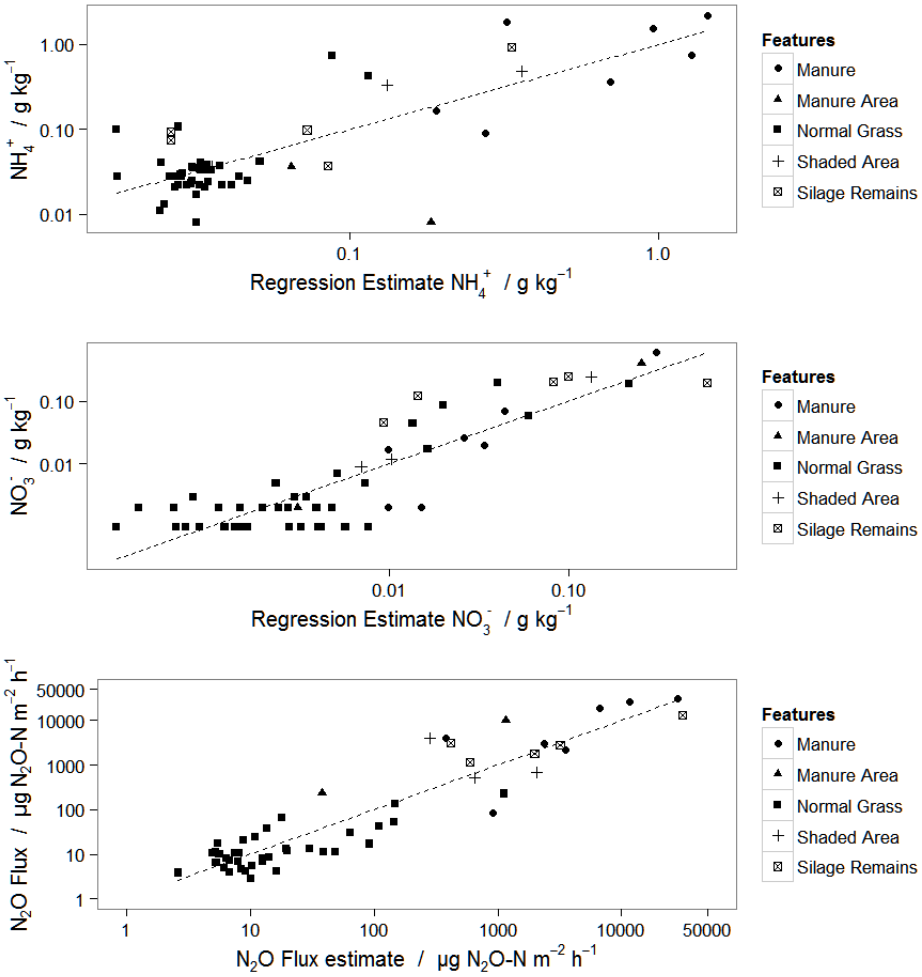

Figure 6.9 Multiple linear regression used to identify relationships between NH_4^+ (a), NO_3^- (b) and N_2O flux (c) with soil properties measured during flux measurements from grazed grassland (See Table 6.2 for fitting parameters). All 55 soil samples collected from multiple features present in the field were included in the regression analysis.

Table 6.2 Multiple linear regression correlation of soil properties and N_2O flux as plotted in Figure 6.9.

	Estimate	S.D.	Statistical significance
a) $Y = \log_{10}(NH_4^+)$			
(Intercept)	- 2.56	0.8	b
pH	0.37	0.05	a
$\log_{10}$(Carbon g Kg^{-1})	- 1.14	0.6	d
$\log_{10}$(Nitrogen g Kg^{-1})	1.53	0.8	d
b) $Y = \log_{10}(NO_3^-)$			
(Intercept)	- 402	205	d
$\log_{10}$(NH_4-N g Kg^{-1})	0.5	0.1	a
$\log_{10}$(Carbon g Kg^{-1})	-6.7	0.9	a
$\log_{10}$(Nitrogen g Kg^{-1})	8.6	1.1	a
WFPS%	0.04	0.01	b
Soil porosity	404	205	d
Bulk density g cm^{-1}	155	77.4	d
c) $Y = \log_{10}(N_2O$ Flux)			
(Intercept)	- 4.3	1.3	b
$\log_{10}$(NH_4-N g Kg^{-1})	- 0.25	0.20	e
$\log_{10}$(NO_3-N g Kg^{-1})	0.76	0.10	a
pH	0.60	0.10	a
WFPS%	0.04	0.01	a
Soil porosity	3.85	1.3	b

Significance of p-value: 0 ‘a’ 0.001 ‘b’ 0.01 ‘c’ 0.05‘d’ 0.1 ‘e’

6.4 Discussion

6.4.1 Variation in N_2O fluxes at the field scale

N_2O fluxes measured from the grazed grassland area of the field (excluding the hotspot areas) were highly variable (between 2 to 227 µg N_2O-N m^{-2} h^{-1}). This is a common phenomenon which is verified in many N_2O flux measurement experiments (e.g. Oenema *et al*., 1997; Skiba *et al*., 2012). Flux magnitude was unpredictable across the grassland and in some cases varied by two orders of magnitude across relatively short distances (<10 m). 80% of the fluxes measured from the grassland area were below 30 µg N_2O-N m^{-2} h^{-1}. Fluxes of N_2O comparable to this magnitude are often measured from grazed fields in different climates in between fertilisation events (Clayton *et al*., 1997; Oenema *et al*., 1997; Luo *et al*., 2013). The advantage of using the closed loop dynamic chamber (Chapter 4) in this experiment was that the extremely high precision (1 µg N_2O-N m^{-2} h^{-1})

allowed us to confidently report very low individual N_2O fluxes across the field and compare these measurements with the relevant soil properties collected from within the measurement plot at each individual location.

The largest fluxes in the field were measured from the hotspot features present (up to 79,000 µg N_2O-N m^{-2} h^{-1}). Fluxes from the shaded area and the silage heap remains were consistently higher than those measured on the grassland area. The shaded area presented an increased number of sheep, with the resultant increase in animal waste freshly deposited there (NH_4^+). Fluxes measured from the silage heap remains were surprisingly high. Decaying plant matter is known to emit N_2O (Hellebrand, 1998), but it is unclear whether the emissions from these patches are due to the additional organic materials present in the soil or to the increased sheep activity and resultant urine and faeces deposits. The larger pH values from the shaded areas, as well as the manure heap and perimeter suggest that animal waste was the most likely source of N_2O. The combination of large concentrations of mineral N and organic C in a high pH environment are ideal conditions for denitrification (Hofstra and Bouwman, 2005; Saggar *et al*., 2013), which is most probably the main source of the N_2O here.

Fluxes of N_2O from the stream were relatively small (1 to 22 µg N_2O-N m^{-2} h^{-1}) compared with those measured from the rest of the field. Significantly higher fluxes have been measured from drainage streams at the Bush Estate in previous experiments (100 to 1000 µg N_2O-N m^{-2} h^{-1}) using different methodology (Reay *et al*., 2003). Dry conditions in the run up to the measurement period had decreased any leachate from the soils entering the stream. Past experiments have reported N_2O flux measurements from agricultural streams similar in magnitude to those made in the surrounding soils (Baulch *et al*., 2011); however, it is likely that the N_2O fluxes measured in this experiment are lower than they would have been had the measurements taken place on a wetter date when drainage waters containing N_2O and other nitrogen compounds from surrounding fields would also have been entering the stream.

Flux measurements made on and around the manure heap were on average 420 times higher than the fluxes measured for the grassland area of the field. The large spatial variability of N_2O flux observed from the heap was similar to that of a previous experiment carried out on the farm estate using static chamber measurements, although reported fluxes are an order of magnitude smaller in this study (Skiba *et al*., 2006). Solid manure heaps are a known large source of N_2O emissions and several studies have estimated emission factors for such heaps (Chadwick *et al*., 1999; Amon *et al*., 2001; Skiba *et al*., 2006). Emission factors for

manure heaps are often calculated by volume of stored manure. This implies a large degree of variability, following from different components of animal waste as well as the age of the waste and how it is stored (Amon *et al*., 2001). Application of the manure as fertiliser is often considered in the emission factor of animal waste as well as storage (Chadwick *et al*., 1999; Velthof *et al*., 2003; Chadwick *et al*., 2011). Measurements made in this experiment did not account for manure volume or calculate an emission factor for the heap; however, this study highlights that an additional factor may also need to be taken into account for a more accurate estimate of the emission factor of solid manure storage (i.e. the legacy emissions of a manure heap). Very high N_2O fluxes (up to 10,825 µg N_2O-N m^{-2} h^{-1}) were measured from the area around the manure heap which had become contaminated with the animal waste. Our data have shown that these areas that are highly enriched with available nitrogen compounds and organic matter remain after the manure heap has been removed, and can continue to emit N_2O for months, as was observed for the patches of silage heap remains (manure was spread in autumn, nine months prior to measurements). The high emissions and lasting effect of these areas may contribute significantly to the overall emission factor of solid manure heaps and agriculture as a whole when the large volumes of animal waste and storage from livestock farms are considered.

6.4.2 Correlation between soil properties and N_2O flux

High concentrations of NH_4^+ and NO_3^- are known to increase N_2O fluxes from soils as they are the primary nutrients required for the microbial processes of nitrification and denitrification in which N_2O is produced and then released to the atmosphere (Davidson *et al*., 2000). Animal urine and droppings are a known source of urea ($CO(NH_2)_2$ and ammonia (NH_3) which are both alkaline and convert to NH_4^+ in the presence of water (Freney *et al*., 1983). A strong positive correlation between NH_4^+ concentrations and soil pH was observed across the field (See Table 6.2). As ruminant (sheep and cattle) urine is normally slightly alkaline the increased pH in the small hotspot areas suggested that increased alkaline animal waste deposition was the reason for the increase in pH and resultant available NH_4^+ in the soil. This relationship has also been observed in other studies (e.g. Haynes and Williams, 1992). Organic matter in the soils (Total C and N) also correlated with NH_4^+ concentrations in the soils (See Table 6.2). Mineralisation of animal waste, and plant materials such as silage, continues to provide NH_4^+ to soils over extended periods (Martins & Dewes, 1992; Van Kessel and Reeves, 2002). All of the N_2O flux hotspot features of the field contained elevated concentrations of NH_4^+ in the soil (See Table 6.1); however the concentration of NH_4^+ was not found to correlate significantly with N_2O fluxes (See Table 6.2).

NO_3^- concentrations in the soil correlated well with available NH_4^+ and organic matter (See Figure 6.9b). The physical properties of the soil were also influential as NO_3^-correlated strongly with WFPS, and weakly with bulk density and soil porosity. Elevated NO_3^- concentrations in the soil can be associated with high rates of nitrification, as NO_3^- is the primary product of the nitrification process. The strong correlation between NO_3^- with the available NH_4^+ and organic material present in the hotspot features of the field provides strong evidence that elevated concentrations of NO_3^- in these areas is due to nitrification occurring at an increased rate. The soils measured in this study were relatively dry (9–50% WFPS), therefore more conducive for nitrification than denitrification (Davidson *et al*., 2000; Bateman and Baggs, 2005). However the presence of organic matter would have created the necessary anaerobic conditions required for denitrification in localised microsites, through increased O_2 consumption required for organic matter decomposition (Sexstone *et al*., 1985). No significant correlation between organic carbon and N_2O flux was observed in this data set. Organic carbon is known to be a limiting factor of denitrification rates in some soils (McCarty and Bremner, 1992); however, it is possible that the lack of correlation between carbon and N_2O flux measured in this experiment is due to the abundance of carbon available in the soils.

Correlation between N_2O flux and the measured soil properties showed that NO_3^- concentrations were the most significant factor (Table 6.2). The strength of the correlation with NO_3^- and lack of correlation with NH_4^+ does not explain if fluxes are predominantly caused by either microbial nitrification or denitrification. The presence of NO_3^- indicates that nitrification is definitely happening at these sites; however, the lack of correlation between NH_4^+ and N_2O flux suggests that denitrification may be the primary source of emissions. The correlations indicate that areas in which the concentrations of available nitrogen compounds are higher emit more N_2O, and therefore, available nitrogen input is likely to be the primary driver of the spatial variability observed in N_2O flux measurements in this study. This relationship between soil NO_3^- and NH_4^+ concentrations and N_2O flux is also observed in similar studies (e.g. Turner *et al*., 2008). Our conclusion from the correlation analysis is that the high spatial variability of N_2O flux across the grazed field is primarily due to the uneven distribution of nitrogen deposition in the form of animal waste.

There remains a high degree of uncertainty in the relationship between the soil properties and N_2O flux. This study suggests NH_4^+, NO_3^- and organic matter can be used as indicators to predict where fluxes will be higher in the field. Exact fluxes are more difficult to estimate due to the large number of variables which affect the rates of microbial processes. Similar studies carried out in different environments predicted very different

significance values for each of the measured soil properties depending on environmental factors (Šimek *et al*., 2006; Turner *et al*., 2008). In order to better understand these processes more detailed experiments would be required in a variety of geographical and environmental conditions to better predict the behaviour of microbial processes in soils with high available nitrogen concentrations. Alternatively, a more controlled analysis of individual soil properties and microbial processes can be examined under laboratory conditions using similar high precision chamber methodology. Ideally the use of this equipment could be paired with 15N labelled nitrogen compounds (such as urea) and denitrification inhibitors to investigate the biological mechanisms in N_2O production and determine relationships between these processes and soil properties.

6.4.3 Interpolation of N_2O fluxes at a field scale

The simplest way to estimate the total daily N_2O flux from the field during the measurement period is to combine the relevant area and mean flux recorded for each of the features of the field. Due to the uneven distribution of flux magnitude and the many large hotspots of flux measured using the chamber method in this experiment, geometric mean values were chosen to determine fluxes across the field scale (Table 6.3).Using the geometric mean values an estimate of 48 g N_2O-N d^{-1} was emitted from the field site during the measurement period. (See Table 3) (123 g N_2O-N d^{-1} estimated using the arithmetic mean). The grassland area of the field which accounts for 98.6% of the study area contributed 45% (21.3 g N_2O-N) of the estimated daily N_2O flux from the field. The silage remains and shaded area contributed 5 and 13% to the total emissions, respectively. The manure heap and soils contaminated by the heap contributed a very large 38% (18 g N_2O-N) of the total flux estimate which comes from a relatively small area of the field (0.8%) (Table 6.3).

Using mean values to interpolate N_2O flux at the field scale results in very high uncertainty values due to the high spatial variability of the N_2O fluxes (Table 6.3). From this experiment the total daily flux is estimated to be between 13 and 215g N_2O-N d^{-1}. These high uncertainties highlight the weakness of the chamber methodologies inability to account for spatial variability of N_2O flux over large areas and the importance of spatial variability when N_2O flux estimates are made using simple interpolation methods on a large scale. These results also highlight the need for a better understanding of how agricultural flux measurements are made using current methodology. Flux chamber placement is vital in understanding the variability of N_2O flux across a field. Without a good understanding of N_2O hotspots and the appropriate positioning of chambers to include (or exclude) these areas, chamber methods will not be able to provide effective comparable results between experiments.

Table 6.3 Geometric mean flux values and estimated cumulative flux from each of the measured features across the field scale. 95% confidence intervals (CI's) are included.

Field Feature	Area (m^2)	Geometric Mean Flux ($\mu g\ N_2O\text{-}N\ m^{-2}\ h^{-1}$)	95% C.I.	Cumulative Flux ($g\ N_2O\text{-}N\ d^{-1}$)	95% C.I.
Grazed grassland	66861	13	(4.7 - 37.2)	21.3	(7.6 - 59.8)
Silage remains	36	2664	(1220 - 5815)	2.3	(1.1 - 5.0)
Shaded area	210	1217	(252 - 5881)	6.1	(1.3 - 29.6)
Stream	183	7	(3 - 17.5)	0	(0.0 - 0.1)
Manure heap	102	3195	(656 - 15562)	7.8	(1.6 - 38.1)
Manure perimeter	50	4470	(573 - 34875)	5.4	(0.7 - 41.9)
Manure outer perimeter	366	551	(66 - 4628)	4.8	0.6
Total	67808			47.7	(12.8 – 215.1)

Other methods of interpolation exist when using chamber measurements, although these also struggle to account for the spatial variability of N_2O at larger scales. Fluxes measured from the field in this experiment showed some predictability in spatial patterns as fluxes were higher in certain hotspot locations, although knowledge of these locations is required to observe this predictability as there was little relationship observed between N_2O flux and distance between measurements. Hotspot locations which are not visible by eye are much more difficult to investigate. Variance diagrams highlight this lack of predictability across the field, showing a random distribution with no clear spatial pattern visible in the flux or the corresponding soil properties across the field scale (Figure 6.10). Variance diagrams describe how similarities between measurements vary with distance between measurement locations. When a spatial pattern is present in a data set the semivariance between measurements should increase with distance, which means that measurements made close together should be more similar than those made far apart. No clear spatial pattern is visible in any of the field scale measurements which highlights the inability to predict N_2O flux between measurement points based on spatial variability. The nature of the unpredictable spatial variability of N_2O fluxes is a difficult barrier to overcome, which limits the use of many methods of spatial interpolation of the flux across a large scale such as a field. Taking many chamber measurements across a small area is one way to improve this method (Turner *et al.*, 2008); however, this becomes impractical at larger scales and a compromise needs to be made between field coverage and the number of chamber measurements taken.

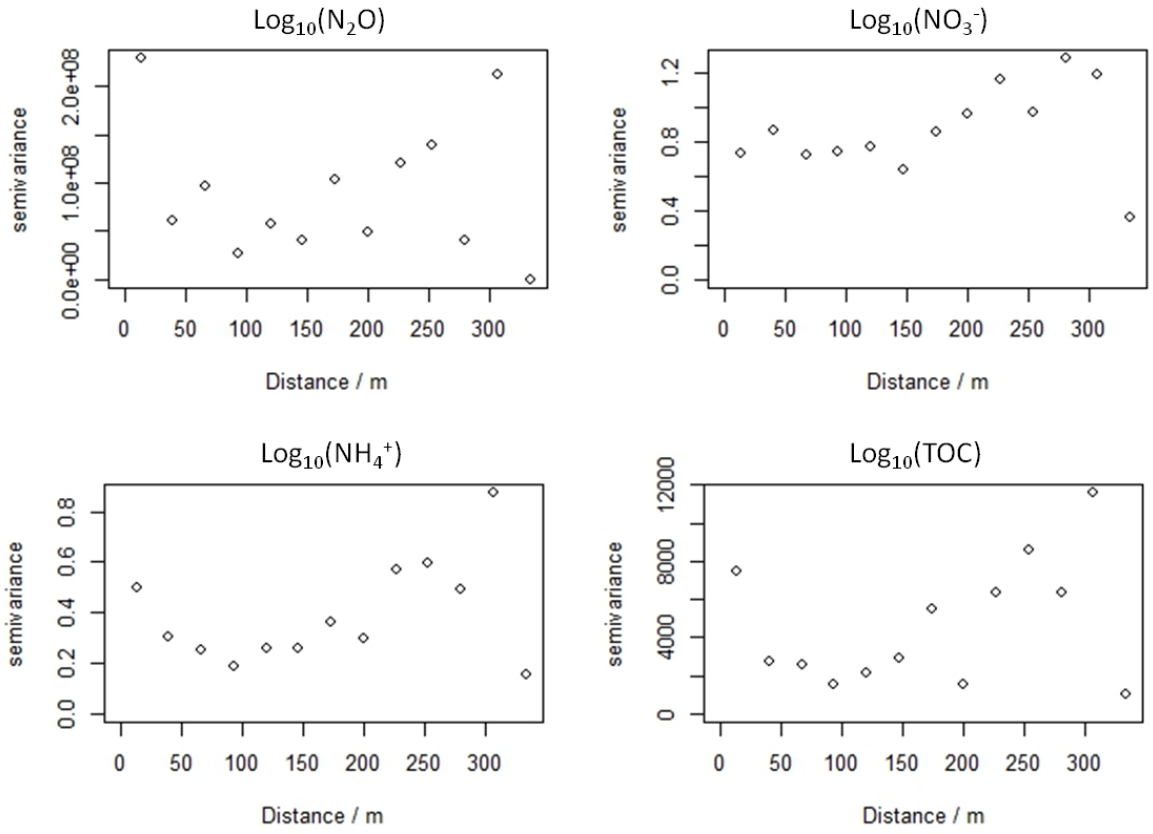

Figure 6.10 Variograms for N_2O flux, NO_3^-, NH_4^+ and total carbon measured across the field scale. Log-normal distributions were used as in Figure 6.9 and Table 6.2. The x-axis is the distance between measurement locations in m and the y-axis is the semi-variance in all of the respective measurements made for the entire field.

Another method of measuring N_2O fluxes at a field scale which has advanced in recent years due to the increasing precision of rapid gas analysers would be eddy covariance (Eugster *et al*., 2007; Kort *et al*., 2011). Eddy covariance does not suffer from the same interpolation issues as the chamber method and can provide a relatively confident estimate of mean N_2O flux across a large area (>100 m^2). The weakness of the eddy covariance method is that it would not be able to distinguish between sources and provide information on hotspot fluxes. Areas in which animals spend a lot of time to shelter from the elements such as the shaded area in this field scale study present problems for eddy covariance measurements as any physical objects which alter turbulence in the air (such as trees or foliage in our case) can prevent measurements from taking place. From the results in this experiment we would suggest that both methods should be deployed in tandem to investigate N_2O flux on a field scale as both methods have significant weaknesses that the other can compliment.

6.5 Conclusions

Spatial variability remains one of the largest sources of uncertainty when measuring N_2O flux from agricultural soils. Results from this study suggest that additional nitrogen applied to fields in the form of animal waste is the primary source of anthropogenic N_2O emissions from grazed agricultural soils (with the exception of fertiliser events). The wide and often random distribution of this nitrogen in the soils is one of the major causes of the spatial variability observed in N_2O emissions. This inherent variability of soil properties limits the ability to reduce uncertainty in N_2O emission estimates that can be achieved by taking a practical number of flux measurements using a chamber method. In order to reduce uncertainties in large scale emission budgets it is effective to identify hotspots of N_2O fluxes and determine the causes of these increased emissions. Identifying areas in which N_2O fluxes are significantly higher than the majority of the experimental area can reduce overall uncertainty in results by defining different emission estimates.

This study highlights the requirement of a better understanding of spatial variability of N_2O fluxes from intensively grazed grasslands. Without a basic understanding of how hotspots of N_2O are formed and the lifetime of these hotspots it is difficult to determine the true effect of these areas, which may be significant over wider areas such as the farm scale. Field, farm, national and global scale emission budgets of agricultural contributions to N_2O emissions are often dominated by emission factors which account for the soil conditions of the majority of the area of a field. These budgets may be significantly underestimating N_2O fluxes in some cases, especially for livestock farms with high stocking densities.

Chapter 7

A farm scale inventory of N_2O fluxes from a livestock farm in Central Scotland

Summary:

Nitrous oxide fluxes, together with soil moisture, mineral N, temperature and meteorological conditions were measured from a selection of arable fields and managed grasslands and from known N_2O hotspots, including manure heaps, livestock feeding areas and animal barns from a typical livestock farm in Central Scotland (124 ha). Measurements were made on six occasions over a one year period (August 2012 to July 2013) using a mobile follow-through chamber system connected to a quantum cascade laser. Fluxes and other measured parameters were combined with farm management data to construct an annual farm scale inventory of biological N_2O emissions, based on existing and new simple regression models. Nitrogen fertiliser application was the largest single source of N_2O emissions at the farm scale contributing approximately 49% of the total 672 Kg N_2O-N annual emission estimate for the farm. Outwith the N fertilisation periods the arable and grazed field soils were responsible for a combined contribution of 46% of the total annual emissions. The hotspots were large point sources of N_2O and flux measurements varied by up to five orders of magnitude (0 to 80,000 µg N_2O-N m^{-2} h^{-1}), but due to their small surface area only contributed to 5% of the total farm N_2O emissions.

(Work presented in this chapter is based on the manuscript submitted as: Cowan, N.J., Famulari, D., Levy, P. E., Anderson, M., Reay, D. S., Skiba, U. M.: A farm scale inventory of N_2O fluxes from a typical livestock farm in Central Scotland, Journal of Agriculture Ecosystems and environment (November 2014).

7.1 Introduction

Nitrous oxide (N_2O) is a powerful greenhouse gas which also contributes to stratospheric ozone depletion (IPCC, 2013; Ravishankara *et al*., 2009). N_2O is produced naturally (primarily as the as a by-product of microbiological processes of nitrification and denitrification) in soils and aquatic environments (e.g. Davidson *et al*., 2000); however, human activities which alter the natural nitrogen cycle in these environments can significantly increase emissions of microbial produced N_2O (IPCC, 2013). The increase in global livestock numbers and wide scale application of artificial fertilisers to agricultural soils over the past 100 years has led to a large increase in concentrations of reactive nitrogen compounds present in the environment, which has resulted in a significant increase in anthropogenic N_2O emissions on a global scale (Reay *et al*., 2012). Quantifying the increase in anthropogenic N_2O emissions has proven difficult due to the high uncertainties involved in measuring and interpolating N_2O fluxes when scaling up emission estimates over large areas (Mathieu *et al*., 2006; Giltrap *et al*., 2014). Accounting for the wide variety of sources of N_2O caused by human activities and the multiple environmental factors involved in N_2O production at a microbial level also increases the complexity of quantifying anthropogenic fluxes of N_2O (Thomson *et al*., 2012; Butterbach-Bahl *et al*., 2013).

Up to 80% of global anthropogenic fluxes of N_2O are believed to be directly or indirectly associated with agricultural activities (IPCC, 2013). Agriculture accounts for 70% of land coverage in the UK (DEFRA, 2009). This land is often intensively managed and regularly treated with nitrogen fertilisers and other nutrients which increase yields of crops or pasture grass. It is estimated that on average 94 kg ha^{-1} of nitrogen fertilisers (organic and mineral) are applied to agricultural land in the UK every year (DEFRA, 2013a). UK farms are estimated to contain a total of 9.7 million cattle, 22.2 million sheep and 4.4 million pigs (DEFRA, 2013b). Waste from these animals is often deposited on pasture fields during grazing or stored (housed animals) and applied to arable fields as a source of nitrogen and other nutrients for crop growth. The large quantity of nitrogen fertilisers applied to agricultural soils is believed to be the largest source of N_2O emissions in the UK (Webb *et al*., 2014).

Accounting for agricultural N_2O emissions on a national scale is highly uncertain due to different farm structures, management approaches and climate. These differences are not reflected in the current greenhouse gas reporting structure (Skiba *et al.,* 2012); only the relationship of N_2O with nitrogen application is included

(IPCC, 2013). As each farm is unique in terms of size, management and environment it is difficult to apply generic emission factors to each source of N_2O at a national scale.

Past experiments have been carried out with the goal of quantifying N_2O emissions from individual farms with some success (Velthof and Oenema, 1997; Brown *et al*., 2001; Ellis *et al*., 2001). These estimates usually involve a combination of regional specific literature values used to estimate emission factors or are calculated from on-site flux measurements, often made using static chamber methodology. Due to the magnitude of the task, several studies have focussed on a particular aspect of N_2O emissions from a farm, such as animal waste management (Chadwick *et al*., 1999), fertiliser use (Smith *et al*., 2012; Smith and Massheder, 2014) or secondary emissions caused by leaching losses from soils (Reay *et al*., 2009). Relatively small areas such as ditches, gateways and feeding troughs can also be sources of high N_2O fluxes (Matthews *et al*., 2010). Under certain conditions, small areas in which soil conditions favour microbial activity (i.e. increased nitrogen content or compaction) can emit N_2O in much greater quantities than an equivalent area of general agricultural soils.

The aim of this experiment was to identify and quantify the most significant sources of N_2O emissions from a typical livestock farm in Scotland using a mixture of on-site flux measurements and literature values.

7.2 Materials and methods

7.2.1 Farm description

The Easter Bush Farm Estate is a combination of several farms near Penicuik, Midlothian in Central Scotland (55° 51' 55.7036"N, 3° 12' 44.3549"W). These farms are owned by both the Scotland's Rural College (SRUC) and the University of Edinburgh (UoE) and are run for commercial and research purposes. The total coverage of the Estate is over 1000 ha and provides for approximately 1600 ewes and 300 cattle. Of this area, a selection of 20 separate fields which covered 124 ha of land was chosen to represent a typical Scottish livestock farm (See Figure 7.1 & Table 7.1). Five of the selected fields (54 ha) were dedicated arable fields used to grow predominantly barley crops and silage grass for animal feed. The other selected fields were used as grazed pasture for cattle and sheep. Several of the fields had multiple purposes (See Table 7.1). The perimeter and area of each field was measured manually using a handheld GPS device (Garmin eTrex Legend HCx, Garmin, Shaffhausen, Switzerland) (See Figure 7.1 & Table 7.1).

Livestock were often moved between the selected fields and the larger farm estate outside the selected area. In order to simulate typical farm conditions the farm managers at the estate estimated that the selected fields would provide for 440 ewes with 835 lambs and 86 cattle with 60 calves over the period of a year (See Table 7.6 for further details). The farm managers at the estate also provided farm records for the selected fields which detailed management data such as animal stocking density, fertiliser applied and crops sown. An animal housing barn, several manure heaps and a silage grass store were also included in the farm scale model as potential sources of N_2O emissions. Cattle and sheep were moved between pasture fields and the barns throughout the year. Silage grass was fed to the animals in barns or placed in pasture fields over autumn and winter. Manure was removed from the barns and stored in various fields which were eventually applied as manure fertiliser. The data provided by the farm managers was combined to create a basic model from which a farm scale N_2O inventory could be created. This "livestock farm" served as the basis for a year long farm scale N_2O inventory starting from August 2012 and ending in July 2013.

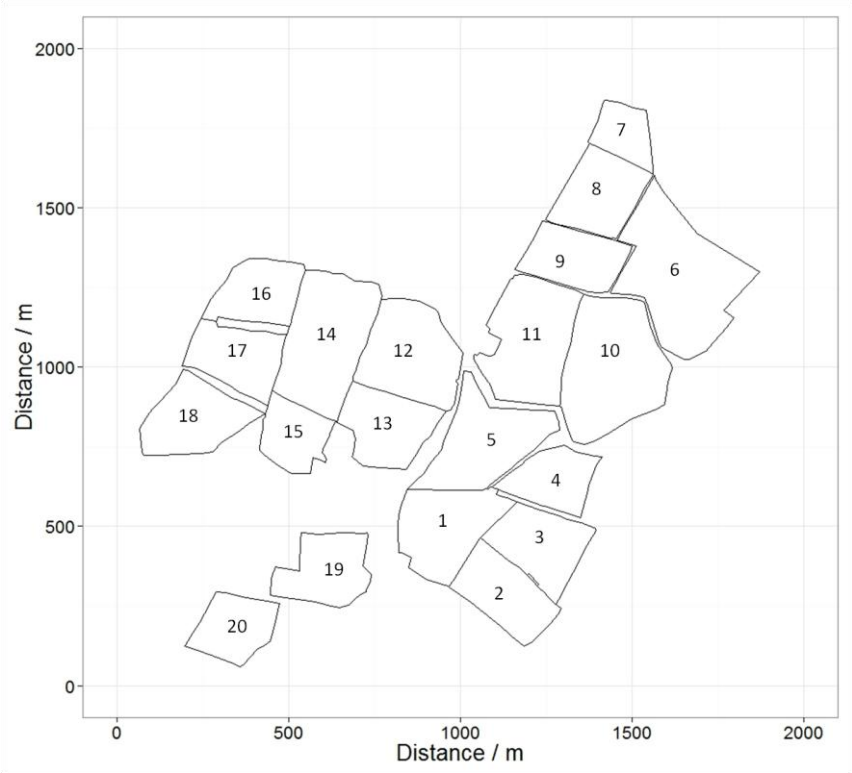

Figure 7.1 Twenty fields (133 ha) from the Easter Bush Farm Estate (Scotland) were selected to represent a typical Scottish livestock farm (See Table 7.1 for details).

Table 7.1 A description of the each of the fields selected to represent a typical Scottish livestock farm in this study (Figure 7.1). Field use during each season is detailed for the year long measurement period from August 2012 to July 2013.

Field Name	Field No.	Area (ha)	Autumn [a] 2012	Winter [b] 2012/2013	Spring [c] 2013	Summer [d] 2013
Corner Field	1	6.72	Sheep	Sheep	Sheep	Sheep
Engineers Field	2	5.30	Sheep	Sheep	Sheep	Sheep
Middle Field	3	5.44	Cattle	Sheep	Sheep	Sheep
Paddock Field	4	4.08	Sheep	Sheep	Sheep	Sheep
Bog Hall Field	5	7.55	Barley	Empty	Barley	Barley
Kimming Hill	6	12.16	Silage	Sheep	Silage	Silage
Anchordales	7	2.67	Barley	Empty	Barley	Barley
Anchordales N.L.T	8	5.36	Barley	Empty	Barley	Barley
Cow Loan	9	4.79	Barley	Empty	Barley	Barley
Hay Knowes	10	10.92	Barley	Oilseed	Oilseed	Barley
Crofts	11	8.67	Barley	Empty	Barley	Barley
Low Fulford	12	7.72	Silage	Sheep	Silage	Silage
Fulford Camp	13	5.37	Sheep	Sheep	Sheep	Sheep
Mid Fulford	14	9.57	Cattle	Empty	Sheep	Sheep
Fulford Stackyard	15	3.68	Sheep	Sheep	Sheep	Sheep
Upper Fulford	16	4.48	Sheep	Empty	Cattle	Cattle
Nuek	17	4.89	Cattle	Empty	Cattle	Cattle
Doo Brae	18	5.76	Sheep	Sheep	Cattle	Cattle
Woodhouselee Camp	19	4.94	Cattle	Cattle	Cattle	Cattle
Lower Terrace	20	4.38	Barley	Empty	Empty	Sheep

([a] 24/09/12 to 28/09/12, [b] 10/02/13 to 12/02/13, [c] 03/05/13 to 16/05/13, [d] 02/07/13 to 10/07/13)

7.2.2 Environmental conditions

Air temperature and rainfall (tipping bucket) were monitored by a permanent meteorological monitoring station within the Bush Estate (Figure 7.2). The meteorological data recorded from this site is assumed to be representative for the entire farm area throughout the inventory measurement period due to the relatively small distance between the fields and the monitoring station.

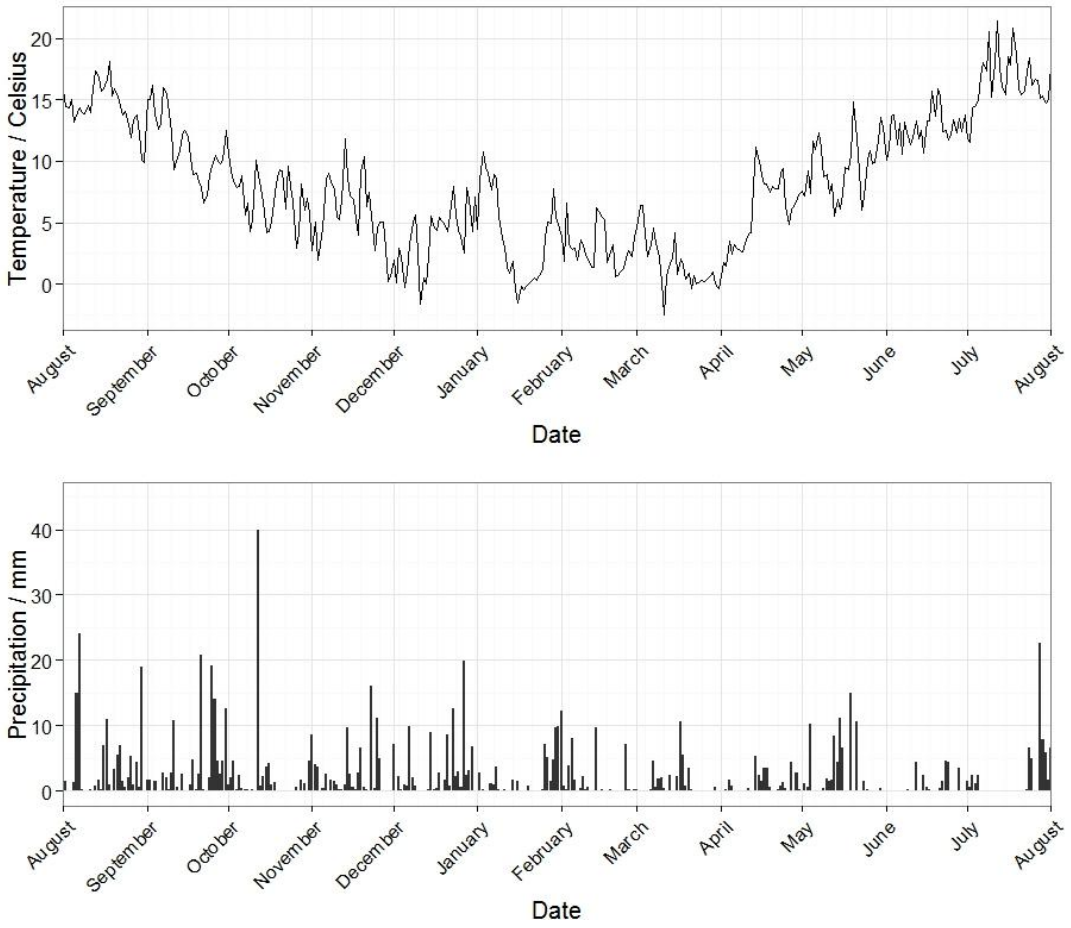

Figure 7.2 A summary of mean daily temperature and daily precipitation recorded at the meteorological monitoring station at Easter Bush Estate between August 2012 and August 2013.

7.2.3 Dynamic chamber flux measurements

A high precision mobile closed loop dynamic chamber system was deployed to measure N_2O fluxes from as many of the fields and identified sources of N_2O as was possible during four seasonal measurement periods between autumn 2012 and summer 2013. The dynamic chamber method circulated air between a flux chamber and a quantum cascade laser (QCL) gas analyser via an air pump (SH-110, Varian Inc, CA, USA) over a three minute period (as in Chapter 4). A compact continuous wave QCL (CW-QC-TILDAS-76-CS, Aerodyne Research Inc., Billerica, MA, USA) was used to measure gas mixing ratios within the dynamic chamber system. The instrument was secured inside a four wheel drive vehicle to allow for mobile measurements around the farm estate which was powered by a diesel generator kept on a tow trailer. The chamber was placed onto circular aluminium collars which were inserted several cm into the soil (on average 5 cm) several minutes prior to each measurement. Neoprene sponge formed an airtight seal between the chamber and the collar which was held in

place by four strong clips. Two 30 m lengths of 3/8 inch ID Tygon® tubing were attached to both the inlet of the QCL and the outlet of the pump. This provided a 30 m radius from the vehicle in which the chamber could be placed (Figure 7.3). The tubing length was limited to 30 m lengths to reduce the strain on the vacuum pump. Lag time between the pump and the chamber was also an issue as longer tubing would have increased the time required to wait between measurements as the contents of the tubing were flushed with atmospheric air.

Figure 7.3 The QCL was mounted in an off road vehicle which was powered by a diesel generator. The dynamic chamber measurements could be made in a 30 m radius around the parked vehicle.

A total of 527 flux measurements were made using the dynamic chamber method from a variety of field soils (Table 7.2), and identified sources of N_2O such as animal barns and manure and silage heaps across the farm. Wet weather, difficult terrain and availability of the QCL instrument were limiting factors in the number of measurements that were possible during each measurement period and the areas in which measurements could take place. Very wet weather during autumn and winter months reduced the number of fields in which measurements could be made. Five or more flux measurements were made per measured field with some fields being investigated in greater detail. Due to logistical constraints, there were some fields in which no flux measurements were made at any point during the year (See Table 7.2).

Table 7.2 The dates and number of N_2O flux measurements that were carried out from each field during four seasonal measurement periods.

	Autumn		Winter		Spring		Summer	
Field Name	n	Date	n	Date	n	Date	n	Date
Corner Field	8	24/09/12			6	09/05/13	55	02/07/13
Engineers Field	10	24/09/12			6	09/05/13	6	02/07/13
Middle Field	10	24/09/12			6	09/05/13	6	02/07/13
Paddock Field					6	09/05/13	6	02/07/13
Bog Hall Field					6	09/05/13	6	02/07/13
Kimming Hill					6	08/05/13	6	03/07/13
Anchordales					6	08/05/13	6	03/07/13
Anchordales N.L.T					6	08/05/13	6	03/07/13
Cow Loan	20	27/09/12	25	12/02/13	6	08/05/13	6	03/07/13
Hay Knowes					6	08/05/13	6	03/07/13
Crofts					6	08/05/13	6	03/07/13
Low Fulford	10	28/09/12			10	13/05/13	10	04/07/13
Fulford Camp	10	28/09/12			10	13/05/13	10	04/07/13
Mid Fulford					15	14/05/13		
Fulford Stackyard								
Upper Fulford								
Nuek								
Doo Brae								
Woodhouselee Camp	12	25/09/12	30	14/02/13	15	16/05/13	12	05/07/13
Lower Terrace					5	16/05/13	6	05/07/13
Total	80		55		121		135	

7.2.4 Soil sampling and analysis

Two types of soil samples were taken from each flux measurement location. "Wet" soil samples (5 cm deep) were taken from within the chamber collar using a 2 cm wide corer immediately after a flux measurement was complete. These soils were frozen to -18 ˚C within six hours of collection for several months until we had time for analysis of pH (in H_2O) and available nitrogen in the form of ammonium (NH_4^+) and nitrate (NO_3^-).Wet soil samples were defrosted in a refrigerated room (5 ˚C) over night prior to analysis. The pH of the soil samples were measured using the method outlined in Rowell (1994). Air dried soil (10 g) was placed in a small plastic cup with 20 ml of deionised H_2O. The mixture was shaken and left for 60 minutes. A pH meter (MP220, Mettler Toledo, Columbus, Ohio, USA) was used to measure pH in the soil solution.

NH_4^+ and NO_3^- was extracted from the wet soil samples using KCl extraction as outlined in Rowell (1994). Soil (15 g) was added to a flask and mixed with 50 ml of 1mol L^{-1} KCl solution. The solution was

shaken automatically using an orbital shaker for 60 mins. The mixture was filtered using 2.5 µm filter paper (Fisherbrand, Hampton, New Hampshire, USA) and the solution was stored and frozen in 20 ml plastic vials. Concentrations of NH_4^+ and NO_3^- were measured using a Bran and Luebbe AutoAnalyser (SPX Flow Technology, Norderstedt, Germany). Available nitrogen content in the soils were calculated using Equation 7.1.

$$N = \frac{C \times V}{m} \quad \text{(Eq. 7.1)}$$

Where N is the mass of nitrogen in the form of NH_4^+ or NO_3^- in mg (per g of dry soil), C is the concentration of NH_4^+ or NO_3^- measured in the analysis of KCl extract in mg L^{-1}, V is the volume of solution in which the soil sample was mixed with KCl in L, and m is the mass of dry soil mixed with the KCl solution in g.

Separate soil samples used to measure bulk density were taken immediately after the flux measurement using a sharp metal cutting cylinder (7.4 cm diameter, 5 cm deep) which was carefully hammered into undisturbed soil. These soil samples were kept in a refrigerated room (5 ˚C) until oven drying (less than seven days after sample collection). These samples were used to calculate soil moisture content (via oven drying at 100 ˚C) which also provided the dry soil mass. Bulk density was calculated by dividing the volume of the cutting ring by the mass of dry soil. A sub sample of the dried soils was taken to be ground (via ball milling) for elemental analysis of total carbon and nitrogen content of the soil (vario EL cube, Elemaentar, Hanau, Germany). WFPS was calculated from the bulk density soil samples as described in Rowell, 1994 (See Equation 7.2).

$$WFPS = \frac{V_{cont} \times 100}{1 - \left(\frac{r_b}{r_d}\right)} \quad \text{(Eq. 7.2)}$$

Where WFPS is the percentage of porous volume in the soil filled by water, Vcont is the volumetric water content of the soil, r_b is the bulk density of the soil in g cm^{-3} and r_d is the particle density of the soil (assumed as 2.65 g cm^{-3}) (Rowell, 1994).

Statistical analysis was carried out using the statistical software R and freely available software packages within R. Multiple linear regression was carried out using (plyr) package and some plots contain built in statistical calculations made using the (ggplot2) package.

7.3 Results

7.3.1 Meteorological monitoring

Annual cumulative rainfall for the 12 month measurement period between July 2012 and August 2013 was 962 mm. The average annual rainfall over the past 10 years is 921 mm which suggested that rainfall during the measurement period was fairly typical (Figure 7.4a); although the summer months of 2012 were wetter than average and the winter and spring months of 2013 were drier than average (See Figure 7.4a). Daily temperatures recorded were considered typical for the year in which measurements took place. Seasonal temperature changes at the farm estate have been fairly consistent throughout the past 10 years (Figure 7.4b). This data was recorded by staff from the Centre for Ecology and Hydrology (Edinburgh) at the Easter Bush meteorological monitoring station.

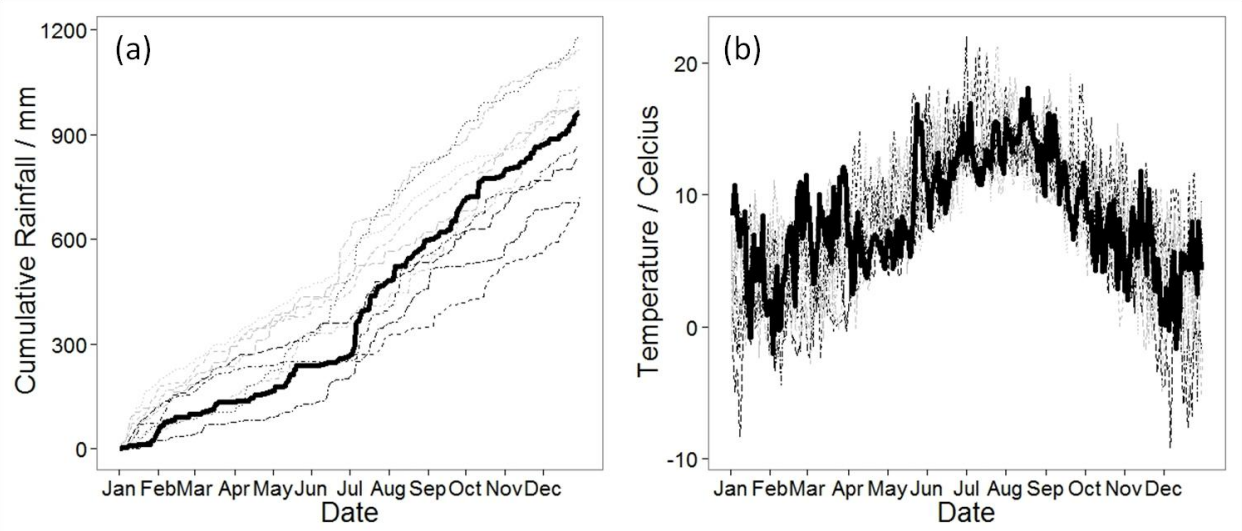

Figure 7.4 (a) Cumulative annual rainfall and (b) daily average temperature were plotted for the past 10 years of meteorological measurements recorded at the Easter Bush Estate. The measurement period of the study is represented with a solid black line in both figures.

7.3.2 Fluxes measured from the fields

Of the 527 flux measurements made across the farm, 353 were representative of the general field conditions (soils which covered the majority of the fields at least two weeks after any fertilisation events) (See Table 7.2). Measurements were made from both arable and grazed fields during each season (Figure 7.5). N_2O fluxes often varied by two orders of magnitude with values recorded between the range of -5.5 and 424 µg N_2O-N m^{-2} h^{-1}

during the study. Individual flux measurements measured from the same field varied unpredictably between measurement locations; however, the range of N_2O flux recorded from the individual fields was similar across the farm throughout the year (0 to 100 µg N_2O-N m^{-2} h^{-1}) (Figure 7.5).

In summer 2013 a more detailed study was conducted from a sheep grazed field 'Field 1' (Table 7.1), when 55 flux measurements were made over a three day period (Chapter 6). Fluxes ranged from 2 to 200 µg N_2O-N m^{-2} h^{-1} (See Figure 7.5, circled). This wide range of N_2O fluxes from this individual field was very similar to that of the farm area as a whole.

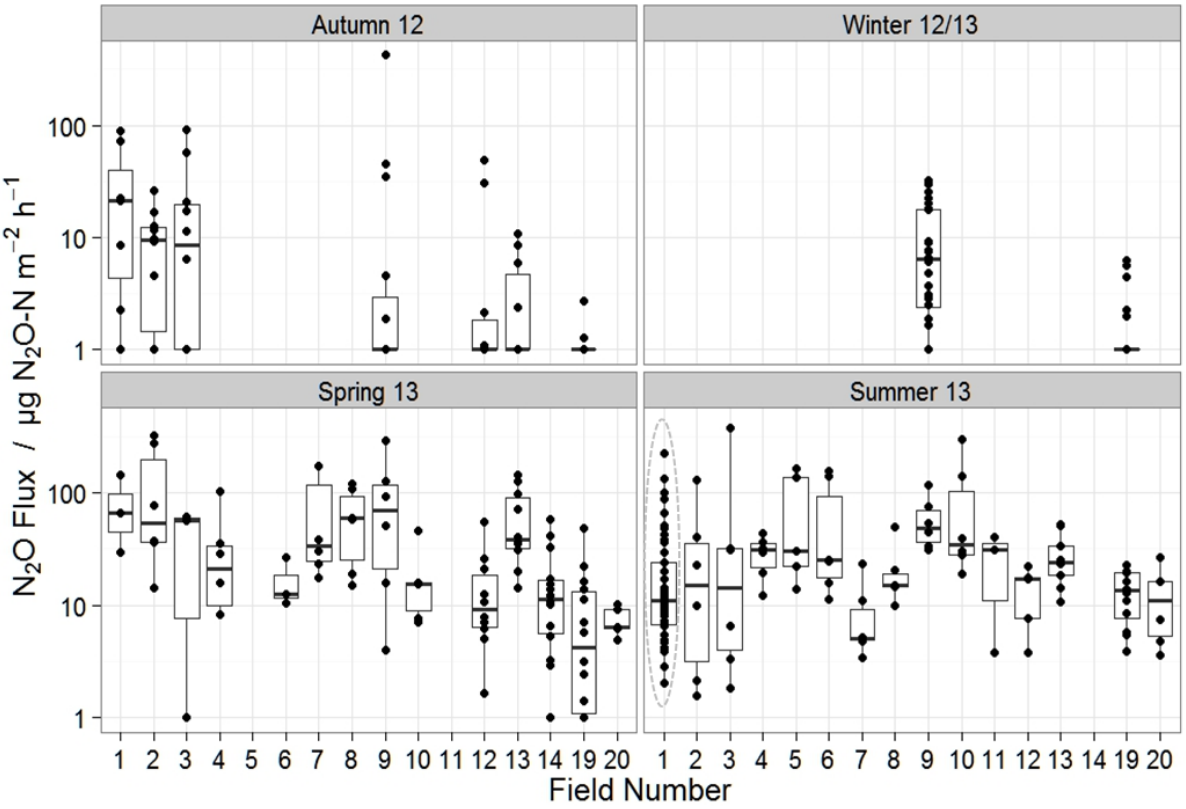

Figure 7.5 A summary of all flux measurements (points) representative of general field conditions from each of the fields described in Table 7.1 during different seasons. The box plot represents the mean flux and the 25th and 75th percentile ranges of uncertainty in the mean flux recorded from each field. The results of the summer field scale experiment are circled (dotted line). Note the log scale of the Y axis (small negative fluxes -5 to 0 µg N_2O-N m^{-2} h^{-1} recorded during the study are plotted as 1 µg N_2O-N m^{-2} h^{-1} for the purpose of the log-scale figure).

A wide range of fluxes were measured across each of the different field types throughout the year (Figure 7.6). The large range of uncertainty associated with mean flux values between each field type overlaps during most seasons, although a seasonal difference is still observed (Figure 7.6). Mean flux values calculated for measurements made in autumn and winter are generally lower than those in spring and summer for each of the field types; however, the range of fluxes measured is similar during most of the year (Figure 7.6). With the exception of winter (for which fewer measurements were made due to the wet and inaccessible conditions of the fields), flux measurements in each season span the range between near zero flux values on the verge of the detection limits of the methodology to over 100 µg N_2O-N m^{-2} h^{-1} (Figure 7.6).

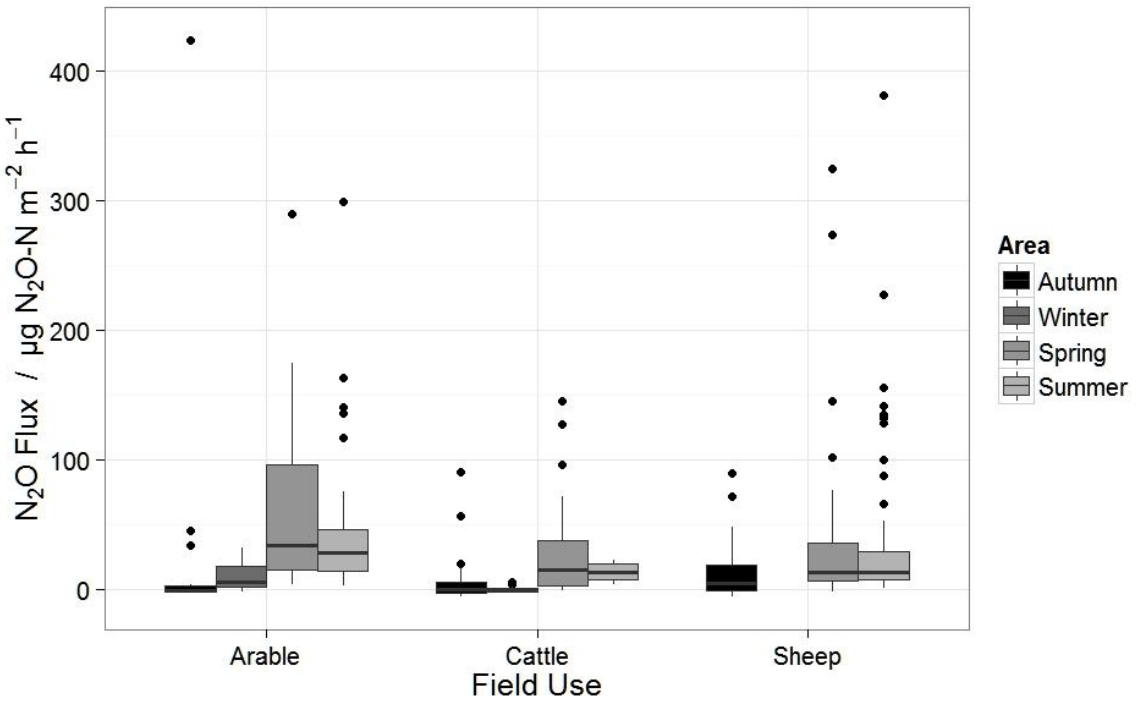

Figure 7.6 A summary of all flux measurements representative of majority field conditions separated by field use for each season. The box plot represents the mean flux and the 25th and 75th percentile ranges of uncertainty in the mean flux recorded from each field. (Winter measurements were not possible on sheep grazed fields due to logistical constraints).

7.3.3 Chamber flux measurements from identified N_2O flux sources

A total of 109 dynamic chamber measurements were made from locations known to be N_2O flux hotspots. These included two recently fertilised fields (Field 12 and 13, Table 7.2) measured less than 14 days after a nitrogen fertiliser application; and nitrogen rich soils such as areas contaminated from the presence of manure heaps, the decayed remains of silage bales and compacted soils where animal waste had collected such as

feeding and drinking trough areas. Variation in fluxes measured from these hotspots was much greater in magnitude than from the fields which represented general unfertilised conditions (Figures 7.8a & b). Some extremely high fluxes (over 10,000 µg N_2O-N m^{-2} h^{-1}) were measured as well as a small number of fluxes similar in magnitude to those measured from soils representative of the general field coverage (between 10 and 100 µg N_2O-N m^{-2} h^{-1}) (Figure 7.8b).

Other known sources of N_2O where no soil was present included animal barns, manure heaps and stored silage grass (Figure 7.7). A combination of 65 fluxes of N_2O were measured from these sources which were similar in magnitude to those of the identified flux sources with a small number of exceptionally high measurements which recorded fluxes over 50,000 µg N_2O-N m^{-2} h^{-1} from manure heaps and one measurement of 352,909 µg N_2O-N m^{-2} h^{-1} from a patch of stored silage grass which showed advanced signs of decay (Figure 7.8c). This was the single largest flux measurement recorded in the study. Fluxes of N_2O measured from manure and silage grass heaps scaled 5 orders of magnitude (Figure 7.8c).

Figure 7.7 Dynamic chamber measurements were made from manure heaps from various fields during the farm scale experiment. The rings fit into the surface of the heap as they would on soils. Fluxes from silage grass and animal barns were measured in a similar way.

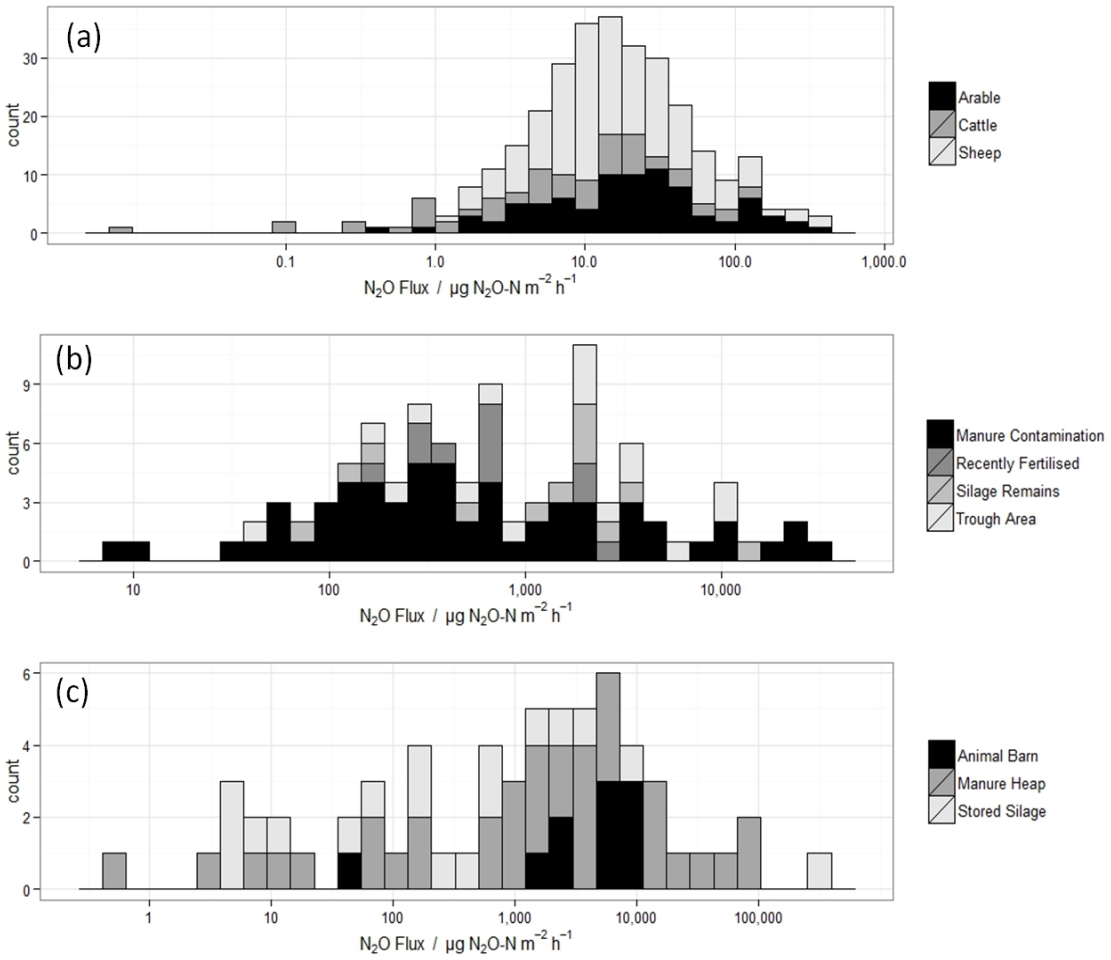

Figure 7.8 Frequency of all N_2O measured fluxes on a log-normal scale. This plot shows that N_2O flux distribution of (a) majority field conditions, (b) flux hotspot soil conditions and (c) recognised sources of N_2O from non-soil sources all follow a similar geometric distribution.

Although several small individual flux values were measured (below 20 µg N_2O-N m^{-2} h^{-1}) it is clear that each of the identified sources is capable of emitting significantly more N_2O than that of an equivalent area of a general field soil coverage (Table 7.3). The uncertainty associated with mean flux values from the known sources of N_2O is very large due to the wide range of flux magnitude recorded in the measurements (See Figure 7.8). The arithmetic mean value of all flux measurements representative of majority field conditions made throughout the year was 28.2 µg N_2O-N m^{-2} h^{-1}. The flux distribution is log-normal (Figure 7.8a) with a geometric mean flux of 9.8 µg N_2O-N m^{-2} h^{-1}. A log-normal distribution is observed for all of the flux measurements at the farm scale (Figure 7.8).

Table 7.3 The range and mean values of N_2O fluxes measured from all sources at the farm scale during the study (units in µg N_2O-N m^{-2} h^{-1}).

Source	Flux Measurements n	Fields Measured n	Flux Range	Arithmetic Mean	95 % C.I.	Geometric Mean	95 % C.I.
Field Measurements							
All Fields	353	40	-6–424	28	-77–132	9.8	0–199
Arable	95	16	-2–424	40	-95–174	13.5	1–315
Cattle	86	8	-5–145	12	-39–62	3.7	0–73
Sheep	172	16	-6–381	30	-73–133	13.2	1–168
Autumn 12	65	7	-6–424	15	-92–122	3.4	0–74
Winter 12/13	51	2	-2–33	4.	-77–160	2.5	1–273
Spring 13	98	16	-2 –325	42	-71–138	18.1	2–150
Summer 13	139	15	2–381	34	-12.1–21.3	17.1	0–25
Known sources							
Manure Contamination	62	4	-1–31,251	2,816	-10,124–15,757	388	5–32,711
Recently Fertilised	11	2	190–2642	907	-708–2522	641	118–3481
Silage Remains	12	4	68–13,393	2376	-4712–9464	1,007	52–19,598
Trough Area	24	8	-3–11,750	1928	-4239–8096	140	0–112,490
Animal Barn	10	1	53–9683	5038	-1,945–12,021	2,888	131–63,730
Manure Heap	35	7	1–80,035	10,542	-30,800–51,883	1,086	4–315,963
Stored Silage	20	4	0–352,909	18,491	-135,830–172,811	126	0–77,873

7.3.4 Measurements of soil properties

Like the measurements of N_2O flux, soil NH_4^+, NO_3^- concentrations and total carbon and total nitrogen contents were log normally distributed and data are presented as geometric rather than arithmetic means (See Figure 7.8 and Table 7.4). All other measured properties such as pH and bulk density were found to fit a normal distribution well.

The largest difference in soil properties observed between general field conditions and the identified sources of N_2O were the concentrations of available nitrogen in the form of NH_4^+ and NO_3^- (See Figures 7.8a,b & Table 7.4). Mean concentrations of NH_4^+ were fairly consistent throughout the year in majority field conditions with a mean value of 17.9 mg kg^{-1}. Higher values were measured in spring and summer, predominantly from sheep grazed fields with a maximum of 766 mg kg^{-1} recorded from an individual measurement in these conditions. This may have been due to the increased stocking density in these fields over these months (ewes and suckling lambs) and the resultant increase in urine patches throughout the field, or alternatively the remnants of nitrogen fertilisers during this period. Measurements made from recently fertilised fields did not record a higher concentration of NH_4^+ in the soils in this study, although the soils taken from the other identified sources all had very high mean concentrations on NH_4^+, exceeding 80 mg kg^{-1} (See Figure 7.9a & Table 7.4). The highest concentration of NH_4^+ recorded from the farm soil was 2482 mg kg^{-1} from an area of soil which had been contaminated by a nearby manure heap.

Generally concentrations of NO_3^- in the soil were lower than that of NH_4^+ with a mean value of 12.2 mg kg^{-1} for all measurements representative of majority field coverage; however, the distribution between locations was fairly similar with large concentrations recorded at soils around troughs, silage residues and areas of manure contamination (Figure 7.9b). Although the highest mean value for NO_3^- concentrations is for soils containing silage residues (127 mg kg^{-1}), the highest individual recorded concentration of NO_3^- was 651 mg kg^{-1} from an area of soil which had been contaminated by a nearby manure heap.

Individual measurements of total carbon content of soils from majority field conditions varied from values near zero to over 100 g kg^{-1} with a mean value of 40 g kg^{-1} (Figure 7.9c). Total carbon content measured from the identified sources of N_2O was generally of the same range and magnitude of the majority field conditions. The exceptions to these measurements were a handful of extremely high values recorded near manure heaps. Soil carbon content of up to 355 g kg^{-1} was recorded in these areas. Measurements of total

nitrogen content of the soils did not indicate a significant difference between the majority field conditions and the known sources of N_2O (See Table 7.4). Slightly higher values were recorded from sheep fields in summer. As with available nitrogen, this may have been due to additional animals present in the field and an increased presence of nitrogen fertilisers during this period, although relationship is observed between animal N input and total nitrogen content of the fields. Due to the DEFRA reporting structure (DEFRA, 2008) the presence of lambs in these months does not increase the estimates of animal nitrogen input in grazed fields reported in this study as it is considered as negligible in the report (See Table 7.6).

The pH values recorded from the different soil types was fairly consistent with a mean value of 6.3 for all typical soil measurements (Figure 7.9d). Maximum recorded pH measurements of 9.2 and 9.4 were made at a feeding trough and manure contaminated soils respectively. As cattle and sheep urine is slightly alkaline it is likely that high pH values indicated the presence of animal waste as would be expected in these soils.

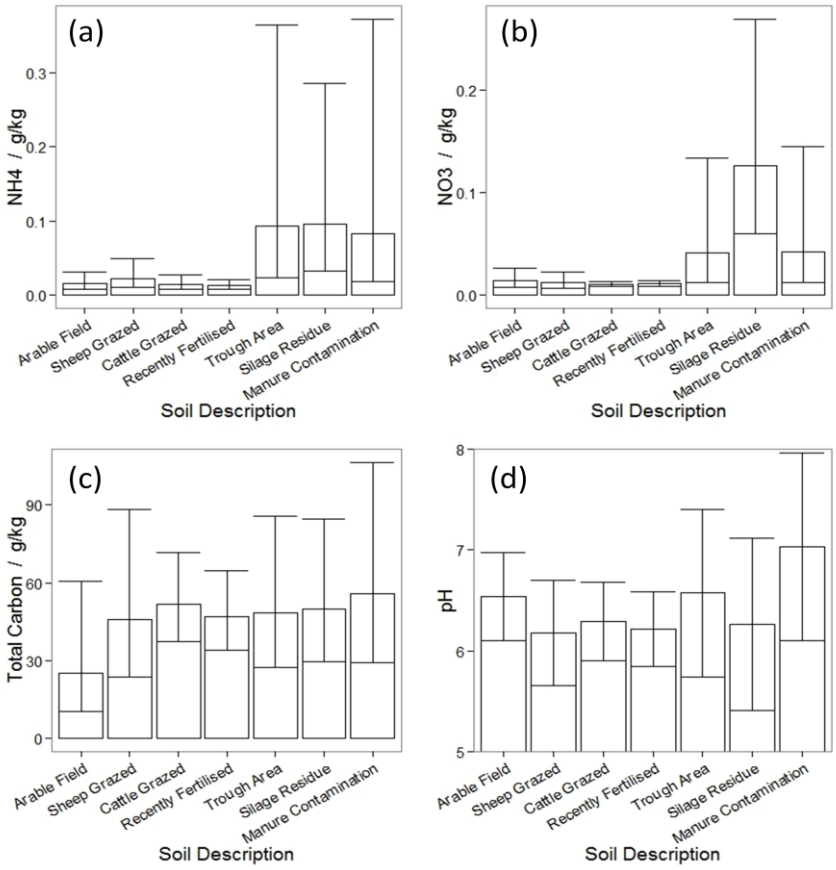

Figure 7.9 Geometric mean values of soil properties were calculated for each of the different soil types measured (Refer to Table 4). Total soil content of (a) NH_4^+, (b) NO_3^-, (c) total carbon content, and (d) the pH of the soil are included in the figures. Standard deviation ranges (bar) is included for each value in the figures.

Table 7.4 A summary of the mean and standard deviation values for all soil properties measured during the farm scale study.

		NH_4^+ / mg kg^{-1}		NO_3^- / mg kg^{-1}		Total Carbon / g kg^{-1}		Total Nitrogen / g kg^{-1}		pH		Bulk density / g cm^{-3}	
Soil Description	n	Geometric Mean	Geometric St. Dev.	Geometric Mean	Geometric St. Dev.	Geometric Mean	Geometric St. Dev.	Geometric Mean	Geometric St. Dev.	Arithmetic Mean	Arithmetic St. Dev.	Arithmetic Mean	Arithmetic St. Dev.
<u>Typical Field conditions</u>													
All Fields	367	18	9 – 37	12	7 – 21	40	20 – 82	4	2–7	6.3	± 0.5	0.9	± 0.2
All Autumn	72	13	8–22	10	0–15	40	29–57	3	2–5	6.3	± 0.3	1.0	± 0.3
All Winter	54	11	9–13	10	0–15	40	29–56	3	2–45	6.4	± 0.3	1.0	± 0.2
All Spring	112	18	9–35	13	8–21	44	31–63	4	3–5	6.3	± 0.5	0.9	± 0.2
All Summer	129	25	11–57	14	7–30	37	12–112	5	2–10	6.3	± 0.5	0.9	± 0.2
Arable Field	105	16	8–31	14	8–26	25	11–61	4	2–7	6.5	± 0.4	1.1	± 0.2
Cattle Grazed	98	15	8–27	11	8–14	52	38–72	4	3– 6	6.3	± 0.4	0.8	± 0.2
Sheep Grazed	146	23	10–50	12	7–22	46	24– 88	5	3– 9	6.2	± 0.5	0.9	± 0.2
<u>Hotspot Features</u>													
Recently Fertilised	29	13	8–21	11	8–15	47	34–65	4	3–5	6.2	± 0.4	1.0	± 0.3
Trough Area	13	93	24–365	41	13–133	48	27–86	4	2–7	6.6	± 0.8	1.0	± 0.1
Silage Residue	10	96	32–286	127	60–269	50	30–85	4	3 – 6	6.3	± 0.9	0.9	± 0.2
Manure Contamination	47	83	19–372	42	12–145	56	29–106	4	2–7	7.0	± 0.9	0.9	± 0.3

7.3.5 Correlation between soil properties and N_2O flux

Multi-linear regression was used to identify which of the measured soil properties correlated most significantly to N_2O fluxes from agricultural soils. Due to the geometric distribution of flux measurement values (See Figure 7.8) a log-normal scale was used for the regression analysis (Figures 7.9a & b). For all individual flux measurements with soil samples (n = 425) the best linear fit between flux and soil properties (R^2 = 0.48) was provided by available nitrogen (in the form of NH_4^+ and NO_3^-), volumetric water content, pH and rainfall over a 60 day period (Equation 7.3 and Table 7.5). Although correlation with N_2O flux was significant for several of the soil properties ($p < 0.001$, see Table 7.5) the comparison between measured and predicted flux is still rather weak with a large scatter of data over two orders of magnitude (See Figure 7.10a). Rainfall and NO_3^- are identified as the measurements which correlate best with N_2O flux ($p < 0.001$). Rainfall and volumetric water content are found to correlate well with flux in this data set (See Table 7.4), although WFPS did not ($p > 0.1$). The overall correlation suggests that N_2O fluxes are higher when more available nitrogen is present and lower when the soil is wetter (See Equation 7.3).

$$\text{Flux} = 3.74 + (NH_4 \times 0.53) + (NO_3 \times 0.91) + (pH \times 0.18) + (Vol.H_2O \times -0.01) + (Rain \times -0.007) \quad \text{(Eq.7.3)}$$

Where Flux is $\log_{10}(N_2O$ flux) in units of µg N_2O-N m^{-2} h^{-1}, NH_4 and NO_3 are concentrations of $\log_{10}(NH_4^+)$ and $\log_{10}(NO_3^-)$ in the soil in g kg^{-1}, pH is soil pH, $Vol.H_2O$ is the ratio of volumetric content of the soil filled by water and Rain is the cumulative rainfall over a 60 day period prior to the flux measurement in mm.

For further statistical analysis the 425 individual flux measurements were grouped into 70 units of three to six measurements. The criterion for each group was that they were made on the same measurement date and from the same flux source with measurements in close proximity of each other. Multi-linear regression was run using the mean values of each of the soil properties (geometric or arithmetic as in Table 7.4) and N_2O flux (Figure 7.10b). Mean concentration of available nitrogen in the form of NH_4^+ and NO_3^- and cumulative rainfall over a 60 day period were the only properties which significant correlated with N_2O flux in the grouped data set (See Table 7.5 & Equation 7.4). The relationship between measured flux and flux estimated using the multi-linear regression coefficients was stronger using the grouped data than the single data points (R^2 = 0.58 (Fig

7.10b) compared with R^2 = 0.48 (Fig 7.10a)); however, differences of several orders of magnitude still exist between these values in some cases (See Figure 7.10b).

$$\text{Flux} = 5.50 + (NH_4 \times 0.69) + (NO_3 \times 1.25) + (\text{Rain} \times -0.007) \quad \text{(Eq. 7.4)}$$

Where Flux is $\log_{10}(N_2O$ flux) in units of µg N_2O-N m^{-2} h^{-1}, NH_4 and NO_3 are concentrations of $\log_{10}(NH_4^+)$ and $\log_{10}(NO_3^-)$ in the soil in g kg^{-1} and Rain is the cumulative rainfall over a 60 day period prior to the measurement in mm.

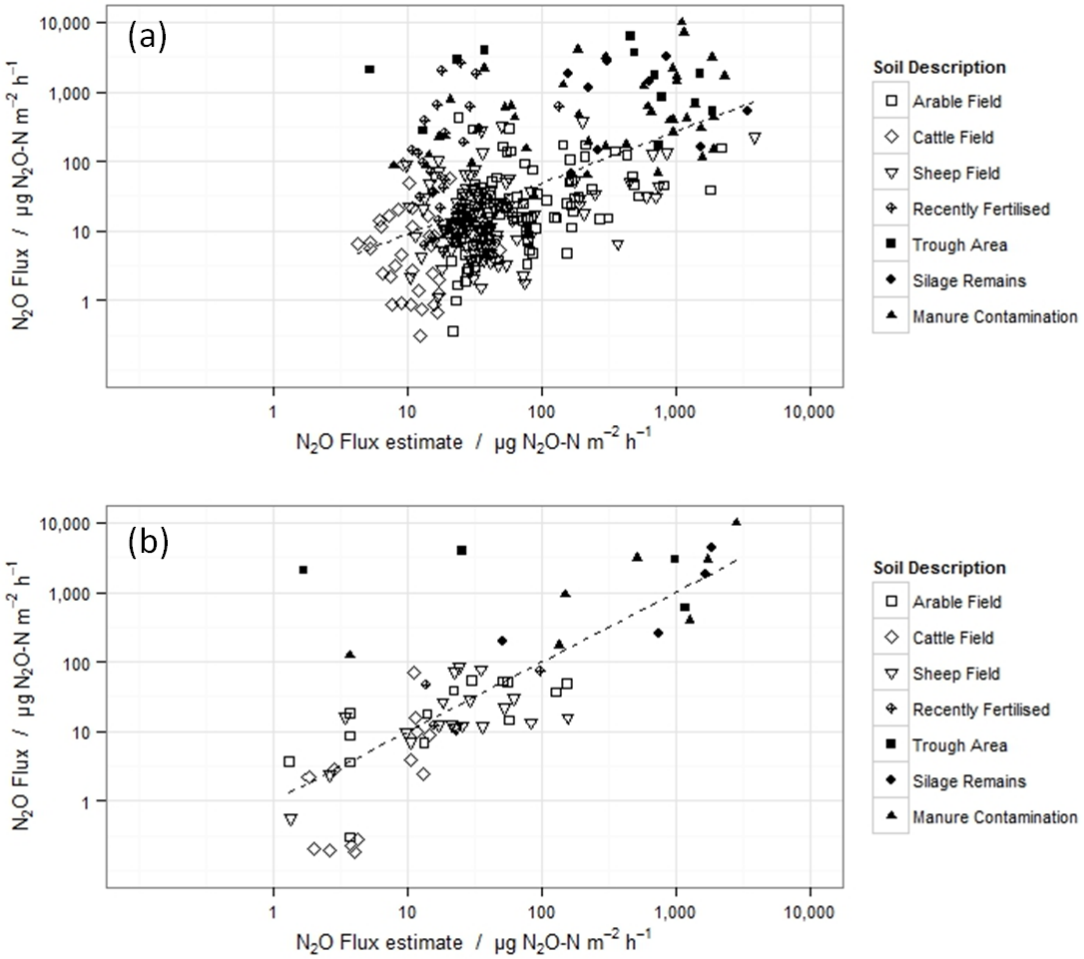

Figure 7.10 Multiple linear regression was used to identify relationships between (a) each of the individually measured soil properties and N_2O fluxes from farm soils (See Table 7.5 & Equation 7.3) and (b) mean values of soil properties and N_2O fluxes from 70 identified groups of farm soils with similar soil types (See Table 7.5 & Equation 7.4).

Table 7.5 Multiple linear regression correlation of soil properties (0–5 cm depth) with $\log_{10}(N_2O$ flux) as plotted in Figure 7.10.

	Coefficient estimate	Coefficient Std. Error	p - value
Individual regression			
(Intercept)	3.7	0.6	<0.001
$Log_{10}(NH_4^+)$	0.5	0.1	<0.001
$Log_{10}(NO_3^-)$	0.9	0.2	<0.001
pH	0.2	0.1	0.025
Vol. water content	-0.01	0.003	<0.001
Rainfall / mm	-0.007	0.001	<0.001
Grouped regression			
(Intercept)	5.5	0.5	<0.001
$Log_{10}(NH_4^+)$	0.7	0.4	0.05
$Log_{10}(NO_3^-)$	1.3	0.4	<0.001
Rainfall / mm	-0.007	0.002	0.004

7.3.6 Estimating farm scale nitrogen input

During this study it was not possible to monitor fluxes from fertiliser events in a way which would have allowed an accurate estimate of N_2O emission factors across the farm from on-site measurements. Multiple linear regression carried out using the measurements recorded during the project (See Figure 7.10 & Table 7.5) implies a strong relationship between N_2O flux and available nitrogen (in the form of NH_4^+ and NO_3^-). This relationship suggests that N_2O flux will correlate with N input as reported in the literature (IPCC 2007; Lesschen et al., 2011; Skiba *et al*., 2012). So to predict a farm scale emission estimate of N_2O an inventory of N input for the farm is required from a number of sources:

7.3.7 Accounting for nitrogen produced by livestock

A detailed account of animal numbers at the farm was created using data provided by farm managers (Table 7.6). This data allowed an approximate estimate of nitrogen produced by livestock to be calculated using the same protocol that UK farmers use to estimate and plan for animal waste management. Values provided by the Nitrate Pollution Prevention Regulations 2008 (DEFRA, 2008) were combined with farm management data to produce an animal waste budget (See Tables 7.6 & 7.7). Nitrogen and the volume of waste produced per animal

can be calculated based on the different animal species, age and type. Using this method nitrogen input from lambs is considered negligible and is accounted for as part of the nitrogen produced by ewes (Table 7.7).

Animal numbers were recorded in barns throughout the year. This allowed an approximation of the volume of farm yard manure (FYM) to be made using further protocol as described in the Nitrate Pollution Prevention Regulations 2008 (DEFRA, 2008) (Equation 7.5). By multiplying the volume of waste generated by the animals kept in barns with constants (provided by DEFRA, 2008) for straw addition (1.15) and density (0.7) an estimate of farmyard manure volume can be made (See Equation 7.5). An estimated total of 686 m^3 of FYM was produced over 12 months in the animal barns. This is equivalent to 4,116 kg of total nitrogen content.

$$V_{FYM} = \frac{V_w \times 1.15}{0.7} \quad \text{(Eq. 7.5)}$$

Where V_{FYM} is volume of FYM produced and V_W is the volume of animal waste produced in the barns (as calculated using values in Tables 7.6 & 7.7).

Table 7.7 Approximate values for nitrogen and volume of waste produced by livestock were provided by the Nitrate Pollution Prevention Regulations 2008 (DEFRA, 2008).

	Nitrogen produced per month / Kg	Volume of waste produced per month / m^3
Cattle		
3 months (All)	0.12	0.21
3 - 13 months (All)	2.33	0.60
13 - 25 months (Steer)	4.17	0.78
13 - 25 months (Female)	4.17	0.96
>25 months (Female Breeding)	5.08	0.96
>25 months > 500 kg (Female Breeding)	6.92	1.35
Sheep		
Lambs	0.00	0.00
< 60 kg (Ewes)	0.63	0.10
> 60 kg (Ewes)	0.99	0.15

Table 7.6 Animal numbers housed in barns and grazing in pasture fields were recorded from the farm area over the year long measurement period. Nitrogen produced by all animals in the farm scale inventory was accounted for. Total nitrogen and FYM produced on a monthly basis was calculated using DEFRA Protocol (See Equation 7.4).

	Age/classification	Aug-12	Sep-12	Oct-12	Nov-12	Dec-13	Jan-13	Feb-13	Mar-13	Apr-13	May-13	Jun-13	Jul-13
Housed in Barns													
Cattle	3 months (All)	0	0	0	0	0	0	0	0	0	0	0	0
	3 - 13 months (All)	0	0	0	0	16	16	16	0	0	0	0	0
	13 - 25 months (Steer)	20	0	0	0	20	20	20	20	20	20	20	20
	13 - 25 months (Female)	0	0	0	0	14	14	14	6	6	6	6	6
	>25 months (Female Breeding)	0	0	0	0	20	20	20	0	0	0	0	0
	>25 months > 500 kg (Female Breeding)	0	0	0	0	16	16	16	0	0	0	0	0
Sheep	Lambs	50	0	0	0	0	0	0	50	50	50	30	30
	< 60 kg (Ewes)	15	0	0	0	0	0	15	35	35	35	35	35
	> 60 kg (Ewes)	15	0	0	0	0	0	15	40	40	40	40	40
Grazed Pasture													
Cattle	3 months (All)	16	16	16	16	16	16	16	44	44	44	44	44
	3 - 13 months (All)	0	0	0	0	0	0	0	16	16	16	16	16
	13 - 25 months (Steer)	20	20	20	20	20	20	20	20	20	20	20	20
	13 - 25 months (Female)	30	30	30	30	30	30	30	30	30	30	30	30
	>25 months (Female Breeding)	20	20	20	20	20	20	20	20	20	20	20	20
	>25 months > 500 kg (Female Breeding)	16	16	16	16	16	16	16	16	16	16	16	16
Sheep	Lambs	835	0	0	0	0	0	0	835	835	835	835	835
	< 60 kg (Ewes)	240	240	240	240	240	240	240	240	240	240	240	240
	> 60 kg (Ewes)	200	200	200	200	200	200	200	200	200	200	200	200
Total N Produced / kg													
	Pasture	773	773	773	773	773	773	773	813	813	813	813	813
	Barns	108	0	0	0	391	391	416	170	170	170	170	170
Volume of FYM Produced / m^3													
	Barn	32	0	0	0	131	131	137	51	51	51	51	51

Animal waste deposited on pasture fields (9476 Kg annually, as calculated in Table 7.6) is assumed to have had an effect on the flux measurements made in grazed pasture fields during the study. High flux 'hotspots' of N_2O measured in typical grazed field soils are believed to be due to additional nitrogen deposited in this manner. If this is the case, then emissions of N_2O released from grazing animal waste is taken into account when mean fluxes from grazed fields are calculated. High fluxes of N_2O around troughs and silage remains are also likely due to this deposition of additional nitrogen to the soil.

Multiple linear regression was carried out to investigate correlation between estimated animal waste nitrogen input and N_2O flux measured from grazed fields (Figure 7.11 & Equation 7.6). Data was grouped into measurements made on the same measurement date and from the same flux source with measurements in close proximity of each other (as in Figure 7.9b). Using only estimated monthly nitrogen input for the field in which measurements were made and cumulated rainfall over 30 days before flux measurements a moderate correlation can be observed with N_2O flux from the grazed fields ($R^2 = 0.65$) (See Figure 7.11a & Equation 7.6). The correlation predicts that N_2O flux from grazed fields will rise with nitrogen input from animals and decrease with more rainfall in the month prior to the flux. The Nitrogen input variable did not correlate well with N_2O flux ($p = 0.54$) and the relationship is dominated by a strong correlation with cumulative rainfall ($p < 0.001$). This relationship suggests that fluxes measured from the majority coverage of grazed fields at the farm were influenced more by rain events than by nitrogen input. The relationship between N_2O flux and cumulative rainfall over 30 days before measurements does not fit so well for the arable fields (Figure 7.11b) ($R^2 = 0.56$); however, there is still a strong correlation between the relationship ($p < 0.001$). No correlations were observed between N_2O flux and soil temperature or air temperature in any of the regression analysis in this study.

$$\text{Flux} = 1.49 + (\text{N-Input} \times 0.0065) + (\text{Rain} \times -0.018) \qquad \text{(Eq. 7.6)}$$

Where Flux is $\log_{10}(N_2O \text{ flux})$ in units of $\mu g\ N_2O\text{-}N\ m^{-2}\ h^{-1}$, N-Input is the monthly input of nitrogen to a particular field in kg-N and Rain is the cumulative rainfall over a 30 day period prior to the measurement in mm.

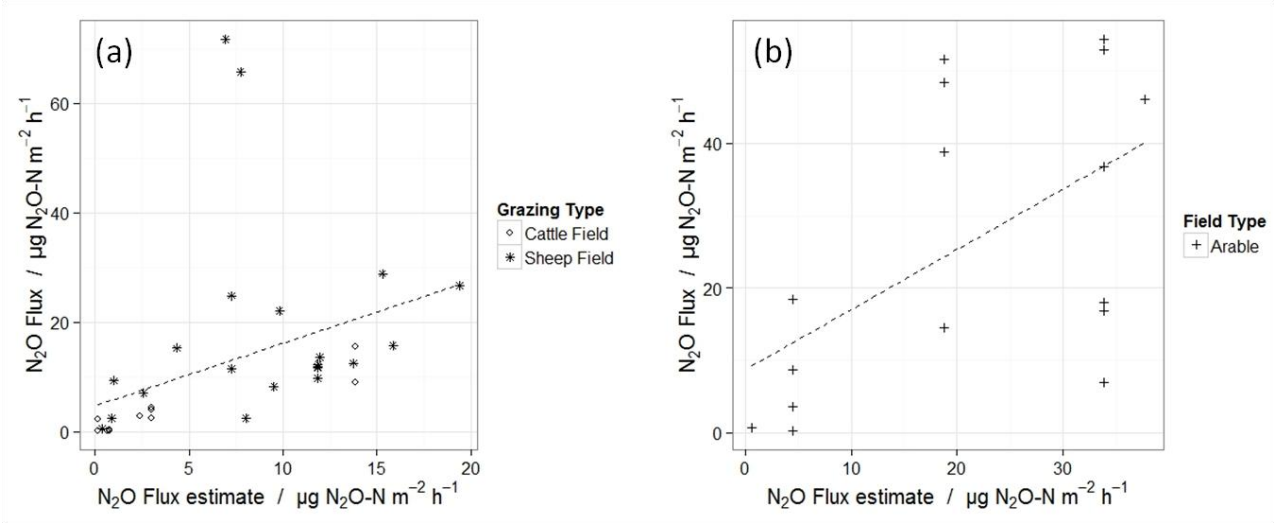

Figure 7.11 Multiple linear regression was used to identify relationships between N_2O fluxes and (a) rainfall and monthly nitrogen input (in the form of animal waste) from 34 groups of flux measurements made in grazed fields (See Equation 7.6), and (b) rainfall from 16 groups of flux measurements made in arable fields.

7.3.8 Estimating nitrogen input from fertiliser application

Farm management data provided by the farm estate managers showed that an estimated 21,863 Kg of nitrogen (a combination of 40 separate applications) was applied to the farm area in the form of mineral nitrogen, mainly as ammonium nitrate, in August 2012 and during the five month period March to July 2013 (Table 7.8). An additional 4116 Kg of nitrogen in the form of farmyard manure (FYM) was estimated to have been generated over a 12 month period from animal barns at the farm (See Table 7.6 & Equation 7.5). This was spread in January onto three arable and two silage fields (See Table 7.8).

Table 7.8 A summary of all nitrogen fertilisation events which occurred on the farm over a year long period (starting in August 2012) and the estimated N_2O emissions calculated using three different methods.

					IPCC 2007				Skiba *et al*., 2012				Lesschen *et al*., 2011			
Fertiliser Type	Month	Field Use	No. app's	Nitrogen applied / Kg	EF %	Emission /Kg	Min /Kg	Max /Kg	EF %	Emission /Kg	Min /Kg	Max /Kg	EF %	Emission /Kg	Min /Kg	Max /Kg
Artificial																
Nitram	August	Pasture	3	1192	1	11.9	3.6	35.8	4.7	56.6	38.3	74.8	2.1	25.3	16.1	34.4
Nitram	August	Silage	2	1193	1	11.9	3.6	35.8	4.7	56.6	38.4	74.9	1.1	12.6	8.1	17.2
Nitram	March	Silage	1	865	1	8.7	2.6	26.0	0.7	5.8	3.7	7.9	1.1	9.2	5.9	12.5
Nitram	April	Arable	5	3696	1	37.0	11.1	110.9	1.0	37.4	18.6	56.3	1.1	39.2	25	53.3
Nitram	April	Pasture	3	1929	1	19.3	5.8	57.9	1.0	19.5	9.7	29.4	2.1	40.9	26.1	55.6
Nitram	April	Silage	1	1459	1	14.6	4.4	43.8	1.0	14.8	7.3	22.2	1.1	15.5	9.9	21.0
Granular	April	Pasture	3	908	1	9.1	2.7	27.2	1.0	9.2	4.6	13.8	2.1	19.2	12.3	26.2
Nitram	May	Pasture	7	3153	1	31.5	9.5	94.6	1.4	44.5	19.9	69.1	2.1	66.8	42.7	90.9
Nitram	June	Arable	1	831	1	8.3	2.5	24.9	0.5	3.8	2.6	5.1	1.1	8.8	5.6	12.0
Nitram	June	Pasture	6	2257	1	22.6	6.8	67.7	0.5	10.3	6.9	13.7	2.1	47.8	30.5	65.1
Nitram	June	Silage	2	1988	1	19.9	6.0	59.6	0.5	9.1	6.1	12.1	1.1	21.1	13.5	28.7
Urea	June	Pasture	2	539	1	5.4	1.6	16.2	0.5	2.5	1.7	3.3	1.1	5.7	3.6	7.8
Nitram	July	Pasture	4	1853	1	18.5	5.6	55.6	1.4	25.5	14.3	36.6	2.1	39.3	25.1	53.4
Animal waste																
FYM	January	Arable	3	2470	1	24.7	7.4	74.1	1.6	39.1	25.3	52.9	0.5	13.3	8.5	18.0
FYM	January	Silage	2	1646	1	16.5	4.9	49.4	1.6	26.1	16.9	35.3	0.5	8.8	5.6	12.0
Total																
Artificial			40	21863		218.6	65.6	655.9		295.7	172.2	419.1		351.4	224.4	477.9
Animal waste			5	4116		41.2	12.3	123.5		65.2	42.2	88.2		22.1	14.1	30.1
All			45	25979		259.8	77.9	779.4		360.9	214.4	507.3		373.5	238.5	508.0

7.3.9 Annual inventory of N_2O flux

From the measurements and regression relationships identified in this study several methods can be used to calculate N_2O flux from the Easter Bush Estate. Sources of N_2O in this study fall into three main categories: the general field coverage of the farm, the identified 'hotspot' sources of N_2O and fertilisation events. Emission estimates for these sources can be calculated using a mixture of the data recorded and previous literature emission factors.

7.3.10 Emissions from general field coverage

Estimating N_2O emissions from the general field coverage of the farm can be done in a variety of ways. Using field area coverage and the arithmetic and geometric mean flux values of the measurements recorded in this study there are three possible methods. 1) All measurements can be classed as one group and a mean value can be calculated and applied over the entire year for the whole farm area. 2) Measurements can be classed separately depending on field use and mean flux values can be associated with the area of each field type on a monthly basis. 3) Measurements can be classed separately depending on season and mean flux values can be associated with the area of the fields on a seasonal basis. Due to missing data it is not possible to use both field type and season together to estimate N_2O emissions associated with typical soil conditions for the farm area.

Using these methods large differences in annual flux values for grazed and arable fields are seen when using arithmetic and geometric mean values (Table 7.9). Emission estimates calculated using arithmetic mean flux values are approximately two to three times larger than those calculated using the geometric method (Table 7.9). Differences in fluxes calculated using either the field use or seasonal variations also result in large differences. The outcome of this emission estimate is entirely dependent on the mean flux values reported in Table 7.3 and are prone to the same high uncertainties in these values.

Table 7.9 Annual emissions of N_2O (kg N_2O-N) from the arable and grazed fields were calculated using multiple methodologies.

Method Used	Arable Fields	95% C.I.	Grazed Fields	95% C.I.
Arithmetic Mean				
All	114.2	-349 – 607	198.9	-540 – 938
By field type	193.7	-518 – 955	150.3	-384 – 685
By season	96	-288 – 505	167.1	-445 – 779
Geometric Mean				
All	39.6	2 – 907	69.1	3 – 1400
By field type	65.5	3 – 1724	63.5	5 – 858
By season	41.6	4 –595	72.5	6 – 920
Rainfall Regression	62.7	39 – 1618	83.7	25 – 162

Another method to estimate annual emissions would be to use the regression equations linking rainfall with N_2O flux from the majority field measurements (See Figures 7.11a & b). Using this method a daily N_2O flux is estimated for the farm which is highly dependent on cumulative rainfall for the previous 30 days. This method also takes into account animal nitrogen input for the grazed fields (See Equation 7.6). N_2O emission estimates for the farm using this method are close in magnitude to those calculated using the geometric means with a similarly large range of uncertainty (Table 7.9).

7.3.11 Emissions from identified sources

Recognised high emission sources of N_2O (as described in Table 7.3) can emit very large fluxes of N_2O from relatively small space. Although a correlation between available nitrogen and flux was observed in these areas it is not possible to predict farm scale emissions from these sources using this relationship due to missing data. Nitrogen input and stocking density around trough and feeding areas is not known and therefore cannot be used to predict emissions from these soils. From the results gathered in this study the only available method to calculate fluxes from these sources over the year long measurement period is to use the mean (arithmetic and geometric) flux value for each source and combine it with estimated area coverage.

For many of these sources it is difficult to estimate the true area of coverage without many measurements of N_2O around the perimeter of each individual area. Over the course of the field work GPS measurements were used to measure outlines of several suspected sources of N_2O such as manure heaps, feeding

troughs and areas which contained silage remains. To estimate the total area coverage of these features for the farm over a period of a year requires some large assumptions and generalisations to be made.

To simplify the process, estimates of 20 and 35 m^2 were used to calculate the area of influence of each animal trough used for sheep and cattle respectively based on GPS measurements carried out at several locations. To estimate the total area of soil affected by troughs around the farm the number of fields which contained a particular animal type was multiplied by the appropriate area of influence on a monthly basis. Estimates of 20 and 40 m^2 were made for the areas of soils which contained silage residues for sheep and cattle grazed pastures respectively which were also estimated from GPS measurements. Unlike the trough areas, the silage residues continued to emit large fluxes throughout the year regardless of whether animals were in the field or not. A constant value of 320 m^2 across the farm is used throughout the year for areas influenced by silage remains as not enough information is known about the temporal properties of these soil types.

Although many manure heaps were present in the farm area, these could not all be associated with the small selected area representative of a typical farm size within the larger farm estate. A simple calculation was done using the volume of FYM produced in barns (See Table 7.6) and an approximate height of 2 m for manure heaps stored around the farm to calculate an estimated of area coverage of manure heap for the simulated farm. The total FYM produced throughout the year is estimated to be 686 m^3. This manure was spread in January resulting in no manure heap coverage for this month. The maximum coverage of manure contaminated soil is estimated to be 342 m^2 which is split between the area coverage of the manure heap and contaminated soils categories on a monthly basis. A similar method was used to estimate the area of FYM coverage in animal barns based on the volume of waste produced per month and an estimated depth of 0.5 m.

Two concrete floored silage heap containment areas were measured to be 800 m^2 each. One heap was selected to be part of the farm inventory. This heap reached maximum volume (100%) in August after silage harvests in June, July and August. The lowest volume of silage was estimated to be in May (10%). The area of coverage of the silage heap was calculated on a monthly value based on incremental 10% decreases in silage between August and May and 30% increases per harvest in June, July and August.

Using the estimated monthly area of coverage of each of the identified sources a yearly estimated flux was produced from the mean flux values in Table 7.3 (Table 7.10). As with the majority field measurements there is a large difference between the estimates made using arithmetic and geometric mean values. Uncertainties in these estimates are extremely large due to uncertainties in mean flux estimates for each source.

Due to the large range of N_2O flux measurements from silage storage a very high arithmetic mean flux and uncertainty are reported. It is likely that one or two extremely high flux measurements which are not a good representation of the silage heap as a whole distorted these values.

Table 7.10 Annual emissions of N_2O (kg N_2O-N) from identified sources of N_2O were estimated for the farm scale using mean flux values reported in Table 7.3.

Flux Source	Arithmetic Method	95% C.I.	Geometric Method	95% C.I.
Trough Area	4.1	-9 – 17	0.3	0 – 239
Silage Remains	6.7	-13 – 27	2.8	0 – 55
Manure Contamination	4.9	-18 – 27	0.7	0 – 57
Manure Heap	13.3	-39 – 65	1.4	0 – 397
Animal Barn	5.0	-2 – 12	2.9	0 – 63
Stored Silage	71.4	-525 – 668	0.5	0 – 301

7.3.12 Emissions from nitrogen fertiliser application

Using the fertiliser data recorded by the farm managers (See Table 7.8) an N_2O emission estimate can be calculated using emission factors reported in previous literature. The most commonly used and simplest method to estimate N_2O emissions from fertiliser events is to apply the IPCC 2007 default emission factor (EF) of 1% of the mass of applied nitrogen. This value comes with an estimated uncertainty which ranges between 0.3 to 3%. Using the IPCC method we estimated that a total of 260 kg of N_2O-N is emitted from the farm over the period of a year due to fertilisation events (Table 7.8). The uncertainty in this estimate ranges from 77.9 to 779.4 Kg of N_2O-N (Table 7.8). Mineral fertilisers account for 81% of emissions from fertiliser events from the farm calculated using this method of calculation with the remainder due to the application of farm yard manure

Previous work carried out at Easter Bush Farm investigating N_2O emissions revealed a relationship between precipitation and the N_2O emission factor for fertilisation events in the area (Skiba *et al.*, 2012). This relationship predicts the emission factor of a nitrogen fertiliser event using the summed cumulative rainfall one week previous and three weeks after the event (Equation 7.7). After applying this equation to the rainfall data collected at the farm (See Figure 7.2), an emission factor can be calculated for each fertiliser event (Table 7.8). Using this method the EF varies on a month to month basis. High rainfall in August 2012 results in a significantly larger EF of 4.7% calculated for this month. In June low rainfall results in an EF of only 0.5%. The

cumulative annual emission estimate of N_2O from fertiliser events calculated using this method is 361 Kg N_2O-N. An uncertainty range of 214 to 507 Kg of N_2O-N is estimated using the standard deviation in mean monthly rainfall for the relevant month in which fertilisation took place although this range may be higher due to the uncertainty in the fit used in Equation 7.7. Mineral fertilisers accounted for 78% of emissions calculated using this method of calculation.

$$\mathrm{EF} = 0.03 \times \mathrm{P} - 0.25 \qquad \text{(Eq. 7.7)}$$

Where EF is the emission factor of N_2O released as a percentage of nitrogen applied during a fertilisation event and P is the cumulative sum of precipitation in mm over a three week period after the event and one week previous to the fertilisation event (Skiba *et al.*, 2012).

Another separate study which investigated fertilisation events also recognised rainfall as a primary contributor to N_2O emissions (Lesschen *et al.*, 2011). In this study N_2O EFs were associated with soil type, fertiliser type, field use and average annual precipitation. The fields in this study can all be classed as clay soils and field type is described in Table 7.1 (Silage production classed as arable). The annual rainfall for the Easter Bush farm estate over the past ten years is 912 mm (SD ± 201 mm). Using the Lesschen method, an estimated annual emission of 374 Kg of N_2O-N was calculated for the year long period (See Table 7.8). An uncertainty in this estimate o 239 to 508 Kg of N_2O-N was calculated using the standard deviation in annual rainfall for the ten year period although uncertainty in the emission factors used in the calculation is likely to increase this value. Mineral fertilisers account for 94% of emissions calculated using this method of calculation (See Table 7.8).

7.4 Discussion

7.4.1 Sources of N_2O flux at the farm scale

Our study has shown that the application of N fertilisers is the largest single contributor to N_2O released from this farm, and thereby agrees with current understanding (IPCC 2007; Thomas *et al.*, 2011). The fertilisation periods from the arable (including silage production) and grazed fields contributed to 49% of the total farm emissions, ranging from 260 to 374 Kg N_2O-N depending on which EF calculation method was used (Table 7.8). Nitrous oxide emissions from field soils during periods not influenced by N fertilisation (the general conditions on the arable and grazed pasture fields) contributed almost equally to the N_2O budget as the fertilisation period, with arable field responsible for 20% of the emissions and grazed grasslands to 26% of the emissions (Table 7.11 & Figure 7.12).

Table 7.11 A budget of annual emission estimates calculated using the arithmetic mean of measured flux values and reported emission factors.

Source	Area Coverage / ha	Annual Emissions per hectare / kg N_2O-N ha^{-1}	Total Annual Emissions / kg N_2O-N	Range of Uncertainty /kg N_2O-N
Trough Area	0.02	169	4.1	0 – 17
Silage Remains	0.03	209	6.7	0 – 27
Manure Contamination	0.02	247	4.9	0 – 27
Manure Heap	0.01	924	13.3	0 – 65
Animal Barn	0.01	439	5	0 – 12
Arable Fields	53.8	2.5	134.6	0 – 955
Grazed Fields	72.8	2.4	172.1	0 – 938
Fertiliser Application	117.0	2.8	331.4	254 – 779
Total	132.7		672.1	254 – 2,820

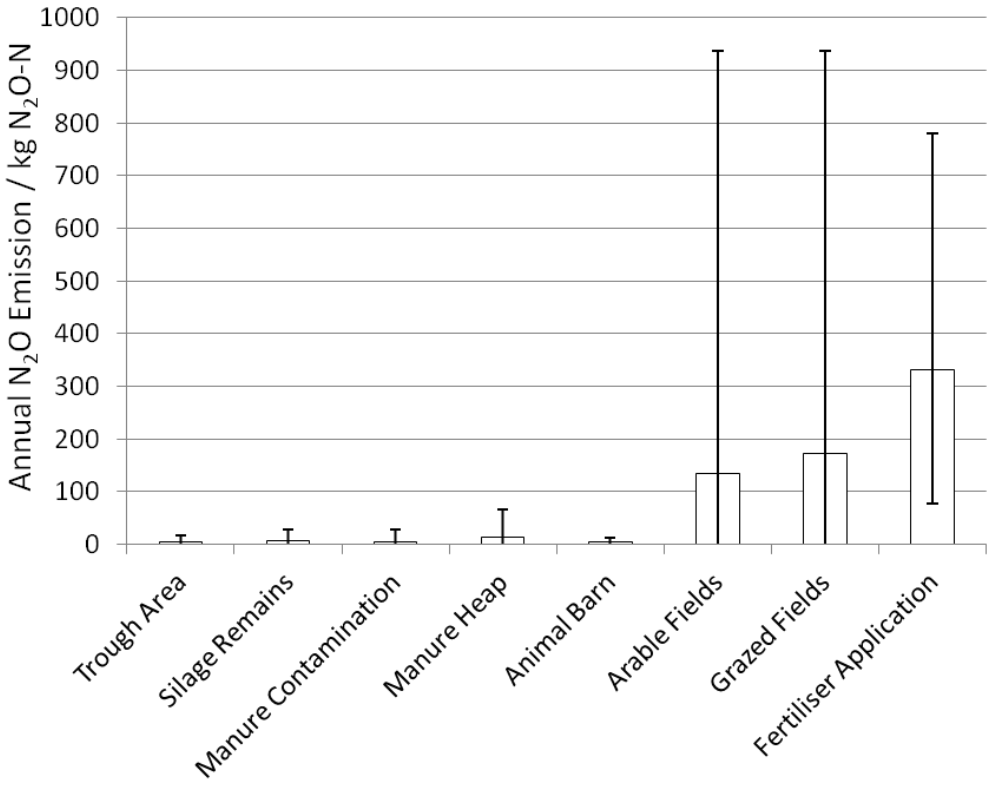

Figure 7.12 Annual emission estimates of N_2O at the farm scale calculated using the arithmetic mean of measured flux values and reported emission factors (See Table 7.11).

The use of three different methods to calculate emissions from fertilisers resulted in three different N_2O flux estimates for the whole farm (See Table 7.8). Estimates using the IPCC method were smaller compared to

the other two methods in this study. The methods outlined in Skiba *et al*. (2012) and Lesschen et al. (2011) take into account variations with rainfall in additions to variations with N applied. Overall the total N_2O emission estimate calculated for fertiliser use by these two methods compare well. However, large differences in EFs due to temporal differences and fertiliser type between the methods are apparent (See Table 7.8). In spite of the extra complexity introduced by the Skiba and Lesschen methods, estimate uncertainties are still high.

The uncertainty in N_2O emissions from fields during the fertilisation periods presents difficulties in creating accurate farm scale emission inventories as it is a large source with no precise estimate method. This uncertainty can only be improved by more detailed temporal and spatial knowledge of the drivers responsible for N_2O production and emission. Our results support a continuing emphasis on studies into understanding the magnitude of N_2O emissions from nitrogen fertiliser events at a regional scale. EFs which can take into account regional meteorological inputs such as those in Skiba *et al*., (2012) and Lesschen *et al*., (2011) are more appropriate for estimating emissions from fertiliser events at the relatively small farm scale than the global scale estimates that the IPCC methodology accounts for; however, uncertainty still remains very large using these methods.

Although generally low in magnitude, fluxes from typical arable and pasture soils contribute a significant proportion of the total N_2O emissions from the farm area due to the wide area coverage (124 ha). Fluxes measured from the general field conditions in spring and summers were larger than those in autumn and winter (See Figure 7.2 & Table 7.3). This difference is likely a response of several factors, such as increased microbial mineralisation, nitrification and denitrification rates and plant growth at higher temperatures (Braker et al., 2010; Wertz et al., 2013), and changes in rainfall patterns during spring and summer. It is likely that temporal variations are caused by several rather than a single definitive factor. Annual emission factors of N_2O calculated from the typical field measurements reported in this study ranged from 0.8 to 4.1 Kg ha^{-1} and 1.0 to 3.1 Kg ha^{-1} for arable and pasture fields respectively. Large uncertainties are associated with these values due to the wide range of flux measurements made and the inability to predict spatial variability of N_2O flux at a wide scale (See Table 7.10).

Relationships between rainfall and fluxes measured in arable and pasture fields indicate that N_2O decreased with increased rainfall (See Figure 7.9). This is the opposite of what is reported in literature when calculating emission factors from nitrogen fertilisation events (Skiba *et al*., 2012 and Lesschen *et al*., 2011). This observation is not fully understood. It is not possible to determine if this relationship is real or an artefact of

the limited seasonal measurement dates. The effect that soil moisture content has on microbiological processes and gas diffusion varies between experiments reported in literature. Further work is required to fully understand the combined effect that soil properties (such as soil moisture, oxygen availability and soil type) on N_2O emissions from agricultural soils.

Some potent sources of N_2O on the farm (such as manure heaps and animal barns) emit far more N_2O per unit area than soils which represent majority field coverage. These areas are estimated to cover only a very small area of the total farm size (approximately 0.1%) and as a result, emit a relatively small amount of N_2O compared to the farm as a whole (See Table 7.10). There are still relatively large isolated emissions from sources of N_2O throughout the farm area. Animal waste, FYM heaps and contamination from manure heaps all contribute to N_2O fluxes from the farm. These sources of nitrogen are difficult to manage in terms of reducing emissions of greenhouse gasses, and like fertiliser use, come with a large range of uncertainty associated with N_2O flux values (> 50%) as has been described in previous literature (Chadwick et al., 1999; Montes et al., 2013).

High N_2O flux measurements made near animal feeding and drinking troughs in this study can be attributed to the higher concentration of animal waste deposited in these areas. This is also the case for areas of silage remains found in the pasture fields. Emission estimates from feeding areas across the farm compared in magnitude to those measured from the animal barns over the period of a year. N_2O emissions from animal barns are believed to be a significant source of N_2O at the national level (Chadwick et al., 1999; Webb, 2014) which suggests that emissions from feeding areas and drinking troughs throughout present on farmland may also contribute in a significant way to N_2O emissions at a national scale. Difficulties remain in accurately identifying the area coverage which these features account for and it is likely that other such areas within pasture fields exist. Animals tend to spend longer amounts of time in areas they are more comfortable (See Chapter 6) which means they will deposit more waste in sheltered or shaded areas depending on weather conditions. This behaviour is unaccounted for in this inventory and presents another source of uncertainty for this study which may increase uncertainty by more than 100% of that reported in this study.

Emission estimates of N_2O released from stored silage grass were the least certain of all sources at the farm scale. A wide range of measured flux values which varied by over five orders of magnitude (zero flux to 352,909 μg N_2O-N m^{-2} h^{-1}) and a low number of measurements (n = 20) prevented an accurate estimate of this contribution. This estimate is also influenced by the state of the grass silage heap. This study found that decayed

grass can emit extremely high N_2O fluxes. As most measurements were taken later in the year it is likely that the grass is more decayed that it may have been when the grass was freshly cut fluxes measured are higher than they would have been. It is likely that the values reported for silage grass storage in this study are not representative of a typical silage heap, although there is little evidence in literature to compare values with (Hellebrand, 1998).

7.4.2 Predicting fluxes of N_2O from soil properties

A common factor between many of the high fluxes measured at the farm scale is the addition of available nitrogen to agricultural soils. From the soil analysis carried out in this study it is clear that available nitrogen in the soil is the primary cause of N_2O emissions from many of the high flux areas. This relationship has been identified in other similar studies (Šimek *et al.*, 2006; Jones *et al.*, 2007). A strong log-normal correlation between NO_3^- content of the soil and N_2O flux was observed at many of the locations in which high fluxes were measured. Available nitrogen in animal waste and decaying plant materials is often available in the form of NH_4^+ (Jarvis *et al.*, 1996). The presence of NO_3^- indicates that nitrification is taking place in these soils and also that it is available for denitrification processes. It is likely in these soils with high available nitrogen contents that both microbiological processes occur simultaneously at greater rates than the surrounding soils, albeit at different rates depending on environmental factors. Oxygen availability, temperature, WFPS and the diffusity of the soil surface are all likely to play a role in determining the rates of microbiological processes in the soils (Turner *et al.*, 2008).

This study identified NO_3^- concentrations as a good indicator of 'hotspots' of N_2O fluxes in agricultural soils; however, there remain significant differences between measured flux and estimated flux using NO_3^- as a proxy (See Figure 7.10). There are multiple reasons for a lack of consistency between N_2O flux and soil properties at different locations. The sampling method used to collect soils for chemical analysis of NH_4^+ and NO_3^- is open to multiple inconsistencies between locations. An example of this is that no increase in available nitrogen was observed in soil measurements made from the recently fertilised fields in the study even though it is certain that nitrogen was applied to the fields. This may indicate that the 5 cm core depth was too deep to measure this short term addition of nitrogen to the system which remained on the surface of the soils. It has been reported in literature that net N_2O flux is determined by the first few mm of soil (Neftel et al., 2000). Animal feeding areas and soils contaminated by manure heaps are relatively long term features in which nitrogen will pass through the layers of the soil with time and core depth is less significant in these soil property measurements.

The variability of nitrogen within a single measurement location is also likely to cause some uncertainty in reported available nitrogen as only one sample was taken from each chamber placement. It becomes impractical to do multiple soil samples from each individual flux measurement and this uncertainty may explain why grouped datasets showed better correlation between mean values of flux and NO_3^- concentrations than individual measurements (See Figure 7.10). A combination of uncertainties in methodology from sampling to analysis combined with the sensitive log-normal relationship between available nitrogen and N_2O flux results in a relatively large difference between many of the measured flux values and the estimated values using correlation of soil properties.

Using soil NO_3^- as a proxy for N_2O flux is not a practical proposition. The analysis of soil NO_3^- and NH_4^+ is more costly and time consuming to measure than N_2O fluxes. Their distribution is similarly variable in time and space as that of N_2O measurements in terms of spatial variability and magnitude. These traits make available nitrogen a poor replacement for flux measurements as even if an accurate correlation between the relevant soil properties and flux could be identified, the same issues of upscaling will arise due to an inability to interpolate available nitrogen measurements as is with N_2O flux. It is also unlikely that a correlation equation using parameters from any one experiment will allow an estimate of N_2O flux to be accurately predicted from a different field site. Multiple studies with similar regression equations often report very different results (Jones et al., 2007; Šimek et al., 2006). Available nitrogen and WFPS are commonly identified as the primary drivers of N_2O emissions from agricultural soils in these studies, although no definitive relationship can be identified.

7.4.3 Unaccounted N_2O sources

Several sources of N_2O emissions associated with agricultural sources have not been estimated in this inventory due to either a lack of available data from the farm or a lack of an appropriate method which would allow an estimate to be made. Primary sources of N_2O emissions not estimated from the farm include fossil fuel emissions and tillage events. Currently literature on N_2O flux emissions from tillage events does not provide sufficient data to create an emission estimate for the farm scale. Secondary emissions of N_2O are not included in this emission inventory as they fall outside of the scope of the experiment. The most significant secondary sources of N_2O emissions from the farm estate are likely to be that of ammonia deposition and emissions and NO_3^- leaching from the fields containing dissolved N_2O and mineral and organic nitrogen compounds. Both of these sources will be directly linked with the application of nitrogen fertilisers and animal waste to fields; however, they are not included in this study for logistical reasons.

7.5 Conclusions

A farm scale budget made from the 133 ha Easter Bush Farm Estate determined that 672 kg N_2O-N was released over a 12 month period between August 2012 and July 2013. This study showed that at the farm scale direct N_2O emissions released from regularly fertilised fields are most likely the largest single source of N_2O. Emissions from identified sources of N_2O such manure heaps and animal troughs contributed only a small fraction (5%) of the total annual budget from the farm. This research verifies that N_2O emissions from agricultural soils are mainly driven by available nitrogen in soils. This nitrogen is deposited in to the soils in the form of, nitrogen fertilisers, animal waste and decaying plant matter. Further research is required to identify relevant regional emission factors for multiple sources of N_2O from agricultural sources to further understand how to apply mitigation strategies at a farm scale.

Chapter 8

Investigating uptake of N_2O in agricultural soils using a high-precision dynamic chamber method

Summary

Uptake (or negative flux) of nitrous oxide (N_2O) in agricultural soils is a controversial issue which has proven difficult to investigate in the past due to constraints such as instrumental precision and unknown methodological uncertainties. Using a recently developed high-precision quantum cascade laser (QCL) gas analyser combined with a closed dynamic chamber, a well defined detection limit of 4 µg N_2O-N m^{-2} h^{-1} could be achieved for individual soil flux measurements. 1220 measurements of N_2O flux were made from a variety of UK soils using this method, of which 115 indicated uptake by the soil (i.e. a negative flux in the micrometeorological sign convention). Only four of these apparently negative fluxes were greater than the detection limit of the method, which suggests that the vast majority of reported negative fluxes from such measurements are actually due to instrument noise. As such, we suggest that the bulk of negative N_2O fluxes reported for agricultural fields are most likely due to limits in detection of a particular flux measurement methodology and not as a result of microbiological activity consuming atmospheric N_2O.

Work presented in this chapter is based on the manuscript published as: N. J. Cowan, D. Famulari, P. E. Levy, M. Anderson, D. S. Reay, U. M. Skiba: Investigating uptake of N_2O in agricultural soils using a high-precision dynamic chamber method, in Journal of Atmospheric Measurement Techniques, June 2014)

8.1 Introduction

N_2O is a naturally occurring greenhouse gas (GHG) which is formed predominantly in soils and aquatic environments as a by-product of the microbial processes of nitrification and denitrification (e.g. Davidson *et al*., 2000). Atmospheric N_2O has increased from pre-industrial concentrations of 280 nmol mol^{-1} to over 320 nmol mol^{-1} (IPCC, 2013). This increase is believed to be primarily due to agricultural activities such as the production and subsequent application of reactive nitrogen fertilisers to agricultural soils, which increases microbial activity and the production of N_2O on a global scale (IPCC, 2007; IPCC, 2013). It is estimated that agriculture contributes either directly or indirectly to over 80% of all anthropogenic N_2O emissions; however, there is a large uncertainty associated with these figures (IPCC 2007). Emission estimates of N_2O from various soils often have large uncertainties associated with them due to the large spatial and temporal variability of N_2O flux measurements (Velthof *et al*., 1996; Zhu *et al*., 2013; Chadwick *et al*., 2014). Accurate measurement of N_2O flux from various agricultural soils can also be difficult to perform due to the relatively low concentrations of N_2O in the atmosphere (nmol mol^{-1}). With the exception of nitrogen fertiliser application events, fluxes of N_2O from agricultural soils are often small, verging on the detection limits of gas analysers (<20 µg N_2O-N m^{-2} h^{-1}) (Smith *et al*., 1994; Flechard *et al*., 2005).

Reported observations of negative fluxes (or uptake) of N_2O from the atmosphere into agricultural soils are relatively common in literature and have been reported in several studies using different methodologies (sometimes exceeding values as high as 50 µg N_2O-N m^{-2} h^{-1}) (Ryden, 1981; Papen *et al*., 2001; Butterbach-Bahl *et al*., 2002; Flechard *et al*., 2005). In these studies the authors attribute the uptake of N_2O to microbial denitrification, which is biologically plausible (Okereke, 1993; Davidson *et al*., 2000). However, there has been much debate over whether the observed negative fluxes of N_2O are genuinely a result of microbial uptake or merely experimental or instrumental artefacts (Chapuis-Lardy *et al*., 2007).

The static chamber approach is generally deployed to monitor N_2O fluxes from agricultural soils (Jones *et al*., 2007; Hensen *et al*., 2013). Fluxes derived from static chamber methods are often prone to high instrumental noise from gas chromatograph (GC) instruments, the choice of regression method used and temperature and pressure changes within the chamber (Venterea *et al*., 2009; Levy *et al*., 2011). N_2O fluxes also show very high spatial variability, which makes it more difficult to judge whether any individual measurement is an erroneous outlier or truly valid (See Chapters 5, 6 & 7).

Recent advances in infra-red laser technology have resulted in the commercial availability of high precision trace gas analysers such as quantum cascade lasers (QCLs) capable of measuring N_2O concentrations with very high precision and accuracy. Here, we used a QCL gas analyser with a closed dynamic chamber, resulting in a measurement system with a significantly lower detection limit than GC-based static chamber methods. We used this system to measure a total of 1220 fluxes at five field sites across the UK at different times of the year. This study aimed to investigate the occurrence and validity of negative fluxes of N_2O within this data set, and their relationship with commonly measured soil properties.

8.2 Materials and methods

8.2.1 Dynamic chamber method

All of the N_2O flux measurements reported in this paper were made using a non-steady-state flow-through (or closed dynamic) chamber system which circulated air between a flux chamber and a quantum cascade laser (QCL) gas analyser (as described in Chapter 4). A compact continuous wave QCL (CW-QC-TILDAS-76-CS, Aerodyne Research Inc., Billerica, MA, USA) was used to measure gas mixing ratios within the dynamic chamber system. The instrumentation was either placed in a stationary cabin or secured inside a four wheel drive vehicle to allow for mobile measurements. The system could be powered from a main power supply when available; and when used in mobile conditions, a diesel generator was required which was kept on a tow trailer to provide a constant supply of electricity to the system.

The chamber consisted of a cylindrical polyvinyl chloride (PVC) plastic pipe of 48 cm inner diameter (ID) and 22 cm height with closed cell neoprene sponge attached to the underside. It was placed onto circular stainless steel collars which were inserted (approximately 5 cm) into the soil and the neoprene sponge formed an airtight seal between the chamber and the collar. Clips were added to the chamber to increase the strength of this seal. Two 30 m lengths of 3/8 inch ID Tygon® tubing were attached to both the inlet of the QCL and the outlet of the pump. This provided a 30 m radius from the analyser in which the chamber could be placed. A flow rate of approximately 6 to 7 L min^{-1} was used between the QCL and the chamber.

The dynamic chamber method records gas mixing ratios at a rate of 1 Hz during flux measurements which allows detailed investigation of an individual flux measurement. During the 180 second enclosure time of each chamber measurement the first 60 seconds of measurements are discarded to give the system time to mix

air between the chamber and the analyser. A total of approximately 120 mixing ratio measurements are then used to calculate fluxes of N_2O from each chamber location

Fluxes of N_2O were calculated using linear and non-linear asymptotic regression methods using the HMR package for the statistical software R (Pedersen *et al*., 2010; Levy *et al*., 2011). Using a mixture of goodness-of-fit statistics and visual inspection the regression method that provided the best fit for the time series of mixing ratio was chosen for each individual measurement. The rate of change in mixing ratio of a particular gas can then be used to calculate soil flux for each measurement (Equation 8.1).

$$F = \frac{dC}{dt_0} . \frac{\rho V}{A} \qquad \text{(Eq.8.1)}$$

Where F is gas flux from the soil (μmol m^{-2} s^{-1}), dC/dt_0 is the initial rate of change in mixing ratio with time in μmol $mol^{-1}s^{-1,}$ ρ is the density of air in mol m^{-3}, V is the volume of the chamber in m^3 and A is the ground area enclosed by the chamber in m^2.

8.2.2 *Field sites*

The dynamic chamber method was developed to improve the precision of N_2O flux measurement from soils and verify other chamber methodologies in a national project (InveN_2Ory; http://www.ghgplatform.org.uk/) to improve the agricultural greenhouse gas emissions inventory in the UK (Skiba *et al*., 2012). The dynamic chamber has been used at a variety of field sites run by different research groups across the UK between 2011 and 2014 where N_2O flux experiments were taking place using more common static chamber methodologies (See Table 8.1; Chadwick *et al*., 2014). The majority of measurements made during the project were from areas within Easter Bush Farm Estate (Penicuik, Midlothian), which is run jointly between the Scottish Rural University College (SRUC) and the University of Edinburgh (UoE).

Soil samples were collected for individual flux measurements during the farm and grazed grassland field experiments at Easter Bush in order to investigate which soil properties were driving N_2O fluxes. From these locations 5 cm deep soil samples were taken from inside the chamber collar using a 2 cm wide corer immediately after the flux measurement was completed. These soils were used to determine soil pH, soil moisture content (via oven drying at 100 ˚C) and available nitrogen in the form of ammonium (NH_4^+) and nitrate (NO_3^-) via KCl extraction. Bulk density soil samples also were taken immediately after the flux measurement

using a sharp metal cutting cylinder (7.4 cm diameter, 5 cm deep), which was carefully hammered into undisturbed soil. Bulk density samples were used to calculate total carbon and nitrogen content of the soil, soil moisture content and WFPS (Rowell, 1994). All soils were frozen after collection from the field sites for preservation before lab analysis was carried out. This provided 455 soil samples with individual flux measurements associated with each of them, 61of which were from locations that reported negative N_2O flux. It was not possible to take destructive soil samples directly from the nitrogen fertiliser manipulation chambers, as this would have interfered with the very frequent (at least weekly) flux measurement programme.

8.3 Results

8.3.1 Measured fluxes of N_2O

Flux magnitude measured from the different field sites across the UK varied between -5.5 to 27,475 µg N_2O-N m^{-2} h^{-1}. A large variety of soil types, fertiliser treatments and agricultural fields which contained different crops and grazing animals were all measured during the experiments which provided many areas of high and low N_2O fluxes. The vast majority of the N_2O fluxes measured were below 50 µg N_2O-N m^{-2} h^{-1}. 887 of the 1220 measurements (73%) fell into this category (Figure 8.1). Of these, 115 of the measurements showed negative fluxes of N_2O, accounting for 9.4% of all of the measurements made.

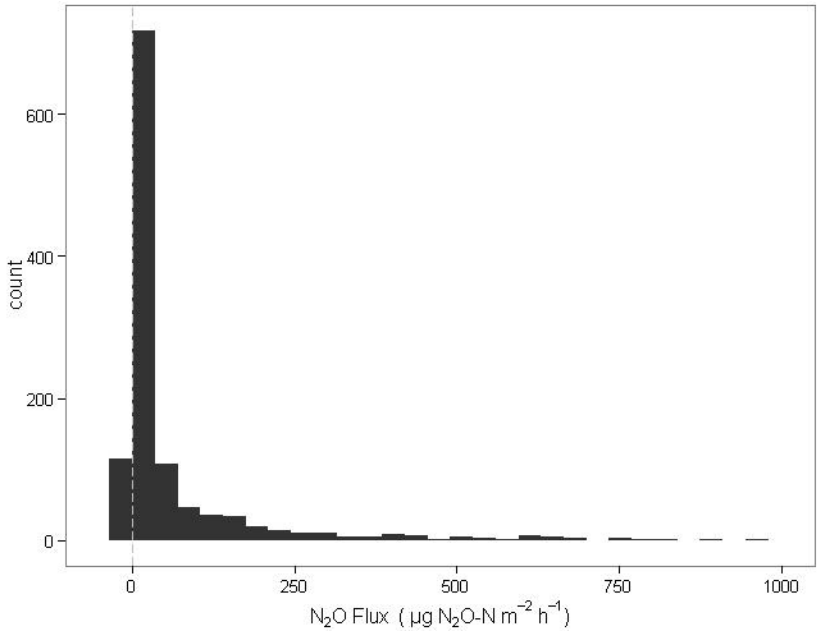

Figure 8.1 Frequency of all N_2O fluxes measured from all locations excluding those above 1000 µg N_2O-N m^{-2} h^{-1}.

Table 8.1 A summary of all InveN_2Ory field sites from which N_2O fluxes were made using the dynamic chamber method.

Location	Dates of measurements	Measurement details	Soil Texture	Total annual rainfall (mm)	Annual average air temperature (˚C)	No. of M'mnts	No. of negative fluxes
Nitrogen fertiliser manipulation plots[a]							
Dumfries (SRUC) [b]	Oct.– Nov. 2012	Grazed Grassland, SW Scotland, Mineral N, or manure applications	Sandy loam	1211	10.2	282	12
Rosemaund (ADAS)[c]	Mar. 2013	Barley, SW England Slurry, manure applications	Silty clay loam	418	10.4	49	0
Easter Bush (SRUC)	Apr.– May 2013	Barley, Central Scotland Slurry, manure applications	Clay loam	937	10.2	105	3
On-farm measurements (UoE and SRUC)							
2 grazed grasslands[d]	Apr. – Jul. 2012	Adjacent tilled and un-tilled sheep grazed grasslands	Clay loam	937	10.2	329	39
Autumn- Farm[e]	Sep. 2012	Mixture of grazed and arable fields across Easter Bush Farm Estate	Clay loam	937	10.2	80	34
Winter- Farm	Feb. 2013	As above	Clay loam	937	10.2	55	23
Spring- Farm	May 2013	As above	Clay loam	937	10.2	127	4
Summer- Farm	Jul 2013	As above	Clay loam	937	10.2	120	0
Grazed grassland[f]	Jul. 2013	Grassland with high stocking density of sheep on Easter Bush Farm Estate	Clay loam	937	10.2	73	0
				Total		1220	115

[a] Overall experimental design is described in Chadwick *et al*., 2014
[b] Bell *et al*., 2014 (In preperation)
[c] Williams *et al*., ADAS, pers comm..
[d] Chapter 5
[e] Chapter 7
[f] Chapter 6

The detection limit of the dynamic chamber system (as defined by double the typical standard deviation (SD) of a zero flux measurement reported in Chapter 4) is approximately 2 to 4 μg N_2O-N m^{-2} h^{-1}. Uncertainty in flux in each chamber measurement is calculated by propagating the uncertainty associated with each of the terms in Equation 1 to estimate the total uncertainty in the flux. Uncertainty in d*C*/d*t* was obtained from the 95% confidence interval in the regression slope parameter. As 1 Hz mixing ratios provide approximately 120 measurements over the three minute enclosure period and both linear and non-linear regression methods are applied for each individual measurement to see which fits best, the uncertainty in d*C*/d*t* caused by the choice of regression method is far less significant than previous studies which used 3–5 mixing ratio measurements over the period of an hour (Parkin *et al*., 2012).

Uncertainty in the chamber volume could be estimated by taking several measurements of height in each chamber, and taking the 95% confidence interval in the calculated chamber volume. Including estimates of the volume of vegetation, this gave values of approximately 10% of the total volume. Uncertainty in the air density term (ρ) arises from uncertainties in the temperature and pressure measurements. The 95% confidence interval for the mean temperature and pressure was calculated from the 1 Hz data, and added to the instrumental precision of the temperature probe (0.4 °C) and pressure sensor (50 Pa). Of the apparent negative fluxes recorded during all of the experiments only four exceed the negative limit of detection (0.3%) (Figure 8.2). Moreover, these fluxes (three of which are shown in Figures 8.3a,b & c) only slightly exceeded the detection limit of the system varying from -4.1 to -5.5 μg N_2O-N m^{-2} h^{-1}.

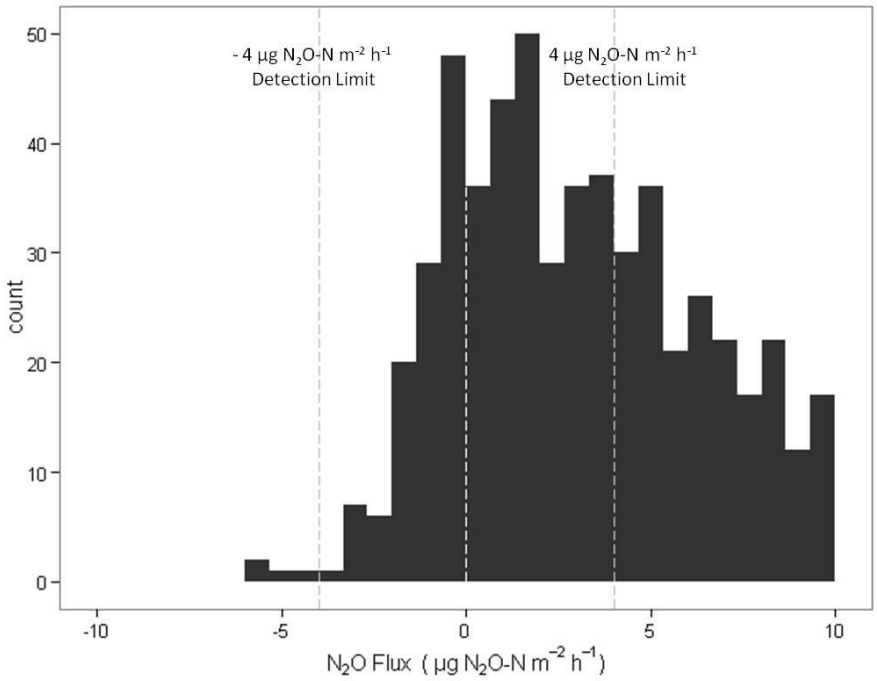

Figure 8.2 Frequency of all N_2O fluxes measured from all locations excluding those above 10 µg N_2O-N m^{-2} h^{-1}. The estimated zero flux detection limit of ± 4 µg N_2O-N m^{-2} h^{-1} is included.

The 1 Hz mixing ratio measurements show that in some cases there is a definite and consistent negative flux occurring in the chamber during the measurement period (See Figures 8.3a,b & c); however, these changes are often very small (less than 1 nmol mol^{-1} over 120 seconds) and several events can distort these measurements such as a small leak within the chamber or a gas analyser issue. In certain conditions the sensitivity of the QCL can change due to a rapid temperature change or for example electronic noise from a generator or power supply. In these situations, at near zero flux conditions, it is difficult to determine whether a negative flux of N_2O is real or an artefact of instrumental noise (Figure 8.3d). Of the 115 apparently negative fluxes measured a mixture of both is likely to have taken place.

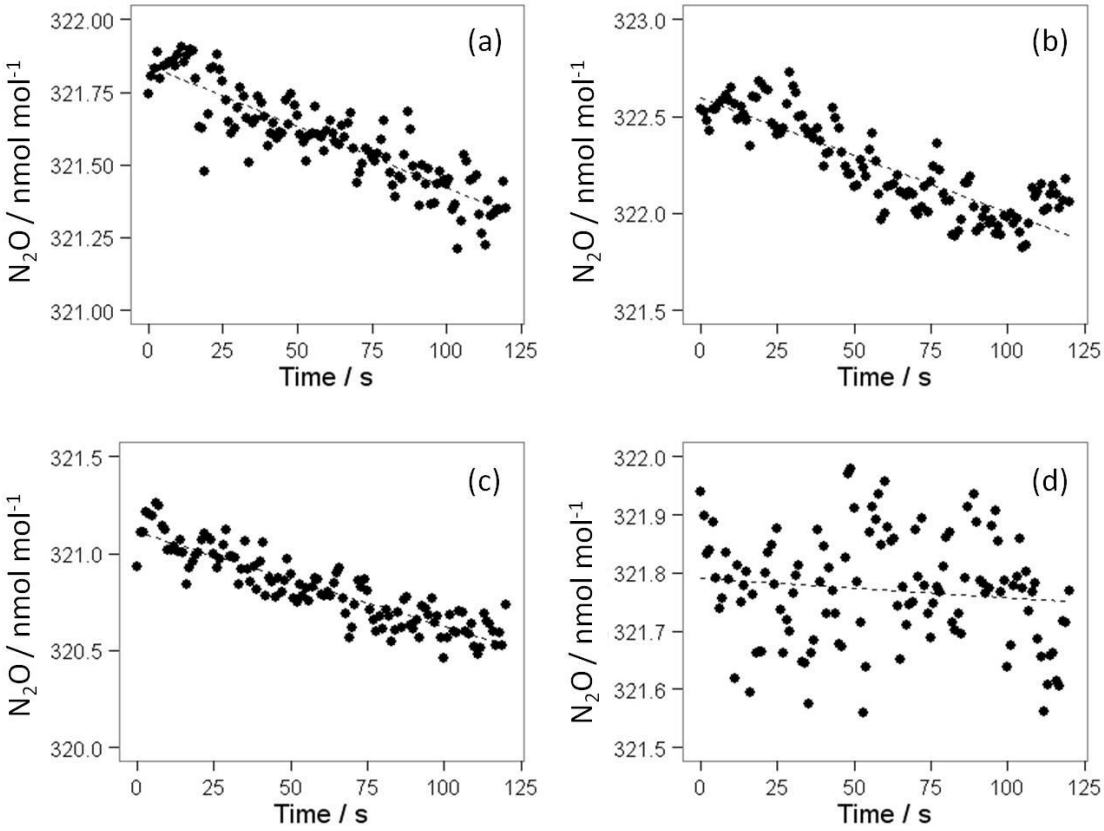

Figure 8.3 Examples of 1 Hz N_2O mixing ratio data recorded during four separate negative flux measurements made using the dynamic chamber method. Each flux measurement uses over 120 individual measurements to calculate the rate of change of N_2O mixing ratio within the chamber over a three minute measurement period. a,b,c are examples of clear and consistent negative fluxes, d is an example of negative flux likely attributable to instrumental noise.

8.3.2 Soil analysis of low flux locations

Soil samples were available for 190 chamber measurements which measured N_2O flux below 10 µg N_2O-N m^{-2} h^{-1}. Multiple linear regression analysis was used to investigate the relationship between flux and soil properties for fluxes reported in the range of -10 to 10 µg N_2O-N m^{-2} h^{-1} (See Table 8.2). The results of the regression analysis suggest that a weak relationship does exist between the measured soil properties and fluxes measured (R^2 = 0.38) (Figure 8.4a). The properties which correlate strongest with measured flux are WFPS, available NO_3^-, pH and bulk density. Individual comparison between flux and each of these soil properties reveals no clear indication of which soil conditions would provide ideal conditions for negative flux observations (Figure 8.4b, c & d). From the soil analysis results it could be suggested that in general, negative

fluxes of N_2O tend to contain very low concentrations of NO_3^- (below 0.01 mg kg^{-1}), and are more likely to occur in damper soils (WFPS >40%) with a pH of approximately 6.5; however the lack of observable difference in the soil properties measured between slightly positive and slightly negative fluxes may indicate that measurement uncertainty in both flux and soil property measurements are too large to investigate these relationships in detail.

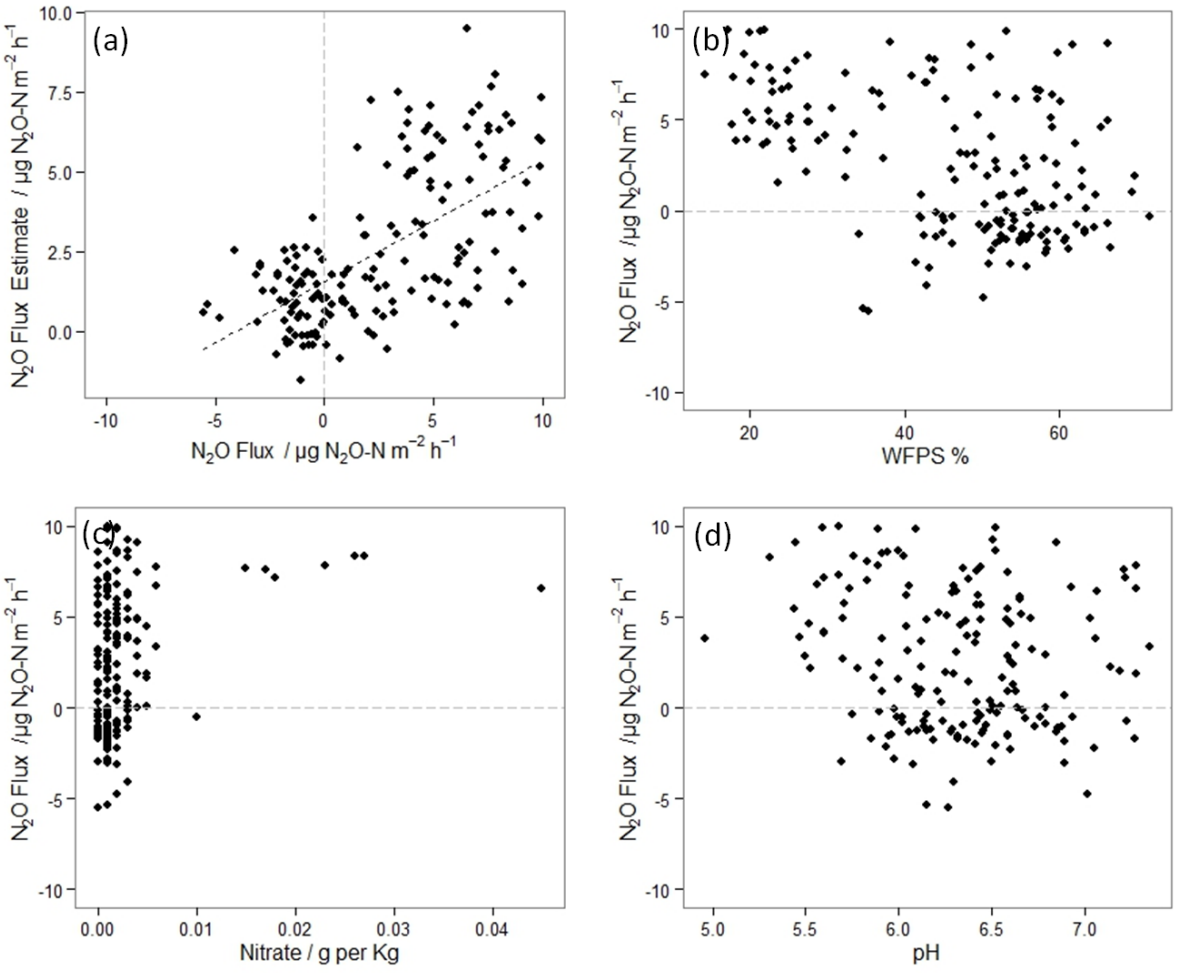

Figure 8.4 Multiple linear regression was carried out to correlate all N_2O fluxes measured below 10 µg N_2O-N m^{-2} and the soil properties measured from these locations (a) (See Table 8.2). Individual comparisons with the three strongest correlating properties are shown (b,c,d).

Table 8.2 Multiple linear regression correlation of soil properties and N_2O flux below 10 µg N_2O-N m^{-2} h^{-1} as plotted in Figure 8.4a.

	Estimate	S.D.	Statistical significance
(Intercept)	-1513	780	.
NH_4-N g Kg^{-1}	14.9	16	
NO_3-N g Kg^{-1}	163.8	55	**
pH	-1.3	0.6	*
WFPS %	-0.2	0.02	***
Bulk density g cm^{-1}	593	300	*
Soil porosity	1527	780	.
Carbon g Kg^{-1}	-0.02	0.02	
Nitrogen g Kg^{-1}	-0.10	0.07	

Significance of p-value: 0 '***' 0.001 '**' 0.01 '*' 0.05 '.' 0.1 ' ' 1

8.4 Discussion

The results in this paper show that even when using a high precision flux measurement methodology a relatively high proportion of apparently negative fluxes are recorded; however, these measurements rarely exceed the detection limit of the measurement method (Figure 8.2). The frequency of near zero fluxes below the detection limit is very high (28% of measurements reported fluxes below 4 µg N_2O-N m^{-2} h^{-1}) and many of the negative flux measurements in this experiment are likely to be caused by noise in the gas analyser (as shown in Figure 8.3d). A look at the change in ratio of negative fluxes with time also supports this theory. In the development stages of the dynamic chamber method (2012 measurements) the signal to noise ratio of the system was slightly lower due to unstable temperature conditions for the analyser and lack of a stable source of power supply. As the system logistics were optimized, the flux detection limit improved slightly and the number of negative fluxes recorded fell rapidly (See Figure 8.5).

It would be too simplistic to assume that instrumental noise is the cause of all of the negative fluxes of N_2O measured in these experiments, as can be seen in Figures 8.3a, b & c. In these examples it is clear that concentrations of N_2O decreased below the ambient concentrations of N_2O in the atmosphere. It is highly unlikely that an increase in N_2O concentration followed by a subsequent leak could cause this effect over the short 120 second measurement period in our dynamic chamber method. However, this explanation would be plausible over the much longer, 30–60 min incubation periods required by static chamber methods (Chapter 4).

Although very rare, consistent decline in N_2O concentrations are observed in some of the measurements (as in Figure 8.3) and the reasons for these observations are yet to be found.

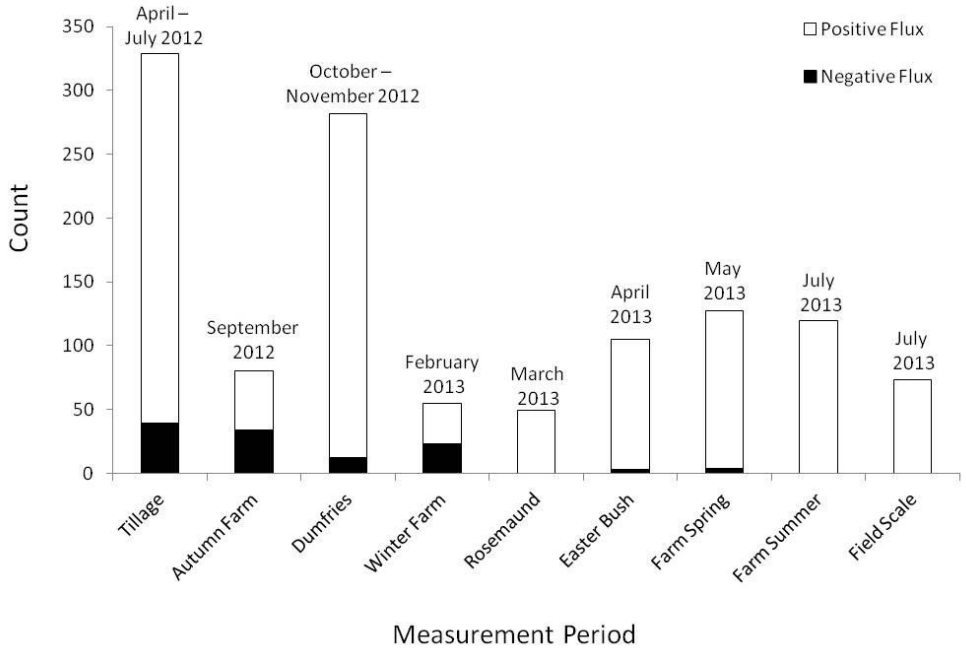

Figure 8.5 The number of negative and positive fluxes measured from all InveN_2Ory field sites using the dynamic chamber method in chronological order (See Table 8.1 for details).

One hypothesis which was tested in laboratory conditions using this methodology is that N_2O may dissolve in moisture in the tubing of the dynamic chamber system in wetter and colder conditions. This theory was tested early in the development of the dynamic chamber system and no effect on N_2O concentration measurements was observed when water was added to the system; however, the effect that humidity may have on the system in different temperature conditions may be very small and difficult to detect in lab conditions. Some interference in N_2O measurements caused by moisture and high humidity remains one explanation of N_2O uptake in the system using this methodology. Very slight laser drift and spectra fitting caused by rough environmental conditions and transportation of the delicate instrumentation are other possible reasons for this uptake effect, although we see no evidence from any of the recorded data that this is the case; moreover, there is no reason to believe the decreased signal to noise ratio due to these disturbances would not produce an equal distortion in the positive range of the fluxes.

It is believed that uptake of N_2O in agricultural soils may be the result of denitrification occurring at the surface layer of soils which converts atmospheric N_2O into N_2 (Yu *et al*., 2000; Wrage *et al*., 2004). Past experiments have linked negative fluxes to soil properties such as moisture content, temperature, pH, oxygen and available nitrogen (Heincke and Kaupenjohann, 1999; Khalil *et al*., 2002). N_2O uptake has also been recorded from forest soils with similar links observed between N_2O flux and available nitrogen (Rosenkranz *et al*., 2006; Goldberg and Gebauer, 2009); however, the influence of these factors seems to vary between different experiments and no clear set of conditions which would favour negative fluxes from different soil types can be established. It remains plausible that various microbial processes in soils are able to remove N_2O from the atmosphere; however, the mechanisms and triggers for N_2O uptake need to be studied further to understand these processes (Chapuis-Lardy *et al*., 2007). The analysis of soil samples taken from locations where negative and low fluxes were measured in this study showed no clear relationship between flux and soil properties. The heterogeneous nature of soils often increases the uncertainty of measured soil properties from a particular location which may be clouding any relationships present, although a more significant concern in this study is that the high number of negative fluxes measured during the wetter period in autumn and winter may bias any relationships with soil properties. It is unclear whether the higher ratio of negative fluxes measured during autumn and winter (2012/2013, as shown in Figure 8.4) is caused by higher instrumental uncertainty which was improved in subsequent measurements or if it is a genuine effect of the wetter soil properties at the time. A moisture effect on the methodology could also have increased the possibility of negative flux measurements during these wetter periods.

What is clear from this study is that true negative fluxes of N_2O from the agricultural soils examined are rare and very small. The issues that still exist in identifying when negative fluxes of N_2O are real or caused by instrumental noise using a high precision QCL instrument suggests that more commonly used N_2O flux measurement methodologies, such as the static chamber method, would have been unable to measure negative fluxes of N_2O with the precision required to identify if they are real or not. The results of this study suggest that large negative fluxes reported in the literature may in fact indicate a larger detection limit of an individual methodology than previously thought, which may explain many reports of negative flux measurements in the literature (Jordan *et al*., 1998; Flechard *et al*., 2005; Jones *et al*., 2011). Certainly, the majority of negative fluxes reported in this study were most likely caused by instrumental noise (as shown by Figures 8.2 and 8.3d). The high frequency of near zero-fluxes of N_2O from soils highlights the need for higher precision measurements

(able to detect in the region of 0 to 10 µg N_2O-N m^{-2} h^{-1}) when wanting to characterise the N_2O exchange processes between soil and air in background or unperturbed conditions.

When negative fluxes of N_2O are measured during field experiments it can be detrimental to the study as it complicates the calculation of cumulative fluxes and emission factors from certain soils and agricultural practices. This issue has been addressed several ways in the past. Negative fluxes are sometimes treated as real and left in all calculations or declared false measurements and removed or set to zero flux values. In theory when using flux chambers a larger number of measurements should help reduce the uncertainty in an average flux measurement, thus reducing the likelihood of measuring a negative flux; however, this is not always the case, especially when detection limits are large. It is our recommendation that propagation of error is investigated thoroughly when negative fluxes are concerned. When calculating cumulative flux estimates over long periods of time it is important to propagate the large uncertainty in measurements with time as well as the average fluxes measured. This may lead to very large uncertainties in these types of experiments; however, if this is the case then it may indicate that a particular cumulative flux methodology is not suitable for purpose.

8.5 Conclusions

Four small negative fluxes of N_2O out of 1220 have been recorded in this study greater than the defined detection limit of the measurement methodology. The reason for these four negative fluxes is still not fully understood and these observations do not provide strong evidence for the occurrence of microbial net uptake of N_2O. This study suggests that it is likely that many recorded negative fluxes of N_2O are significantly smaller and rarer than reported in previous literature. We also highlight the need to fully understand whether negative flux measurements are real or simply readings below the detection limit of the measurement methodology. For these reasons we wish to highlight the importance of specifying the "real" flux detection limit associated to each dataset, as opposed to a theoretical detection limit associated exclusively with the factory-declared precision of the gas analysers: this would allow a more robust estimate of the net contribution of each agricultural environment investigated. The drivers of true negative N_2O flux in agricultural soils cannot be identified in this study. We suggest that, from the evidence presented here, it can be assumed that negative fluxes measured from agricultural soils are a good indicator of the true detection limit of a flux measurement methodology. The results of this study provide strong evidence against the theory that negative fluxes of N_2O in agricultural soils can be a significant sink of atmospheric N_2O, as most of the negative N_2O fluxes reported are likely to be an artefact of measurement methodology.

Chapter 9

Synthesis and conclusions

9.1 Improvements in N_2O flux measurement precision

The development of the dynamic chamber method (as outlined in Chapter 4) has helped investigate and quantify several sources of uncertainty in chamber measurements to a level of precision that was previously not possible. The most significant improvement that the dynamic chamber design provided over alternative chamber methodologies was the ability to drastically reduce and quantify the uncertainty in flux measurements caused by limitations in instrumental precision and regression fitting, which are regarded to be the major contributors to uncertainties in chamber measurements (Kroon *et al.*, 2008; Pedersen *et al.*, 2010; Levy *et al.*, 2011; Parkin *et al.*, 2012). These advances were made possible through the use of a high precision gas analyser capable of making gas mixing ratio measurements at a rate of 1 Hz. This frequency of measurements also allowed observation of the effect that high winds and temperature and pressure changes had on the system in much greater detail than previous methodologies allowed. The combination of all of these factors provided a detailed analysis of the inner workings of chamber methodology which could in principle be applied to other chamber methods as well.

The results from the comparison of methodologies (in Chapter 4) shows that in using linear or non-linear regression fitting to calculate fluxes from static chambers closed for a period of 60 mins can result in very high and sometimes unquantifiable errors. Such methods suggest that a systematic underestimate of fluxes may be present in many studies which use chamber measurements with enclosure times that last up to an hour. This type of uncertainty can be unaccounted for even with large numbers of measurements as the error is biased towards lower fluxes. These findings are significant as over 95% of published work on N_2O fluxes contain the use of various chamber methods which could be prone to these systematic uncertainties (de Klein & Harvey, 2013). The same principles may also apply to measurements of CH_4 and other gases made using chamber methodologies which rely on the same basic principles.

The high precision of the dynamic chamber method allowed investigation into several current topics discussed by the N_2O flux research community. The two main findings that the studies were able to contribute towards were the problems of regression fitting in chamber measurements and investigating negative fluxes of

N_2O. During the project it was identified that each individual chamber measurement followed different linearity in concentration change with time (See Chapter 4). Currently there is debate over whether linear or non-linear fitting is best to use in chamber measurements (Kroon *et al.*, 2008; Parkin *et al.*, 2012). From the results in this study it can be concluded that each method may require a slightly different approach based on instrumental precision and number of measurements during chamber closure, and that both methods of regression fitting should be applied when possible to identify which choice is best for each measurement instead of a single approach applied to all.

During the project it was possible to confidently state that most negative fluxes of N_2O measured using the dynamic chamber method were highly likely to be caused by instrumental noise and the high frequency of near zero fluxes measured. This conclusion was possible as a result of the well defined detection limit (4 µg N_2O-N m^{-2} h^{-1}) of the measurement method (See Chapter 8). The lack of any large negative fluxes (below -6 µg N_2O-N m^{-2} h^{-1}) in over 1200 measurements showed that negative fluxes reported in much of the literature was likely due to issues with uncertainties rather than a real negative flux caused by microbial denitrification of N_2O to N_2.

When investigating areas with very large fluxes of N_2O it was clear in the field and farm scale experiments (Chapters 6 & 7) that high concentrations of available nitrogen and other soil properties (such as moisture content, rainfall and pH) were the cause of these large flux measurements. These relationships are more difficult to assess in areas where fluxes are lower such as general field conditions which were found to cover over 99% of the farm area in this project. Investigating relationships between individual N_2O flux measurements and soil properties from these soils required high precision measurements with a low limit of detection (<10 µg N_2O-N m^{-2} h^{-1}). The dynamic chamber method was capable of providing flux measurements which allowed for this type of analysis. The log-normal distribution of N_2O flux observed in these data sets was also possible because of the high precision of the individual measurements. This observation helped during statistical analysis of low flux data sets in which $\log_{10}(N_2O\ Flux)$ correlated well with $\log_{10}$(Available Nitrogen).

A total of 70% of all flux measurements fell below 40 µg N_2O-N m^{-2} h^{-1} during this project (Figure 9.1). This is an important observation as this is the detection limit reported for the static chamber method in Chapter 4. The static chamber method is often used due to its cheap and simple operating procedure; however, there are some severe limitations to the results that can be obtained using this method. The inability to accurately measure low fluxes prevents any attempt to investigate the distribution of data in these measurements

which may be vital when spatial interpolation is concerned. By comparison a total of 28% of all fluxes measured fell below the detection limit of the dynamic chamber method (Figure 9.1). As no spatial pattern can be predicted from N_2O measurements at a wider (field) scale, mean values are often relied upon which are highly dependent on the statistical methodology used (i.e. arithmetic or geometric). Increasing the precision of flux measurements is important as it improves the ability to investigate the spatial aspect of N_2O in more detail.

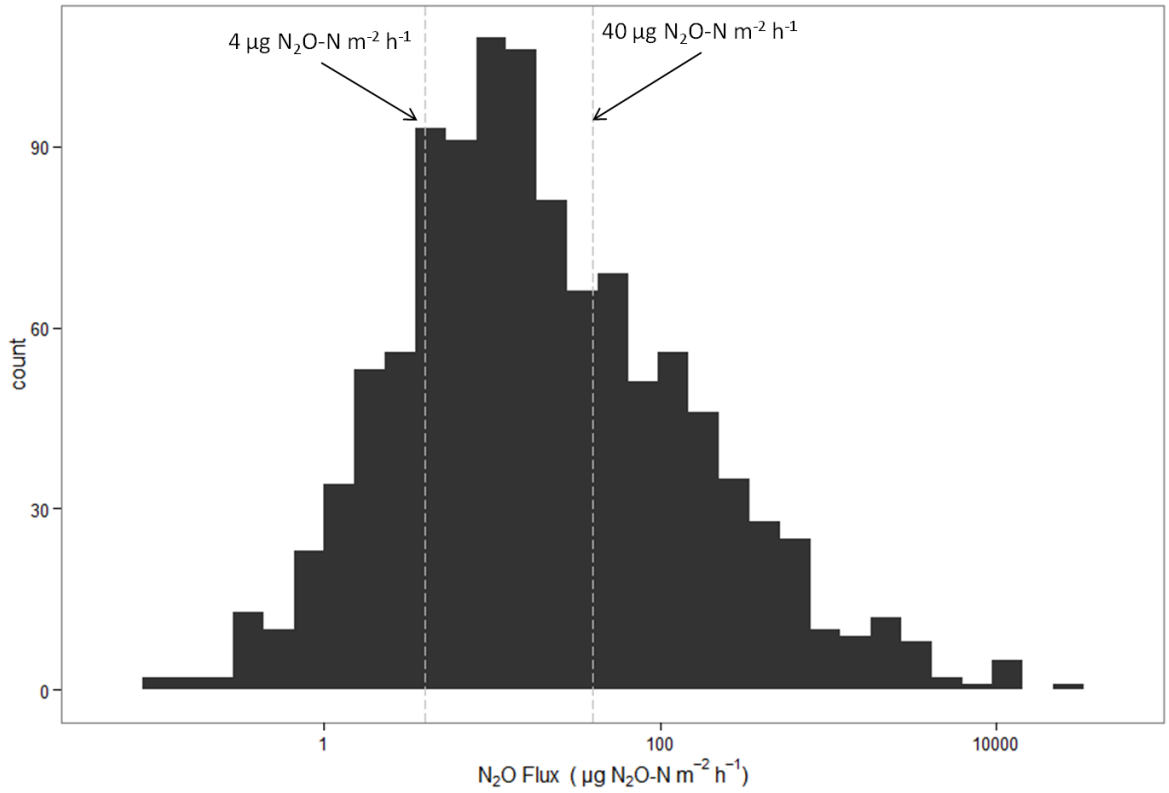

Figure 9.1 A distribution plot of all 1220 flux measurements made from the dynamic chamber throughout Chapters 4 to 8. The detection limits of the dynamic chamber (left) and static chamber (right) as reported in Chapter 4 are included.

9.2 Spatial and temporal interpolation of N_2O flux measurements

Although the precision of chamber measurements was improved, the issue of spatial variability remains. The detailed spatial analysis of low flux emissions that is made capable using the dynamic chamber method was demonstrated during the tillage experiment (See Chapter 5). These measurements showed the extent of spatial variability in N_2O fluxes across a small scale which varied several orders of magnitude over just a couple of metres. This work encountered difficulties when it came to interpolating measurements to represent a wider

area. Spatial and temporal variability of N_2O measurements are believed to be the largest sources of uncertainties in large scale emission estimates made using chamber measurements. Increasing the precision of measurements allowed us to examine the spatial variability of low flux environments in greater detail; however, the issue of interpolating these measurements to wider scales remained.

Several attempts were made to interpolate chamber flux measurements at different scales during the project (See Chapters 5, 6 & 7). Using basic linear interpolation between points was simple but difficult to justify. The tillage experiment showed that fluxes varied several orders of magnitude over just a few metres which meant that fluxes measured even short distances apart will not accurately represent the area between two points. This was also shown during the field scale experiment as a lack of any evident pattern in the variogram analysis of fluxes across the field scale was observed (See Chapter 6). During the field scale measurements linear interpolation between the points (~ 30 m apart) was incapable of predicting hot spot locations across most of the field and suffered when two high fluxes were made consecutively, as it would predict a large area of high flux between and around the points which is unlikely to have been the case. Ultimately it was decided that linear interpolation offered no advantages and was no more accurate than applying a mean flux value with the relevant uncertainties across the field.

Other interpolation methods (kriging and polynomial) suffered from the same problems as linear interpolation (Figure 9.2). These methods were capable of providing informative graphics from which spatial variability of flux measurements could be displayed, although it was not possible to confidently predict N_2O between points made using chamber measurements at a field scale without an impractically large number of measurements being made. Multiple methods were used to plot N_2O at a spatial scale during the project. These methods all suffered from the same weakness that N_2O does not have a predictable spatial pattern, and therefore interpolating over large areas is not possible without large uncertainties. These plots were considered to provide varying degrees of qualitative information rather than a desired quantitative flux interpolation. It was decided during the project that using mean values of flux measurements was the only viable way to represent N_2O flux emission estimates over the field to farm scale; however, choosing which type of mean value best represents the field and farm scale was also an issue.

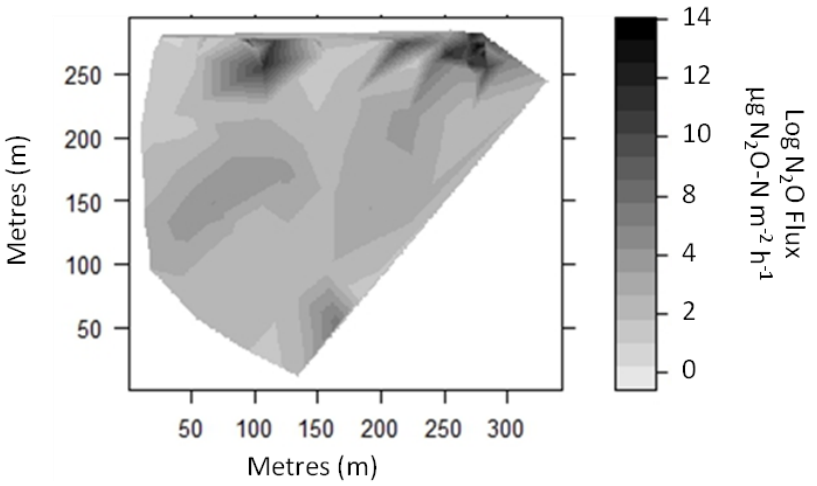

Figure 9.2 An example of N_2O flux plotted for a grazed grassland field (See Chapter 6) using locally weighted scatterplot smoothing (LOESS). High fluxes were recorded at the manure heap (top right) and shaded (top left) areas.

The log-normal distribution of N_2O fluxes measured using the dynamic chamber method is shown in several of the experiments in this project (See Chapters 6 & 7). The many high flux measurements which are typically two to three orders of magnitude higher than the remainder of the values recorded in chamber measurements complicates mean calculations of N_2O flux. An arithmetic mean assumes a normal distribution of flux magnitude and that the frequency of high flux measurements is an accurate representative of the wider scale. If this is not the case then a small number of high fluxes which are several orders of magnitude higher than other measurements are able to raise an arithmetic mean value significantly to unrealistic values. Alternatively if high fluxes are missed from a particular source then mean values can be underestimated. The high uncertainty associated with arithmetic mean flux values in this project was often caused by the wide distribution of flux measurements from a particular source.

Geometric means may be more representative of group of measurements if large outliers are not representative of the wider scale in which measurements will be scaled to. This may be the case if a single small "hotspot" of N_2O flux is present in the field which is measured. For example in a situation where one in ten measurements were made from a high flux area that actually only represents 1% of the field then an over estimate will occur. During the field and farm experiments identifiable hotspot measurements were segregated from the majority coverage, general field soil measurements when possible to increase the accuracy of emission estimates for these sources. By identifying individual high flux areas a more representative emission estimate

for a field could be made rather than using a generic mean value of all of the measurements; however, this method required the measurement of each individual field feature which may be contributing to a high N_2O flux. As these areas were often not possible to identify by eye it is difficult to ensure all of these features are accounted for.

Temporal variability also remains a large source of uncertainty in N_2O flux measurements. During the study no evidence of changes in N_2O fluxes during the day were observed from chamber measurements. Measurement days often lasted up to seven hours in which measurements were made from morning to evening. No night time fluxes were observed using the chamber measurements which prevents study of any diurnal effects in this project. The largest temporal uncertainties in N_2O emissions are caused by an inability to gap fill between measurement dates using models. The farm scale experiment in this project assumed linear temporal viability between seasons when using arithmetic and geometric mean based emission estimates. The correlation between rainfall and N_2O flux observed in the farm scale experiment as well as other rainfall correlations reported in previous literature suggest that linear interpolation between measurement dates may not be a good representation of N_2O flux over these time periods as daily flux estimates will change based on numerous meteorological conditions such as rainfall.

9.3 Modelling N_2O fluxes from agricultural soils

Modelling N_2O emissions is a complicated task due to the multiple factors involved which influence microbiological pathways. During this project several equations were identified from linear regression fitting between N_2O flux and measured soil properties (Table 9.1). Each of these fitting exercises provided different equations with differing significance values for the relevant soil properties. An increased presence of available nitrogen (in the form of NH_4^+ and NO_3^-) was found to be a strong indicator that N_2O flux would be high in all of the regression fits in this project (See Table 9.1). This is a commonly reported observation in similar studies; however, the relationship between concentrations of NH_4^+ and NO_3^- and N_2O flux can vary unpredictably between soil types in different meteorological conditions. The log scale relationship between flux and available nitrogen and the wide scatter in the reported correlations (Table 9.1) result in high uncertainties in using these regression fitting methods to predict N_2O flux at a particular location. Using the information gathered in this project it is clear that available nitrogen contributes significantly to N_2O flux from soils, but it is not possible to quantify this relationship in a way that could confidently estimate emissions of N_2O using only soil measurements.

Table 9.1 All multiple linear regression equations carried out during the project are presented in one final table. The relevant figures are plotted in parallel to the regression coefficients (See Chapters 6,7 & 8 for more detail).

	Coefficient Estimate	S.D.	Sig.
Chapter 6			
(Intercept)	-4.3	1.3	**
$log_{10}(NH_4\text{-N g Kg}^{-1})$	-0.25	0.2	
$log_{10}(NO_3\text{-N g Kg}^{-1})$	0.76	0.1	***
pH	0.6	0.1	***
WFPS	0.04	0.01	***
Soil porosity	3.85	1.3	**
Chapter 7			
Individual regression			
(Intercept)	3.7	0.6	***
$log_{10}(NH_4\text{-N g Kg}^{-1})$	0.5	0.1	***
$log_{10}(NO_3\text{-N g Kg}^{-1})$	0.9	0.2	***
pH	0.2	0.1	*
Vol. water content	-0.01	0.003	***
Rainfall / mm	-0.007	0.001	***
Grouped regression			
(Intercept)	5.5	0.5	***
$Log_{10}(NH_4^+)$	0.7	0.4	.
$Log_{10}(NO_3^-)$	1.3	0.4	***
Rainfall / mm	-0.007	0.002	**
Chapter 8			
(Intercept)	-1513	780	.
$NH_4\text{-N g Kg}^{-1}$	14.9	16	
$NO_3\text{-N g Kg}^{-1}$	163.8	55	**
pH	-1.3	0.6	*
WFPS	-0.2	0.02	***
Bulk density g cm^{-1}	593	300	*
Soil porosity	1527	780	.
Carbon g Kg^{-1}	-0.02	0.02	
Nitrogen g Kg^{-1}	-0.1	0.07	

Significance of p-value: 0 '***' 0.001 '**' 0.01 '*' 0.05 '.' 0.1 ' ' 1

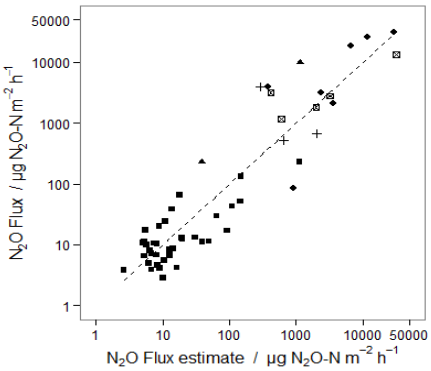

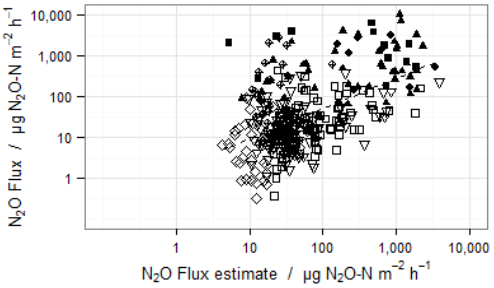

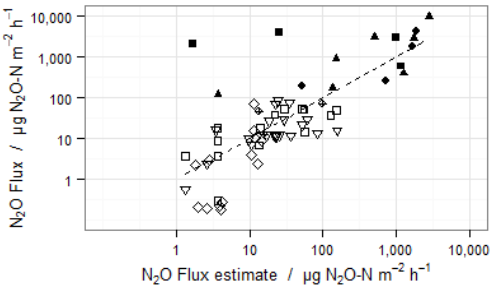

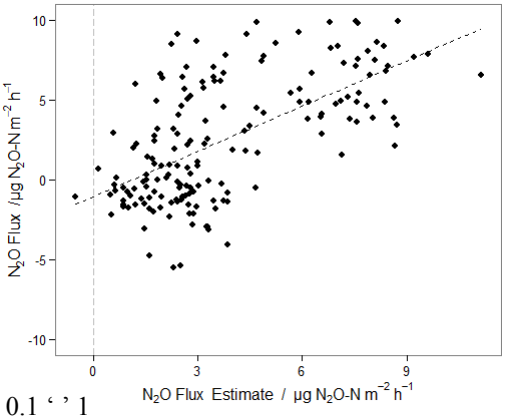

Even if regression fitting between soil properties and N_2O was consistent at different locations, modelling N_2O from soil measurements has practical drawbacks. The soil measurements which would be required to estimate N_2O emissions are often more time consuming and expensive to measure than the actual N_2O flux would be. The same issues with spatial and temporal interpolation that N_2O flux estimates suffer from would also apply to soil property measurements as concentrations of various nitrogen compounds in the soil change on a daily basis. This prevents the soil data recorded in this study from modelling Tier 1 farm scale emission estimates based on the reported regression relationships. This method may become possible in the future if a relevant model is built which can confidently predict available nitrogen on a daily basis based on nitrogen input at the field scale.

Rainfall and soil moisture often correlated strongly with N_2O flux during the project. During the tillage experiment it was found that very high fluxes of N_2O were released from the wetter area of poorly drained soils within the measurement plot. This suggested that soil moisture content was a key factor in N_2O emissions after tillage events. The opposite of this relationship was observed during the farm scale experiment. It was found that high rainfall had a negative effect on N_2O emissions in this experiment, which disagrees with the general consensus in literature that rainfall increases N_2O flux. The relationship between moisture content in the soil and N_2O flux is complicated and is often described as non-linear in nature. The complete lack of water in soils results in a reduction of microbial activity and high water content can prevent gas transport from the soil to the atmosphere as well as promoting complete denitrification to N_2 instead of N_2O. The effect of rainfall on N_2O emissions from the farm area will therefore depend on factors such as the soil moisture content prior to rain events, soil type, the quality of drainage, crop type and evaporation (temperature and sunlight).

Soil moisture content effects both the rates of nitrification and denitrification and the fraction of N_2O released from each of these processes. For Tier 2 modelling purposes further research would be required to investigate the effect of rainfall and soil moisture content on the individual microbial processes to explain the lack of consistency in relationships between soil moisture and N_2O flux observations between experiments. Advantages of using rainfall in these scenarios to model N_2O emissions would be that the meteorological data is often readily available and can be modelled at a national scale (Tier 2 model) with relative ease compared to soil moisture content which would require numerous soil data inputs.

No relationship was observed between stocking density and available nitrogen measured from the individual field measurements. Animal waste as calculated using values provided by DEFRA (DEFRA, 2008)

was used as an estimate of how much N was produced from each animal. These values were used as it is a simple method that the farming community were already familiar with, although the estimates were fairly basic and no range of uncertainty was reported in the methodology of the report. The method also considered nitrogen input from lambs as negligible, although results may suggest otherwise. Estimates of nitrogen calculated from animal waste were also prone to error, as especially detailed knowledge of animal numbers were difficult to obtain. Studies in this project (Chapters 6 & 7) show that animal waste is a source of available nitrogen which results in high fluxes of N_2O in certain areas. From the data and relationships observed it is not possible to confidently model emissions based on calculations of animal waste. Ideally if animal waste and rainfall could predict N_2O emissions then basic models of farm scale emissions (such as those presented in Chapter 7) would be simple and easy to use to calculate a national inventory (Tier 2 model) of N_2O from grazed fields. It was not possible to construct a well defined model from the data presented in this project; however, with a larger data set further research may provide a simple model which could provide a basic national inventory of N_2O from grazing livestock.

9.4 Mitigation of N_2O flux from agriculture

Currently several mitigation methods are applied to agricultural practices to reduce N_2O emissions. The farm scale experiment agrees that optimised use of nitrogen fertilisers is an important mitigation strategy. N_2O emissions from fertiliser treatments are highly uncertain; however, it is still clear that they play a large role in agricultural N_2O emissions and even relatively small reductions in the use of nitrogen applied may result in a large reduction in N_2O emissions. The exponential relationship between N_2O flux and available nitrogen during this project agrees with work recently carried out which suggests that fertiliser induced N_2O emissions are not linear in nature with N-input (Ma et al., 2010; Shcherbak et al., 2014). Literature has identified that larger applications of fertilisers may have larger N_2O emission factors associated with them. These findings suggest that reductions in N_2O emissions may be achieved by splitting nitrogen input into multiple smaller applications; however, this is entirely dependent on the effect that such practices would have on crop yields and practicality issues for farmers and land owners.

Precision farming is one way in which nitrogen input may be reduced. Precision farming requires knowledge of soil properties such as available nitrogen content, soil moisture content, soil pH, and mineral carbon and nitrogen content. With this knowledge it becomes possible to determine which areas of a particular field require further fertiliser and which do not, thus reducing total nitrogen input without loss of crop yield.

This information is not easy to obtain on the scale which is required for precision farming and further improvements in measurement methodology are required before this method could become practical for most farmers.

The exponential relationship between available nitrogen and N_2O flux may suggest that stocking density could be managed in a way which would disperse animal waste over a larger area. The relationship predicts that if animals are kept in smaller spaces that N_2O fluxes may increase exponentially if available nitrogen concentrations in soils increase even fractionally. Mitigation may involve practices such as moving feeding areas and troughs occasionally to prevent areas of extremely high fluxes. Results from the farm scale experiment suggest that this kind of practice may not be worthwhile depending on logistical effort as fluxes from these areas are estimated to only contribute a small proportion to N_2O emissions at the farm scale (<5%).

9.5 Future work

To mitigate N_2O emissions effectively further work is required to improve the accuracy of emission estimates of the largest sources of agricultural emissions. Accurate emission estimates from fertiliser applications are difficult to model at large scales using current methodologies and emission factors. Further work is required to understand the drivers of emissions from these events so as to predict and mitigate fluxes of N_2O at the regional and national scales. Without methodology capable of reducing uncertainties in N_2O emissions from fertiliser events it would be difficult to provide solid evidence describing how nitrogen fertiliser applications can be optimised to increase crop yield with the lowest associated fluxes of N_2O. This is an area of concern in terms of reducing climate change and improving the nitrogen economy in agricultural areas.

Improvements in spatial and temporal gap filling in N_2O emission models is also required to advance progress in the understanding of N_2O emissions at the wider scale. Further research using automated measurement methodologies such as eddy covariance which are capable of interpolating fluxes on a 24 hour a day basis over large scales is required to investigate temporal patterns and the integration of flux measurements over a given area. Identifying key variables which alter N_2O fluxes such as nitrogen input, rainfall and soil properties in a way that can be applied to a regional scale would also improve modelling at wider scales. Eddy covariance may provide some interesting opportunities to model N_2O fluxes with meteorological changes such as rainfall events and changing temperatures.

This study identified several sources of N_2O emissions such as remains of manure heaps, silage grass remains and stored silage grass. Although contributing relatively small quantities of N_2O emissions at the farm scale in this project, each of these sources was capable of emitting significant quantities of N_2O from a small area. Further research into these point sources may better quantify emissions at a wider scale and also provide information on how to prevent these emissions without significant cost to farm management (i.e. combustion of rotten silage grass).

A lack of data is still an issue for many sources of N_2O. During the farm scale experiment it was not possible to account for N_2O emissions caused by tillage events at the farm scale. The tillage experiment revealed that emissions from such events can be of the same order of magnitude to that of a nitrogen fertiliser event which suggests that tillage can be a large N_2O source at the farm scale; however, the long lasting effects of tillage events are less well understood. It has been reported in some studies that tilled soils may emit less N_2O from nitrogen fertiliser events carried out later in the year than if no tillage took place, and due to this uncertainty we are unable to declare if tillage events resulted in a net increase or decrease annual emissions of N_2O from a field or farm scale. Further research is required to quantify this effect.

9.6 Recommendations for future field work

Work presented in this thesis highlights the complex nature of N_2O flux measurements. The new high precision chamber methodology used throughout has resulted in novel data sets which provide a clearer understanding of the underlying processes involved in N_2O emissions than previous methodology has allowed. I would recommend that if future researchers want to investigate N_2O fluxes from soils using a chamber method, then they should strive to maximise the precision of their methodology in order to gather as much information as possible. A detailed understanding of the limitations of a particular methodology is also required to fully make use of a measurement data set. Being able to determine what is real or artefact in measurements can help identify when data can be trusted which helps considerably when trying to analyse the results.

Regarding linear and non-linear regression in chambers I believe it is important to understand that both may be used depending on circumstance. Although non-linear regression may seem like a more accurate choice to use for some measurements made using the dynamic chamber method ($n > 120$) this may not be the case for static chambers ($n < 5$). It is often difficult to identify the true linearity present in a static chamber measurement and fitting non-linear curves to a small number of data points (<5) may increase uncertainty in regression

estimates more than using a linear regression estimate would. What is more important than choosing a particular regression estimate is that the confidence interval of the regression is accurately calculated to observe the true range of uncertainty in a measurement. This involves using at least three samples per static chamber flux measurement. Increasing the number of measurement points will decrease regression uncertainty when using static chamber methodologies, although there is a worry that the effects of an increased internal pressure caused by removing more air samples from the chamber may influence the measurement. Understanding the underlying chamber specific variables for each methodology will allow a balance to be made when deciding how best to measure fluxes for a particular experiment and chamber design.

From my work I have found no clear spatial pattern in N_2O flux from soils which can be used to interpolate to large scales without the need for an impractical number of flux or soil measurements. The lack of a practical method able to interpolate N_2O flux at the field scale means that in most cases an averaging method has to be used instead. Some significant assumptions are made in using simplistic averages to interpolate N_2O flux to larger scales which leaves room for uncertainty. It is important to identify areas of a field which may not be well represented by a sampling methodology (as in Chapter 6). I would recommend that when averaging N_2O flux measurements over a plot or field scale that the distribution of data is examined as this may have a profound effect on the way that mean values are calculated. The use of arithmetic and geometric statistics should both be considered when this work is carried out.

The eddy covariance method has recently grown in popularity as a way to measure N_2O fluxes. As new instrumentation with high measurement precision becomes available it is likely more research groups will begin to measure eddy covariance for N_2O. During my project eddy covariance measurements were made for a tilled field; however, a change in wind direction prevented this experiment from going ahead. It was not possible to delay the tillage or move the eddy covariance tower due to the requirement of mains power. I would recommend that any research group who wish to use eddy covariance should make plans to avoid this situation. Ideally a tower surrounded by a homogenous measurement area prevents wind direction from becoming an issue, but as there is currently no commercial open-path N_2O analysers available for eddy covariance measurements then tubing length and power limitations may prevent this. The use of two analysers is also not an option in most cases due to the high cost of these instruments. The example of the failed tillage measurements highlights the need to be aware of what a particular methodology is capable of in practical terms.

9.7 Conclusions

In conclusion the work presented in this project has contributed some significant findings in the field of N_2O fluxes from agricultural soils. The project has yielded some large data sets of both flux measurements and soil properties which have contributed to several investigations into sources of N_2O fluxes. Much of this work was made capable by the development of high precision chamber measurements, although this was not enough to address the issue of reducing uncertainty in N_2O emissions across various scales. It was possible to measure and identify some factors which contributed to spatial variability of N_2O fluxes and several methods of spatial interpolation were investigated using measured data. The studies conclude that further research is required into spatial and temporal variability of N_2O to further improve emission estimates at various scales. This research may require further improvements in the way that N_2O flux activity data is recorded over various spatial scales and how this data is interpolated to provide wider coverage flux estimates.

Chapter 10

References

Abdalla, M., Jones, M., Ambus, P., and Williams, M.: Emissions of nitrous oxide from Irish arable soils: effects of tillage and reduced N input, Nutrient Cycling in Agroecosystems, 86, 53-65, 2010.

Amon, B., Amon, T., Boxberger, J., and Alt, C.: Emissions of NH_3, N_2O and CH_4 from dairy cows housed in a farmyard manure tying stall (housing, manure storage, manure spreading), Nutrient Cycling in Agroecosystems, 60, 103-113, 2001.

Baggs, E. M., Stevenson, M., Pihlatie, M., Regar, A., Cook, H., and Cadisch, G.: Nitrous oxide emissions following application of residues and fertiliser under zero and conventional tillage, Plant Soil, 254, 361-370, 2003.

Baggs, E. M.: A review of stable isotope techniques for N_2O source partitioning in soils: recent progress, remaining challenges and future considerations, Rapid Commun Mass Sp, 22, 1664-1672, 2008.

Ball, B. C., Crichton, I., and Horgan, G. W.: Dynamics of upward and downward N_2O and CO_2 fluxes in ploughed or no-tilled soils in relation to water-filled pore space, compaction and crop presence, Soil Till Res, 101, 20-30, 2008.

Bateman, E. J. and Baggs, E. M.: Contributions of nitrification and denitrification to N_2O emissions from soils at different water-filled pore space, Biology and Fertility of Soils, 41, 379-388, 2005.

Baulch, H. M., Schiff, S. L., Maranger, R., and Dillon, P. J.: Nitrogen enrichment and the emission of nitrous oxide from streams, Global Biogeochem Cy, 25, GB4013, 2011.

Beauchamp, E. G.: Nitrous oxide emission from agricultural soils, Canadian Journal of Soil Science, 77, 113-123, 1997.

Beaulieu, J. J., Tank, J. L., Hamilton, S. K., Wollheim, W. M., Hall, R. O., Mulholland, P. J., Peterson, B. J., Ashkenas, L. R., Cooper, L. W., Dahm, C. N., Dodds, W. K., Grimm, N. B., Johnson, S. L., McDowell, W. H., Poole, G. C., Valett, H. M., Arango, C. P., Bernot, M. J., Burgin, A. J., Crenshaw, C. L., Helton, A. M., Johnson, L. T., O'Brien, J. M., Potter, J. D., Sheibley, R. W., Sobota, D. J., and Thomas, S. M.: Nitrous oxide emission from denitrification in stream and river networks, Proceedings of the National Academy of Sciences of the United States of America, 108, 214-219, 2011.

Bell, M. J., Rees, R. M., Cloy, J. M., Topp, C. F. E., Bagnall, A., and Chadwick, D. R.: Nitrous oxide emissions from cattle excreta applied to a Scottish grassland: Effects of soil and climatic conditions and a nitrification inhibitor, Science of The Total Environment, 508, 343-353, 2015.

Berger, A. and Tricot, C.: The greenhouse effect, Surv Geophys, 13, 523-549, 1992.

Boeckx, P., Van Nieuland, K., and Van Cleemput, O.: Short-term effect of tillage intensity on N_2O and CO_2 emissions, Agron Sustain Dev, 31, 453-461, 2011.

Bouwman, A. F., Van der Hoek, K. W., and Olivier, J. G. J.: Uncertainties in the global source distribution of nitrous oxide, Journal of Geophysical Research: Atmospheres, 100, 2785-2800, 1995.

Bouwman, A. F.: Direct emission of nitrous oxide from agricultural soils, Nutrient Cycling in Agroecosystems, 46, 53-70, 1996.

Bouwman, A. F., Boumans, L. J. M., and Batjes, N. H.: Modeling global annual N_2O and NO emissions from fertilized fields, Global Biogeochem Cy, 16, 2002.

Braker, G., Schwarz, J., and Conrad, R.: Influence of temperature on the composition and activity of denitrifying soil communities, Fems Microbiol Ecol, 73, 134-148, 2010.

Brown, L., Jarvis, S. C., and Headon, D.: A farm-scale basis for predicting nitrous oxide emissions from dairy farms, Nutrient Cycling in Agroecosystems, 60, 149-158, 2001.

Butterbach-Bahl, K., Breuer, L., Gasche, R., Willibald, G., and Papen, H.: Exchange of trace gases between soils and the atmosphere in Scots pine forest ecosystems of the northeastern German lowlands: 1. Fluxes of N_2O, NO/NO_2 and CH_4 at forest sites with different N-deposition, Forest Ecology and Management, 167, 123-134, 2002.

Butterbach-Bahl, K., Baggs, E. M., Dannenmann, M., Kiese, R., and Zechmeister-Boltenstern, S.: Nitrous oxide emissions from soils: how well do we understand the processes and their controls?, Philos T R Soc B, 368, 2013.

Cabello, P., Roldán, M. D., and Moreno-Vivián, C.: Nitrate reduction and the nitrogen cycle in archaea, Microbiology, 150, 3527-3546, 2004.

Chadwick, D. R., Sneath, R. W., Phillips, V. R., and Pain, B. F.: A UK inventory of nitrous oxide emissions from farmed livestock, Atmos Environ, 33, 3345-3354, 1999.

Chadwick, D., Sommer, S., Thorman, R., Fangueiro, D., Cardenas, L., Amon, B., and Misselbrook, T.: Manure management: Implications for greenhouse gas emissions, Anim Feed Sci Tech, 166–167, 514-531, 2011.

Chadwick, D. R., Cardenas, L., Misselbrook, T. H., Smith, K. A., Rees, R. M., Watson, C. J., McGeough, K. L., Williams, J. R., Cloy, J. M., Thorman, R. E., and Dhanoa, M. S.: Optimizing chamber methods for measuring nitrous oxide emissions from plot-based agricultural experiments, European Journal of Soil Science, 65, 295-307, 2014.

Chapuis-Lardy, L., Wrage, N., Metay, A., Chotte, J.-L., and Bernoux, M.: Soils, a sink for N_2O? A review, Global Change Biol, 13, 1-17, 2007.

Christensen, S., Ambus, P., Arah, J. R. M., Clayton, H., Galle, B., Griffith, D. W. T., Hargreaves, K. J., Klemedtsson, L., Lind, A. M., Maag, M., Scott, A., Skiba, U., Smith, K. A., Welling, M., and Wienhold, F. G.: Nitrous oxide emission from an agricultural field: Comparison between measurements by flux chamber and micrometerological techniques, Atmos Environ, 30, 4183-4190, 1996.

Clayton, H., McTaggart, I. P., Parker, J., Swan, L., and Smith, K. A.: Nitrous oxide emissions from fertilised grassland: A 2-year study of the effects of N fertiliser form and environmental conditions, Biology and Fertility of Soils, 25, 252-260, 1997.

Conen, F., Dobbie, K. E., and Smith, K. A.: Predicting N_2O emissions from agricultural land through related soil parameters, Global Change Biol, 6, 417-426, 2000.

Crutzen, P. J., Mosier, A. R., Smith, K. A., and Winiwarter, W.: N_2O release from agro-biofuel production negates global warming reduction by replacing fossil fuels, Atmos Chem Phys, 8, 389-395, 2008.

Davidson, E. A. Fluxes of nitrous oxide and nitric oxide from terrestrial ecosystems. Microbial production and consumption of greenhouse gasses: methane, nitrogen oxides, and halomethanes. 219-235, 1991

Davidson, E. A., Keller, M., Erickson, H. E., Verchot, L. V., and Veldkamp, E.: Testing a conceptual model of soil emissions of nitrous and nitric oxides, Bioscience, 50, 667-680, 2000.

Davidson, E. A.: The contribution of manure and fertilizer nitrogen to atmospheric nitrous oxide since 1860, Nature Geosci, 2, 659-662, 2009.

de Klein, C. & Harvey, M., et al. Nitrous oxide chamber guidelines; Global Research Alliance on Agricultural Greenhouse Gases. (At: www.globalresearchalliance.org/research/livestock/activities/nitrous-oxide-chamber-methodology-guidelines/. Accessed: 16/6/14), 2013

DEFRA, 2012, Agriculture in the United Kingdom (Report). UK government

DEFRA, 2008: The Nitrate Pollution Prevention Regulations 2008 (At: http://www.legislation.gov.uk/uksi/2008/2349/pdfs/uksi_20082349_en.pdf /. Accessed: 16/9/14)

DEFRA, 2009: Agriculture in the United Kingdom, 2009. (At: https://www.gov.uk/government/uploads/system/uploads/attachment_data/file/208436/auk-2012-25jun13.pdf. Accessed: 16/9/14)

DEFRA, 2013: (a) The British survey of fertiliser practice. Fertiliser use on farm crops for crop year 2013 (At: https://www.gov.uk/government/uploads/system/uploads/attachment_data/file/301474/fertiliseruse-report2013-08apr14.pdf. Accessed: 16/9/14)

DEFRA, 2013 (b): Farming Statistics - Livestock Populations at 1 December 2013 – UK (At: https://www.gov.uk/government/uploads/system/uploads/attachment_data/file/293717/structure-dec2013-uk-19mar14.pdf. Accessed: 16/9/14)

Del Grosso, S. J., Parton, W. J., Mosier, A. R., Walsh, M. K., Ojima, D. S., and Thornton, P. E.: DAYCENT national-scale simulations of nitrous oxide emissions from cropped soils in the United States, J Environ Qual, 35, 1451-1460, 2006.

Denmead, O. T.: Approaches to measuring fluxes of methane and nitrous oxide between landscapes and the atmosphere, Plant Soil, 309, 5-24, 2008.

Dobbie, K. E., McTaggart, I. P., and Smith, K. A.: Nitrous oxide emissions from intensive agricultural systems: Variations between crops and seasons, key driving variables, and mean emission factors, J. Geophys. Res., 104, 26891-26899, 1999.

Dobbie, K. E. and Smith, K. A.: The effects of temperature, water-filled pore space and land use on N_2O emissions from an imperfectly drained gleysol, European Journal of Soil Science, 52, 667-673, 2001.

Eckard, R. J., Grainger, C., and de Klein, C. A. M.: Options for the abatement of methane and nitrous oxide from ruminant production: A review, Livest Sci, 130, 47-56, 2010.

Elmi, A. A., Madramootoo, C., Hamel, C., and Liu, A.: Denitrification and nitrous oxide to nitrous oxide plus dinitrogen ratios in the soil profile under three tillage systems, Biology and Fertility of Soils, 38, 340-348, 2003.

Ellis, S., Webb, J., Misselbrook, T., and Chadwick, D.: Emission of ammonia (NH3), nitrous oxide (N_2O) and methane (CH4) from a dairy hardstanding in the UK, Nutrient Cycling in Agroecosystems, 60, 115-122, 2001.

Eugster, W., Zeyer, K., Zeeman, M., Michna, P., Zingg, A., Buchmann, N. & Emmenegger, L. Methodical study of nitrous oxide eddy covariance measurements using quantum cascade laser spectrometery over a Swiss forest. Biogeosciences, 4, 927-939. 2007

Flechard, C. R., Neftel, A., Jocher, M., Ammann, C., and Fuhrer, J.: Bi-directional soil/atmosphere N_2O exchange over two mown grassland systems with contrasting management practices, Global Change Biol, 11, 2114-2127, 2005.

Folorunso, O.A. & Rolston, D.E. Spatial and spectral relationships between field-measured denitrification gas fluxes and soil properties 1. Soil Science Society of America Journal, 49, 1087-1093, 1985

Fowler, D., Coyle, M., Skiba, U., Sutton, M. A., Cape, J. N., Reis, S., Sheppard, L. J., Jenkins, A., Grizzetti, B., Galloway, J. N., Vitousek, P., Leach, A., Bouwman, A. F., Butterbach-Bahl, K., Dentener, F., Stevenson, D., Amann, M., and Voss, M.: The global nitrogen cycle in the twenty-first century, Philos T R Soc B, 368, 2013.

Freney, J. R., Simpson, J. R., and Denmead, O. T.: Volatilization of ammonia. In: Gaseous Loss of Nitrogen from Plant-Soil Systems, Freney, J. R. and Simpson, J. R. (Eds.), Developments in Plant and Soil Sciences, Springer Netherlands, 1983.

Giltrap, D. L., Li, C., and Saggar, S.: DNDC: A process-based model of greenhouse gas fluxes from agricultural soils, Agriculture, Ecosystems & Environment, 136, 292-300, 2010.

Giltrap, D. L., Berben, P., Palmada, T., and Saggar, S.: Understanding and analysing spatial variability of nitrous oxide emissions from a grazed pasture, Agriculture, Ecosystems & Environment, 186, 1-10, 2014.

Goldberg, S. D., and Gebauer, G.: Drought turns a Central European Norway spruce forest soil from an N_2O source to a transient N_2O sink, Global Change Biol, 15(4), 850-860, 2009

Grossel, A., Nicoullaud, B., Bourennane, H., Rochette, P., Guimbaud, C., Chartier, M., Catoire, V., and Hénault, C.: Simulating the spatial variability of nitrous oxide emission from cropped soils at the within-field scale using the NOE model, Ecol Model, 288, 155-165, 2014.

Haynes, R. J. and Williams, P. H.: Changes in soil solution composition and pH in urine-affected areas of pasture, J Soil Sci, 43, 323-334, 1992.

Hellebrand, H. J.: Emission of Nitrous Oxide and other Trace Gases during Composting of Grass and Green Waste, Journal of Agricultural Engineering Research, 69, 365-375, 1998.

Hensen, A., Groot, T.T., van den Bulk, W.C.M., Vermeulen, A.T., Olesen, J.E. & Schelde, K. Dairy farm CH_4 and N_2O emissions, from one square metre to the full farm scale. Agriculture, Ecosystems & Environment, 112, 146-152, 2006

Hensen, A., Skiba, U. & Famulari, D. Low cost and state of the art methods to measure nitrous oxide emissions. Environmental Research Letters, 8, 025022, 2013.

Heincke, M., and Kaupenjohann, M.: Effects of soil solution on the dynamics of N_2O emissions: a review, Nutrient Cycling in Agroecosystems, 55(2), 133-157, 1999

Hirsch, A. I., Michalak, A. M., Bruhwiler, L. M., Peters, W., Dlugokencky, E. J., and Tans, P. P.: Inverse modeling estimates of the global nitrous oxide surface flux from 1998-2001, Global Biogeochem Cy, 20, 2006.

Hofstra, N. and Bouwman, A. F.: Denitrification in Agricultural Soils: Summarizing Published Data and Estimating Global Annual Rates, Nutrient Cycling in Agroecosystems, 72, 267-278, 2005.

Hutchinson, G.L. & Mosier, A.R.. Improved soil cover method for field measurement of nitrous-oxide fluxes. Soil Science Society of America Journal, 45, 311-316, 1981

IPCC, 2007: Climate Change 2007: The Physical Science Basis. Contribution of Working Group I to the Fourth Assessment Report of the Intergovernmental Panel on Climate Change [Solomon, S., D. Qin, M. Manning, Z. Chen, M. Marquis, K.B. Averyt, M. Tignor and H.L. Miller (eds.)]. Cambridge University Press, Cambridge, United Kingdom and New York, NY, USA, 996 pp

IPCC, 2013: Climate Change 2013: The Physical Science Basis. Contribution of Working Group I to the Fifth Assessment Report of the Intergovernmental Panel on Climate Change (eds. Stocker, T. F., D. Qin, G.-K. Plattner, M. Tignor, S. K. Allen, J. Boschung, A. Nauels, Y. Xia, V. Bex and P. M. Midgley). Cambridge University Press, Cambridge, United Kingdom

Isermann, K.: Agricultures Share in the Emission of Trace Gases Affecting the Climate and Some Cause-Oriented Proposals for Sufficiently Reducing This Share, Environmental pollution, 83, 95-111, 1994.

Jahangir, M. M. R., Roobroeck, D., van Cleemput, O., and Boeckx, P.: Spatial variability and biophysicochemical controls on N_2O emissions from differently tilled arable soils, Biology and Fertility of Soils, 47, 753-766, 2011.

Jarecki, M. K., Parkin, T. B., Chan, A. S. K., Hatfield, J. L., and Jones, R.: Comparison of DAYCENT-Simulated and Measured Nitrous Oxide Emissions from a Corn Field, J. Environ. Qual., 37, 1685-1690, 2008.

Jarvis, S. C., Stockdale, E. A., Shepherd, M. A., and Powlson, D. S.: Nitrogen Mineralization in Temperate Agricultural Soils: Processes and Measurement. In: Advances in Agronomy, Donald, L. S. (Ed.), Academic Press, 1996.

Jones, S. K., Rees, R. M., Skiba, U. M., and Ball, B. C.: Influence of organic and mineral N fertiliser on N2O fluxes from a temperate grassland, Agriculture, Ecosystems & Environment, 121, 74-83, 2007.

Jones, S.K., Famulari, D., Di Marco, C.F., Nemitz, E., Skiba, U.M., Rees, R.M., et al. Nitrous oxide emissions from managed grassland: a comparison of eddy covariance and static chamber measurements. Atmospheric Measurement Techniques, 4, 2179-2194. 2011.

Jordan, T. E., Weller, D. E., and Correll, D. L.: Denitrification in surface soils of a riparian forest: Effects of water, nitrate and sucrose additions, Soil Biology and Biochemistry, 30(7), 833-843. 1998.

Khalil, M. I., Rosenani, A. B., Van Cleemput, O., Fauziah, C. I., and Shamshuddin, J.: Nitrous oxide emissions from an ultisol of the humid tropics under maize-groundnut rotation, Journal of Environmental Quality, 31(4), 1071-1078. 2002

Karl, T. R. and Trenberth, K. E.: Modern global climate change, Science, 302, 1719-1723, 2003.

Kool, D. M., Van Groenigen, J. W., and Wrage, N.: Source Determination of Nitrous Oxide Based on Nitrogen and Oxygen Isotope Tracing: Dealing with Oxygen Exchange, Method Enzymol, 496, 139-160, 2011.

Kort, E.A., Patra, P.K., Ishijima, K., Daube, B.C., Jiménez, R., Elkins, J., et al. Tropospheric distribution and variability of N_2O: Evidence for strong tropical emissions. Geophysical Research. Letters, 38, L15806. 2011

Kroeze, C., Dumont, E., and Seitzinger, S.: Future trends in emissions of N_2O from rivers and estuaries, J Integr Environ Sci, 7, 71-78, 2010.

Kroon, P.S., Hensen A., Jonker, H.J.J., Zahniser, M.S., van 't Veen, W.H. & Vermeulen, A.T. Suitability of quantum cascade laser spectroscopy for CH_4 and N_2O eddy covariance flux measurements. Biogeosciences, 4, 715-728. 2007.

Kroon, P.S., Hensen, A., Bulk, W.C.M., Jongejan, P.A.C. & Vermeulen, A.T. The importance of reducing the systematic error due to non-linearity in N_2O flux measurements by static chambers. Nutrient Cycling in Agroecosystems, 82, 175-186. 2008.

Kroon, P. S., Schrier-Uijl, A. P., Hensen, A., Veenendaal, E. M., and Jonker, H. J. J.: Annual balances of CH_4 and N_2O from a managed fen meadow using eddy covariance flux measurements, European Journal of Soil Science, 61, 773-784, 2010.

Laville, P., Jambert, C., Cellier, P. & Delmas, R. Nitrous oxide fluxes from a fertilised maize crop using micrometeorological and chamber methods. Agricultural & Forest Meteorology, 96, 19-38. 1999.

Laville, P., Lehuger, S., Loubet, B., Chaumartin, F. & Cellier, P. Effect of management, climate and soil conditions on N_2O and NO emissions from an arable crop rotation using high temporal resolution measurements. Agricultural & Forest Meteorology, 151, 228-240. 2011.

Lesschen, J. P., Velthof, G. L., de Vries, W., and Kros, J.: Differentiation of nitrous oxide emission factors for agricultural soils, Environmental pollution, 159, 3215-3222, 2011.

Leuenberger, M. and Siegenthaler, U.: Ice-age atmospheric concentration of nitrous oxide from an Antarctic ice core, Nature, 360, 449-451, 1992.

Levy, P.E., Gray, A., Leeson, S.R., Gaiawyn, J., Kelly, M.P.C., Cooper, M.D.A., et al.. Quantification of uncertainty in trace gas fluxes measured by the static chamber method. European Journal of Soil Science, 62, 811-821. 2011

Linn, D. M. and Doran, J. W.: Effect of Water-Filled Pore Space on Carbon Dioxide and Nitrous Oxide Production in Tilled and Nontilled Soils1, Soil Sci. Soc. Am. J., 48, 1267-1272, 1984.

Livingston G. & Hutchinson G. Enclosure-based measurement of trace gas exchange: applications and sources of error. Biogenic trace gases: measuring emissions from soil and water, 14-51. Blackwell Science, Cambridge University Press, Cambridge. 1995.

Luo, J., Hoogendoorn, C., van der Weerden, T., Saggar, S., de Klein, C., Giltrap, D., Rollo, M., and Rys, G.: Nitrous oxide emissions from grazed hill land in New Zealand, Agriculture, Ecosystems & Environment, 181, 58-68, 2013.

Lynch, L., Bussel, J., Mcfarland, J. G., Chitkara, U., and Berkowitz, R. L.: Antenatal Treatment of Alloimmune Thrombocytopenia - Reply, Obstet Gynecol, 80, 1057-1057, 1992.

Machida, T., Nakazawa, T., Fujii, Y., Aoki, S., and Watanabe, O.: Increase in the Atmospheric Nitrous-Oxide Concentration during the Last 250 Years, Geophysical Research Letters, 22(21), 2921-2924. 1995

Ma, B. L., Wu, T. Y., Tremblay, N., Deen, W., Morrison, M. J., McLaughlin, N. B., Gregorich, E. G., and Stewart, G.: Nitrous oxide fluxes from corn fields: on-farm assessment of the amount and timing of nitrogen fertilizer, Global Change Biol, 16, 156-170, 2010.

Martins, O. and Dewes, T.: Loss of nitrogenous compounds during composting of animal wastes, Bioresource technology, 42, 103-111, 1992.

McCarty, G. W. and Bremner, J. M.: Availability of organic carbon for denitrification of nitrate in subsoils, Biology and Fertility of Soils, 14, 219-222, 1992.

Mcfarland, M. and Kaye, J.: Chlorofluorocarbons and Ozone, Photochem Photobiol, 55, 911-929, 1992.

Mathieu, O., Lévêque, J., Hénault, C., Milloux, M. J., Bizouard, F., and Andreux, F.: Emissions and spatial variability of N_2O, N_2 and nitrous oxide mole fraction at the field scale, revealed with 15N isotopic techniques, Soil Biology and Biochemistry, 38, 941-951, 2006.

Matthews, R. A., Chadwick, D. R., Retter, A. L., Blackwell, M. S. A., and Yamulki, S.: Nitrous oxide emissions from small-scale farmland features of UK livestock farming systems, Agriculture, Ecosystems & Environment, 136, 192-198, 2010.

Merbold, L., Eugster, W., Stieger, J., Zahniser, M., Nelson, D., and Buchmann, N.: Greenhouse gas budget (CO_2, CH_4 and N_2O) of intensively managed grassland following restoration, Global Change Biol, 20, 1913-1928, 2014.

Montes, F., Meinen, R., Dell, C., Rotz, A., Hristov, A. N., Oh, J., Waghorn, G., Gerber, P. J., Henderson, B., Makkar, H. P. S., and Dijkstra, J.: SPECIAL TOPICS-Mitigation of methane and nitrous oxide emissions from animal operations: II. A review of manure management mitigation options, J Anim Sci, 91, 5070-5094, 2013.

Mosier, A. R., Duxbury, J. M., Freney, J. R., Heinemeyer, O., and Minami, K.: Nitrous oxide emissions from agricultural fields: Assessment, measurement and mitigation, Plant Soil, 181, 95-108, 1996.

Mutegi, J. K., Munkholm, L. J., Petersen, B. M., Hansen, E. M., and Petersen, S. O.: Nitrous oxide emissions and controls as influenced by tillage and crop residue management strategy, Soil Biol Biochem, 42, 1701-1711, 2010.

Neftel, A., Blatter, A., Schmid, M., Lehmann, B., and Tarakanov, S. V.: An experimental determination of the scale length of N_2O in the soil of a grassland, J Geophys Res-Atmos, 105, 12095-12103, 2000.

Oenema, O., Velthof, G. L., Yamulki, S., and Jarvis, S. C.: Nitrous oxide emissions from grazed grassland, Soil Use Manage, 13, 288-295, 1997a.

Oenema, O., Wrage, N., Velthof, G., Groenigen, J. W., Dolfing, J., and Kuikman, P.: Trends in Global Nitrous Oxide Emissions from Animal Production Systems, Nutrient Cycling in Agroecosystems, 72, 51-65, 2005.

Okereke, G. U.: Growth yield of denitrifiers using nitrous oxide as a terminal electron acceptor, World Journal of Microbiology and Biotechnology, 9(1), 59-62. 1993

Omonode, R. A., Smith, D. R., Gal, A., and Vyn, T. J.: Soil Nitrous Oxide Emissions in Corn following Three Decades of Tillage and Rotation Treatments, Soil Sci Soc Am J, 75, 152-163, 2011.

Palma, R. M., Rimolo, M., Saubidet, M. I., and Conti, M. E.: Influence of tillage system on denitrification in maize-cropped soils, Biology and Fertility of Soils, 25, 142-146, 1997.

Papen, H., Daum, M., Steinkamp, R., and Butterbach-Bahl, K.: N_2O and CH_4-fluxes from soils of a N-limited and N-fertilized spruce forest ecosystem of the temperate zone, Journal of Applied Botany and Food Quality, 75(3-4), 159-163. 2001

Park, S., Croteau, P., Boering, K. A., Etheridge, D. M., Ferretti, D., Fraser, P. J., Kim, K. R., Krummel, P. B., Langenfelds, R. L., van Ommen, T. D., Steele, L. P., and Trudinger, C. M.: Trends and seasonal cycles in the isotopic composition of nitrous oxide since 1940, Nature Geosci, 5, 261-265, 2012.

Parkin, T. B.: Soil Microsites as a Source of Denitrification Variability1, Soil Sci. Soc. Am. J., 51, 1194-1199, 1987.

Parkin, T.B., Venterea, R.T. & Hargreaves, S.K. Calculating the detection limits of chamber-based soil greenhouse gas flux measurements. Journal of Environmental Quality, 41, 705-715. 2012.

Parry, M. L., Rosenzweig, C., Iglesias, A., Livermore, M., and Fischer, G.: Effects of climate change on global food production under SRES emissions and socio-economic scenarios, Global Environmental Change, 14, 53-67, 2004.

Pedersen, A. R., Petersen, S. O., and Schelde, K.: A comprehensive approach to soil-atmosphere trace-gas flux estimation with static chambers, European Journal of Soil Science, 61, 888-902, 2010.

Petersen, S. O., Schjonning, P., Thomsen, I. K., and Christensen, B. T.: Nitrous oxide evolution from structurally intact soil as influenced by tillage and soil water content, Soil Biol Biochem, 40, 967-977, 2008.

Pinto, M., Merino, P., del Prado, A., Estavillo, J. M., Yamulki, S., Gebauer, G., Piertzak, S., Lauf, J., and Oenema, O.: Increased emissions of nitric oxide and nitrous oxide following tillage of a perennial pasture, Nutrient Cycling in Agroecosystems, 70, 13-22, 2004.

Prinn, R. G., Weiss, R. F., Fraser, P. J., Simmonds, P. G., Cunnold, D. M., Alyea, F. N., O'Doherty, S., Salameh, P., Miller, B. R., Huang, J., Wang, R. H. J., Hartley, D. E., Harth, C., Steele, L. P., Sturrock, G., Midgley, P. M., and McCulloch, A.: A history of chemically and radiatively important gases in air deduced from ALE/GAGE/AGAGE, Journal of Geophysical Research: Atmospheres, 105, 17751-17792, 2000.

Rowell D Soil Science; Methods and Application, Longman Scientific & Technical, 1994

Ravishankara, A.R., Daniel, J.S. & Portmann, R.W. Nitrous oxide (N_2O): the dominant ozone-depleting substance emitted in the 21st century. Science, 326, 123-125. 2009.

Reay, D. S., Smith, K. A., and Edwards, A. C.: Nitrous oxide emission from agricultural drainage waters, Global Change Biol, 9, 195-203, 2003.

Reay, D. S., Edwards, A. C., and Smith, K. A.: Importance of indirect nitrous oxide emissions at the field, farm and catchment scale, Agriculture, Ecosystems & Environment, 133, 163-169, 2009.

Reay, D. S., Davidson, E. A., Smith, K. A., Smith, P., Melillo, J. M., Dentener, F., and Crutzen, P. J.: Global agriculture and nitrous oxide emissions, Nature Clim. Change, 2, 410-416, 2012.

Rochette, P.: No-till only increases N_2O emissions in poorly-aerated soils, Soil Till Res, 101, 97-100, 2008.

Rosenkranz, P., Bruggemann, N., Papen, H., Xu, Z., Seufert, G., and Butterbach-Bahl, K.: N_2O, NO and CH_4 exchange, and microbial N turnover over a Mediterranean pine forest soil, Biogeosciences, 3(2), 121-133, 2006

Rowell D Soil Science; Methods and Application, Longman Scientific & Technical, 1994

Ryden, J. C.: N_2O Exchange between a Grassland Soil and the Atmosphere, Nature, 292, 235-237, 1981.

Rypdal, K. and Winiwarter, W.: Uncertainties in greenhouse gas emission inventories — evaluation, comparability and implications, Environmental Science & Policy, 4, 107-116, 2001.

Saggar, S., Bolan, N. S., Bhandral, R., Hedley, C. B., and Luo, J.: A review of emissions of methane, ammonia, and nitrous oxide from animal excreta deposition and farm effluent application in grazed pastures, New Zeal J Agr Res, 47, 513-544, 2004.

Saggar, S., Jha, N., Deslippe, J., Bolan, N. S., Luo, J., Giltrap, D. L., Kim, D. G., Zaman, M., and Tillman, R. W.: Denitrification and N_2O:N_2 production in temperate grasslands: Processes, measurements, modelling and mitigating negative impacts, Science of The Total Environment, 465, 173-195, 2013.

Sala, O. E., Chapin, F. S., Armesto, J. J., Berlow, E., Bloomfield, J., Dirzo, R., Huber-Sanwald, E., Huenneke, L. F., Jackson, R. B., Kinzig, A., Leemans, R., Lodge, D. M., Mooney, H. A., Oesterheld, M., Poff, N. L., Sykes, M. T., Walker, B. H., Walker, M., and Wall, D. H.: Biodiversity - Global biodiversity scenarios for the year 2100, Science, 287, 1770-1774, 2000.

Schneider, S. H.: The Greenhouse Effect: Science and Policy, Science, 243, 771-781, 1989.

Schlesinger, W.H. Biogeochemistry: an analysis of global change: Academic Press, California, 2, 1997

Sexstone, A. J., Revsbech, N. P., Parkin, T. B., and Tiedje, J. M.: Direct Measurement of Oxygen Profiles and Denitrification Rates in Soil Aggregates1, Soil Sci. Soc. Am. J., 49, 645-651, 1985.

Seitzinger, S. P., Kroeze, C., and Styles, R. V.: Global distribution of N2O emissions from aquatic systems: natural emissions and anthropogenic effects, Chemosphere - Global Change Science, 2, 267-279, 2000.

Shcherbak, I., Millar, N., and Robertson, G. P.: Global metaanalysis of the nonlinear response of soil nitrous oxide (N_2O) emissions to fertilizer nitrogen, Proceedings of the National Academy of Sciences of the United States of America, 111, 9199-9204, 2014.

Sheehy, J., Six, J., Alakukku, L., and Regina, K.: Fluxes of nitrous oxide in tilled and no-tilled boreal arable soils, Agr Ecosyst Environ, 164, 190-199, 2013.

Shoun, H., Kim, D.-H., Uchiyama, H., and Sugiyama, J.: Denitrification by fungi, FEMS Microbiology Letters, 94, 277-281, 1992.

Šimek, M., Brůček, P., Hynšt, J., Uhlířová, E., and Petersen, S. O.: Effects of excretal returns and soil compaction on nitrous oxide emissions from a cattle overwintering area, Agriculture, Ecosystems & Environment, 112, 186-191, 2006.

Skiba, U., et al. (2012), UK emissions of the greenhouse gas nitrous oxide, Philosophical Transactions of the Royal Society B: Biological Sciences, 367(1593), 1175-1185. 1981

Skiba, U., DiMarco, C., Hargreaves, K., Sneath, R., and McCartney, L.: Nitrous oxide emissions from a dung heap measured by chambers and plume methods, Agr Ecosyst Environ, 112, 135-139, 2006.

Skiba, U., Jones, S. K., Drewer, J., Helfter, C., Anderson, M., Dinsmore, K., McKenzie, R., Nemitz, E., and Sutton, M. A.: Comparison of soil greenhouse gas fluxes from extensive and intensive grazing in a temperate maritime climate, Biogeosciences Discuss., 9, 10057-10085, 2012.

Smith, K. A., et al.: Micrometeorological and chamber methods for measurement of nitrous oxide fluxes between soils and the atmosphere: Overview and conclusions, Journal of Geophysical Research: Atmospheres, 99(D8), 16541-16548, 1994

Smith, K. A. and Dobbie, K. E.: The impact of sampling frequency and sampling times on chamber-based measurements of N2O emissions from fertilized soils, Global Change Biol, 7, 933-945, 2001.

Smith, K., Dobbie, K., Thorman, R., Watson, C., Chadwick, D., Yamulki, S., and Ball, B.: The effect of N fertilizer forms on nitrous oxide emissions from UK arable land and grassland, Nutrient Cycling in Agroecosystems, 93, 127-149, 2012.

Smith, K. and Massheder, J.: Predicting nitrous oxide emissions from N-fertilized grassland soils in the UK from three soil variables, using the B-LINE 2 model, Nutrient Cycling in Agroecosystems, 98, 309-326, 2014.

Stevens, R. J., Laughlin, R. J., Burns, L. C., Arah, J. R. M., and Hood, R. C.: Measuring the contributions of nitrification and denitrification to the flux of nitrous oxide from soil, Soil Biology and Biochemistry, 29, 139-151, 1997.

Tan, I. Y. S., van Es, H. M., Duxbury, J. M., Melkonian, J. J., Schindelbeck, R. R., Geohring, L. D., Hively, W. D., and Moebius, B. N.: Single-event nitrous oxide losses under maize production as affected by soil type, tillage, rotation, and fertilization, Soil Till Res, 102, 19-26, 2009.

Thomas J, Thistlethwaite G et al Greenhouse gas inventories for England, Scotland, Wales and Northern Ireland: 1990–2009. Department of Energy and Climate Change, The Scottish Government, The Welsh Government, The Northern Ireland Department of Environment, Didcot. 2011

Thomson, A. J., Giannopoulos, G., Pretty, J., Baggs, E. M., and Richardson, D. J.: Biological sources and sinks of nitrous oxide and strategies to mitigate emissions, Philos T R Soc B, 367, 1157-1168, 2012.

Turner, D. A., Chen, D., Galbally, I. E., Leuning, R., Edis, R. B., Li, Y., Kelly, K., and Phillips, F.: Spatial variability of nitrous oxide emissions from an Australian irrigated dairy pasture, Plant Soil, 309, 77-88, 2008.

Ussiri, D. A. N., Lal, R., and Jarecki, M. K.: Nitrous oxide and methane emissions from long-term tillage under a continuous corn cropping system in Ohio, Soil Till Res, 104, 247-255, 2009.

Van Kessel, J. and Reeves, J.: Nitrogen mineralization potential of dairy manures and its relationship to composition, Biology and Fertility of Soils, 36, 118-123, 2002.

Vallejo, A., Skiba, U. M., Garcia-Torres, L., Arce, A., Lopez-Fernandez, S., and Sanchez-Martin, L.: Nitrogen oxides emission from soils bearing a potato crop as influenced by fertilization with treated pig slurries and composts, Soil Biol Biochem, 38, 2782-2793, 2006.

Velthof, G.L., Jarvis, S.C., Stein, A., Allen, A.G. & Oenema O. Spatial variability of nitrous oxide fluxes in mown and grazed grasslands on a poorly drained clay soil. Soil Biology & Biochemistry, 28, 1215-1225. 1996.

Velthof, G. L. and Oenema, O.: Nitrous oxide emission from dairy farming systems in the Netherlands, Neth J Agr Sci, 45, 347-360, 1997.

Velthof, G., Kuikman, P., and Oenema, O.: Nitrous oxide emission from animal manures applied to soil under controlled conditions, Biology and Fertility of Soils, 37, 221-230, 2003.

Venterea, R. T., Spokas, K. A., and Baker, J. M.: Accuracy and Precision Analysis of Chamber-Based Nitrous Oxide Gas Flux Estimates All rights reserved., Soil Science Society of America Journal, 73(4), 1087-1093. 2009

Wrage, N., Velthof, G. L., van Beusichem, M. L., and Oenema, O.: Role of nitrifier denitrification in the production of nitrous oxide, Soil Biology and Biochemistry, 33, 1723-1732, 2001.

Wrage, N., Lauf, J., del Prado, A., Pinto, M., Pietrzak, S., Yamulki, S., Oenema, O., and Gebauer, G.: Distinguishing sources of N_2O in European grasslands by stable isotope analysis, Rapid Commun Mass Sp, 18(11), 1201-1207. 2004

Webb, N. Broomfield, M. Brown, P. Buys, G. Cardenas L. Murrells T. Pang Y. Passant N. Thistlethwaite G. Watterson J. 2014. UK Greenhouse Gas Inventory 1990 to 2012: Annual Report for submission under the Framework Convention on Climate Change (At: https://www.gov.uk/government/uploads/system/uploads/attachment_data/file/310779/UK_National_Inventory_Report_Main_1990-2012.pdf. Accessed: 16/9/14)

Wertz, S., Goyer, C., Zebarth, B. J., Burton, D. L., Tatti, E., Chantigny, M. H., and Filion, M.: Effects of temperatures near the freezing point on N_2O emissions, denitrification and on the abundance and structure of nitrifying and denitrifying soil communities, Fems Microbiol Ecol, 83, 242-254, 2013.

Yamulki, S. Y. and Jarvis, S. J.: Short-term effects of tillage and compaction on nitrous oxide, nitric oxide, nitrogen dioxide, methane Yamulki, S. & Jarvis, S.C. Automated chamber technique for gaseous flux measurements: Evaluation of a photoacoustic infrared spectrometer-trace gas analyzer. Journal of Geophysical Research-Atmospheres, 104, 5463-5469, 1999.

Yamulki, S. Y. and Jarvis, S. J.: Short-term effects of tillage and compaction on nitrous oxide, nitric oxide, nitrogen dioxide, methane and carbon dioxide fluxes from grassland, Biology and Fertility of Soils, 36, 224-231, 2002.

Yu, K., Chen, G., Struwe, S., and Kjoller, A.: Production and reduction of nitrous oxide in agricultural and forest soils, Ying yong sheng tai xue bao, The journal of applied ecology, 11(3), 385-389, 2000

Zahniser, M.S., Nelson D.D., McManus J.B., Herndon S.C., Wood E.C., Shorter J.H., et al. Infrared QC laser applications to field measurements of atmospheric trace gas sources and sinks in environmental research: enhanced capabilities using continuous wave QCLs. Quantum Sensing & Nanophotonic Devices VI, 7222, 2009.

Zhu, J., Mulder, J., Wu, L. P., Meng, X. X., Wang, Y. H., and Dorsch, P.: Spatial and temporal variability of N_2O emissions in a subtropical forest catchment in China, Biogeosciences, 10, 1309-1321, 2013.